The University of Edinburgh

Collage of Science and Engineering

School of Chemistry

SYNTHESIS and APPLICATIONS of TRIFLUOROMETHYL ARYLDIAZIRINE PHOTOPHORE

By

Mariona Vallès Miret

Thesis for the degree of Doctor of Philosophy

April 2011

To my parents and Ton,

UNIVERSITY OF EDINBURGH

College of Science and Engineering
School of Chemistry

ABSTRACT

Synthesis and Applications of the
Trifluoromethyl Aryldiazirine Photophore

by *Mariona Vallès Miret*

Photoreactive groups have been used in photoaffinity labelling of chemical macromolecules *via* the generation of highly reactive species upon short wave light irradiation. One of the most efficient photoreactive functional groups is trifluoromethyl aryldiazirine (TFMAD). This compound was synthesised as part of the work discussed in this thesis, making use of microwave irradiation to shorten reaction times (**Chapter I**). An investigation of properties allowed the development of three different applications for conjugation to biomolecules. The first application consisted of the development of an approach for generation of small-molecule microarrays, where a 2,000 compound library was immobilised onto the glass surface through carbene insertion. The microarray was then used to screen for potential binders to beta-transducin repeat containing protein (β-TrCP1) allowing the reduction of possible candidates to less than 25 compounds (**Chapter II**). The second application was the synthesis of two probes to allow the selective delivery of active compounds inside specific organelles or cells. The diazirine moiety was used as a rapid way to covalently capture a number of cargos. The approach allowed a peptoid and an anticancer drug to be conjugated to the two probes and their cell penetrability properties and therapeutic effect were studied, respectively (**Chapter III**). Finally, the insertion properties of TFMAD were used to develop approaches to attach DNA onto microspheres and the efficiency of this delivery system was evaluated (**Chapter IV**).

Declaration of Authorship

I, Mariona Vallès-Miret, declare that the thesis entitled "Synthesis and Applications of Trifluoromethyl Aryldiazirine Photophore" and the work presented in it are my own.

I confirm that the research described in this thesis was carried out under the supervision of Prof. Mark Bradley at the University of Edinburgh (September 2007-September 2010). Where I have consulted the published work of others, this is always clearly attributed; where I have quoted from the work of others, the source is always given. With the exception of such quotations, this thesis is entirely my own work; I have acknowledged all main sources for help; Where the thesis is based on work done by myself jointly with others, I have made clear exactly what was done by others and what I have contributed myself; No part of this thesis has been previously submitted at this or any other university for any other degree or a professional qualification.

Signed: 

Date: 18th August 2011

Acknowledgments

Firstly, I would like to express my sincere gratitude to my supervisor, Professor Mark Bradley, for his support, trust, personal guidance and encouragement throughout my research project.

I would like to thank the entire Bradley group, both former and current members, for sharing their knowledge and friendship in equal measure and making the lab a nice place to work. In particular, I would like to thank Rosario who has helped me enormously with her advice, not only to complete this dissertation but also for cheering me up in hard times. I appreciate all the help I received form Juanma for training me to work with microspheres, not to mention his friendship. I would also like to show my gratitude to Jeff, Juanjo, Rong and Albert who always kindly granted me their time to answer any of my questions, and supporting me in my work. I am especially thankful to the biolab team and Geraldine, for introducing me to the world of biology, which is nice only when there are no contaminations, and for their patience, advice and explanations.

Much of this experience has been possible thanks to Adam and Frank who have helped me with my English and inspired me in research and life during our deep discussions in the office, as well as Juanma and Mentxu whose energy motivated anybody to do sport. A warm regard goes to Ferdous with whom I shared lab cabinet and to Ola who warmly welcomed me and took care of me in my first days. Furthermore, Geraldine, Guilhem, Nicos and Effie have been a constant source of encouragement during the long hours in the lab and outside. I have been great to share this part of my life with you.

I would like to thank my family, specially my parents, for their unflagging love and encouragement throughout my life and for being always next to me. Thanks to them I am the person who I have become, and together with my friends from back home they have helped me to stay sane and reminded me of the important things in life.

Finally, I owe my deepest gratitude to Ton who has contributed enormously to the sentimental aspect of this thesis. I confess that without his love, friendship, support and comprehension this work would have never been possible. You have given me the happiest moments of this experience and supported me unconditionally during my hardest times. I love you more and more every day!

Table of contents

Abbreviations

5-(6)-FAM	5-(6)-Carboxyfluorescein
Ac	Acetyl
APTES	Aminopropyltriethoxysilane
Aq	aqueous
Boc_2O	Di-*t*-butyl carbonate
br	broad
^{t}Bu	*tert*-Butyl
Boc	*tert*-Butoxycarbonyl
calcd	calculated
δ	chemical shift in ppm downfield from tetramethylsilane
d	doublet
DCM	Dichloromethane
DCC	Dicyclohexylcarbodiimide
DIC	*N,N'*-Diisopropylcarbodiimide
DIPEA	*N,N*-Diisopropylethylamine
DMAP	4-(dimethylamino) pyridine
DMF	*N,N*-Dimethylformamide
DMSO	Dimethyl sulfoxide
DSC	N,N'-Disuccinimidyl carbonate
ELSD	Evaporative Light Scattering Detector
Eq	Equivalent
ES^{+}	Electrospray mass spectrometry, positive ionisation
ES^{-}	Electrospray mass spectrometry, negative ionisation
Et	Ethyl
EtOAc	Ethylacetate
EtOH	Ethanol
FA	Formic acid
Fmoc	9-Fluorenylmethyloxycarbonyl
g	Grams
h	Hours
HCl	Hydrochloric acid
HOBt	*N*-Hydroxybenzotriazole
HMBA	4-[4-(hydroxymethyl)phenoxy]butanoic acid
HTS	High Throughput Screening
HRMS	High Resolution Mass Spectrometry

Hz	Hertz
IR	Infrared
LCMS	Liquid Chromatography-Mass Spectrometry
J	Coupling contant
λ	Wavelength
m	multiplet, meters
M	Molarity
Me	Methyl
MeOH	Methanol
min	minutes
mP	milli-Polarisation level
mp	melting point
MG-oxalate	Malachite Green oxalate salt
MS	Mass Spectrometry
MW	Microwave irradiation
NMP	*N*-methylpyrrolidone
NMR	Nuclear Magnetic Resonance
PEG	Polyethyleneglycol
q	quartet
q_5	quintet
RP-HPLC	Reverse Phase-High Performance Liquid Chromatography
RT	Room temperature
s	Singlet, seconds
t	Triplet
TEA	Triethylamine
TFA	Trifluoroacetic acid
THF	Tetrahydrofuran
TIS	Tri-*iso*-propylsilane
TLC	Thin Layer Chromatography
t_R	Retention time
UV	Ultraviolet

Amino Acids

D	Aspartic acid	R	Arginine
G	Glycine	S	Serine
K	Lysine	V	Valine
P	Proline		

***Chapter I*:**

THE TRIFLUOROMETHYL ARYLDIAZIRINE PHOTOPHORE

1.1. Introduction

Photophores are stable reagents that become highly reactive species when activated by UV light, often forming new covalent bonds with surrounding molecules. These may be biopolymers or surfaces with typically few, if any, restrictions on selectivity towards different functional groups. Their use adds variation and opportunity for studying systems where little is known.

This chapter introduces the most common photoactivatable groups, describes how they work and looks at their reactivity and applications. Finally, it focuses on the synthesis, properties and behaviour of the trifluoromethyl aryldiazirine photophore, which is the photoactivatable group that has been used in this thesis.

1.1.1. Photoactivatable Reagents

Photoprobes are important tools used in drug discovery and drug development.[1-4] For example, photoactivatable groups have been widely used in photoaffinity labelling approaches, a method that is based on the chemical modification of biological macromolecules (i.e. proteins). It is an efficient and reliable tool used to identify, isolate and characterise novel biological molecules as well as to identify potential drug targets, particularly when the target molecule is unknown. This method also helps to define relationships on biomolecules within an assembly, and to provide information on the spatial relationship between components in complex systems.[1, 5]

One important feature of this technique is the preparation of an effective probe. The photoaffinity probe incorporates a photoactivatable group in its structure which is activated by light when complexed to its target. Until they are photolysed, photosensitive functional groups are relatively non-reactive in typical thermochemical processes. Because they are stable in the dark, reagents designed with a photophore can be assessed for their bioactivity before being used in highly controlled photoactivated reactions.

Upon activation, photoactivatable groups generate highly reactive species which allows formation of a new covalent bond between the ligand and the target molecule. In addition, the probe often incorporates a reporter group in order to identify and facilitate the isolation of the labelled molecule. These reporter groups can be a radioactive label,[6, 7] biotin[8, 9] or a fluorescent tag[10] (**Figure 1.1**).

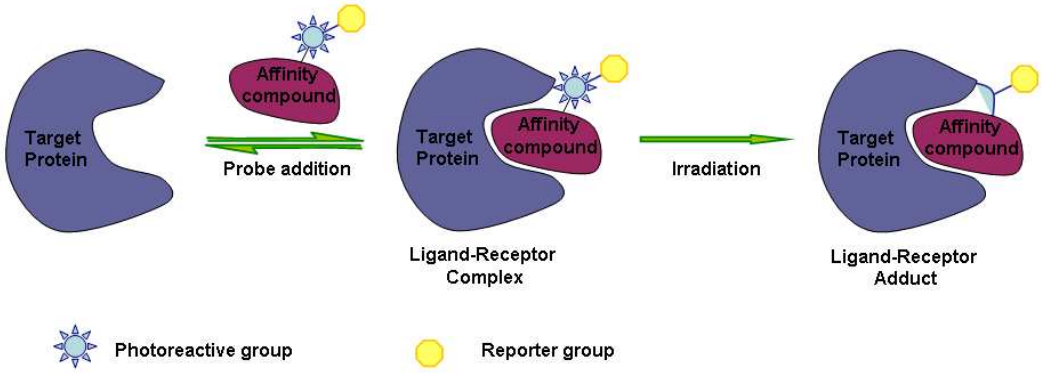

Figure 1.1: Schematic representation of photoaffinity labelling approach. In this case, the probe consists of a high affinity compound that has been derivatised with a photoreactive group and reporter group. Once the complex between probe and protein has ocurred, the sample is irradiated leading to the formation of a covalent bond between them. Then, the reported group is used to identify or purify the adduct.

Photoactivatable reagents form short-lived, high-energy intermediates upon UV irradiation. Thus, an important feature of these reagents is that they should be activated at wavelengths that do little or no damage to the other components of the system. In general, this means that irradiation at wavelengths absorbed by proteins and nucleic acids (<300 nm) should be avoided. In addition, photolysis should be highly efficient; that is the reagent should have a high extinction coefficient (ε) and the reactive group should be formed in high quantum yield (Φ).

The most common photoactivatable functional groups are benzophenones, aromatic azides and aromatic diazirines generating reactive intermediates such as ketyls, nitrenes, and carbenes.

1.1.1.1. ***Ketyl-Reactive Species:***

Acetophenones, benzophenones and anthraquinones form highly reactive species after exposure to UV light (ranging from 340 to 360nm).[11-13] The photoactivatable group of these reagents are conjugated carbonyl functionalities which can be excited by UV light, generating an nπ* triplet state (**Figure 1.2**).[14] In the exited state the molecule can interact with weak C-H σ-bonds, resulting in hydrogen abstraction to form a ketyl radical. The ketyl readily recombines with the alkyl radical generated in the substrate, forming a new C-C bond (**Scheme 1.1**). Unreacted excited species rapidly relax to the ground state, as a result, conjugated ketones usually need quite long irradiation times,[15, 16] which can be problematic for some applications. However, they can be manipulated in aqueous solutions as they do not react with water or bulk nucleophiles.[12]

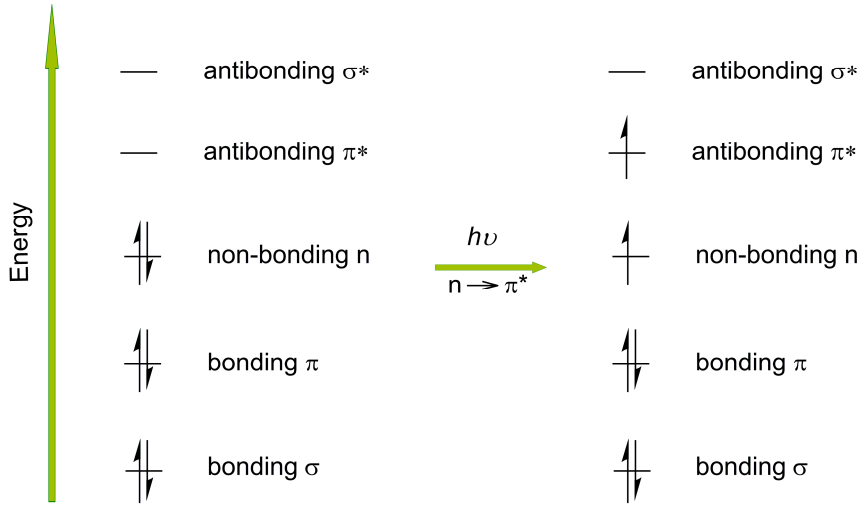

Figure 1.2: Generation of nπ* triplet state after excitation with UV light.

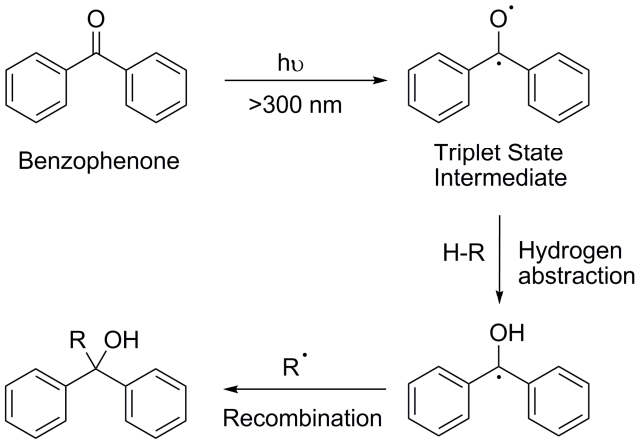

Scheme 1.1: Conjugated carbonyl excited by UV light form a triplet excited state that abstracts a hydrogen atom from a donor yielding two radicals which subsequently couple.

1.1.1.2. ***Nitrene-Reactive Species:***

Nitrenes are highly reactive species generated by azide photolysis. They can insert non-specifically into different chemical bonds of target molecules, including addition reactions to double bonds and insertion reactions to bonds at C-H and N-H sites.

One of the most widely applied photolabelling reagents are phenyl azides.[17, 18] Their popularity is mainly due to the ease of their synthesis and commercial availability. Although phenyl azides possess high stability, the nitrenes generated are much less reactive than many other classes of nitrenes. For example, photolysis of phenyl azides in hydrocarbon solvents at room temperature gives almost none intermolecular C-H insertion products.[19, 20] This lack of reactivity may in part be due to the ring expansion of the generated singlet phenyl nitrene after photolysis forming azirine and dehydroazepine,[21, 22 23] which tends to be intercepted by a nucleophile such as an amine or undergo polymerisation to form poly-1,2-azepines[24] in the absence of a nucleophile (**Scheme 1.2**).

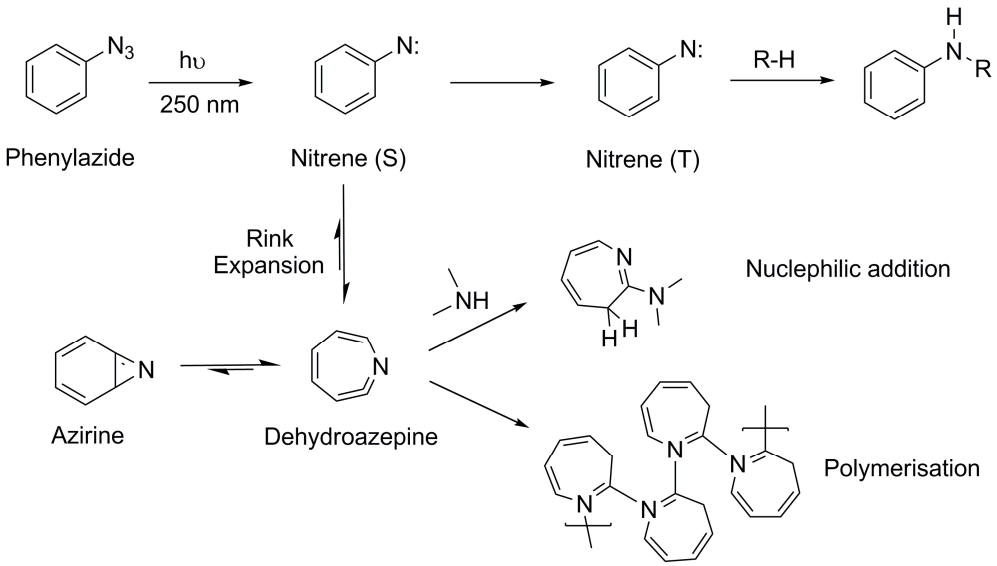

Scheme 1.2: Photolysis of phenyl azides at 250 nm produces phenyl nitrenes which insert into different chemical bonds or they can undergo a ring expansion forming dehydroazepine which reacts with nucleophiles such as amines and thiols to form substituted azepines or polymerise to form poly-1,2-azepines.

New azide reagents that promise an improved series of photolabels are perfluorophenyl azides (PFPA). They give higher yields of C-H insertion than their non-fluorinated analogues, possibly due to the higher reactivity of the nitrenes by favouring triplet state formation and consequently lacking the side reaction of

the singlet nitrene ring expansion (**Scheme 1.3**). Moreover, its photolysis can be conveniently monitored by ^{19}F NMR. However, all 4-substituted perfluorophenyl azides have UV absorption maxima around 260 nm which can damage biomolecules. Fortunately, photolysis tends to be complete before appreciable photolytic damage takes place due to the greater molar absorptivity and photochemical liability of the photoreactive reagent relative to biopolymers.[25]

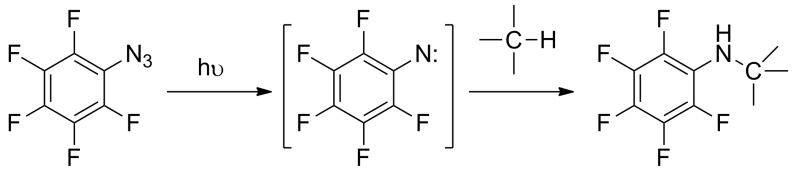

Scheme 1.3: Photolysis of perfluroinated azides produce singlet and triplet nitrenes, without ring expansion, which they undergo C-H insetion to form secondary amines or radicals by proton atom abstraction followed by radical coupling.

1.1.1.3. ***Carbene-Reactive Species:***

Diazo and diazirine compounds undergo irreversible nitrogen liberation upon UV irradiation forming short-lived and highly reactive carbenes that react rapidly with the surrounding chemical environment.[26] Carbenes insert non-specifically into chemical bonds, preferably addition reactions to double bonds[27] but also insertion reactions into C-H and O-H bonds[28, 29] (**Scheme 1.4**).

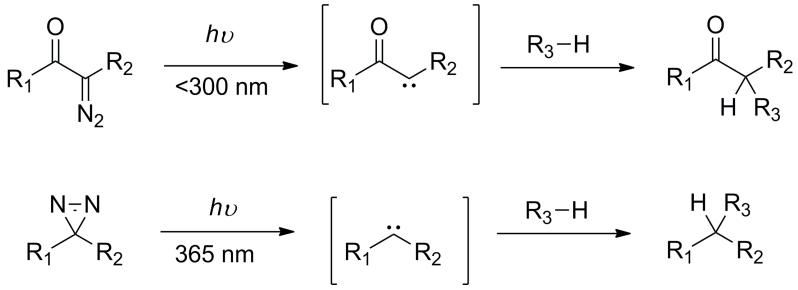

Scheme 1.4: Photolysis of diazo or diazirine compounds generate carbenes which react non-specifically with the surrounding molecules.

Although diazo compounds were one of the first photoactivatable reagents to be used, their photolysis properties are not ideal for photoaffinity labelling for several reasons. Firstly, they generally possess a strong absorption band in the ultraviolet (<300 nm, $\varepsilon \approx 10^4$ $M^{-1}cm^{-1}$) and a very weak band at longer wavelengths (340 nm, $\varepsilon \approx 11$ $M^{-1}cm^{-1}$).[5] Irradiation at >300 nm must thus be prolonged to achieve complete photolysis which can damage biological samples, however it has been shown that photolysis at 254 nm can be achieved

in a reasonable time-frame without causing damage to proteins if care is taken.[30] They are not very stable but it is known that they are stabilised by electron withdrawing substituents at the α-position to the diazo carbon. The diazoacetyl compound family is one of the most stable.[31]

Secondly, the carbene formed after irradiation can undergo Wolff rearrangement yielding a ketene as a major product (**Scheme 1.5**). This fact is one of the reasons why nowadays diazoacetyl compounds are seldomly used for photoaffinity labelling.[32, 33]

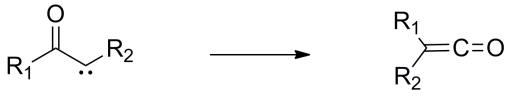

Scheme 1.5: Formation of ketene from carbene by Wolf rearrangement.

Finally, diazoacetyl compounds have very low stability. They are unstable at low pH and they have been seen to react in the dark towards protein functional groups. For instance, modification of histidine occurred in an acid-catalysed rather than a light-induced process with the percentage yield depending on the pH. [33, 34] In addition, like phenyl azides, diazo compounds are susceptible to reduction by a number of thiols used commonly as protective agents for proteins.[35] However, the two diazo reagents, diazotrifluropropionyl (**1**)[36] and *p*-toluenesulfonyldiazoacetyl (**2**),[37] are considerably improved in these respects and are stable in 1 M hydrochloric acid.

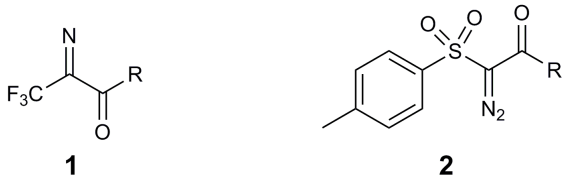

Scheme 1.6: Structures of diazotrifluoropropionyl and *p*-toluenesulfonyldiazoacetyl group.

On the contrary, the use of diazirines as stable carbene precursors has increased dramatically over the past twenty years and these reagents are rapidly becoming the most popular photophores for photoaffinity labelling and biological applications. They have also become important in radical chemistry to prepare heterocyclic compounds.[38, 39]

Among diazirines, trifluoromethyl aryldiazirines appear to come closest to satisfying the chemical and biological criteria required for an optimal photoreagent.[40-44] The diazirine functionality is remarkably stable under a range

of different physical and chemical conditions and it is rapidly photolysed at 350 nm to generate a carbene capable of reacting with the full range of functional groups, including paraffinic C-H bonds.

1.1.2. Trifluoromethyl Aryldiazirine Photophores

Diazirines were first synthesised and characterised in the early 1960s.[45-47] These unsaturated species (**3**) are three-membered heterocycles featuring an azo group and an sp^3 hybridised carbon atom.

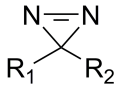

3

The most outstanding property of diazirines is their ability to form highly reactive carbenes with concomitant liberation of nitrogen upon suitable activation *via* exposure to light, pyrolysis or ultrasonification.[48] In addition to reactions with nucleophilic groups, carbenes are capable of reacting *via* insertion into saturated and unsaturated hydrocarbons including aromatic systems.[49] Reaction with carbenes involve the formation of stable carbon-based bonds under most of the conditions necessary for further studies.[50]

a **b**

Figure 1.3: Structures of a) dialkyldiazirines and b) 3H-diazirines.

The first diazirines to be prepared were dialkyl diazirines and 3H-diazirines (**Figure 1.3**), the latter being extremely difficult to synthesise in acceptable yields since they have low stability. The problem of these diazirines is their susceptibility to undergo intramolecular rearrangement by 1,2-hydrogen migration[51] (**Scheme 1.7**). Adamantanediazirine, a constrained caged ring, and 3-halodiazirines have been prepared as they can not rearrange to olefins. However, adamantanediazirines are not exempted of intramolecular rearrangements[52, 53] and 3-halodiazirines were found to have a potentially explosive nature and they are typically only utilised for structural and kinetic studies.[48]

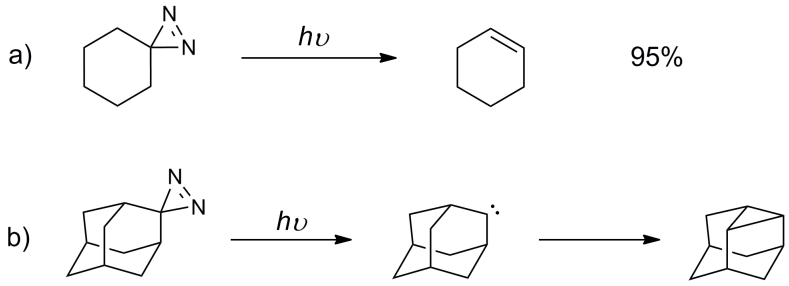

Scheme 1.7 : Examples of unwanted photolysis products by intramolecular rearrangement. a) Rearrangement of carbenes from alkyl diazirines to give olefins. b) Adamantanediazirine carbenes undergo intramolecular insertion.

A more recent addition to the diazirine family were 3H-3-aryldiazirines described by Knowles *et al.*,[54] which were found to be relatively stable to intramolecular rearrangements. However, a serious problem of this family is the high percentage of diazo isomer generation when irradiated, which can vary between 30 and 70%.[54, 55] Lastly, Brunner *et al.*[42] introduced the trifluoromethyl aryldiazirines family which properties come close to satisfying the criteria required for photoprobes while rearrangement to the linear diazo form is less significant.

Photolysis of trifluoromethyl aryldiazirines can be conducted at wavelengths that biomaterials are inert to, thus preventing any unwanted photochemical or structural changes in the target receptor.[54] They are readily photolysed to produce highly reactive carbenes, in high quantum yield, whose life-time is on the nanosecond time-scale, so that no reactive species are left after photolysis. Although a certain proportion of trifluoromethyl aryldiazirines undergo isomerisation to its linear diazo isomer upon photolysis (**Scheme 1.8**)[42], the resulting diazo species (**6**) are stable under the conditions used to decompose trifluoromethyl diazirines and the biological environments, therefore not giving undesired intermediates.[42] This stability is enhanced by the introduction of the trifluoromethyl group which decreases the ability to undergo rearrangement and increase the stability of the corresponding diazo derivative **6**, which becomes a precursor of carbene **5** with the use of a shorter wavelength (302 nm) or with longer irradiation times at 365 nm.[42, 56] An additional advantage of the trifluoromethyl group next to the diazirine ring is that all compounds generated from the photolysis are suitable for ^{19}F NMR analysis.

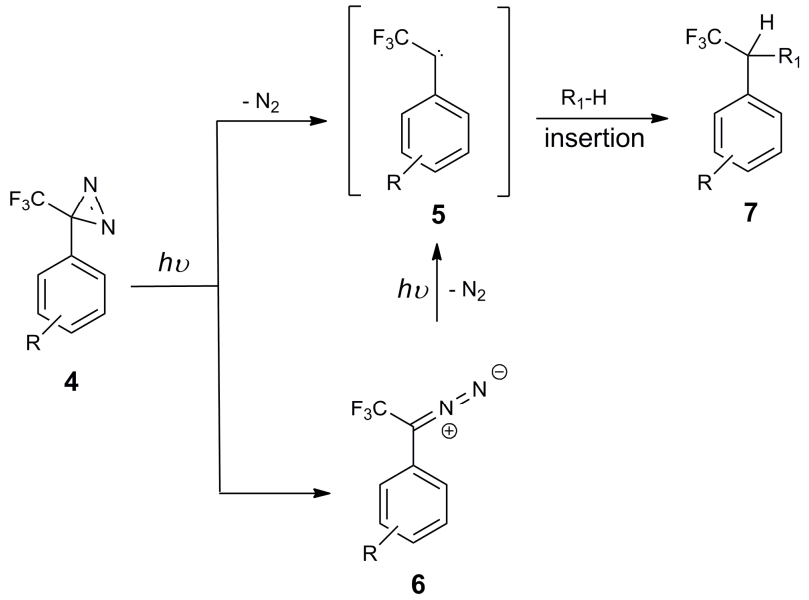

Scheme 1.8: Photolysis of aryl(trifluoromethyl)diazirines generates a carbene which react non-specifically with surrounding molecules. Simultaneously, the diazo isomer form is also generated and with further irradiation also becomes a precursor of carbenes.

Despite the strained ring structure of diazirines, these systems possess excellent chemical and thermal stability, being far more stable than their linear diazo isomers. Aryldiazirines have been shown to be stable towards a wide range of reagents; they are resistant to dilute acids and strong bases, oxidising agents and mild reducing agents such as sodium borohydride.[10, 44, 57, 58] Such information is of great importance in designing synthetic strategies. Diazirines are also stable under physiological conditions including the presence of thiols, which attack azides and diazo compounds,[42] and can be stored for long periods of time.[31, 59] The reason why these systems have not been employed as widely as other photophores (such as azides) is the lack of commercial availability of a wide range of trifluoromethyl ketones used as starting materials in addition to the often complex synthesis required.[60]

1.1.3. Diazirine Reactivity

Carbenes are neutral molecules that have divalent carbons and react in various ways to complete their valence shells. The typical reactions of carbenes are shown in **Scheme 1.9**. Besides reacting with nucleophilic groups, carbenes are capable of reacting by insertion with saturated hydrocarbons and by addition to unsaturated hydrocarbons including aromatic molecules.[26]

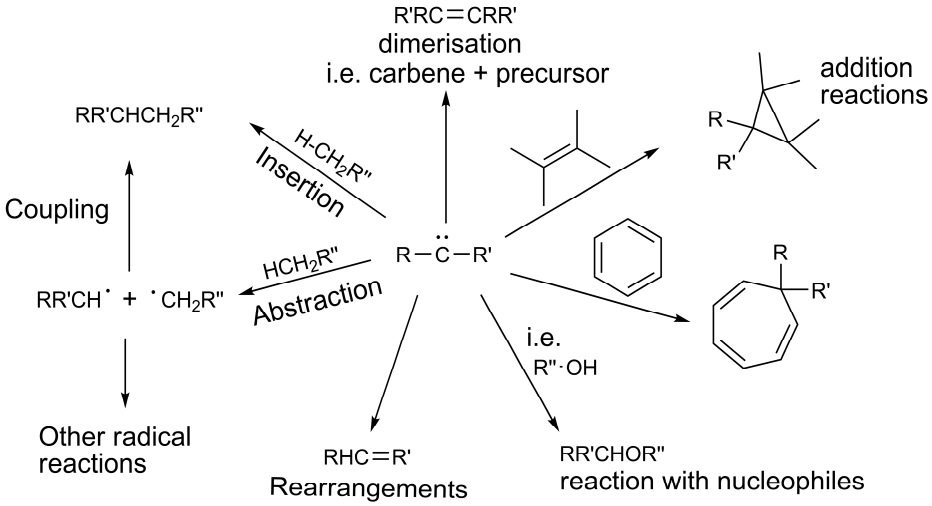

Scheme 1.9: Typical reactions of carbenes.

Carbenes can be classified as either being in a triplet or a singlet state, depending on whether the nonbonding electrons are of the same or opposite spin (**Figure 1.4**). The bonds in triplet carbenes are formed from *sp* orbitals, with unpaired electrons being in two equivalent *p* orbitals and possessing a linear structure (H-C-H angle of 125-140º). The singlet carbene assumes sp^2 hybridisation, with the two unshared electrons in an sp^2 orbital. The *p* orbital is unoccupied. The R-C-R angle is contracted slightly from the normal 120º because of the electronic repulsions between the unshared electron pair and the electrons in the two bonding orbitals (H-C-H angle of 102º).

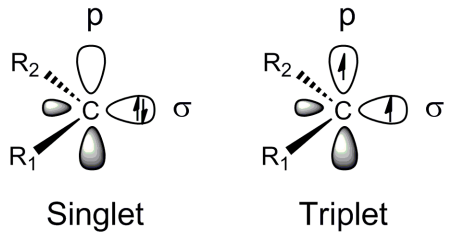

Figure 1.4: Two varieties of carbenes: singlet carbenes have no unpaired electrons, spin multiplicity zero and they are diamagnetic, whereas triplet carbenes have two unpaired electrons, a total spin of one and they are paramagnetic.

The spin states of carbenes are important since singlet and triplet carbenes not just have different geometries but also different chemical reactivities. Singlet carbenes are believed to be involved in rearrangements to fully bonded species, stereospecific reactions with σ and p bonds and the addition of nucleophiles. In contrast, triplet carbenes take part in abstractions, non-stereospecific additions to double bonds and radical-like reactions.[26]

Although carbenes are extraordinarily reactive, they exhibit an appreciable degree of selectivity in reactions with various functional groups. This selectivity depends upon the molecular structure of the carbene. For example, a photogenerated singlet methylene reacts with nucleophiles more readily than with C-H bonds, even when the number of C-H bonds is much higher than for example O-H bonds.[28, 61, 62] On the other hand, carbenes such as $:CF_2$ react with alkenes substituted with groups with a variety of electronic properties, and do not insert at all into C-H bond.[49]

The selective reactivity of trifluoromethyl aryldiazirines used in this thesis have been explored in just one detailed study in the literature.[63] The study showed that trifluoromethyl aryl carbenes generated in alcoholic solutions, preferably inserted into O-H groups, accounting for around 70% of insertion products. This behaviour could be explained by singlet methylene formation. On the other side, the insertion degree of C-H bonds gradually decreases as methylene and methyl groups move away from the hydroxyl group. Different preferable selectivity towards methylene or methyl groups was not seen in this study, but when methine groups were present, insertion was preferred over methylene or methyl groups wherever its position was. This tendency can be explained *via* application of triplet carbene as an intermediate: the carbene's rate-limiting abstraction of a hydrogen atom produces a radical pair which give the formal insertion product.[64] Thus, it is clear that the trifluoromethyl aryldiazirine group generates both singlet and triplet carbenes.

Selectivity of carbenes also varies between thermal and photolysis generation and also between photogenerated carbenes in solution or in solid phase.[64] Kanoh *et al.*[63] studied the reactivity of trifluoromethyl arylcarbenes in a semi-solid state (photolysis in solution at -196 ºC) demonstrating that the insertion reactions in the solid state is less selective since C-H and O-H insertion products were formed in close to equivalent amounts.

1.1.4. Applications

The majority of applications for photophores have been directed to photoaffinity labelling techniques to investigate structural and functional properties of biological systems.[3, 5, 32, 65-67] These labelling reagents can be divided into three main classes: firstly, probes designed to report on general properties of a system, for example, small apolar molecules or lipids which partition into membranes and label selectively integral proteins upon

activation;[40, 68-71] secondly, affinity labelling reagents intended to interact with label components (receptors) in a specific, functionally relevant manner; and thirdly, heterobifunctional photocross-linkers, containing a photoactivatable and a thermal reactive function, preferentially connected *via* a cleavable linker to study the spatial relationship between components in complex systems, or to make macromolecular affinity probes.

Photoreactive groups have also been used for producing reactive (bio)polymers. Polymers of biological or synthetic origin have been modified to feature photolabile groups along the polymer chain which have been used to covalently immobilise bioactive ligands onto it and simultaneously covalently bind it to the substrate surface.[48] Photoreactive amino acid analogues have been synthesised[72, 73] to allow reactive peptides to be made by standard solid-phase techniques as well as photoreactive proteins. This allows the study of structural properties from the interaction of peptides with proteins[74] and protein-protein interactions within cells.[75] Similarly, photoreactive DNA have also been prepared, which retain the ability to form double strand.[76, 77] The photoreactive DNAs are useful tools for analysing the interactions between nucleotides and proteins, such as transcriptional complexes and regulators,[78-82] chromatin structure,[83] and chromatin-remodeling complexes.[84]

Finally, photoreactive groups have been used for modification of inert surfaces. One method is the pretreatment of the surface to achieve a reactive-functionalised surface capable of attaching different biomolecules. Another method is the preparation of biomolecules containing a photoreactive group at a specific position. By positioning the photoreactive group on specific positions, the molecule can be bound onto the surface with the desirable orientation. These two methods have been used to modify different surfaces or particles, including polymer-base microplates,[85] slides[29, 86-90] and beads.[91, 92]

1.2. TFMAD Synthesis

For all the advantages previously mentioned, the photoactivatable trifluoromethyl aryldiazirine reagent was selected for this thesis. Trifluoromethyl aryldiazirines (TFMAD) are generally prepared from the corresponding trifluoromethyl acetophenone in a four step sequence: oximation, tosylation, diazirinylation and oxidation to form the diazirine ring.[41, 43, 44, 72, 93, 94] The main drawbacks of its application are the number of steps involved and the difficulty in

preparing trifluoromethyl acetophenones. In addition, a tether is usually introduced into the ring to allow further functionalisation for latter applications.

The synthetic target chosen for this thesis was {4-[3-(trifluoromethyl)-3*H*-diaziren-3-yl]phenoxy}acetic acid (**4**). This compound contains a carboxylic acid group, which would be used later on and could be safely protected with the bulky *tert*-butyl group while the diazirine ring was generated.

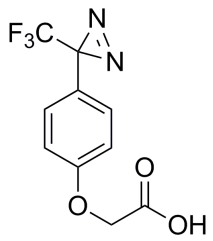

4

Figure 1.5: {4-[3-(trifluoromethyl)-3*H*-diaziren-3-yl]phenoxy}acetic acid (TFMAD).

The synthesis started with the alkylation of 4-hydroxybenzaldehyde **8** (**Scheme 1.10**) with *t*-butyl bromoacetate giving *t*-butyl(4-formyl-phenoxy)acetate **9** using microwave irradiation. Trifluromethyl acetophenone was synthetised in two steps: introduction of the trifluromethyl group by reacting the aldehyde with Ruppert's reagent[95] and oxidation of the resulting alcohol **10** with Dess-Martin periodinane to give **11**. Next, oxime **12** was prepared with hydroxylamine hydrochloride in pyridine which was subsequently tosylated with *p*-toluenesulfonyl chloride to give **13**. Both reactions were performed under microwave irradiation which shortened reaction times and improved the yields. Formation of diaziridine **14** was accomplished by treating the tosylated oxime with liquid ammonia overnight at high pressure. Iodine was used for the oxidation of **14** to give trifluromethyl aryldiazirine **15**. Finally, the *t*-butyl group was removed with 50% trifluoroacetic acid in DCM. This synthetic route allowed the synthesis of **4** with a reasonable overall yield of 21%.

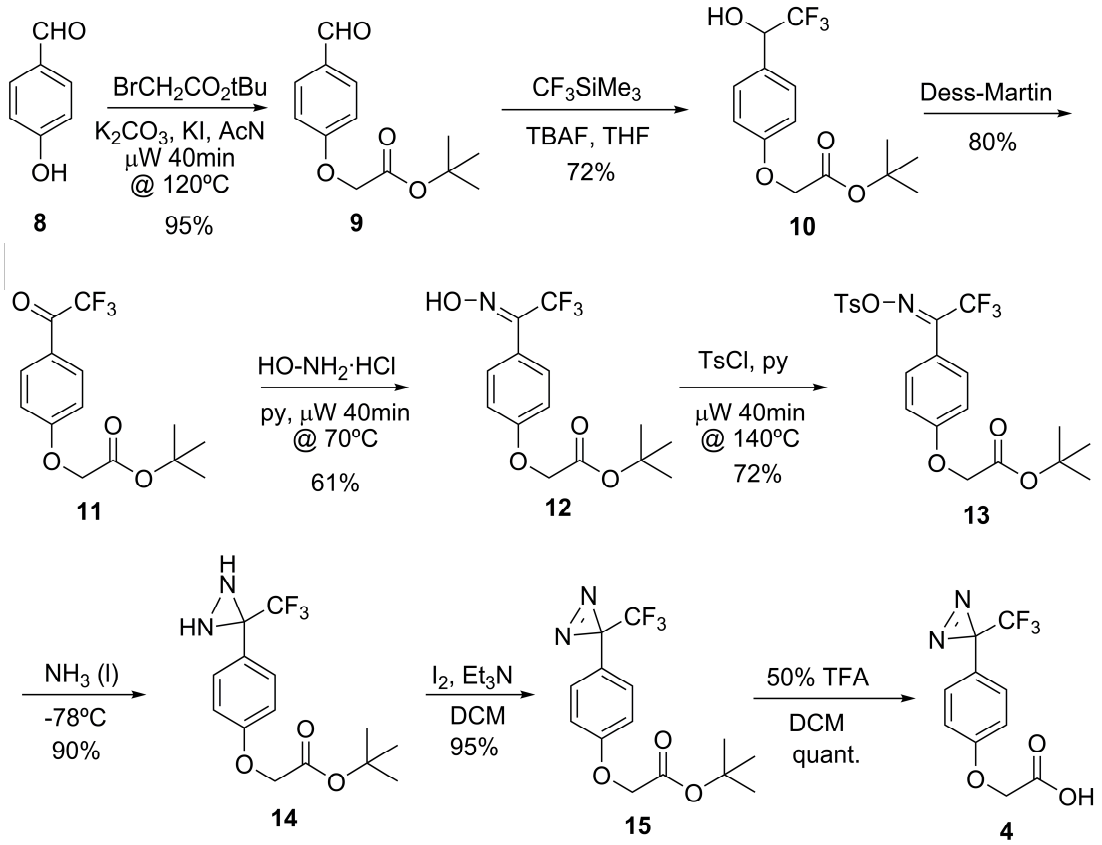

Scheme 1.10: Synthetic route for TFMAD **4** synthesis.

This synthetic route was slightly modified when it was scaled up (**Scheme 1.11**). Although Ruppert's reagent and Dess-Martin oxidation gave good yields on small scale, Dess-Martin oxidation was very temperamental and lower yields were achieved when large amounts were required.

For the large scale synthesis, 4-bromophenol was used as starting material, the bromo group allows the introduction of the trifluoromethyl acetate group by Grignard or *n*BuLi reaction. Both reactions were carried out with *N*-(trifluoromethyl)piperidine as an electrophile[56, 93, 94, 96] under different reaction conditions. Although *n*BuLi reactions worked better than Grignard reagent, the yields were very poor. One way to improve the *n*BuLi reaction yield was the protection of the phenol. Finally, different electrophiles were tested and the best yields were found when trifluoromethyl ethylacetate was used.

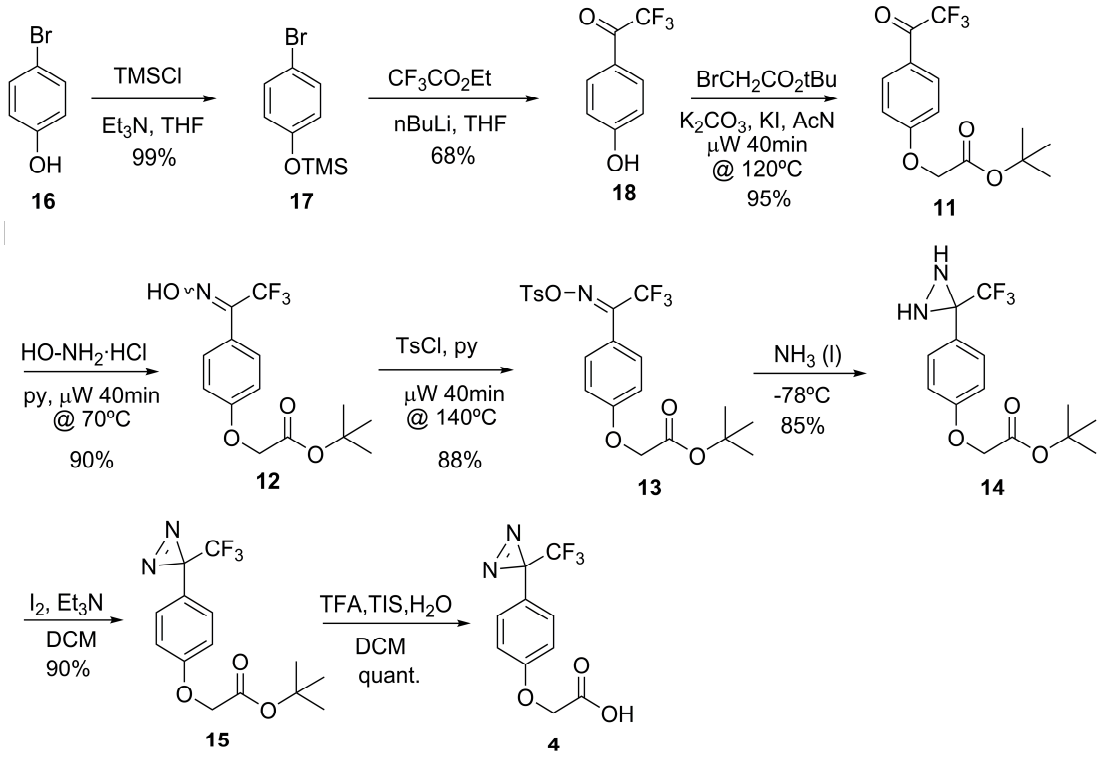

Scheme 1.11: Large amount synthesis of TFMAD **4** photophore (about 1 gram).

Thus, the synthetic route started by protecting the phenolic OH of 4-bromophenol **16** with trifluoromethylsilane group and reaction with *n*BuLi and trifluoromethyl ethylacetate to give **18** as the deprotected alcohol in 68% yield. The rest of the synthesis was carried out as previously described in scheme **1.10** giving **4** in overall 35% yield.

1.3. Photochemical Properties

As introduced in **section 1.1.2**, photolysis of diazirine ring leads to the generation of the diazo compound as well as the desired carbene. TFMAD and its diazo isomer can be differentiated from each other by their characteristic UV-Vis spectra and ^{19}F NMR.[42, 72, 97] These two techniques were used to characterise the synthesised TFMAD photophore **4**, to evaluate its reactivity and determine the optimal irradiation time for its complete photolysis in solution and in solid phase.

1.3.1. Spectrophotometric Measurements

For this study, a 3.54 mM solution of TFMAD **4** in deuterated methanol was introduced into a quartz cuvette and irradiated with a UV light lamp (UVP, B100AP, 100 W), which emits monochromatic light with a wavelength of 365 nm above 10 cm for different periods of time. The photolytic process is summarised

in **Scheme 1.12**, where diazirine **4** is photolysed, losing nitrogen to generate a carbene **5** and partially rearranging to its linear diazo isomer **6**. The carbene reacts with deuterated methanol to form presumably compound **19** while the diazo isomer generates carbene upon further irradiation.

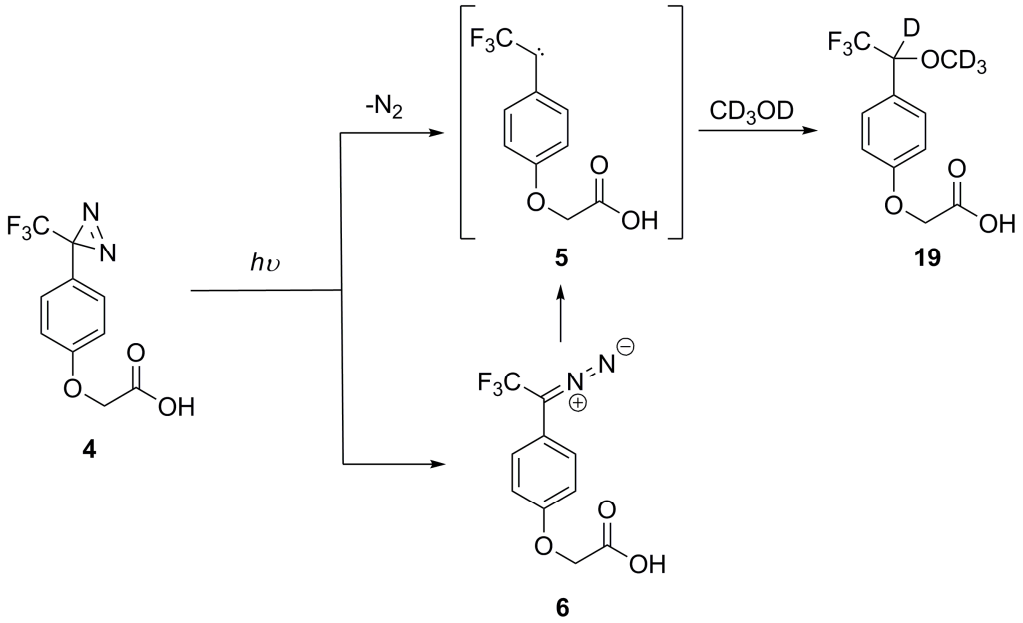

Scheme 1.12: Photolysis of TFMAD leads to the generation of carbene species, which gives product **19** after insertion into the O-D bond of d_4-methanol. Its diazo isomer is a precursor of carbene with further irradiation.

Consistent with the spectral properties of other trifluoromethyl aryldiazirienes,[40, 42, 72] the TFMAD photophore **4** showed characteristic absorption at around 360 with a maximum at 371 nm with an extinction coefficient of 291 $M^{-1}cm^{-1}$ (**Figure 1.6**).

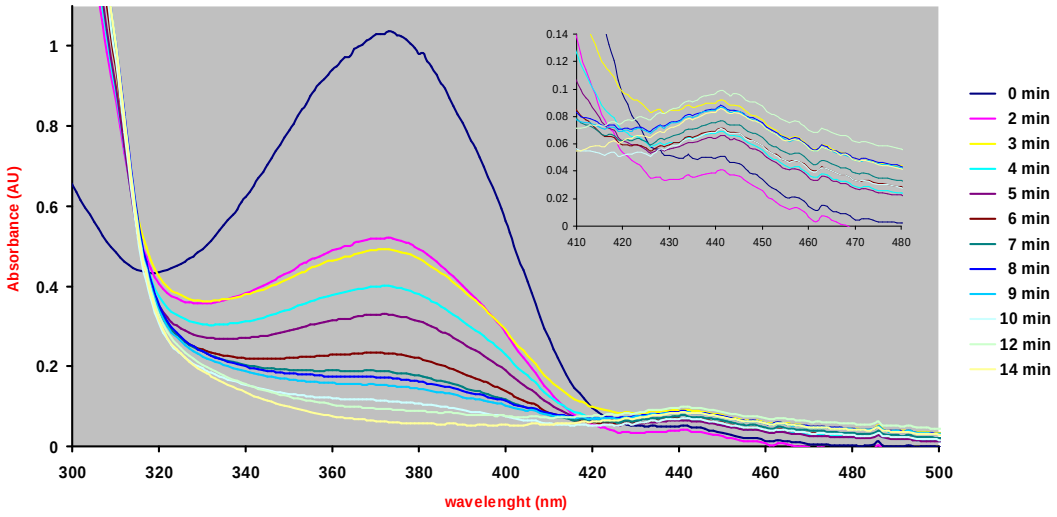

Figure 1.6: UV-Vis spectra of the reaction products from photolysis of TFMAD **4**. A solution of **4** in methanol was irradiated for increasing periods of time (in minutes) as indicated.

The wavelength region between 410 and 480 nm have been expanded as it corresponds to the characteristic diazo absorption (**Figure 1.6**).[40-42, 72] Although the diazo characteristic band is 10 times lower than that of the diazirine absorption due to a low molar extinction coefficient, a band with maximum intensity at 441 nm could be observed to increase with the decrease of the diazirine band. The UV-Vis spectra also showed the decay of the diazirine characteristic band with a maximum at 371 nm within 12 min with a half-life of *ca.* 495 seconds (8.25 min) for a 3.54 mM solution following apparent first-order kinetics as has been reported in the literature (**Figure 1.7**).[56, 98]

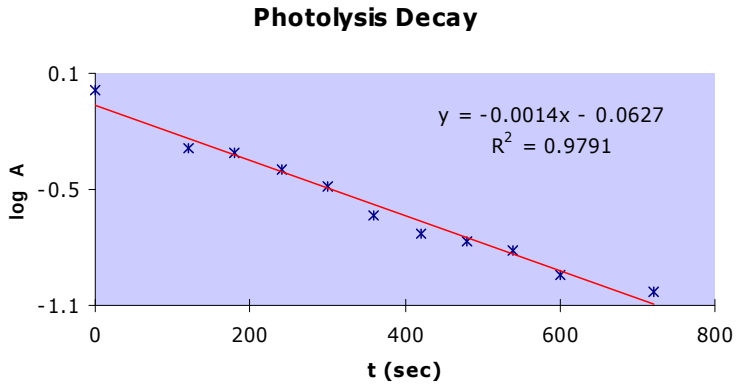

Figure 1.7: Representation of the decay of a 3.54 mM solution of **4** in methanol as a function of time of photolysis at 365 nm.

This study was useful in that it characterised the synthesised diazirine, determining its maximum absorption wavelength and extinction coefficient and confirmed its photoisomerisation to the linear diazo form.

1.3.2. NMR Studies

NMR studies are very useful to study the reactivity of diazirines. ^{1}H- and ^{19}F NMR have been used to determine the irradiation time necessary for complete photolysis of samples in solution and in solid state. Furthermore, all compounds generated from the photolysis of TFMAD bear a trifluoromethyl group that makes them suitable for the estimation of the formation of different species by ^{19}F NMR.

1.3.2.1. ***Photolysis in Deuterated methanol***

A solution of compound **4** in deuterated methanol (1.5 mL, 3.5 mM) containing trifluoroacetic acid as a reference standard was introduced into a glass vial and exposed to a 365 nm UV irradiation at room temperature. At

different times, aliquots of the solution were taken for ^{1}H and ^{19}F NMR analysis. After 40 minute exposure, complete consumption of the starting material was observed. This could be seen by both, ^{1}H and ^{19}F NMR, although ^{19}F NMR was much clearer.

In the ^{1}H NMR, the two aromatic signals of the starting material were indicative of the reaction progress as seen in **Figure 1.8** (For the complete NMR spectra, see **Appendix I**). The most deshielded signal disappears with an increase in the irradiation time to form a new signal at a lower field. The other aromatic signal experienced a reverse effect, not as drastic as the former, becoming a more shielded signal. After 40 minutes irradiation, there was no existence of the two initial signals and two new peaks were observed.

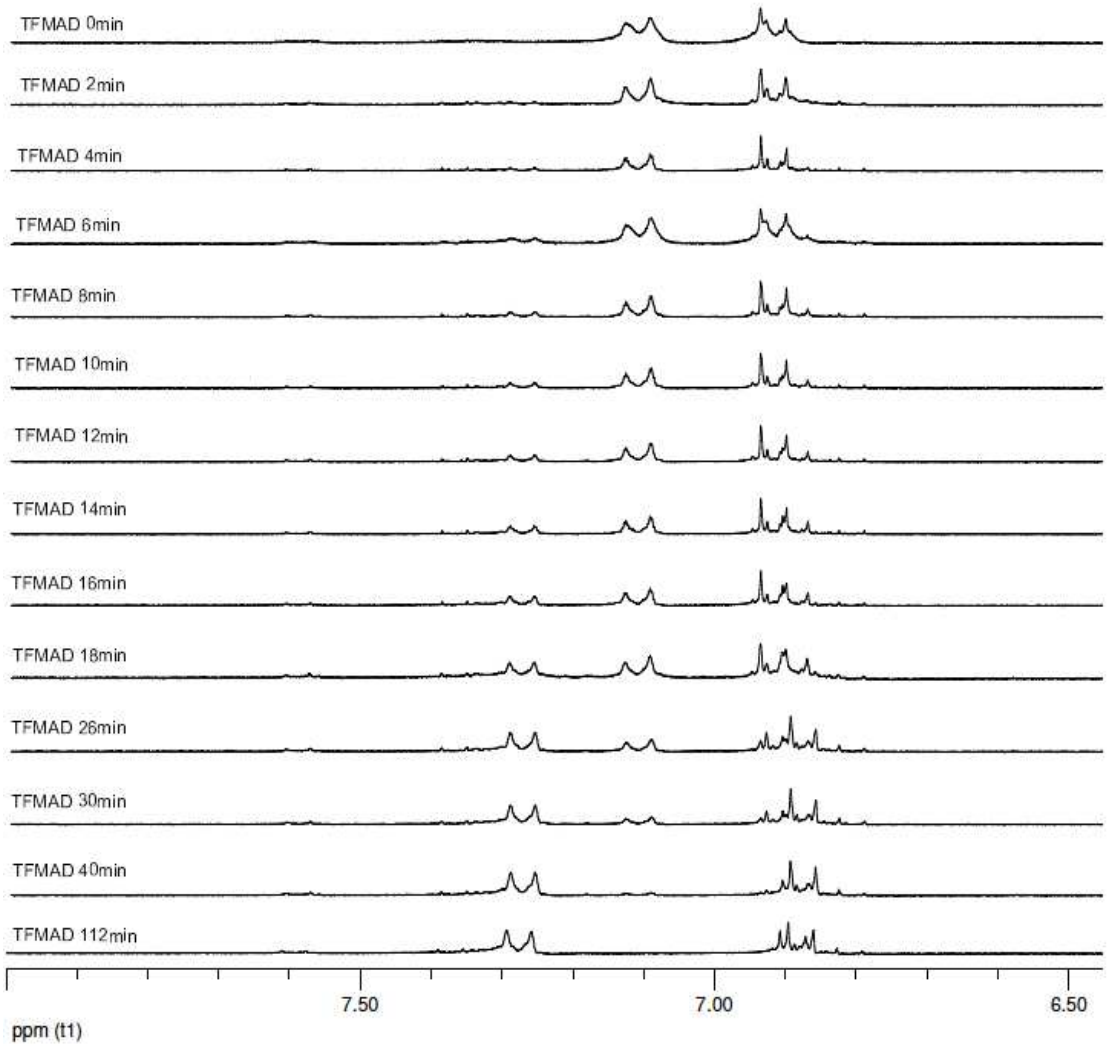

Figure 1.8: Expanded view of the aromatic region from the monitored photoreaction of TFMAD **4** in CD_3OD as determined by ^{1}H NMR.

^{19}F NMR showed the complete disappearance of the TFMAD **4** resonances at -66.7 ppm in 40 min (**Figure 1.9**). The resonance peak for the diazo form **5** was expected at -58 ppm,[45, 99, 100] however, there was no trace of it. The reason for that was the use of trifluoroacetic acid as a reference standard (resonance peak at -78 ppm). Although it is well established that diazirine decomposition is unaffected by acid,[31] the decomposition of the diazo compounds is acid catalysed.[101] For example, one way for the diazo and the diazirine absorption bands identification in the UV spectra was the use of acid. A solution of diazirine that had been irradiated for 2 min was treated with acetic acid, the diazo compound band was eliminated, but the diazirine absorbance band was maintained, and a new product was identified by NMR examination corresponding to trifluorobenzyl acetate derivative **20** (**Scheme 1.13**).[54]

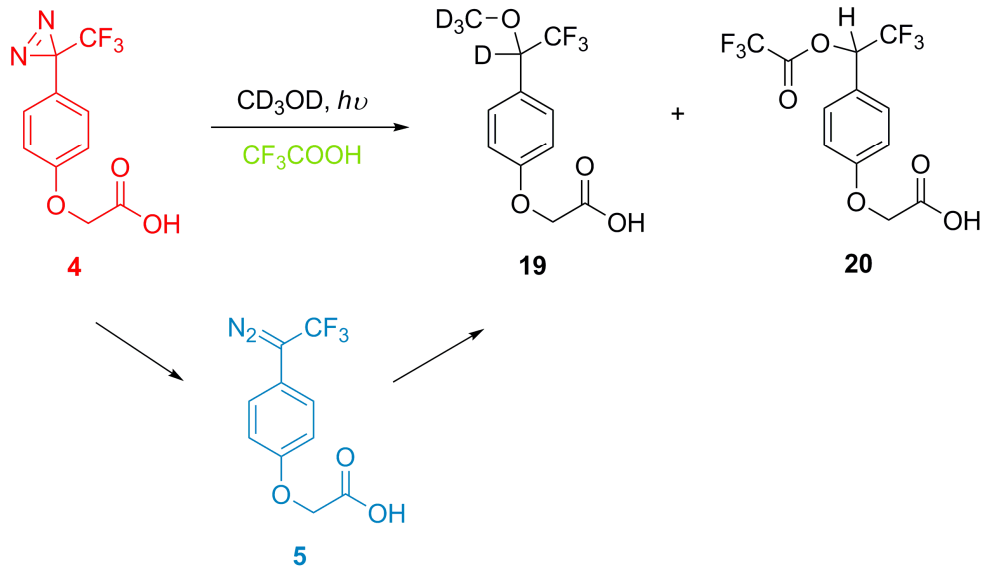

Scheme 1.13: Suggested products of the photolysis of TFMAD **4** in presence of TFA.

In other words, by using trifluoroacetic acid as a reference standard during photolysis, the formed diazo isomer **5** was rapidly reacted with TFA to form **20** (**Scheme 1.13**). As a result, resonance of diazo compound was not detectable and two new signals corresponding to the formed adducts were observed in this study. This was supported by the decrease in intensity of trifluoroacetic acid resonance peak (**Figure 1.9**). The product peaks have not been identified but it is reasonable to think that peak at -79 ppm could correspond to the product formed when the diazo compound reacts with trifluoroacetic acid as here a trifluoromethyl group would be next to an ester (trifluorobenzyl trifluoroacetate, **20**) and the peak at -77 ppm would correspond

to the adduct formed from the carbene with methanol **19**, which have been reported in the literature for other TFMAD derivatives.[100, 102]

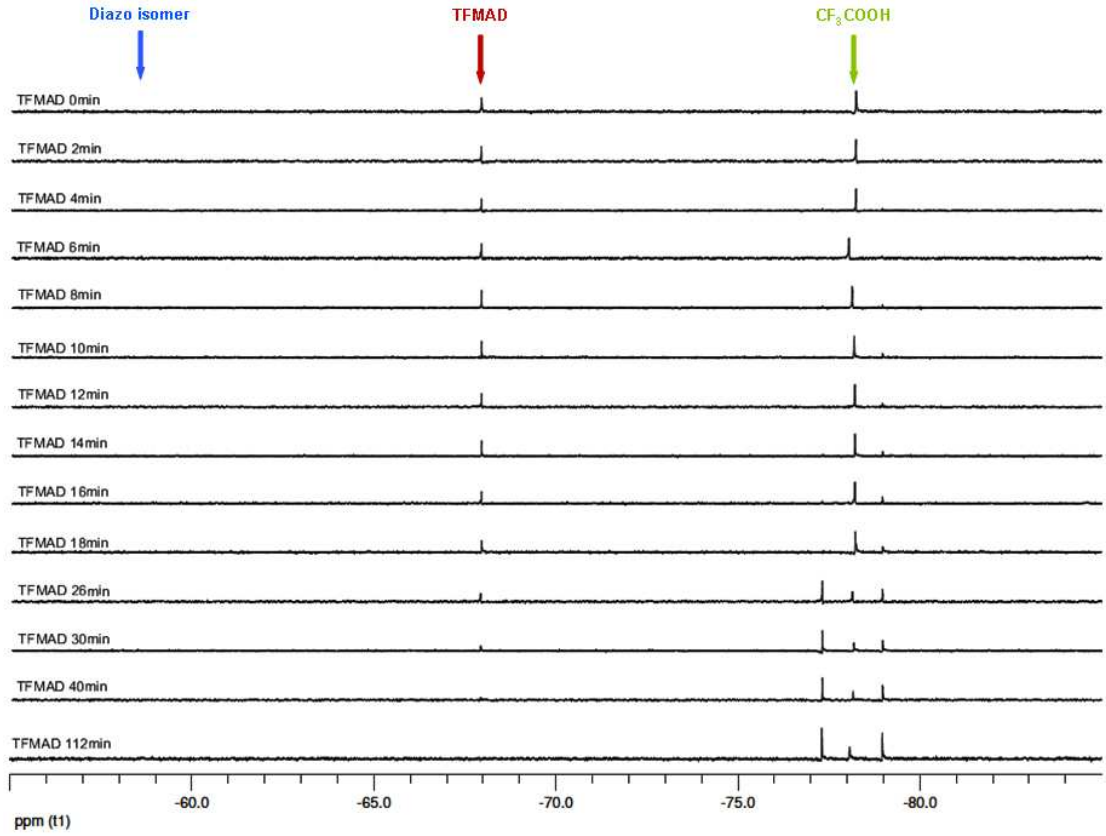

Figure 1.9: Expanded view from the monitored photoreaction of TFMAD 4 in CD_3OD as determined by ^{19}F NMR. The blue arrow points the diazo isomer 5 resonance; the red, TFMAD 4 compound resonance and the green, TFA external standard resonance as shown in **Scheme 1.13**.

1.3.2.2. ***Photolysis in Solid State***

The reactivity of carbenes in solution or solid phase differs highly. This fact has already been seen by carbenes derived from parent diazo compounds in solidified organic molecules.[64] Recently, another group has studied the reactivity of trifluoromethyl aryldiazirines in a semi-solid state and highly concentrated states with 7 different alcohols.[63] They demonstrated that photolysis of diazirine in solution gave O-H insertion products in more than 70%, whereas solid phase reactions gave C-H and O-H insertion products in equivalent amounts.

Another advantage of carbenes generated from photolysis in the solid state is that they are not quenched by reacting with water or buffer components coexisting in the media, making the yields of cross-linking more efficient and random toward functional groups due to the low mobility of molecules.

To find out the conditions and the time necessary for irradiating samples in the solid state, the same studies performed before in methanol were carried out with a dry sample consisting of biotin and TFMAD **4** in a mole ratio of 10:1 (**Scheme 1.14**), but this time without TFA as an external standard. Six identical solutions of TFMAD **4** and biotin in methanol were prepared in 1 mL glass vials and solvent was evaporated until complete dryness. The vials were irradiated above 10 cm and every 10 minutes one of them was removed from the light, dissolved in deuterated methanol and analysed by ^{1}H and ^{19}F NMR.

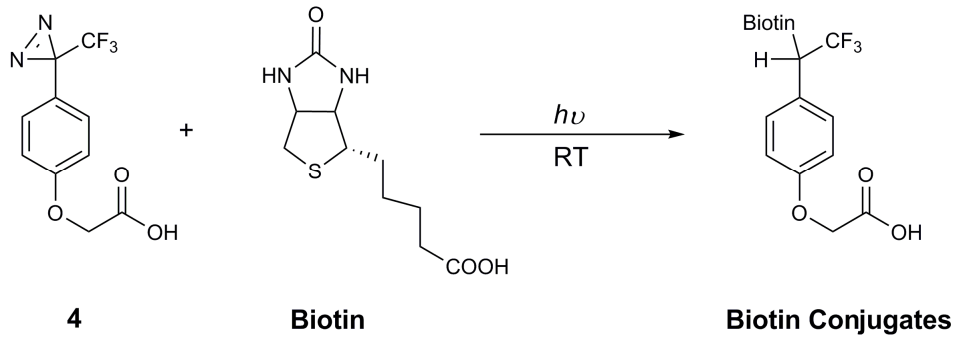

Scheme 1.14: A sample of biotin:TFMAD (10:1) was irradiated at 365 nm in a solid state for different periods of time to give several conjugated products.

The changes in ^{1}H NMR were quite similar to those achieved previously. The same effect on the two aromatic doublets was seen as shown in **Figure 1.10**, which was the clearest change for determining the irradiation time for complete photolysis. As before, photolysis was almost completed at 30 min and finished at 40 min.

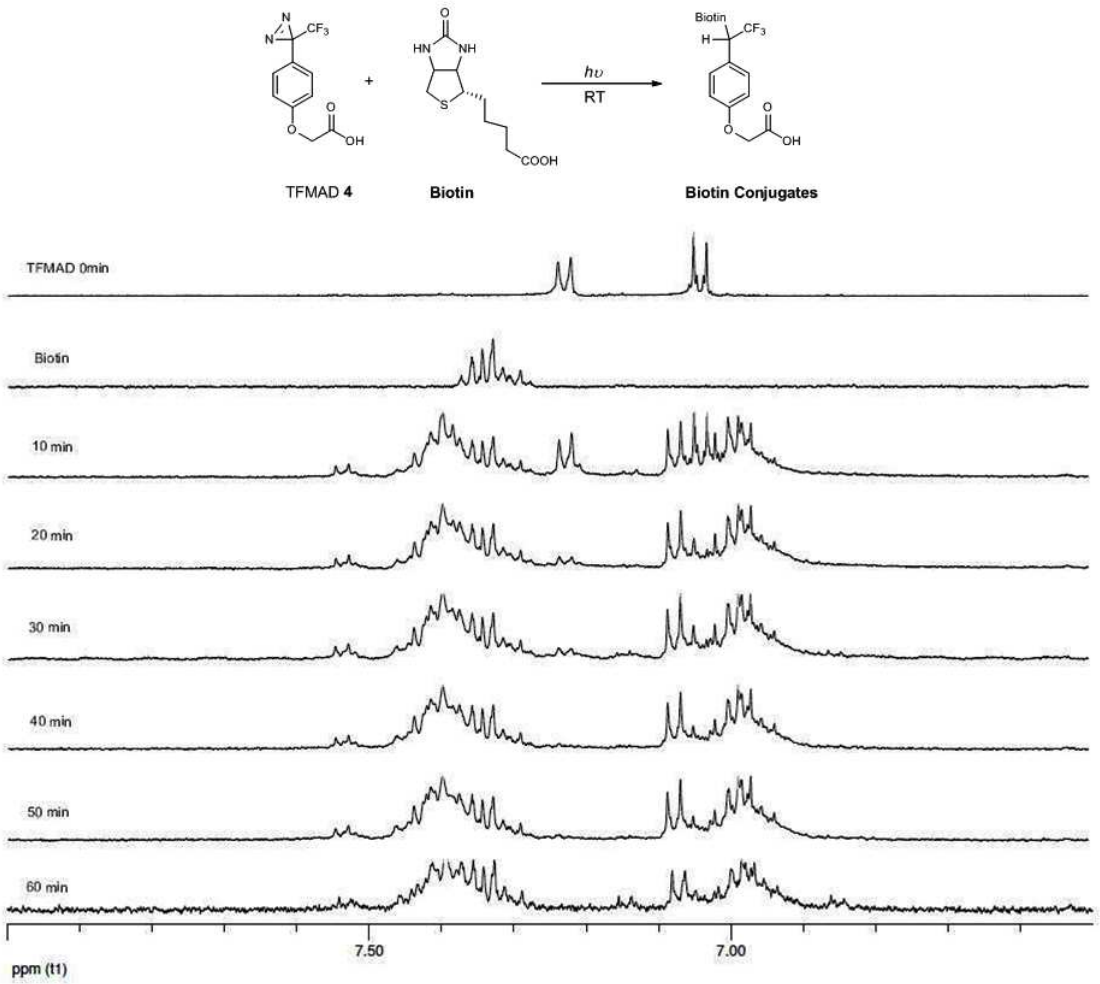

Figure 1.10: Expanded view of the aromatic region of ^{1}H NMR at different irradiation times.

^{19}F NMR also showed that photolysis of the diazirine derivative in solid phase was complete within 40 minutes as in solution phase. Unlike in solution phase, the diazo isomer resonance appeared with short irradiation times and disappeared with further irradiation periods (**Figure 1.11**). From this, two conclusions could be extracted. Firstly, the use of trifluoroacetic acid was the responsible for the absence of the diazo isomer form in solution studies as hypothesised. And secondly and more importantly is the fact that the diazo isomer decreases after longer irradiation times with only tiny traces observed after 40 min irradiation. Thus, no short UV wavelength lamp (302 nm) needs to be used to rapidly decompose the diazo form (as has been recommended for samples with high percentage of diazo isomer form).[99]

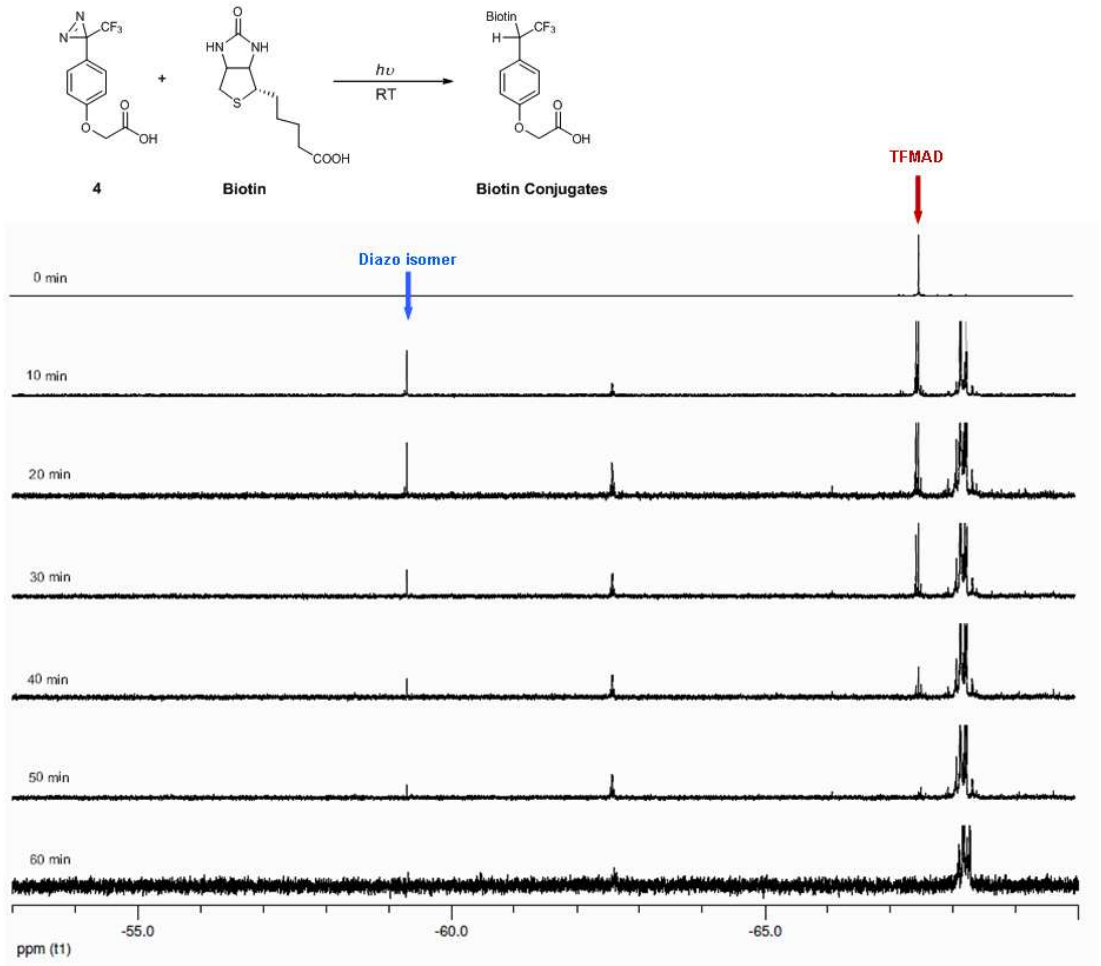

Figure 1.11: Expanded view of the full ^{19}F NMR spectra (**Figure 1.13**). The blue arrow points to the signal corresponding to the diazo isomer byproduct from photolysis of TFMAD **4** and the red one shows the signal corresponding to TFMAD **4**. The rest of signals are biotin-TFMAD conjugated products as shown in the sturcture.

^{19}F NMR also showed that large amounts of conjugate product were formed, all corresponding to the chemical shift region of the trifluoromethyl group (**Figure 1.12**) and no other signals outside this region were observed (**Figure 1.13**). Some of the peaks, for example peak -77 ppm, are multiplets instead of singlets, suggesting the formation of different products without inducing large changes to the electronic environment of the trifluoromethyl group. This fact is in agreement with the non-specificity of the reaction.

a)

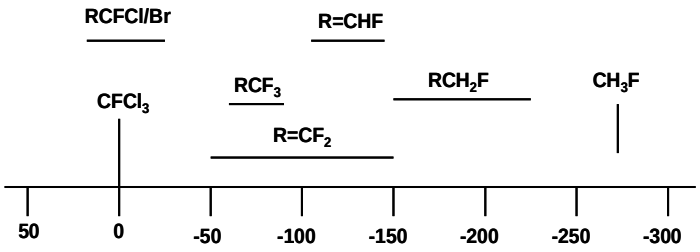

b)

Type	shift ranges (ppm)
CF_3CR_3	-70 to -55
CF_3-O-	-70 to -55
CF_3-CO-	-90 to -70
CF_3-CF_2-	-95 to -80

Figure 1.12: a) ^{19}F spectrum showing the typical chemical shift ranges for each type of signal; b) Table specifying the values of CF_3- shift ranges.

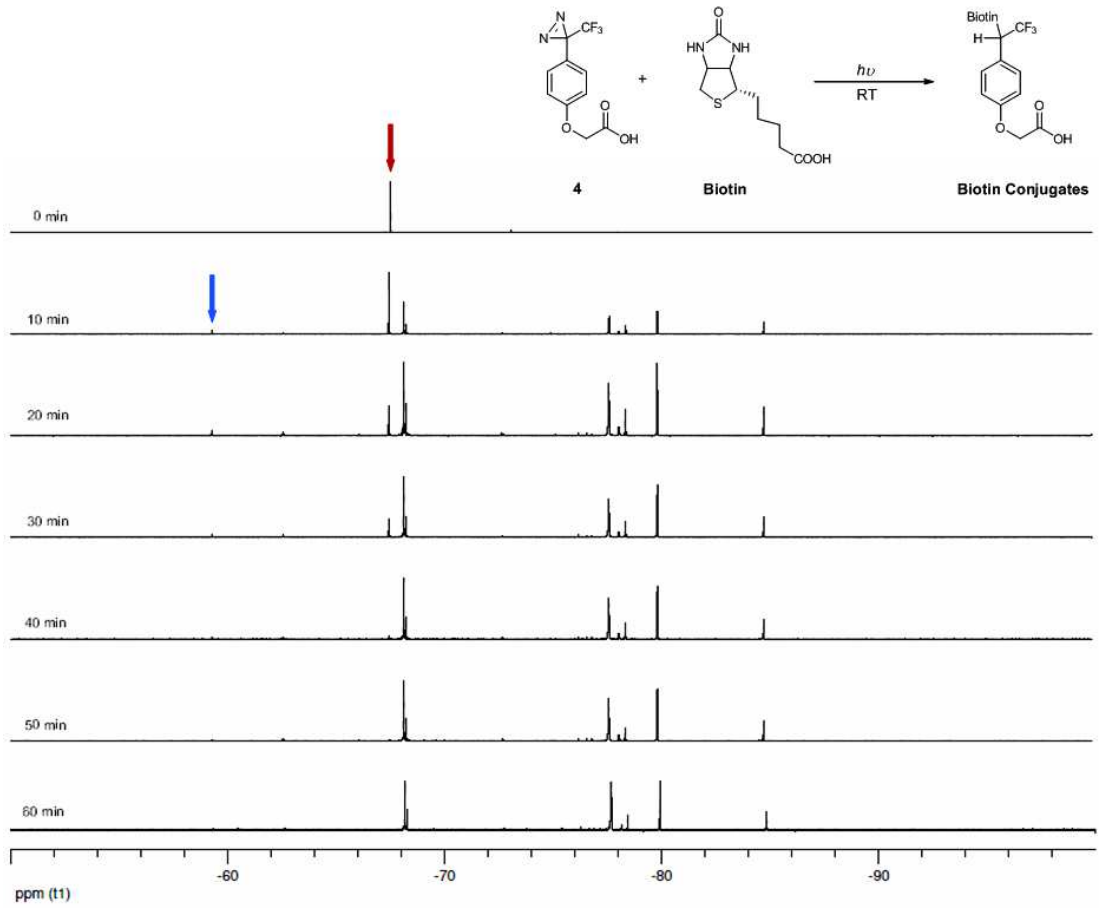

Figure 1.13: ^{19}F NMR of TFMAD **4** before and after irradiation in dry conditions in the presence of biotin for different periods of time. The blue arrow points to the signal corresponding to the diazo isomer by-product **6** from photolysis of TFMAD. The red arrow shows the signal corresponding to TFMAD **4**. The other signals are biotin-TFMAD conjugated products.

If ^{19}F NMR signals are integrated, the relative integration ratios can be used to represent the percentage of each product formed. Thus, taking the multiplet at -77 ppm as one signal, **Figure 1.14** was obtained. The peak with the highest percentage was at -77.6 ppm which accounts for 72% of the total adducts formed. The next two highest percentages corresponded to peaks -68.2

and -79.9 ppm with 9 and 7.5%, respectively. Peak -84.8 ppm, which contributed in 4%, could correspond to the adduct **21** as its chemical shift was in the range of CF_3- next to an ester (**Figures 1.14 & 1.15**). Finally, the rest of contribution on the adduct percentage is shared equally between two signals at -84.8 and -68.3 ppm.

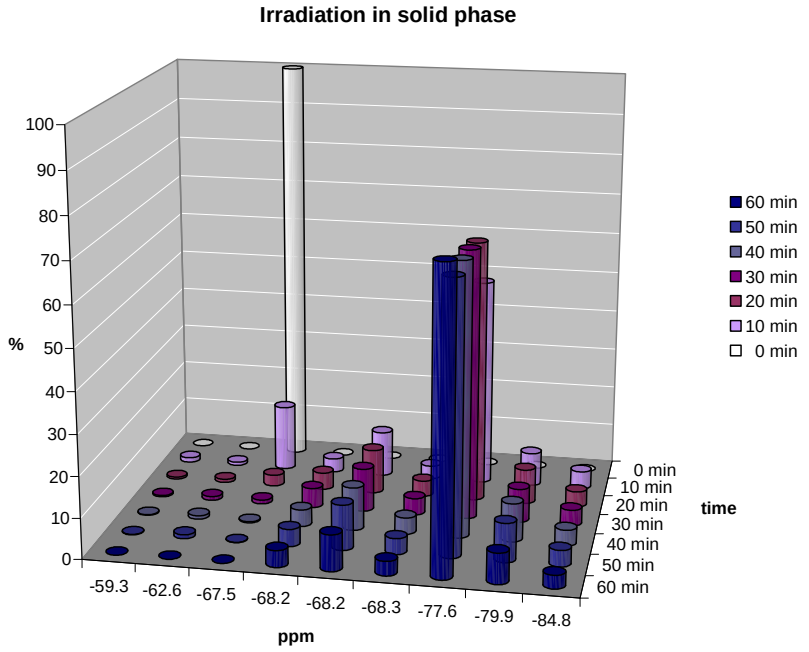

Figure 1.14: Representation of the percentage of each adduct formed in **Scheme 1.14** at different irradiation times.

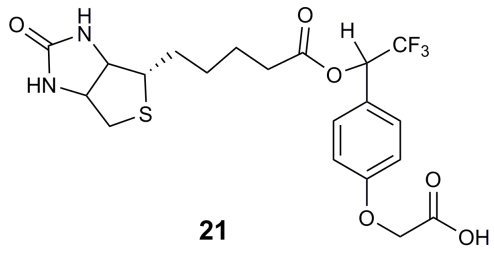

21

Figure 1.15: Probable conjugated structure for the resonance at -84.8 ppm.

In conclusion, this study showed that within 40 minutes the photolysis of diazirine in solid state was completed with the formation of a large quantity of different products as a result of the non-specificity of the reaction. Moreover, it was also clear that despite the formation of the diazo form, it disappeared within the irradiation time determined for the complete photolysis of TFMAD **4**.

1.4. Conclusions

Trifluoromethyl diazirine photophore **4** was synthesised in good overall yield of 35%, from a synthetic route consisting of nine steps where reaction time were shortened by using microwave-assisted reactions. The characterisation and the study of the photo-reactive properties of photophore **4** allowed the determination of the irradiation time necessary for complete photolysis under different conditions, such as in solution or solid phase. The non-selective reactivity of the carbene generated was also observed. Moreover, the introduction of a carboxylic group would allow the presence of this moiety to other structures or surfaces, where photo-crosslinking strategy is needed for the application development.

***Chapter II*:**

SMALL-MOLECULE MICROARRAYS

2.1. Introduction

A recent development in the area of high-throughput screening is the use of microarrays; a flexible and versatile platform that has been applied to the analysis of DNA, RNA, proteins, cells and tissues.[103] Microarrays represent a powerful and advantageous alternative to existing high-throughput techniques, and DNA microarrays have become an essential tool in many areas.[103-106] Although small-molecule microarrays have recently been receiving growing recognition for the identification of molecules capable of binding to biologically relevant targets;[107] there still remains a need to find new approaches to convert this techniques into a routine and essential tool such as DNA microarrays.

2.2. Small-Molecule Microarrays

A small-molecule microarray consist of a microscope slide on which very small amounts of different molecules, such as peptides, drug-like molecules, natural products or sugars, have been captured in an ordered manner through a variety of immobilisation reactions. In this way several thousands or even tens of thousands of molecules can be addressed in parallel for interactions with a biological target of interest, which for example have been fluorescently labelled (**Figure 2.1**). Protein-compound interactions are then monitored by a microarray scanner with high sensitivity that rapidly quantitates the fluorescence of each microspot. Since arrays are addressable, the identity of small molecules interacting with the protein is revealed by their location without further analysis.

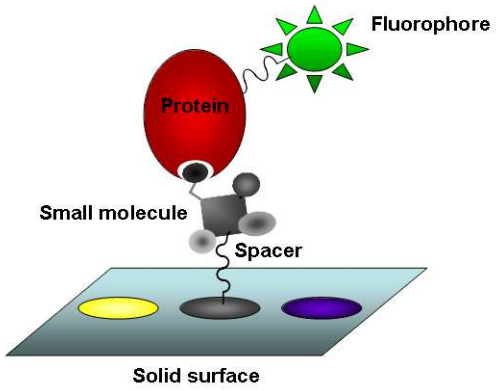

Figure 2.1: Small molecule-protein interactions on a microarray surface. Each spot contains one compound type and just those spots where there is small molecule-protein interaction will be visible.

The advantages of microarrays as a screening tool are the ability to mass-produce large numbers of arrays, the ability to perform massively parallel binding assays, and the high sensitivity of detection that result from concentrating molecules to a microspot while using only tiny amounts of compound. Despite all these advantages, several factors may affect the success of the small-molecule microarray screen, such as the quality of the compound library, the choice of target, and the sensitivity and specificity of the signal.

2.3. Microarray Surfaces

Regarding the chemical nature of the surfaces, there is a huge range on offer depending on the desired application and the compounds to be immobilised. Both the molecular structure of the spacer and the nature of the reactive group on a given surface determines the properties towards probe immobilisation, such as the density of immobilised probes, their molecular arrangement, the accessibility by the target, and the prevention of non-specific binding of the target. The surface chemistry also determines the spot morphology and the distribution of spotted probe on the surface which depends on the wettability and the surface tension.

The most widely used substrates for microarray manufacturing are based on microscope glass slides with standard dimensions, typically 25 by 75 mm and about 1 mm thick. Glass surfaces are reasonably flat, transparent, resistant to high temperatures and easy to handle, but more importantly, there is a wide range of well established protocols for the modification of their surface properties to allow immobilisation of the desired compound or to prevent/reduce non-specific binding of proteins, cells or DNA.

2.3.1. Surface Activation

Organosilanes are a versatile class of reagents widely used to attach different functionalities onto the glass slide.[108-112] They consist of an organic arm which contains the functional or reactive group that is wanted on the surface. This alkyl chain is attached to the central silicon atom, which also can have up to three hydrolysable groups attached to it. They have been shown to efficiently react with available surface silanols of inorganic substrates and pack to densities that render any remaining surface silanols essentially nonreactive (**Scheme 2.1**).[113]

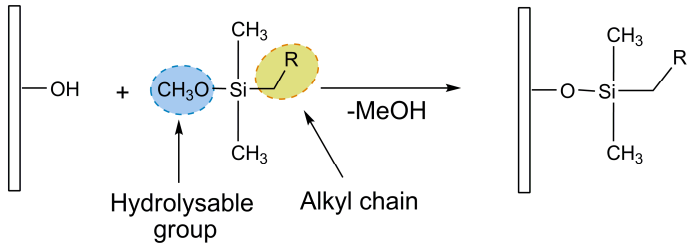

Scheme 2.1: Reaction of monofunctionalised organosilane with a glass surface in order to modify the surface with the desired functional group R.

Assemblies of monoalkoxy (or chloro) silanes ($R(CH_3)_2Si\text{-}X$) attach covalently to the surface through one bond per molecule due to its single hydrolysable group (**Scheme 2.1**). However, microarray technology tends to use di- and trialkoxy silanes ($RCH_2\text{-}Si(OEt)_3$) to form close-packed monolayers which attach covalently to the substrate with higher density of reactive groups on the surface (**Scheme 2.2**).[114-116]

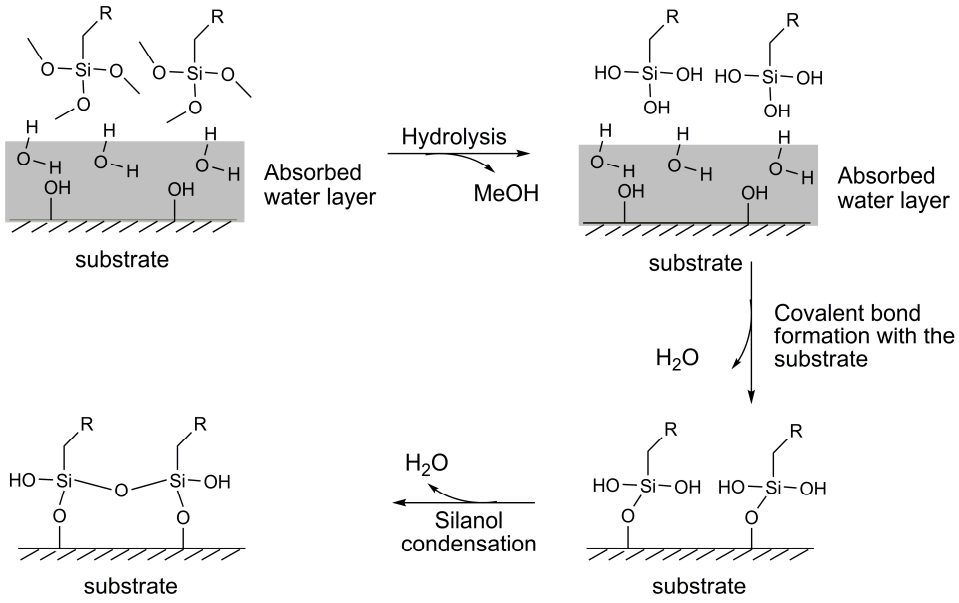

Scheme 2.2: Monolayer formation with trimethoxysilanes bearing a desired functional group (R) for surface functionalisation.

As the success of the microarray experiment depends on the uniformity across the entire substrate by ensuring identical coupling of compounds at each microarray location,[117] steric control of the reaction conditions is essential for the formation of a single monolayer.[118] Reactions can be carried out in aqueous solution, entirely in organic solvents, organic solutions containing a small amount of water, and even in the vapor phase. The choice of reaction strategy often is governed by the inorganic reactive groups on the silane.

Glass slides have also been coated with polymers (e.g. agarose or polyacrylamide or PEG-based hydrogels) to provide a three dimensional architecture with greater capacities of immobilisation and thus enhanced detection sensitivities.[119] Some of these slides have been commercialised such as HydroGel™ (PerkinElmer Life Sciences) and Codelink™ (Amersham Biosciences) slides.

Alternatively, glass slides coated with gold can easily be functionalised by self-assembled monolayers (SAMs) of thiolates. These arrays are based on the ability of thiols to spontaneously organise themselves on gold surfaces. The advantages of these surfaces are the prevention of non-specific interactions between the biological target and the surface[120] and the photosensitivity of the Au-S bond, which can be cleaved by exposure to ultraviolet light, allowing molecules attached onto the gold surface to be detected by mass spectrometry.[121] In addition, surface plasmon resonance (SPR) can be used as a detection method to analyse low affinity interactions between small molecules and proteins.[87, 122]

2.3.2. Spacers

Screening microarrays can be problematic due to steric hindrance or congestion with the surface.[123, 124] While it has been demonstrated that a small molecule-protein interaction is possible with small molecules attached directly to the glass surface,[125] it has generally been noted that higher sensitivity and better signal-to-noise ratios are obtained when spacers are used.[86, 126-128] Spacers separate the glass surface from the small molecule giving flexibility and making them more accessible to the biological target. They also reduce protein adsorption and cell adhesion, reducing background noise.[129, 130] Alternatively, dendrimers have also been used to increase the separation between the small molecule and the surface while increasing the loading capacity of the surface.[126, 131, 132]

2.4. Immobilisation Strategies

One of the most critical steps in small-molecule microarray preparation is perhaps the decision over the way in which a large variety of small molecules will be efficiently immobilised at specific locations on the surface while maintaining the binding properties of the molecules. Efforts over the past decade have introduced a plethora of options for the immobilisation which they have been extensively reviewed[133-138] and they can be classified into two types: chemoselective or non-specific immobilisation strategies.

In chemoselective approaches, a small molecule library is designed in which all members contain a specific functional group which is required for the specific-coupling reaction towards a functional group displayed on the solid support. Thus, compounds with other functional groups will not be immobilised onto the surface (**Figure 2.2**). Consequently, this strategy is suitable for synthetic compounds that can be designed for the specific application, but general libraries or natural products cannot be attached unless modified.

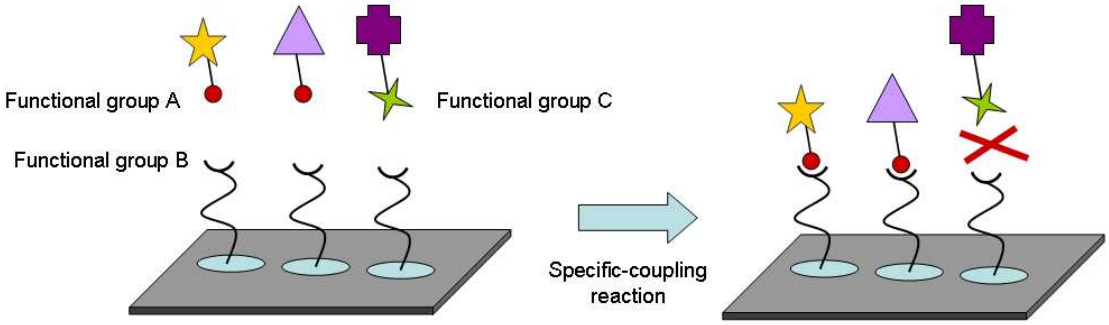

Figure 2.2: Chemoselective immobilisation of small molecules. A library of compounds is prepared with a specific functional group A that is able to selectively react with the functional group B on the surface. Compounds not containing functional group A will not be able to be immobilised onto the solid support and after washing they will be removed.

In addition, site-specific immobilisation chemistries facilitate the directed and uniform presentation of small molecules across the arrays by specific reaction between the chemical group incorporated into the library during the synthesis and a complementary group on the slide. Therefore, part of the molecule is used to link it to a spacer for the specific-coupling reaction to take place. If the binding protein recognises the portion that is used for linking, the binding protein will not bind to the small molecule on the slide and information would be lost (**Figure 2.3a** and **b**).

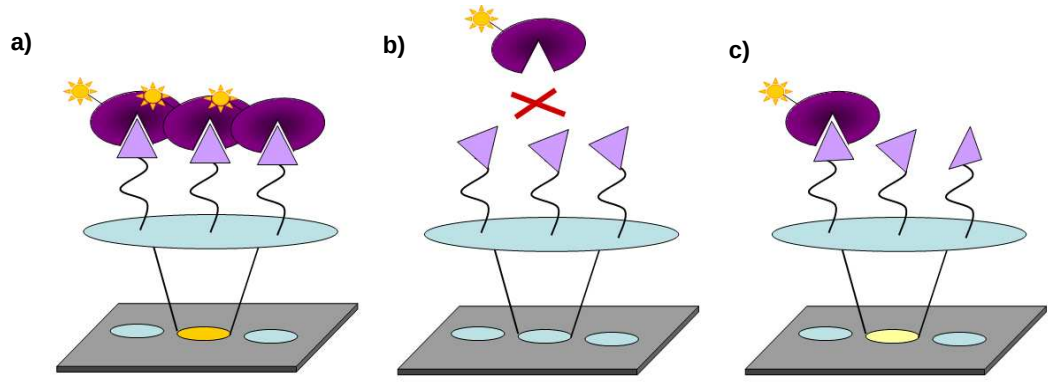

Figure 2.3: Possible situations within a microspot: a) chemoselective immobilisation where the recognised part of the small molecule by the protein is accessible; b) chemoselective immobilisation where the binding site of the compound is facing the slide surface; and c) non-specific immobilisation of small molecules provokes a heterogeneous display of orientations which decrease the fluorescence intensity as just a few molecules are recognised by the target protein.

In contrast, using a non-selective coupling reaction, small molecules are randomly attached onto the solid support exhibiting all potential interaction sites to the biological probe (**Figure 2.3c**). The advantage is that no binding interaction is lost although the sensitivity of this strategy is lower.

The different approaches for microarray preparation can also be classified into two different methods, where libraries are built *in situ* by solid phase techniques or are spotted onto the surface once they have been synthesised.

2.4.1. In situ Synthesis

This immobilisation method applies solid phase techniques for the *in situ* generation of combinatorial libraries of small molecules (mainly linear polymers) at specific positions over planar solid supports. The resulting libraries can be then screened for active compounds while still bound to the solid support used for their synthesis. Light-directed synthesis and SPOT-synthesis are the two different techniques for this method.

2.4.1.1. ***Light-Directed Synthesis:***

Light-directed *in situ* synthesis was initially developed for peptide synthesis[139] but is now widely used for the synthesis of DNA. This method enables the production of peptide libraries on microarray slides by using amino acids with photolabile protecting groups (e.g. nitroveratryloxycarbonyl, NVOC) as a building block and photolithographic masks to selectively deprotect this *N*-terminal protecting group (**Scheme 2.3**).

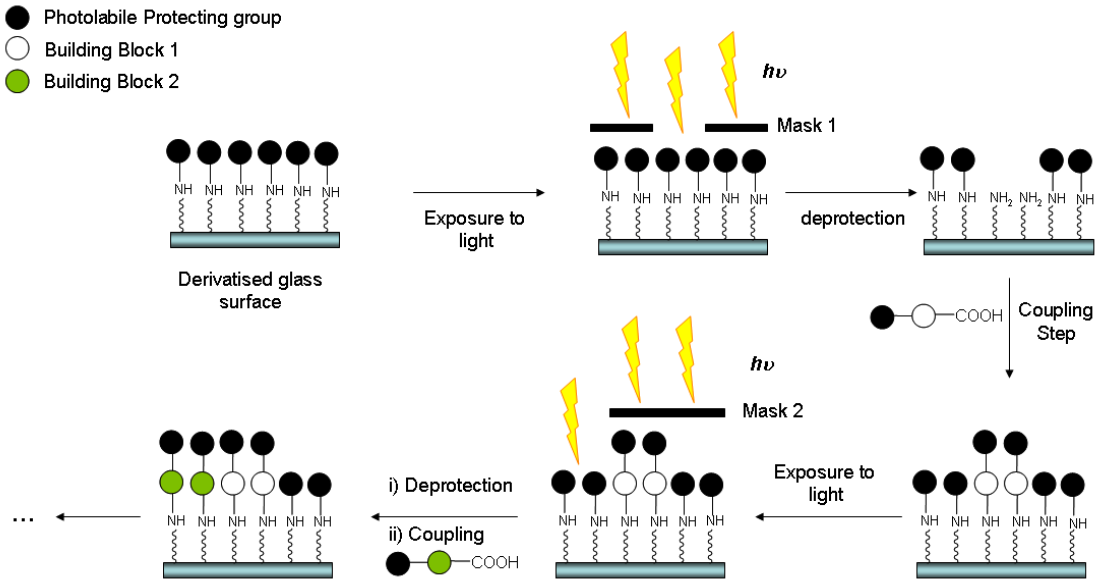

Scheme 2.3: Representation of light-directed synthesis. On a derivatised glass surface with amino groups protected with a photolabile protecting group, light is exposed through a photolithographic mask that allows the light through only at specific positions. Where light have gone through, the building blocks have been deprotected and are available to react with the next building block. A second mask is then applied and other positions are deprotected and reacted with other building blocks. By repeating the process and changing the masks a linear polymer library can be built.

In order to improve the microarray density, new methods have been developed such as the use of polymeric photoresist films to construct the masking pattern on selected regions of the substrates or the use of digital micromirror devices to avoid the cost of photolithographic masks. These methods have been used to prepare oligonucleotide,[140] peptoid[141, 142] and cyclic peptide[143] microarrays.

2.4.1.2. ***SPOT-Synthesis:***

The SPOT-synthesis, developed by Frank *et al.*,[144] is an easy and flexible method for parallel chemical synthesis on membranes.[145, 146] SPOT-synthesis is used for the synthesis of different peptides or peptide mixtures at clearly defined positions on a modified cellulose membrane by manually or automated dispensing of *N*-terminally and side chain-protected amino acids plus coupling agents to defined positions. After the coupling reaction is complete, the whole membrane is washed and the *N*-terminal protecting group is deprotected prior to the next coupling cycle.

This method requires no specialised infrastructure to synthesise the library immobilised onto the support and experimental procedures are simple. The mean spot size is *ca.* 60-times larger (6 mm in diameter) than microarrays prepared by other techniques, due to higher volumes of reagent spotted and the solid support wicking ability, and they are usually called macroarrays. As a result, macroarrays displays three orders of magnitude more compound than microarrays (nanomoles vs. picomoles) and thus, the spots are sufficiently large that they can be cleaved from the membrane and submitted to routine analysis or transferred to a microtiter plate where several solution phase assays can be carried out.[145]

These peptide macroarrays have been used namely to study protein-protein and protein-peptide interactions[147] and for epitope mapping of antibodies.[148-150] SPOT method applications and SPOT synthesis optimisations have been reviewed.[151-153] Recent advances in the field have expanded this technique beyond peptidic systems into the complexity of small-molecule synthesis, including the use of microwave assisted organic reactions and multicomponent reactions.[154] The chemical structures accessed to date are 1,3,5-triazines,[155] cyclic peptidomimetics,[156] 1,3,5-hydantoins,[157] natural product fragments,[158] chalcones,[159] and α-acyl amino amides,[160] with purities reported as good to excellent.

2.4.2. Microspotting

As an alternative to *in situ* synthesis, molecules can be immobilised onto the surface after their synthesis. The advantages of microspotting over *in situ* synthesis are the wider scope of small molecules to be immobilised, the ability to check compound purity before use, and the efficient generation of many copies of the same chip from a stock solution.

2.4.2.1. ***Covalent Immobilisation:***

For covalent attachment onto the surface, small molecule libraries need to be designed to include a common handle with a specific functionality, which can be used to ligate small molecules to an appropriately functionalised surface. Several immobilisation strategies have been used for the covalent attachment of molecules onto surfaces and they can be classified into selective and non-selective immobilisation reactions (**Table 2.1**).

	Slide Coating	Small Molecules	Immobilisation Reaction	Refs.
Selective Immobilisation	Maleimide	Thiols	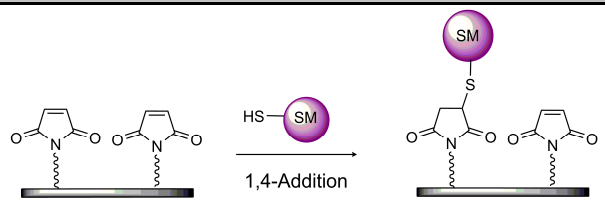	161, 162-164
	Thionyl chloride	Primary alcohols except phenols	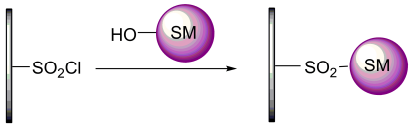	125, 86, 165
	Diazo-benzyliene	Carboxylic acids, phenols, and sufonamides	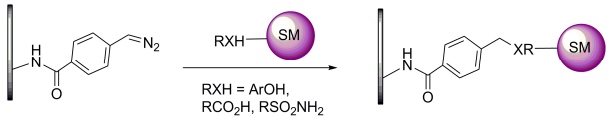	166
	Glycoxylyl	Hydroxyl-amine and cysteines	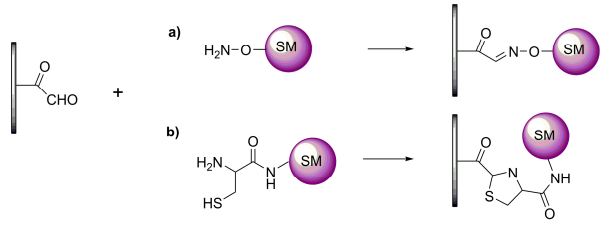	126, 136, 167
	Semi-carbazide	Glycoxyl-containing molecules	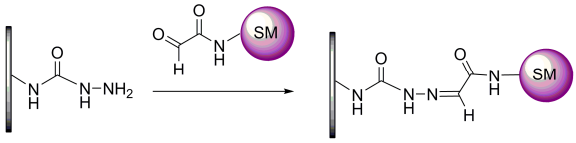	168-170
	Thioester	N-terminal cysteine containing peptides	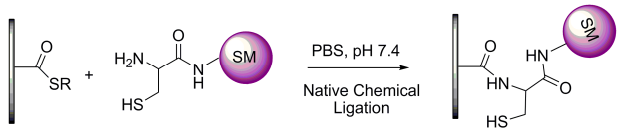	171-174
	Alkyne	Azides	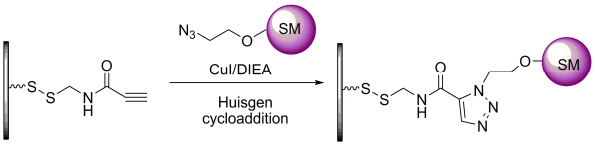	175-180
	Phosphane	Azides	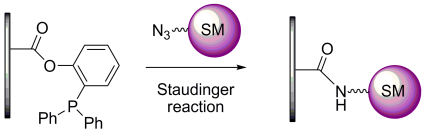	131, 181, 182
	Epoxides	Hydrazines	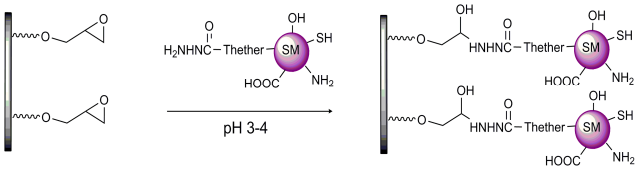	3, 128, 183

Table 2.1: Covalent immobilisation approaches where SM stands for small molecule (Continued).

Non-Selective Immobilisation	Isocyanate	Nucleophilic groups	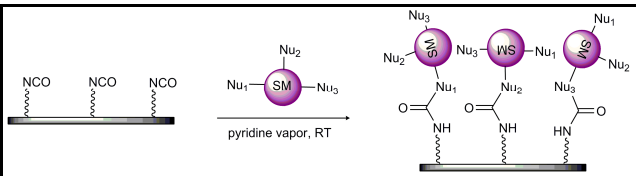	109-111
	Multi-functional	Universal	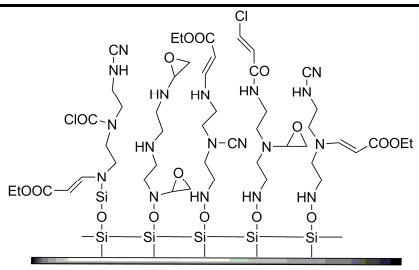	184

Table 2.1: Covalent immobilisation approaches.

2.4.2.2. ***Photochemical Immobilisation***

Several approaches for light-dependent biomolecule immobilisation on surfaces have been developed as it offers the prospect of facile and addressable attachment of substrates with the possibility to structure surfaces by light exposure through a mask (**Table 2.2**).[138, 185, 186]

	Slide Coating	Small Molecules	Immobilisation Reaction	Refs.
Selective Immobilisation	Thiols	Alkenes	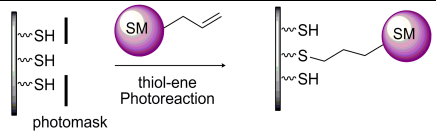	181, 186
	NVOC-protected hydro-quinone	Cyclopenta-diene-tagged molecules	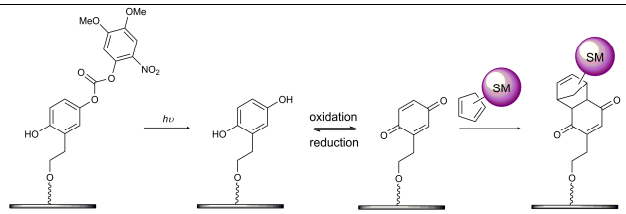	122, 187, 188
	Maleimide	Furan-tagged molecules	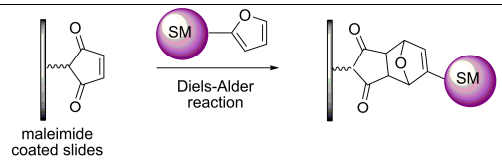	189
Non-selective	Azides, diazirines, and benzo-phenones	Universal	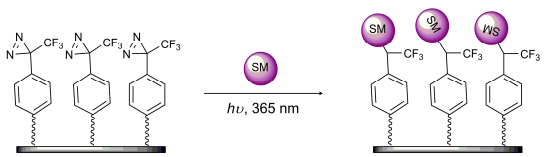	87, 88, 190

Table 2.2: Photoimmobilisation strategies.

Typical photoselective methods are the thiol-ene photoreaction[181, 186] and Diels-Alder reactions.[122, 187-189] Both strategies are compatible with most functional groups and are carried out under mild conditions. Alternatively, the use of photoreactive groups as an anchor for immobilisation of compounds onto surfaces is usually classified as a non-selective method as slides are derivatised with photosensitive groups which after activation with UV light immobilise proximal molecules in a random manner.[87, 88] In addition, the same strategy has been used for selective immobilisation where the photoreactive moiety has been introduced to the compound library and then used to attach those molecules to any type of surface.[190]

2.4.2.3. ***Non-Covalent Immobilisation***

The different non-covalent immobilisation methods use small molecules tagged with biotin, lipophilic or fluorinated chains or peptide nucleic acids which are retained onto a functionalised surface by strong interactions.

a) Ligand-Receptor Pairing

These approaches use small-molecule libraries that have been tagged with biotin and are attached onto an avidin/streptavidin-coated surface by non-covalent interactions (**Scheme 2.4**).[191] Avidin also provides a molecular layer between the glass surface and the proteins interacting with the immobilised molecules which eliminates blocking procedures and minimise non-specific binding on the glass surface. Overall, this method is highly robust and flexible and it has been used for the successful preparation of peptide[173, 192, 193] and carbohydrate[194] microarrays.

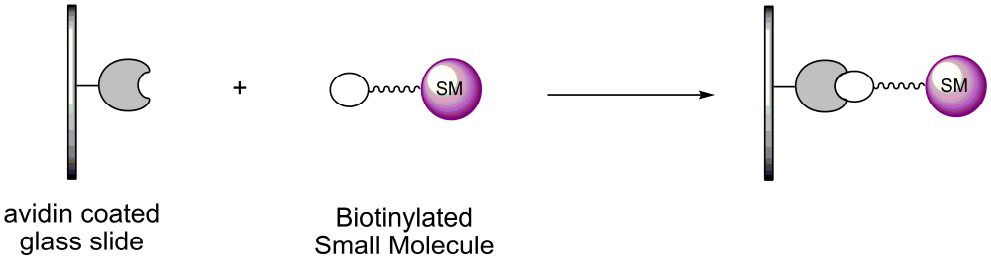

Scheme 2.4: Biotinylated small molecules are immobilised onto a pre-coated surfaces with a monolayer of streptavidin or avidin.

b) Physisorption Using Lipophilic or Fluorous tags

This method consists of a small molecule tagged with a tail having specific physical properties which adhere to a surface by physical absorption. This

method has been applied using two different tags: hydrocarbons and fluorocarbons.

The first approach was used for the preparation of carbohydrate arrays where carbohydrates bear a long saturated hydrocarbon chain, between 13 and 15 carbons, were spotted on a hydrophobic surface (**Scheme 2.5**). It was seen that they were resistant to aqueous washings.[176, 195]

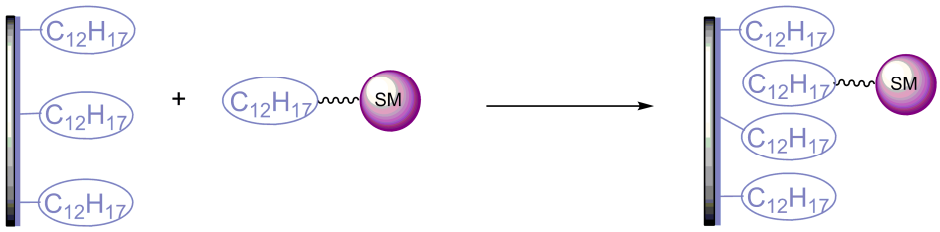

Scheme 2.5: A C12-hydrophobic alkyl-functionalised glass surface is used to immobilise molecules labelled with a lipophilic tag of the same length by physisorption.

The second approach uses the unique properties of fluorinated alkanes, which have prompted the development of perfluorocarbon chains linked to small molecules as a handle for purification.[196] Fluorous tags are hydrophobic and lipophilic, preferring to be in a fluorous phase. In addition, fluorous tags are relatively unreactive and often contain a small aliphatic linker designed to insulate the molecule from the electron withdrawing effects of the fluorous chain.

Carbohydrate microarrays were prepared using fluorous chemistry where sugar derivatives with fluorous tags linked to the anomeric position were synthesised and spotted onto a fluorous-modified glass slide (**Scheme 2.6**). The study showed that a single C_8F_{17} tail was sufficient enough to attach molecules to a fluorinated surface and able to withstand washing with buffer solutions, even in the presence of detergents, with high reproducibility.[197] As a result, several groups have used this approach,[197-204] although as discussed in this thesis there are a number of precautions necessary.

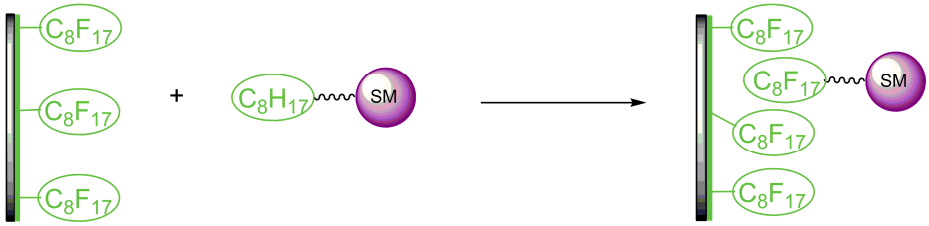

Scheme 2.6: Small molecules functionalised with a fluoroalkyl chain were spotted and immobilised onto a fluoroalkyl-fucntionalised glass slide by physical absorption.

c) ***Self-Assembling Immobilisation***

In this method, a small molecule is covalently tethered to a peptide nucleic acid (PNA) tag whose sequence encodes the structure of the molecule and localises it to a specific site upon hybridisation to an oligonucleotide array containing complementary sequences (**Scheme 2.7**).[205, 206]

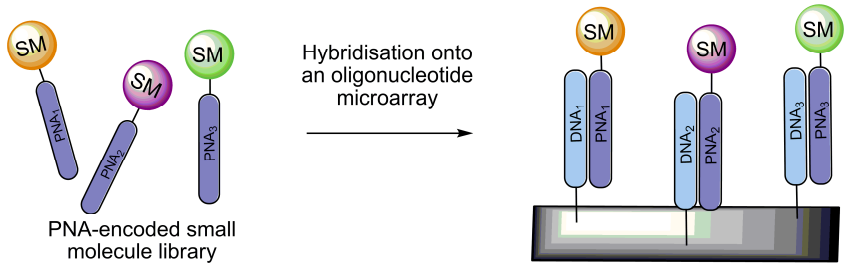

Scheme 2.7: The PNA tags address each substrate from a library to a predefined location on the oligonucleotide microarray through hybridisation, thus allowing the deconvolution of multiple compounds from solution.

An advantage of PNA-encoded libraries compared to covalent immobilisation of small molecules is the possibility to carry out the bioassay in solution prior to the read out by hybridization onto the microarray. In addition, compounds bound to a protein in solution can be selected from the unbound ones prior to hybridisation by size-exclusion filtration or gel separation, which simplifies the screening (**Scheme 2.8**). The methodology and validation of this approach has been described for profiling proteolytic activity from single proteases and from those in crude cell lysates as well as clinical blood samples.[206, 207]

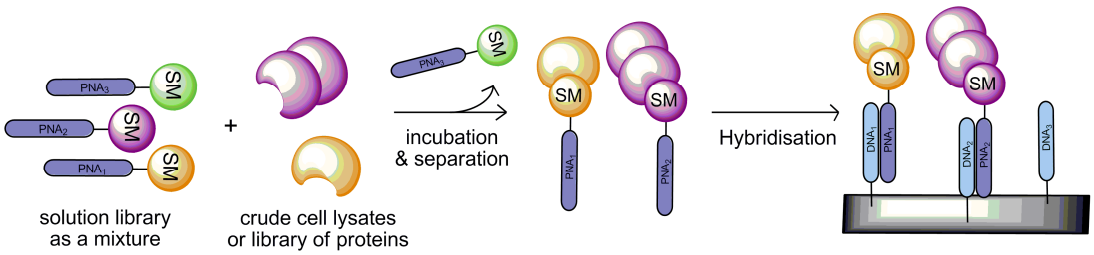

Scheme 2.8: A PNA-tagged library is incubated with the target proteins and then the compounds that have been recognised by the proteins are separated form the ones that are not bound by different techniques and hybridised onto a DNA microarray to know their identity.

A drawback of these approach is when large PNA-tagged compound libraries are hybridised and screened as they involve a broad range of melting temperatures, variations in hybridisation efficiency, differences in concentrations between library members and variations across the microarray itself in terms of

DNA synthesis. To minimise this, dual colour approaches have been developed for profiling tyrosine kinases[208] and proteases.[209-211]

2.5. Printing Technologies

There are many aspects to take into account when printing. Firstly, microarray spots should be small and discernible from each other and be deposited in a grid-like fashion, at equal distances from each other. Secondly, the size and the shape of the spots is also important, they should contain equal amounts of material. For this reason, it is important to control the humidity level, as high humidity may cause spots to smear whereas low humidity may cause the rapid evaporation of solvents from printed spots, which can cause changes in concentration across the spot as well as evaporation of solvents from the source plate.

Two methods for microarray fabrication are photolithography and mechanical microspotting. Photolithography methods are used for *in situ* synthesis of small-molecules onto the slide surface (**Section 2.4.1**), while mechanical microspotting consists of the deposition of pre-synthesised compounds onto the surface by contact or inkjet methods.

Contact deposition methods are based on a high precision robot that holds one or more pins which are dipped into wells containing the solutions of the desired material and pins are then brought in contact with the slide surface where they deliver the sample as a small spot. When moving the pins away from the surface, the adhesion forces between sample and substrate lead to retention of small volumes on the substrate. Thus, the main factors affecting this printing are the viscosity and surface tension of the liquids, the wetting characteristics of both substrate and pins, and parameters controlling the robot. External factors such as humidity and temperature can also affect the quality of printing.[212]

There are various pin technologies available for microspotting (**Figure 2.4**). Solid pins need to be re-dipped for sample loading after each deposition, thus spot size and sample delivery is dependent on the number of stamps per spot. Alternatively, split pins have a reservoir capacities ranging from 0.25 to 1.25 μL and therefore, there is no need of dipping into the solutions repeatedly. Another way to circumvent re-dipping is the pin and ring technology, where a small ring is dipped into the sample solution. The surface tension of the sample is used to form a fluid layer within the ring. A solid pin is pushed through the

fluid layer and the trapped sample is deposited onto the surface. After retraction of the pin the fluid film is still intact and fluid is replenished from the ring.[213]

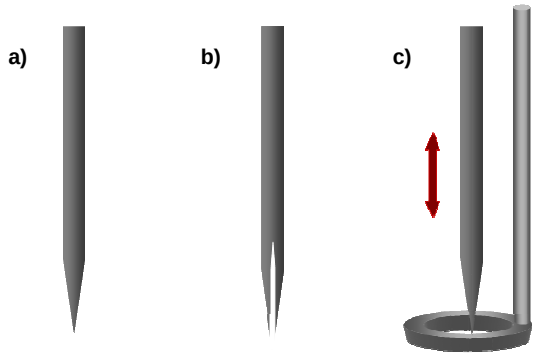

Figure 2.4: Representation of the diferent pins available: a) solid pins; b) split pin; and c) pin and ring.

In inkjet deposition, extremely small volumes (pL) of solution are deposited without contact between the dispensing tip and the surface. Although contact deposition requires less probe solution and results in smaller spots that can be packed more densely on the microarray surface, inkjet printing allows a mild deposition on fragile substrates and better control of the quantities of liquid delivered, allowing a wider range of spot sizes to be printed.[214] Piezoelectric printing and syringe-selenoid methods are the most common variations of this method.

In piezoelectric printing, the target solution is drawn into a glass capillary which is surrounded by a piezoelectric crystal. Application of voltage to the crystal results in a slight conformational change, squeezing the capillary and creates a pressure wave which propagates through the glass into the liquid. In the nozzle region the pressure wave accelerates and a small liquid column leaves the nozzle, breaks off and forms a droplet which flies freely through the air (**Figure 2.5**). The liquid delivery is controlled by the duration and amplitude of the voltage applied to the piezo material allowing very rapid spotting times. The ejected droplet size mainly depends on the size of the nozzle. However, this deposition method is prone to problems caused by air bubbles, which can cause poor spot morphology.

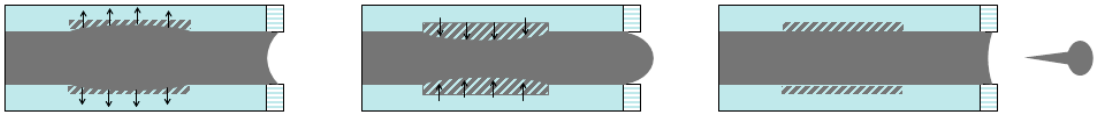

Figure 2.5: Cross sectional view of the fluid channel and nozzle, illustrating the mechanism of droplet ejection. When an electric field is applied, the piezoelectronic crystal undergoes distortion, implying the rapid expansion and contraction, which provokes a pressure pulse in the fluid channel that causes a drop to be ejected from the nozzle.

2.6. Detection Methods

Screening of small-molecule microarrays generally involves the binding of a protein target to the immobilized compound which needs to be detected.[215] The existing detection techniques can be classified into two different methods:

a) Labelling methods

The preferred method of detection is fluorescence detection because these methods are extremely sensitive, simple, have very high resolution, and are compatible with standard microarray scanners. A disadvantage of labelling proteins with fluorophores is a reduction of the quantitative accuracy of the assay, as incorporation of the label may alter the binding properties of the proteins.[216] However, other detection methods have been used with reporter groups such as alkaline phosphatase, radionuclides[126] or epitope tags[155, 217] which in turn can be detected by secondary reagents. Moreover, functional assays for substrates of enzymes have also been applied and the modification of the immobilised compounds is detected with fluorescent quench assay[209, 218] or radiolabel assay.[126]

b) Label-free detection methods:

Although direct protein labelling detection methods are still widely used, non-labelling methods are evolving as a viable complement to traditional labelled-based throughput screening efforts.[219] Label-free technologies offer a number of distinct advantages. First, they are non-invasive and require minimal manipulation of reaction components. This enhances the potential for measuring biologically meaningful data. Second, label-free methods do not suffer from potential assay artefacts such as compound autofluorescence or quenching as no fluorescent dye or label is involved. Finally, they can be used to characterise the affinities, kinetics, and other properties of molecular binding interactions. The most common label-free detection methods are atomic force microscopy

(AFM),[220] and surface plasmon resonance (SPR),[87, 122, 221] reflectometry,[216, 222-224] interferometry,[129] and oblique-incidence reflectivity difference (OI-RD) microscopy.[225]

2.7. Applications

Microarrays of small molecules have already been successfully applied in important areas ranging from protein profiling to the discovery of therapeutic leads. Therefore, they represent a way forward in high-throughput exploration and in combining their vast potential towards medicinal and diagnostic applications.

2.7.1. Protein-Binding Assays

Small-molecule microarrays have proven to be useful tools in the discovery of new protein-small molecule interaction.[138, 226] In chemical genetics research, they are routinely used for identifying small molecules that can selectively modulate either a given protein function or a specific biological phenotype,[227] and in general drug discovery research, they are used for searching potential "hits" for therapeutic targets. Direct binding assays using microarrays have identified small-molecule ligands of varying affinities for many purified proteins, including transcription factors (Hap3p, Ure2p),[165, 228] immunoglobulins (TNF-α),[229, 230] proteases,[207, 231, 232] histone deacetylases,[199] calcium-binding proteins (Calmodulin),[166] kinases,[233, 234] and HIV integrase.[235]

Fragment-based low-affinity microarray screening technology has been developed to allow the rapid experimental characterisation of protein-binding properties and the identification of potential ligands. In this platform, low-complexity drug fragments or pharmacophores, selected from pharmacophores models or virtual screening approaches, are immobilised on microarrays and incubated with the protein or proteins of interest. Binding of the protein to specific molecules on the array is detected and quantified by wavelength shifts of the surface plasmon resonance. A surface plasmon resonance imager is used to record the mass change, which depends on the amount of protein binding to the chemical surface, creating protein-ligand affinity fingerprints. After SAR analysis, the first generation of "hit" compounds and analogues are synthesised and tested, and lead candidates can be further optimised. Graffinity Pharmaceuticals have applied this technology to the search of novel fragments binding to FVIIa[22, 236] and Neri *et al.* found binders with submicromolar dissociation

constants against bovine carbonic anhydrase and human serum albumin.[237] Alternatively, Carlson *et al.* used this approach for the differentiation of proteins based on their binding patterns.[238]

A similar approach is that of small-molecule binding environments microarrays where combinations of pharmacophores are immobilised and screened against a protein of interest. Osada *et al.* used this technology to find a novel bivalent ligand for carbonic anhydrase II (CAII) with high affinity.[239]

Some potential applications to small-molecule microarrays have been limited by challenges in protein biochemistry involving expression of large proteins, solubility, post-translational modification state, activity and yield. For that reason, this technology has been extended to the use of proteins from crude cell lysates. Bradner *et al*. incubated small-molecule microarrays with cellular lysates containing overexpressed epitope-labelled proteins from mammalian cells. Detection of small molecule–protein interactions was achieved by treatment of the microarrays with fluorescently labelled antibodies that interact with the epitope tag.[217] Osada *et al.* also used their small molecule-based binding environments microarrays to screen cellular lysates to identify important moieties for fragment binding to the Shble protein.[240]

2.7.2. Protein Specificity Profiling

Enzyme assays are one of the most popular applications for characterisation of kineases and proteases. Such assays are also highly sensitive since they allow intrinsic signal amplification owing to multiple turnovers by the enzyme.[241] Various microarray-based approaches can be examined in that respect, namely functional annotation,[171, 242] substrate fingerprinting[126, 161] and inhibition fingerprinting.[243, 244]

Functional enzymatic assays with small-molecule microarrays have been developed where surface-bound reporter group translates enzymatic activity into fluorescent readouts. For example, the use of a coumarin substrate immobilised on glass slides in a screen of hydrolytic enzymes has been reported by several groups.[204, 218, 242] Hydrolysis of the non-fluorescent coumarin–substrate complexes results in the fluorescent coumarin being unmasked and indicates substrate-dependent enzyme profiles.

Profiling of tyrosine kinases have been developed by several groups using different approaches. Lam *et al.* studied the non-receptor tyrosine kinase x-SRC

using [γ^{33}P]ATP as the phosphoryl donor to label peptide substrates in order to improve the resolution of the radiolabelled microarray.[126] Houseman *et al.* studied the same protein by three different detection methods and found three inhibitors.[187] Bradley *et al*. screened a 10,000-membered PNA-tagged peptide library against tyrosine kinase and ATP and peptides that were phosphorylated were detected using a primary/secondary antibody approach.[208]

Protease profiling has been carried out by means of a PNA self-sorting approach. Bradley *et al.* used DNA microarrays to self-sort a 10,000 PNA-tagged peptide library where each library substrate incorporated a FRET system in order to interrogate Chymopapain and Subtilisin.[209, 210] Winssinger *et al.* used a PNA-tagged compound library which was labelled with a single fluorescein molecule and used to probe the presence or absence of functionally active cysteine proteases by incubation in solution. The fluorescence intensity of a particular microarray feature is a direct reflect of the amount of the corresponding functional protein present in the sample (**Scheme 2.9**).[206]

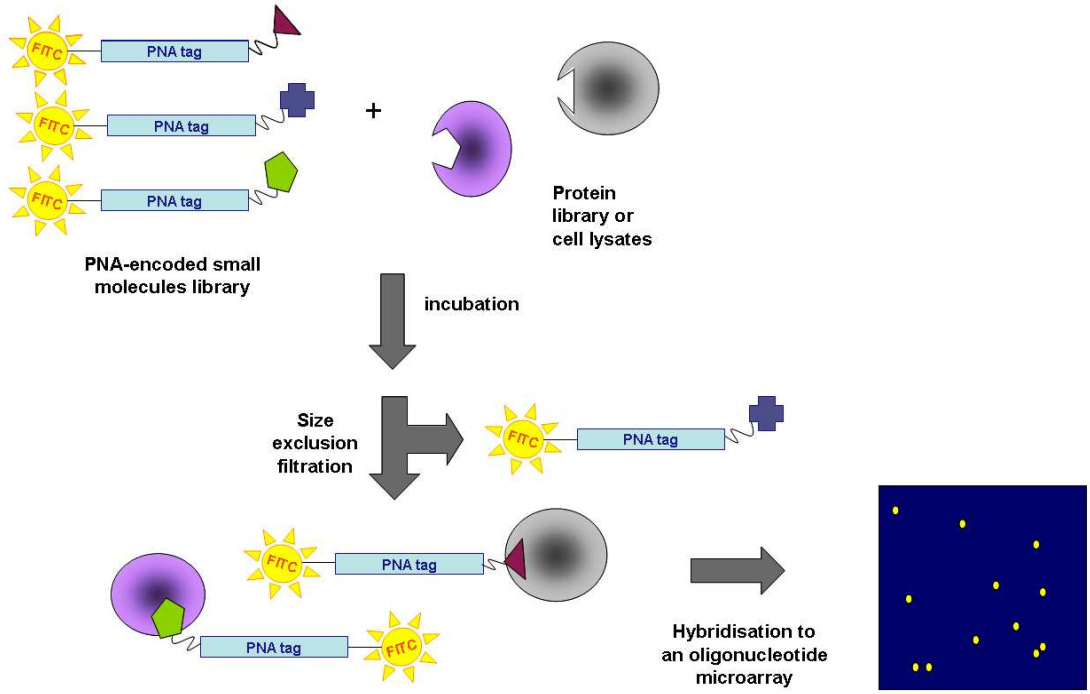

Scheme 2.9: Screening of PNA-encoded libraries. Individual small molecules are tethered to a unique fluorecently labelled PNA sequence, which encodes both their synthetic history and their location following hybridisation to an oligonulceotide microarray. The library of PNA-encoded small molecules were incubated with a protein mixture of interest, passed through a size-exculsion filter to separate the small molecule-PNA adducts bound to a micromolecule from the unbound ones, and the high molecular weight fraction hybridised to the oligonucleotide microarray.

2.7.3. Diagnostic Applications

Recent studies suggest that small-molecule microarrays are useful tools in the discovery of biomarkers for various illnesses, such as autoimmune diseases.[245, 246] Peptide microarrays have been used for antibody detection, where a collection of referenced sera permitted the demonstration of a large gain in sensitivity and specificity compared to the standard ELISA tests.[168] The ligands indentified could be used for a variety of therapeutic and diagnostic applications.[247] Alternatively, carbohydrate microarrays have been extensively used for serum antibody profiling. Human serum contains a wide variety of carbohydrate-binding antibodies, and the population of these antibodies changes as a result of disease, exposure to pathogens, and vaccination.[248]

Alternatively, Disney *et al.* developed a small-molecule microarray to study the binding of ligands to the surface of a variety of pathogens, from Gram-negative bacteria (*P. aeruginosa* and *E. coli*) to fungi (*C. albicans*). These studies have identified a pathogen "fingerprint" for ligand recognition which can be used for a variety of therapeutic and diagnostic applications.[249] Small-molecule microarrays have also been used for the simultaneously and quantitatively detection of three veterinary drug residues in foodstuff: Chloramphenicol, Clenbuterol, and Tylosin.[250]

2.8. Aim of the Project

The aim of this project was to broaden the scope of small-molecule microarray technology to encompass any compound library. We envisaged achieving this by developing a generic approach for the immobilisation of compounds onto glass slides (microarrays). The immobilisation would be possible by using the photoreactive diazirine derivative **4** (**chapter I**) to functionalise the glass surface *via* two different strategies. Either the covalent attachment of **4** onto the surface using standard solid phase coupling chemistry, or alternatively, by physisorption using fluorine chemistry. Small-molecule libraries could then be printed onto the treated slides to provide close contact between the compound and the photoreactive group. Activation of the photoreactive group by irradiation would generate a carbene, which would react with the small molecules in a non-selective manner. We planned to apply this technology to the immobilisation of a 2,000 member compound library and utilise it for the biological screening of β-TrCP1.

2.9. Microarray Fabrication

For the development of the small-molecule microarray approach, the first step was the preparation of photoreactive surfaces which were prepared by two different strategies, compared and optimised.

2.9.1. Strategy I: Photospacer Covalent Immobilisation

Strategy I was based on the covalent immobilisation of the photospacer onto the slide surface. As the TFMAD photophore **4** obtained in chapter I contained a carboxylic acid group, it could be attached to an amino-functionalised surface by standard solid phase coupling conditions. However, instead of derivatising the whole slide with this photophore, a masking process was carried out to localise the probe in order to reduce the non-specific interactions between the target probe and the surface. Once the photoreactive slide was prepared, solutions of small molecules could be dispensed and immobilised by UV irradiation (**Scheme 2.10**).

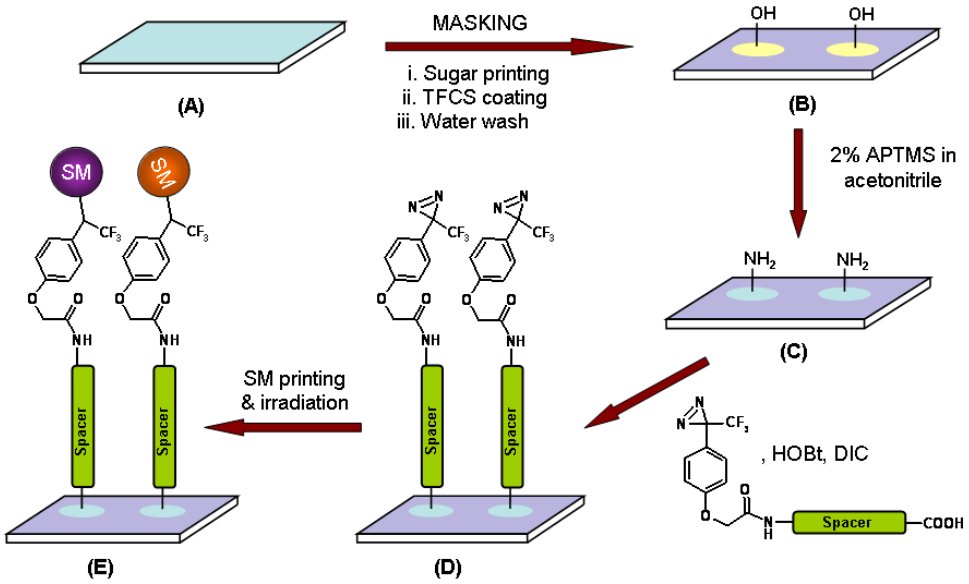

Scheme 2.10: Glass slides were printed with drops of 20% sucrose in water and then treated with tetrahydrooctyl-1-trimethoxysilane (TFCS) to functionalise the slide with fluorous chains everywhere except where sugar had been printed. Removal of sucrose with water allowed derivatisation of the surface with amino groups which were reacted with the preactivated photospacer. Slides were then used for small molecule printing and immobilisation by UV light.

2.9.1.1. ***Surface Preparation***

The first step of this strategy consisted of a masking treatment of the glass surface in order to create a pattern which prevents non-specific

interactions with proteins or cells. In this case, masking was created by spotting a concentrated sugar solution (20% sucrose in water (w/v)) onto pre-cleaned glass slides. The slide was then derivatised with tridecafluoro-1,1,2,2-tetrahydrooctyl-1-trimethoxysilane (TFCS) except at the masked positions where the sugar had been deposited. As a result, once the sugar was dissolved in water and washed away, localised areas with free hydroxyl groups could be converted to other functionalities (**Scheme 2.11**).

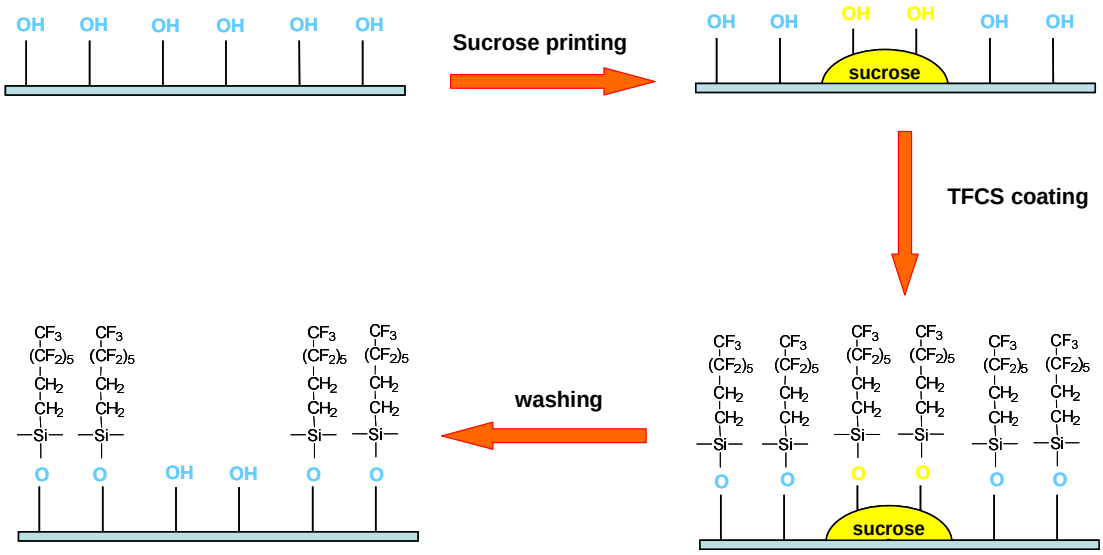

Scheme 2.11: The masking process consitst of 3 steps: first, a solution of sucrose in water is printed on a precleaned slide and let to dry. TFCS is used to modify the surface which interacts with the alcohol groups on the sucrose where the masking have been done. Finally, the slide was washed, firstly with acetone to remove excess TFCS, and then with water to dissolve the mask.

The free hydroxyl groups were reacted with a solution of 2% 3-aminopropyl trimethoxysilane (APTMS) in acetonitrile to convert them into amino groups. These amino groups were further functionalised by dispensing a solution of the photospacer with HOBt/DIC in DMF to give the final photoreactive slide (**D**, see **Scheme 2.10**). After extensive washing in DMF, slides were kept in the dark until small molecule printing.

2.9.1.2. *Photospacer Synthesis*

To optimise the distance of the small molecule from the glass surface and maximise sensitivity, three different length photospacers were synthesised by solid-phase synthesis. For this purpose, it was essential to synthesise compound **23** and Fmoc-protected spacer **27**.

The acid-cleavable linker **23** was readily prepared in 2 steps from hydroxybenzaldehyde (**Scheme 2.12**). Firstly, alkylation of the phenol was carried out with ethyl 4-bromobutyrate under microwave irradiation at 120 ºC to give **22**. Subsequent hydrolysis with sodium hydroxide and reduction of the aldehyde to an alcohol with sodium borohydride was carried out in a single pot reaction to give **23** in an overall yield of 83%.

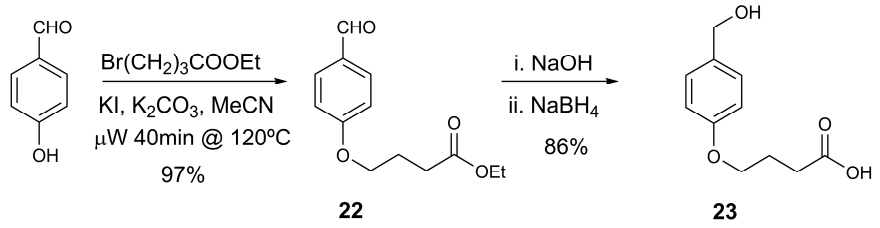

Scheme 2.12: Synthetic route to 4-[4-(hydroxymethyl)phenoxy]butanoic acid **23**.

The Fmoc-8-amino-3,6-dioxaoctanoic acid was synthesised by a slightly modified procedure of Visitin *et al.*[251] (**Scheme 2.13**). The amino group of 2-(aminoethoxy)ethanol was di-protected with benzyl bromide to give **24**. Then, the alcohol was alkylated with bromoacetate in the presence of sodium hydride to give **25**. Deprotection of the benzyl group was performed by hydrogenation on palladium. Final protection of the amino group with Fmoc chloride gave **27** with an overall yield of 49% and a spacer unit ready for use in Fmoc chemistry on a solid support.

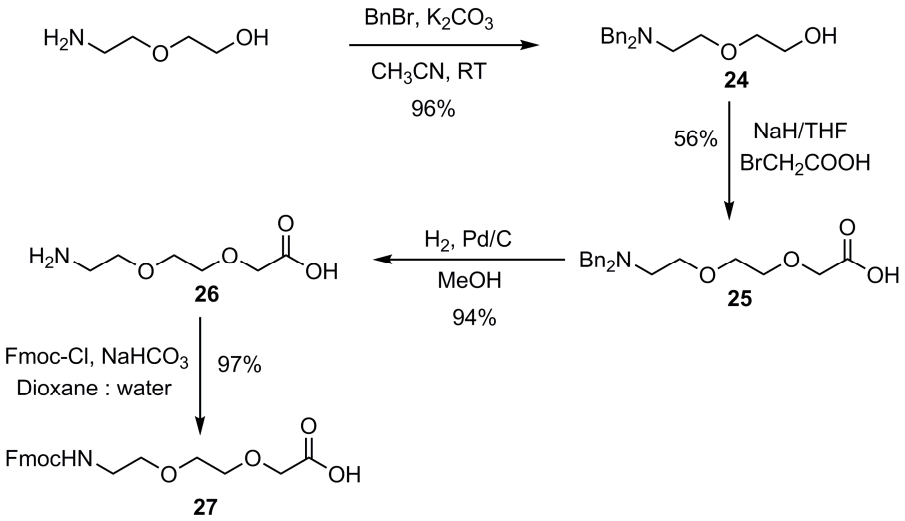

Scheme 2.13: Synthesis of Fmoc-8-amino-3,6-dioxaoctanoic acid spacer unit **27**.

The assembly of building blocks to prepare the photospacer started with the covalent attachment of the linker to aminomethyl resin by standard solid phase coupling conditions (**Scheme 2.14**). Saponification was performed with

aqueous sodium hydroxide to eliminate oligomers formed during the reaction. The spacer unit was then attached to resin **28** by esterification. The success of these couplings was monitored by the colorimetric Malachite Green test, which indicated incomplete coupling when beads were green after washing and gave colourless beads when the coupling was completed. Deprotection of the Fmoc group was carried out with 20% piperidine in DMF and reaction completion was monitored by a ninhydrin test. At that point, one third of the resin was separated and reacted with TFMAD **4**. The first photospacer was cleaved from the resin with a standard acidic cocktail to give **PS1**. Another spacer unit was coupled to the rest of the resin with subsequent Fmoc deprotection. The resin was divided into two parts, one was reacted with TFMAD **4** and cleaved to give **PS2** and the cycle was repeated with the other half to give **PS3**. By this method, photospacers with one, two or three units of the PEG spacer were prepared with high purity (**Figure 2.6**).

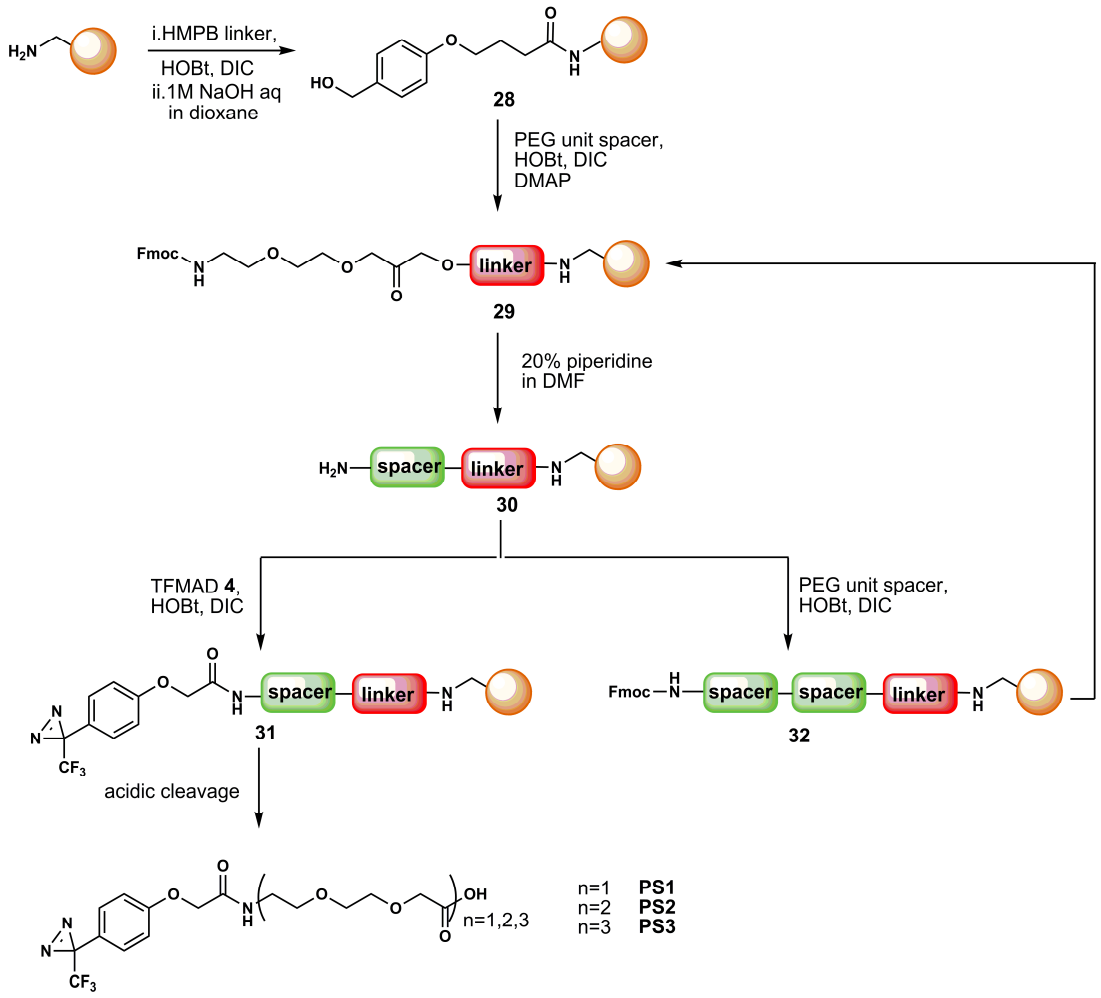

Scheme 2.14: Synthesis of photospacers by solid phase synthesis.

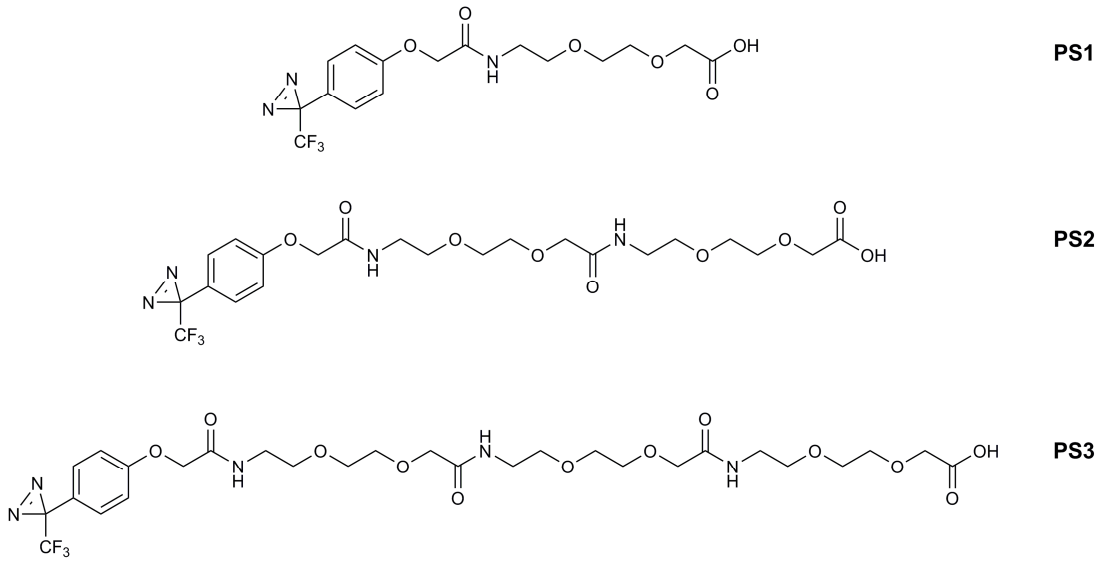

Figure 2.8: Photospacers synthesised with different PEG spacer lengths.

2.9.1.3. ***Experimental Validation***

To validate the robustness and sensitivity of the developed method, the strong interaction between Biotin and Streptavidin was used as a model. Biotin was printed on the photoreactive slide and immobilised by irradiation for 40 min with UV light at -196 ºC. After washing, the slide was incubated with fluorescently labelled Streptavidin for 1 h at 37 ºC. If the photospacers were able to immobilise biotin, fluorescently labelled Streptavidin would be detected just at those locations where biotin had been immobilised (**Scheme 2.15**).

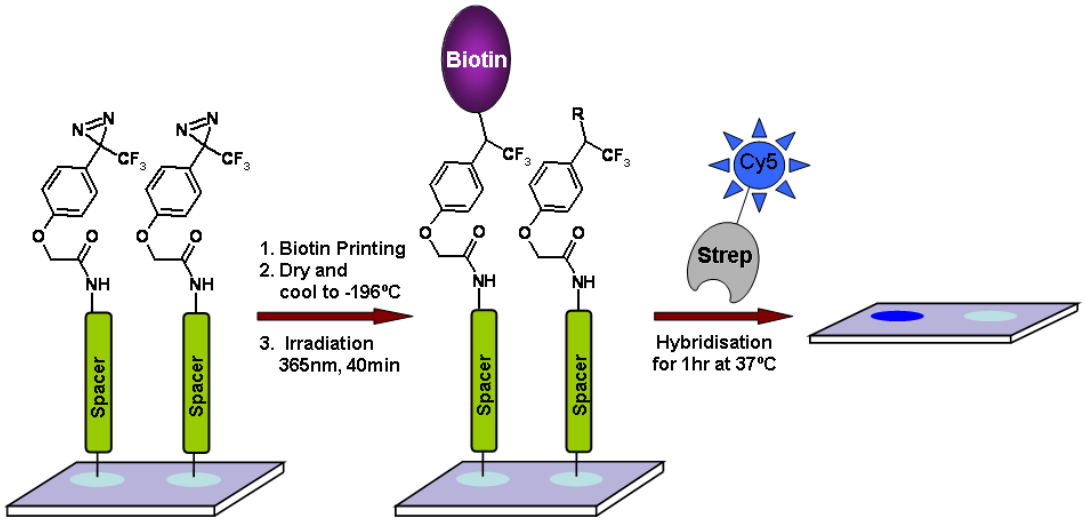

Scheme 2.15: Representation of the validation strategy performed. Biotin was printed at the same positions of the photospacer. Slides were dried and cooled to -196 ºC and then irradiated with a UV lamp for 40 min. After washing, the slides are incubated with Cy5-labelled Streptavidin for 1 h at 37 ºC. Slides are washed and scanned using a Cy5 filter.

The experiment was designed as follows. Each sample was printed in quadruplicate (2x2 spots) and the experiment was duplicated on the same slide (**Figure 2.7**). Negative controls were printed in the first and fifth column where either photospacer or Biotin was printed and treated under the same conditions. Each photospacer was deposited in different columns, from shorter to longer length spacer, and rows were printed with different concentrations of Biotin solutions, ranging from 100 mM to 0.1 mM. **Figure 2.7** corresponds to the slide scanned image (La Vision BioTech, Bielefeld, Germany).

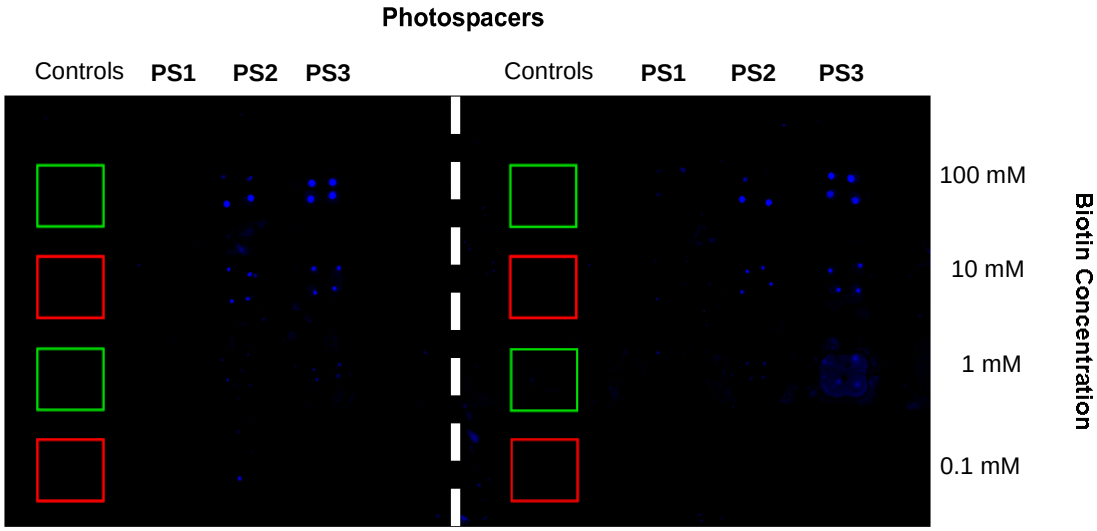

Figure 2.7: Scan of the experimental validation slide with a Cy5 filter. The experiment was duplicated in two grids. In each grid, negative controls were printed in the first and the fifth column, where green squares correspond to only photospacer **PS1** printing and red squares to only biotin solution printing. Columns 2 to 4 and 6 to 7 contain a different photospacer each, ranging from shorter (**PS1**) to longer (**PS3**) spacer lenght and each row corresponds to the printing of different concentration of Biotin solutions on top of the photospacer. The slide was irradiated, washed, incubated with Streptavidin-Cy5 and scanned.

The results showed that the spacer length and the concentration of printed small molecule solutions were important factors for the assay sensitivity. On one side, it was clear that the longer the photospacer the better was the signal, where the signal could be detected down to 1 mM of printed solution. On the other side, no signal was detected when 0.1 mM biotin solutions were printed and minimal for 1 mM concentration. However, 10 mM and 100 mM solutions gave good signal-noise ratios. As a result, further studies were carried out with concentrations of 10 mM solutions.

2.9.2. *Strategy II: Fluorous Tag Physisorption*

Rather than using a covalent reaction to immobilise the photospacers onto the slide surface, photospacers tagged with a perfluoroalkyl chain could be adhered to a fluoroalkylated surface by fluorous affinity. The strategy would simplify slide preparation, without the need of masking steps or amino functionalisation (**Scheme 2.16**).

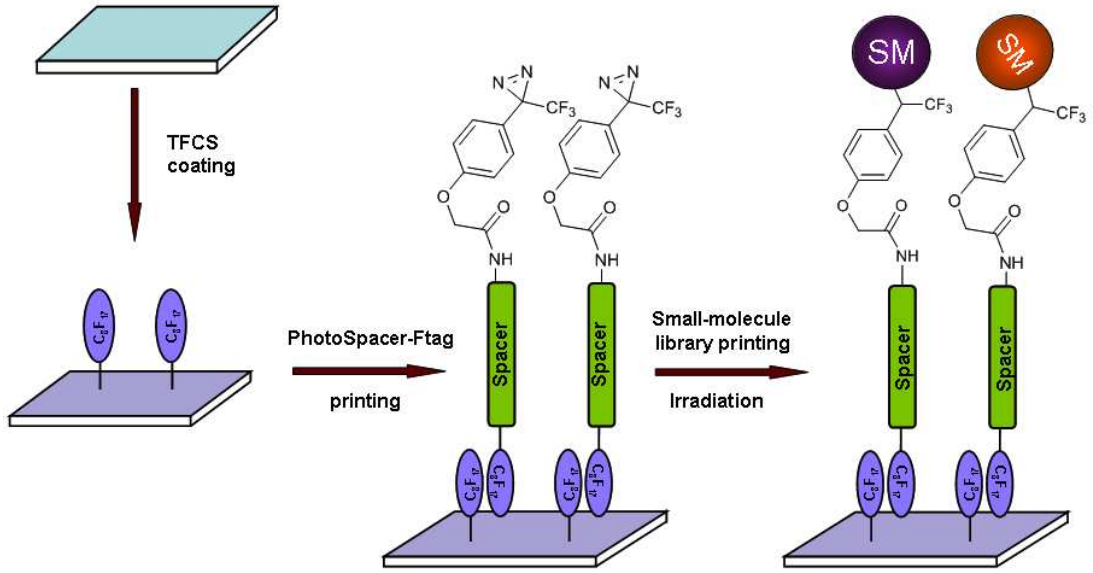

Scheme 2.16: Glass slides treated with TFCS were printed with photospacers tagged with the same fluoralkyl chain and immobilised by fluorous affinity. After washing, small molecules were printed at the same photospacer locations and covalently immobilised by carbene reactions after UV activation.

2.9.2.1. ***Fluorous Tagged Photospacer Synthesis***

Fluorinated tagged photospacers were synthesised by coupling the photospacers **PS1**, **PS2** and **PS3** with 1-amino-1H,1H,2H,2H-perfluorodecane, using PyBOP and DIEA and purified *via* a fluorous silica column (**Scheme 2.17**).

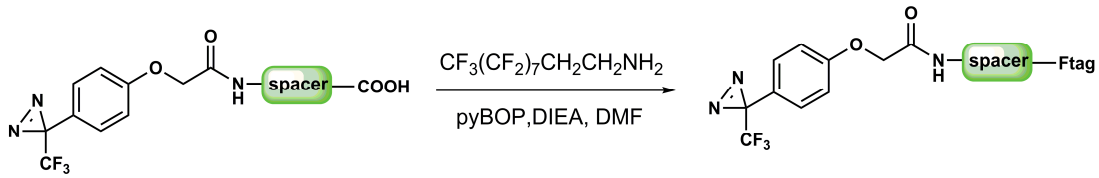

Scheme 2.17: Synthesis of fluorous tagged photospacers.

Positive controls were also synthesised for this strategy. Carboxyfluorescein and biotin were derivatised with the same fluorous tag and reaction. All products were obtained with yields between 60 and 75% (**Figure 2.8**).

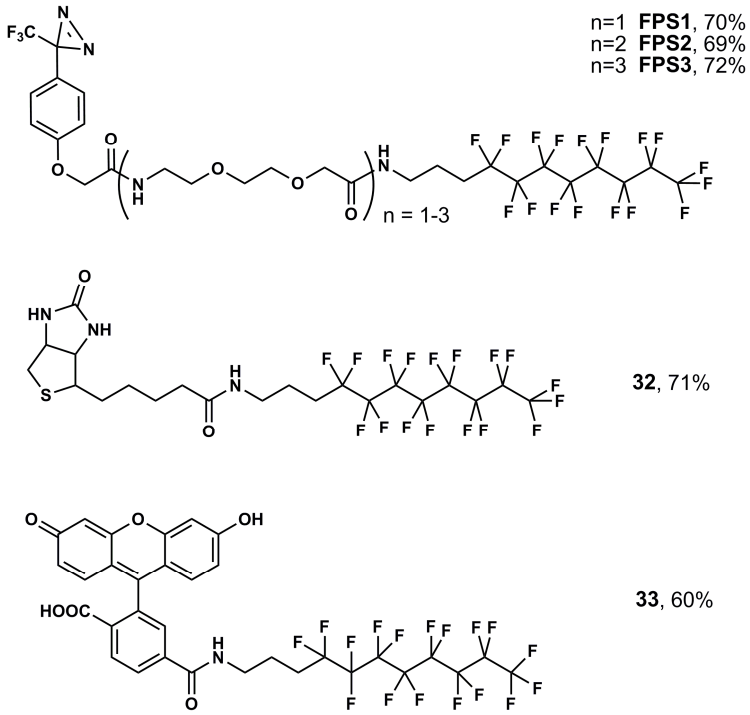

Figure 2.8: Fluorous tagged compounds prepared for strategy II.

2.9.2.2. ***Preparation and Manipulation of Fluorinated Slides***

Preparation of slides for this strategy was simpler than for strategy I, in which pre-cleaned standard glass slides were functionalised with TFCS and printed with fluorous tagged photospacers.

In order to find the optimal conditions for manipulation, different strategies for printing and washing the slides were assessed. Thus a 10 mM solution of fluorous tagged Fluorescein **33** in DMF was used to print different numbers of drops per spot onto the fluorinated slide. Once printed solutions were dried, spot size and morphology were investigated as well as solvents for slide washing after printing and drying methods such as centrifugation or nitrogen. As shown in **Figure 2.9**, when slides are washed in water the spots remained exactly as before and with the same range of intensities. However, if the washing was performed with sonication for 1 min some shadows could be seen surrounding the spots indicating compound movement. Slide drying by centrifugation showed the worst results and it was clear that fluorine affinity was

not strong enough to survive this treatment. As expected, organic solvents completely washed away the fluorous tagged compound from the slide; however water washings with up to 20 % methanol could be used without compound diffusion.

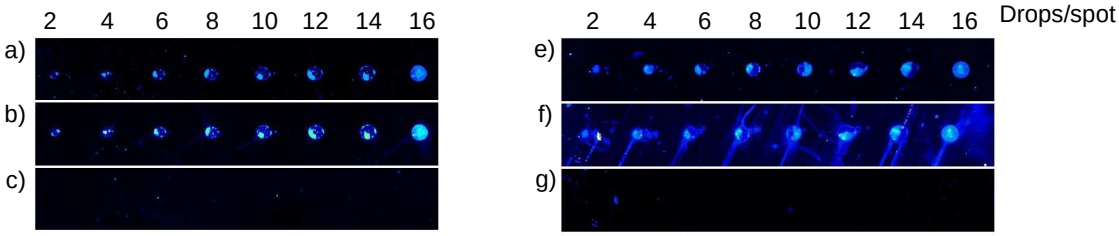

Figure 2.9: Scan of fluorous tagged Fluorescein **33** printed slides after different washing and drying techniques: a) slide without washing; b) slide washed with water for 10 minutes and then 1 minute sonication; c) slide washed with DMSO; e) slide washed with water for 10 minutes; f) slide washed for 10 minutes in water and then dried by centrifugation; g) slide washed with ethanol.

To assess the ability of fluorous tagged photospacers once adhered onto the surface to capture Fluorescein the following experiment was carried out. A fluorinated slide was printed with a solution of 10 mM of **FPS1** in DMF with different number of drops. Slides were left to dry overnight and then a solution of 10 mM carboxyfluorescein in DMF was printed at the same position with the same number of drops as the photospacer. Slides were left to dry and then irradiated for 40 min at 365 nm. Scanning of the slide was done before and after washing twice with a 10% MeOH solution in water for 10 min (**Figure 2.10**). As anticipated, the intensity of the spot decreased after washing due to the removal of exces fluorescein, however, the spot shape and homogeneity was still good. The results showed that a fluorous tagged photospacer was attached to the surface and it remained after washing and that it was capable of capturing carboxyfluorescein. In addition, signals were detected with as less as 2 drops per spot, although the signal fluorescence incresed with the number of spots.

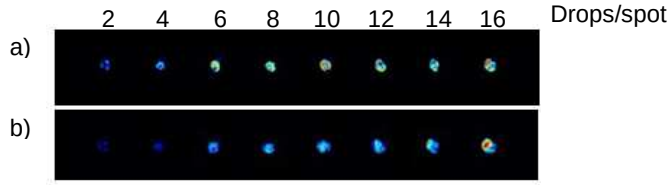

Figure 2.10: Scan of carboxyfluorescein immobilised onto a surface printed with FPS1. From left to right, increasing drop number of FPS1 solution printed. a) slide without wash; b) slide washed with 10% MeOH in water.

A second method used for immobilisation of compounds consisted of mixing **FPS1** and carboxyfluorescein prior to solvent evaporation and irradiation.

The sample was then redissolved in DMF and printed onto a fluorinated slide with the same number of drops as the previous experiment. The slide was left to dry and then washed before scanning. Although this strategy seemed to work, the spot morphology was not as homogeneous as with the previous method (**Figure 2.11**).

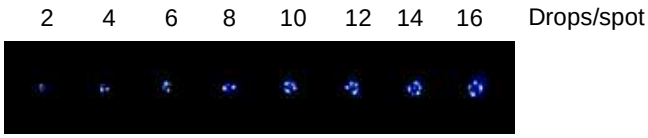

Figure 2.11: A carboxyfluorescein and **FPS1** were irradiated for 40 min and then dissolved in DMF to make a 10 mM solution and printed onto a fluorinated slide.

In conclusion, these experiments established the best way to immobilise compounds by fluorous tag physisorption onto fluorinated slides. Firstly, slides could be washed in water without fear of compound diffusion but when washed with organic solvents compounds were completely washed away. Secondly, slide quality was superior when no sonication or centrifugation was applied. And finally, the simpler and the better signal-to-noise ratio and spot morphology was achieved when irradiation was performed over the slide after spotting of both the photospacer and the small molecule to be immobilised.

2.9.2.3. ***Experimental Validation***

To determine the sensitivity of this strategy and the optimal photospacer length, a validation experiment was carried out. As for strategy I, every structure was printed in quadruplicate and the experiment was duplicated within the slide. The left array was printed with 8 drops/spot and the right one with 10 drops/spot of a photospacer solution. The controls used were the same as before where only one of both, photospacer (**FPS3**) or the small molecule, was printed and highlighted with green and red squares, respectively. From left to right, the three different photospacers were printed, and from top to bottom the concentration of the small molecule increases. This experiment was carried out with the immobilisation of carboxyfluorescein (**Figure 2.12**) and Biotin (**Figure 2.13**).

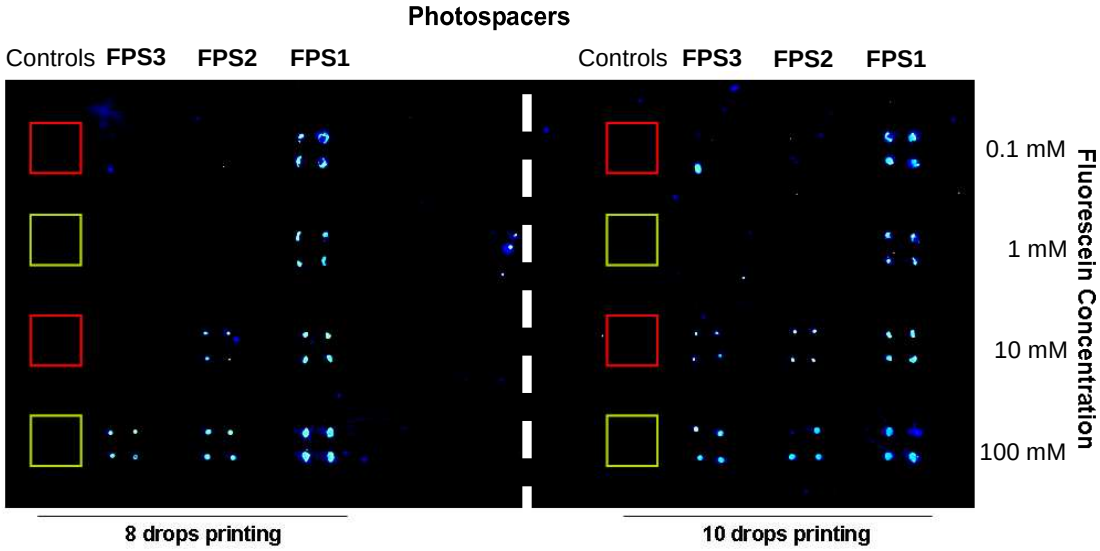

Figure 2.12: All photospacers were printed using a 10 mM solution in DMF. Green squares show where **FPS3** photospacer had been printed and red squares where 10 mM solution of Fluorescein. The left grid was printed with 8 drops/spot and the right one with 10 drops/spot of both photospacer and carboxyfluorescein solutions. After printing, the slides were left overnight and then irradiated for 40 min at 365nm, washed with water and scanned with a FITC filter.

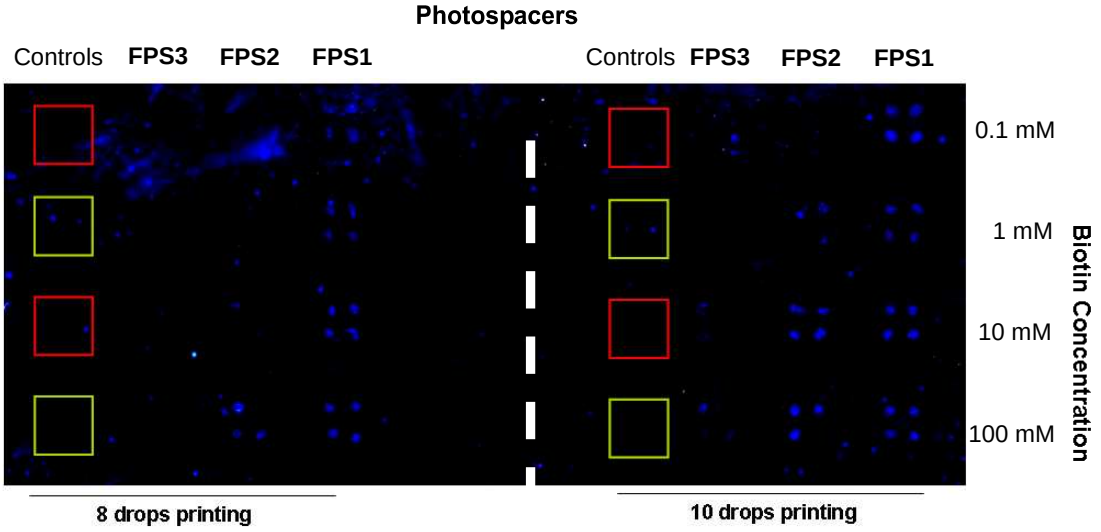

Figure 2.13: Photospacer length and sensitivity experiment by immobilising Biotin. Detection of Biotin was carried out by incubation of Cy5-labelled Streptavidin for 1 h at 37 ºC. After washing, slides were scanned using a Cy5 filter.

Unlike strategy I, the shortest fluorous tagged photospacer **FPS1** gave the best results and intensive signals could be detected when the lowest concentrations of small molecule were used. Fluorous tagged photospacers **FPS2** and **FPS3** signal was detected when the small molecule concentration was at least 10 mM or higher. Thus, the sensitivity of strategy II seemed to be higher than strategy I as signals could be detected at lower concentrations of the small molecule solutions.

In conclusion, strategy II has some advantages over strategy I. Firstly, the preparation of slides for strategy I is longer, involving an additional printing step for the masking process. Moreover, each slide needs to be specially prepared for each designed experiment, making sure that the photospacer and the small molecule to be immobilised are printed at the same position where the masking was disposed. On the contrary, slides prepared by strategy II involve only one step without printing and do not need the removal of slides from the printer station until all processes are completed. In addition, when the experiment is finished there is the possibility to wash the slides with organic solvents and reprint them.

2.10. Printing of a 2,000 Compound Library

A small-molecule microarray was prepared by strategy II to screen a library of 2,000 compounds. For statistical reasons, each compound had to be assessed in triplicate. As a consequence, a small-molecule microarray needed to be designed where at least 6,000 spots could fit into the printing area. Thus, a SciFlexarrayer printer was used to achieve higher spot density on the slide instead of the Microdrop printer used for previous experiments. In addition, the Sciflexarrayer software allows programming of the printing method in a simple manner which is an important advantage when 6,000 spots need to be deposited.

2.10.1. SciFLEXARRAYER printer

In order to see if the preliminary experiments could be extrapolated to the SciFlexarrayer technology the following experiment was carried out where an array of 5x5 spots was printed with **FPS1** and used to immobilise biotin. In addition, the experiment was used to determine the best photospacer:biotin ratio by printing a different number of drops/spot in each column. Column 1 corresponded to 1:1 ratio, column 2 to 2:1, and up to 5 times more photospacer than Biotin. Each condition was replicated five times. The positive control corresponded to the printing of a 2 mM solution of fluorous tagged Biotin **32** and the negative control corresponded to a 10 mM Biotin solution. The slides were left to dry and then irradiated for 40 min at 365 nm and washed extensively before incubation with Streptavidin-Cy3 for 1 h at 37 ºC, washed and scanned with a Cy3 filter (**Figure 2.14**).

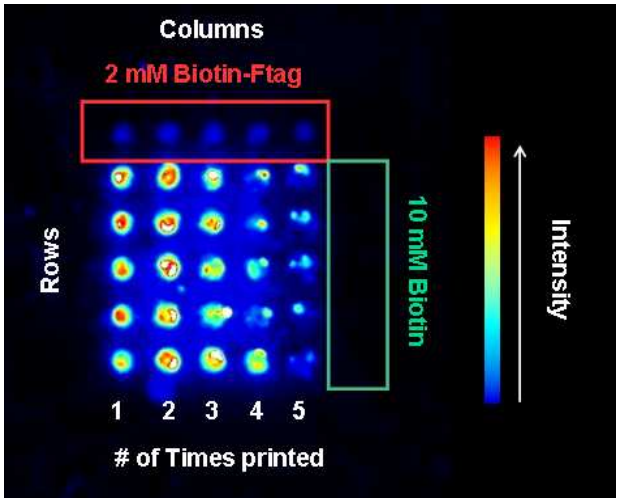

Figure 2.14: Scanning of a slide generated using strategy II and a SciFlexarrayer printer in order to optimise the amount of photospacer to be used for a 10 mM small molecule solution (Biotin). The different photospacer:Biotin ratios (columns 1 to 5) were produced by depositing the same volumes of **FPS1** but varying the number of printing times, ranging from 5:1 ratio in the first column to 1:1 ratio in the fifth column. Each ratio was quintupled (rows), generating a 5x5 grid. The same volume of a 10 mM Biotin solution was printed equally everywhere. The negative control consisted in an extra column (green rectangle) where a 10 mM Biotin solution was printed without previous photospacer printing. A 2 mM fluorous tagged Biotin **32** solution was used as a positive control (red rectangle).

The experiment showed that the strategy II could be performed with the SciFlexarrayer printer and that a large excess of photospacer did not give a better signal, the 5:1 ratio giving the lowest intensity. The 3:1, 2:1 and 1:1 ratios gave high fluorescent signals, with the 2:1 ratio the most intensive. However, the 1:1 ratio was used for the development of the small-molecule microarray as the spots were smaller, showed high intensity and required less photospacer.

2.10.2. Slide Reuse

The reuse of the printed slides was studied with the biotin printed slide used in the previous section (**Figure 2.14**). The fluorescence mean data of each spot was analysed before and after water washings at 70 ºC (for 1 or 2 h) to induce protein denaturation and to wash away the Cy3-labelled Streptavidin. Subsequently, the slide was incubated again with Streptavidin-Cy3 and fluorescence data was compared in order to determine how well the washing steps were performed and if the slide was still functional after the washing step in comparison with the first incubation of the slide with Streptavidin-Cy3 (**Figure 2.15** and **Graph 2.1**).

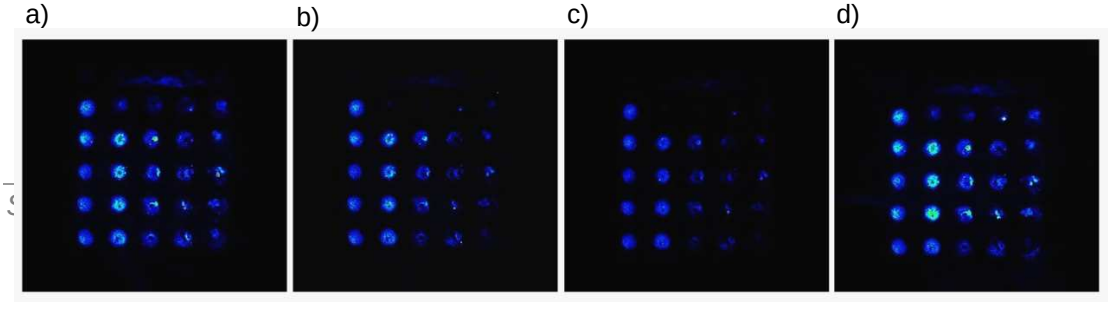

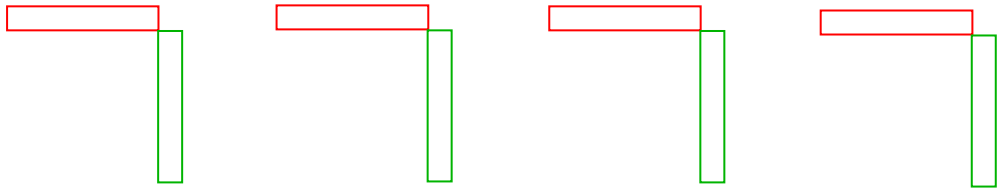

Figure 2.15: Scanning of the same slide in **Figure 2.14** where a 10 mM Biotin solution was immobilised by different amounts of photospacer-Ftag generating a grid of 5x5 (5 different ratios (columns) by 5 replicates of each condition (rows)) on a Genetix Scanner after a) first incubation with Streptavidin-Cy3 (the same as **Figure 2.14**); b) washing for 1 h at 70 ºC; c) washing for 2 h at 70 ºC; and, d) repeated incubation with Streptavidin-Cy3. Red squares correspond to the area where Biotin-Ftag was printed and green squares were Biotin solution was printed without previous photospacer printing.

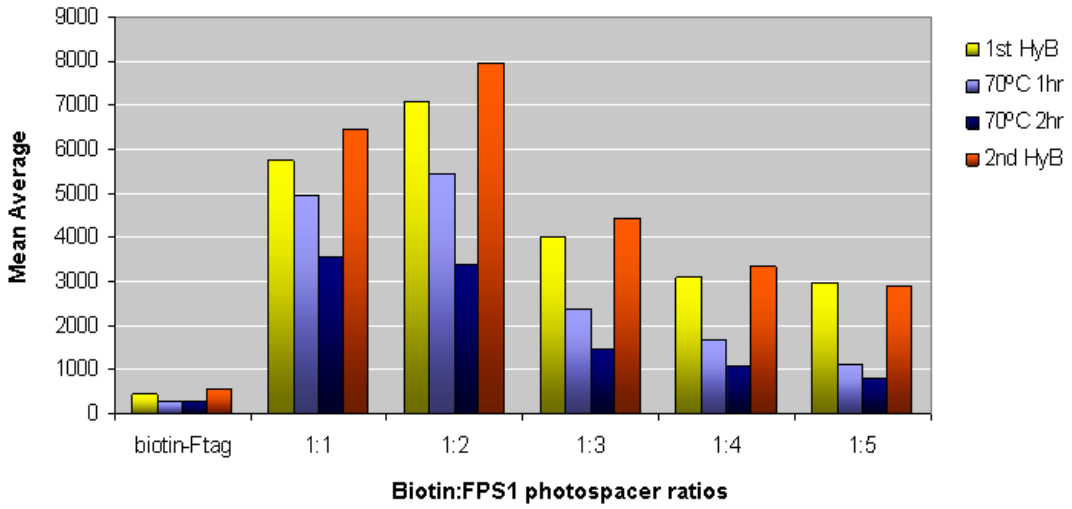

Graph 2.1: Intensity values of each spot condition after each treatment: yellow bars correspond to the first incubation with streptavidin-Cy3; light blue to wash treatment at 70 ºC for 1 h; dark blue to wash treatment at 70 ºC for 2 h; and orange bars show means after the slide have been incubated for a second time with Streptavidin-Cy3. Mean is shown as an average of 5 spots and x-axis represents the different ratios of Biotin:**FPS1** photospacer.

The results showed that intensity decreased after washing for 1 h at 70 ºC. After a second wash at 70 ºC for 1h, the intensity further decreased to half and re-incubation of the slide with Streptavidin-Cy3 restored the fluorescence achieving the same or higher values than the first hybridisation.

In conclusion, the data indicate that after washing the entire signal was removed but fluorescent signals could be restored after protein re-incubation with the same intensity values of the first incubation. Thus, printed slides already used for binding assays can be reused. In addition, degradation of immobilised compounds under washing conditions can be spotted when intensity is not restored to initial values after washing and re-incubation.

2.10.3. Spectum Library

The 2,000 compounds (Spectrum collection of MicroSource Discovery Systems, Inc. (Gaylordsville, CT)) encompass a wide range of biologically active compounds. Approximately 50% of the library consists of known drugs. Natural products with unknown biological properties make up 30% of the library and the remaining 20% of the compounds represent non-drug enzyme inhibitors, receptor blockers, membrane active compounds, and cellular toxins.

2.10.4. Beta-Transducin Repeat Containing Protein

Beta-Transducin Repeat Containing Protein (β-TrCP1) is an F box protein which interacts with Skp1 through the 40 amino acid F box motif and with substrates through C-terminal protein-protein interaction domains consisting of seven WD40 repeats. The F-box domain subunit, together with the adaptor protein Skp1, the scaffold protein Cullin1, and the RING-domain protein RBX1, makes up the SCF complex (Skp1-Cul1-F-box protein) or E3 ubiquitin ligase. All known $SCF^{\beta\text{-}TrCP1}$ substrates contain the DSGØXS destruction motif (Ø representing a hydrophobic and X any amino acid) in which the serine residues are phosphorylated by specific kinases. The binding of β-TrCP1 results in ubiquitination and subsequent degradation by the proteasome (**Figure 2.16**).[252]

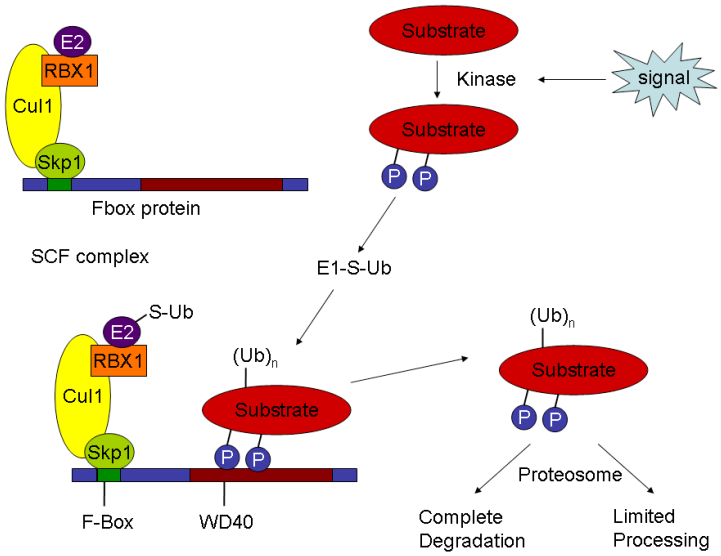

Figure 2.16: Diagrammatic drawing showing the SCF complex and how it recognises its substrate for degradation by the proteasome. (Ub)n, polyubiquitn; P, phosphate group; E1 and E2, ubiquitin E1 and E2 enzymes; Cul1, RBX1,Skp1, and Fbox protein, SCF complex components.

β-TrCP1 is implicated in various cancers, by being overexpressed or having mutations. β-TrCP1 controls the stability of proteins involved in

transcription, including β-catenin[253] and IkB.[254] For example, the degradation of IkB is an essential step for releasing the transcription factor NFkB (Nuclear Factor-kB) which translocate to the nucleus and bind their cognate DNA binding sites to regulate the transcription of a large number of genes, regulating and activating key molecules that are associated with diseases ranging from inflammation to cancer.[254, 255] Thus, finding molecules that interact with β-TrCP1 could help to study and regulate its activity in cancer cells where it is overexpressed.

2.10.5. Microarray Experiments

A small-molecule microarray was prepared by printing 8 drops per spot of 10 mM **FPS1** solution in DMF (53 rows x 114 columns = 6,042 spots). The SPECTRUM library (2,000 compounds) was then printed in triplicate, spotting 8 drops per spot of 10 mM compound solutions, and then irradiated (**Figure 2.17**).

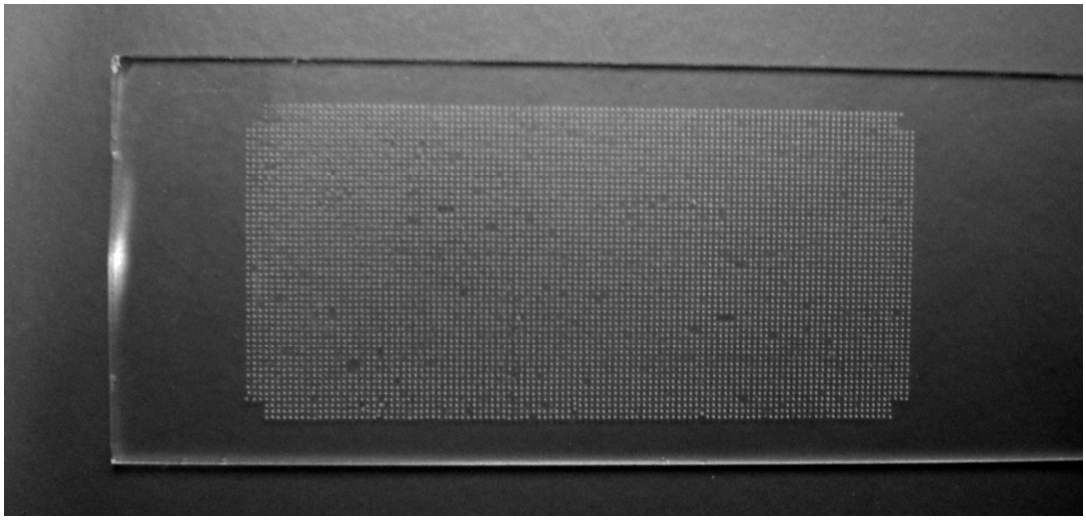

Figure 2.17: Image of the prepared small-molecule microarray following strategy II (6,042 spot/slide with an average spot diameter of 200 μm).

This small-molecule microarray was used to screen ligands for β-TrCP1. Compounds that interact with the target protein were detected by incubating the microarray with an anti-β-TrCP1 primary mouse antibody which was recognised by a secondary antibody containing a fluorescent label (Cy3-conjugated Donkey anti-Mouse IgG secondary antibody).

To eliminate assay false positives, non-specific interactions from the antibodies used for the assay towards the small molecules immobilised onto the

array were investigated. Firstly, the small-molecule microarray was incubated with the Cy3 conjugated donkey anti-mouse IgG secondary antibody and the comparison of fluorescence before and after incubation was evaluated. No false positives were detected as a result of the interaction between the secondary antibody and the immobilised compound library.

Secondly, incubation of the small-molecule microarray with the two antibodies used for the assay was investigated in order to detect possible non-specific interactions between the first antibody and the compound library. The slide was first treated with monoclonal mouse anti-β-TrCP1 for 4 h and subsequently incubated with the secondary antibody as previously. Slides were washed and dried and finally scanned with a Cy3 filter with a microarray scanner (Genetix 4200AL, Axon). Fluorescence intensities before and after the antibody binding clearly showed the existence of non-specific interactions. In order to eliminate these false positives, the fluorescence data collected from this assay was used as the background to be substracted from the posterior binding assay experiments with β-TrCP1.

Finally, the binding assay of β-TrCP1 was carried out by incubation of the protein with the small-molecule microarray at 4 ºC overnight and subsequent incubation with antibodies (**Figure 2.18**).

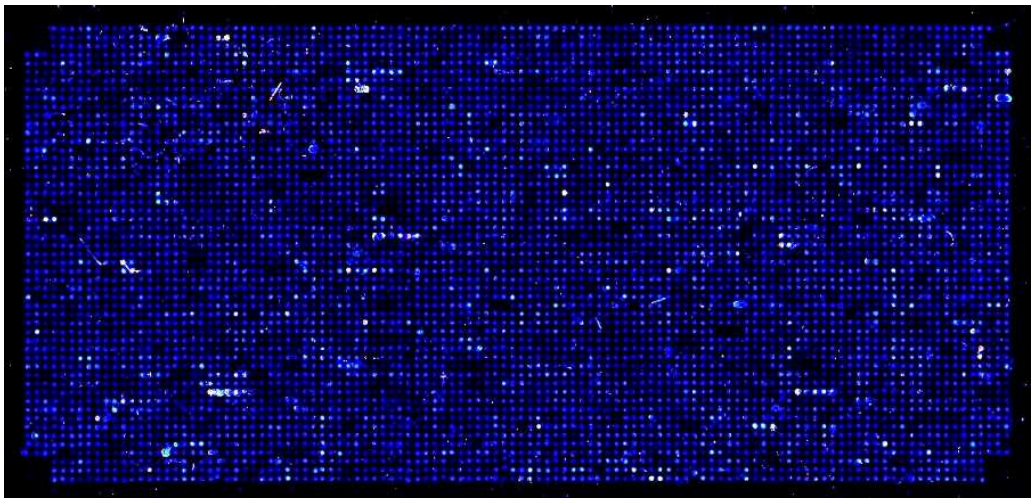

Figure 2.18: Fluorescence image of the microarray after incubation with β-TrCP1 and primary and secondary antibodies. Each compound of the library was printed in triplicate in different positions of the slide.

After the first set of data was collected, the slide was washed at 70 ºC for 1 h with water and the bioassay was carried out for a second time. Data were collected and the process was repeated, thus giving three sets of data for

binding. Data treatment generated a list of binders, with many compounds seen in all three lists (**Table 2.3**). Some of the compounds found as potential binders had been already assessed by fluorescence polarisation solution assays and showed inhibition activity towards β-TrCP1. This was indicative of a good assay performance and background correction.

	Binding Assay 1	Binding Assay 2	Binding Assay 3
1	Rutilantinone	Pyrromycin	Pyrvinium Pamoate
2	Pyrromycin	Pyrvinium Pamoate	Pyrromycin
3	Derrubone	Doxorubicin	Fenofibrate
4	Quinacrine Hydrochloride	Dehydrovariabilin	Grayanotoxin I
5	Chlorhexidine	Bisanhydroturilantinone	Phloretin
6	Pyrimethamine	Fenofibrate	Dichlorophene
7	Doxorubicin	Rutilantinone	Benzbromarone
8	Thioridazine Hydrochloride	Dichlorophene	Pimozide
9	Grayanotoxin I	Naphazoline Hydrochloride	Auraptene
10	Pyrvinium Pamoate	Hexachlorophene	Hexachlorophene
11	Tyrothricin	Bithionate Sodium	Pararosaniline Pamoate
12	Purpurin	Auraptene	Gentian Violet
13	Perillyl Alcohol	Pararosaniline Pamoate	Pomiferin
14	Tannic Acid	Tannic Acid	Tannic Acid
15	Daunorubicin	Benzbromarone	Bithionate Sodium
16	Thiostrepton	Daunorubicin	3,4'-Dimethoxyflavone
17	Indapamide	Gentian Violet	1,4,5,8-tetrahydroxy-2,6-Dimethylanthroquinone
18	Epirubicin Hydrochloride	Gambogic Acid Amide	Pyrimethamine
19	Aristolochic Acid	3,4'-Dimethoxyflavone	Pachyrrhizin
20	Hexachlorophene	Probucol	Tyrothricin
21	Bithionate Sodium	Trazodone Hydrochloride	Thioridazine Hydrochloride
22	Bisanhydrorutilantinone	Dibutyl Phthalate	Aristolochic Acid
23	Dehydrovariabilin	Pyrimethamine	Resveratrol
24	Dichlorophene	Gossypol	Gossypetin
25	Pimozide	Pomiferin	Gossypol

Table 2.3: 25 first hits of the 3 binding assays carried out where those compounds that are in all three assays in these positions have been highlighted.

In order to reassess potential binders found from the whole library screens, a "short list" of 80 compounds was generated (**Appendix II**). This list was built up of putative ligands found in the first positions of the three binding assays and compounds that showed no activity (as negative controls). These compounds were spotted again in quadruplicate and in 6 different grids distributed along the slide and screened against β-TrCP1 (**Figure 2.19**).

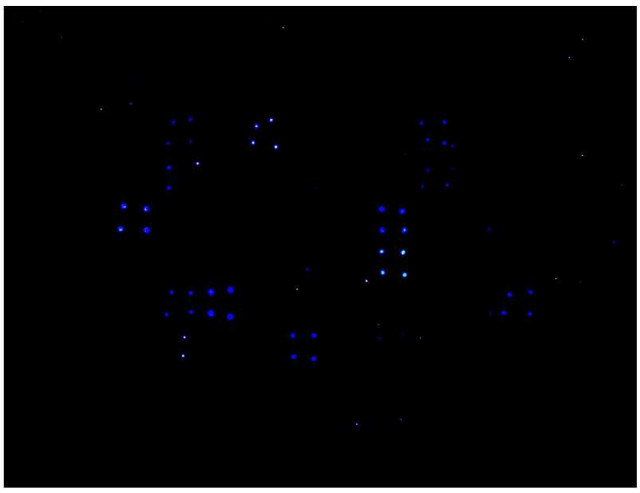

Figure 2.19: Scanning of one of the six grids with quadruplicates of the 80 printed compounds after incubation with β-TrCP1.

The top 10 potential binders identified for β-TrCP1 are shown in **Table 2.4**. These compounds were analysed by fluorescence polarisation solution assay to determine their inhibition activity towards β-TrCP1. The fluorescence polarisation assay consists of a modified sustrate with a fluorophore for the target protein (β-TrCP1), in this case β-catenin was modified with fluorescein. The fluorophore is excited with polarised light. Only fluorophores parallel to the light absorb and are excited. The excited state has a lifetime before the light emission occurs. During this time the labelled fluorophore molecule rotates and the polarisation of the light emitted differs from the excitation plane, giving a fluorescence polarisation response as mP (milli-polarisation level). The rotational speed of a molecule is dependent on the size of the molecule. The basic principle is that the substrate is small and rotates rapidly (low polarisation), however, when the labelled compound binds to a larger molecule, its rotation slows down considerably and its fluorescence becomes polarised. As a result, when a molecule which can displace the substrate form the target is added, the inhibition activity can be measured as a change in polarisation (mP).

Compound	mP (10 µM)	% inhibition	mP (100 µM)	% inhibition	Conclusion
4'-Methoxy Chalcone	110.3	10.2	112.6	6.5	Inactive
Curcumine	232.2	-	261.2	-	Fluorescent
Trazodone HCl	110.4	10.0	111.5	8.3	Inactive

Tyrothricin	116.1	-	251.3	-	Fluorescent
Grayanotoxin I	111.0	9.1	107.8	14.2	Inactive
Dehydrovariabilin	108.8	12.6	109.2	12.0	Inactive
Derrubone	111.1	9.0	108.3	13.5	Inactive
Dichlorphene	105.3	18.4	97.5	30.9	Weakly active
Thiostrepton	110.3	10.2	110.6	9.8	Inactive
Gambogic Acid Amide	114.5	-	144.6	-	Fluorescent

Table 2.4: Top 10 potential binders identified after screening the 80 selected compounds from SPECTRUM library and the results from fluorescence polaritsation solution assays in mP values and percentage of inhibition for each concentration.

The results from the solution assay showed that one compound was weakly active with 30% of inhibition activity at a 100 μM concentration and the rest were inactive or could not be determined as a result of the intrinsic fluorescence of the compound.

2.11. Conclusions

The experiments presented demonstrated two different ways to immobilise compounds in an array format by means of carbene insertion chemistry. Both methods use fluorinated surfaces which avoid or limit non-specific interactions of proteins with the glass surface, and thus improve the signal-to-noise ratio. Comparison of the two methods suggested that the second strategy, in which the slide surface was functionalised with TFMAD **4** by non-covalent interactions using a fluorous surface, was more sensitive as it could detect lower concentrations of printed small molecules and involved a much simple surface preparation procedure. In addition, it was shown that the slides of immobilised compounds could be re-used several times with simple washing away of the protein that was being interrogated under de-naturing conditions.

Once the approach was optimised, a 2,000 compound library was immobilised and screened against β-TrCP1, a protein with oncologic interest. The β-TrCP1 screens produced a ranking of 25 molecules that would bind and potentially act as inhibitors or inducers of β-TrCP1. These compounds were re-printed and reassessed again to obtain the top 10 "hit" list. These compounds were analysed by fluorescent polarisation based assays in order to detect displacement of the natural β-TrCP1 ligand. The assay identified one of the compounds as weakly active with 30% of inhibition activity towards β-TrCP1 at 100 μM concentration. However, three of the top ten hits could not be analysed

in depth due to their intrinsic fluorescence. This highlights one of the weaknesses of the affinity based assays in that compounds might well bind to the target, but actually be totally passive with respect to β-TrCP1 inhibition (i.e they could bind in non-responsive positions).

Although the results reported have not identified potent inhibitors for β-TrCP1, the approach developed could be a useful tool for the screening of other libraries of compounds where potential binders could be found or for the screening of other proteins of interest. However, more experiments would be needed to make this approach a reliable tool for protein screening.

***Chapter III*:**

Fluorescent Probes for Cargo Attachment and Cell Delivery

3.1. Introduction

Many biologically active compounds, including various large molecules, need to be delivered intracellularly to exert their therapeutic effect. These compounds need to be sufficiently soluble in the intracellular media and at the same time sufficiently hydrophobic to allow membrane penetration as the lipophilic nature of the biological membranes restricts direct intracellular translocation. As this is difficult to accomplish, several carrier-mediated delivery systems have been developed.[256, 257] One of these approaches involves tethering molecules to peptides that can translocate through the cellular membrane, thereby enhancing delivery into the cell.[258]

3.1.1. Cellular Membrane

The cellular membrane is a complex fluidic phospholipid bilayer embedded with proteins that control the intracellular flux of compounds circulating extracellularly due to its selective permeability (based predominantly on ionic charge, hydrophobicity, and size).[259] The phospholipid bilayer is arranged such that the polar ends of the molecules form the outermost and innermost surface of the membrane while the non-polar ends mingle at the center of the membrane (**Figure 3.1**). Other complex lipids are also present in lesser amount such as cholesterol, which makes the membrane less permeable to most biological molecules and adds rigidity. Lipids allow diffusion control across the

membrane: prevent loss of polar compounds such as proteins, acid or ions but permit the passive diffusion of hydrophobic materials.

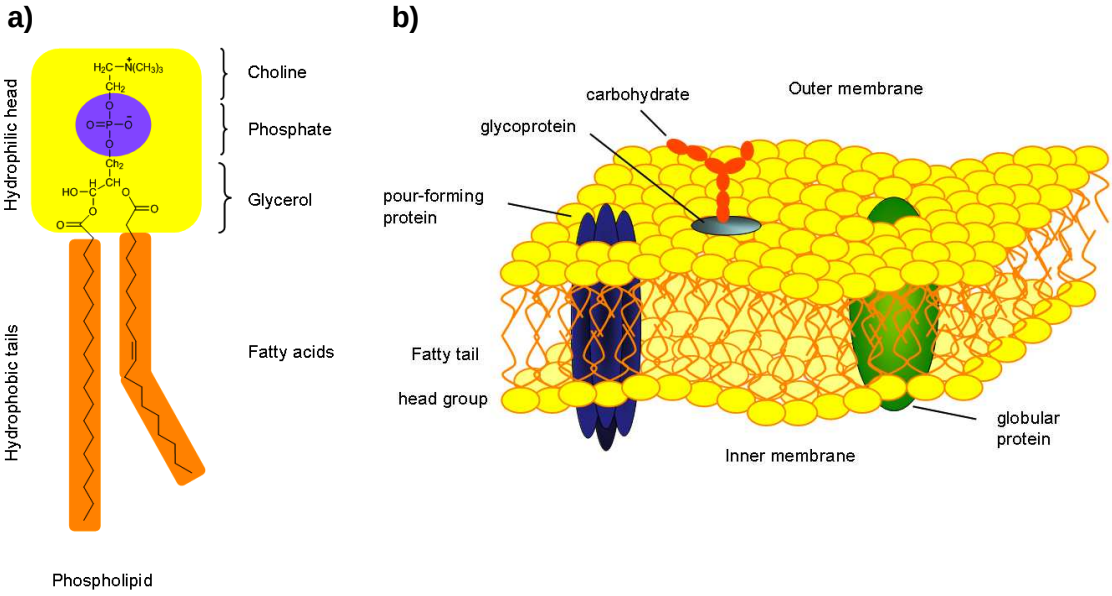

Figure 3.9: Schematic representation of a) the phospholipid structure that makes up the lipid bilayer and b) the cellular membrane and its components.

Membrane proteins allow numerous cellular functions to occur such as transport, cell signalling, and adhesion. Channel proteins form pores for the free transport of small molecules and ions to pass through without coming in direct contact with lipid interior. Carrier proteins facilitate diffusion and active transport of specific molecules and ions that cannot cross on their own. For cell signalling, receptor proteins bind to specific molecules such as hormones and cytokines, this interaction triggering a series of membrane and intracellular events that alters the activity of the target cell. Finally, cell adhesion molecules are important in the cell's ability to recognise "self" and in cell-to-cell interactions. As a result of this complexity, selective substances cross the cytoplasmic membrane of eukaryotic cells by different transport methods such as simple diffusion, osmosis, active transport, endocytosis, and exocytosis.

The complexity and the selective permeability of the cellular membrane represent a challenge for drug development as foreign materials such as nucleic acids and proteins are not able to translocate the cellular membrane alone and require a delivery vehicle. The principal delivery vehicles being explored include: microspheres,[260] cationic lipids,[261] polymers[262] and dendrimers,[263] multi-walled carbon nanotubes (MWNTs)[264] and cell penetrating peptides (CPPs).[258, 265]

3.1.2. Cell-Penetrating Peptides

A strategy for promoting cellular delivery of poorly permeable materials into cells is based on the conjugation to cell-penetrating peptides which enhance translocation across the cellular membrane, while organelle specific targeting can also be mediated by specific peptides. The mechanism of translocation occurs by a non-toxic process, apparently independent of membrane receptors although the mode of action is still subject to debate.[266] Cell-penetrating peptides are short peptides of less than 30 amino acids and are classified into two structural types: polycationic or amphiphatic.

Polycationic peptides are highly rich in basic residues (lysine and arginine) such as the TAT peptide (GRKKRRQRRRPPQ),[267-269] and they posses an overall positive charge. Short oligomers sequences made of Arginines[267, 269] or Lysines[270] have also been shown to enable or enhance uptake of agents into the cells that do not enter or do so poorly.

In contrast, amphiphatic cell-penetrating peptides consist of sequences with an alternating pattern of polar and non-polar residues, such as transportan (GWTLNSAGYLLGKINLKALAALAKKIL),[271] penetratin (RQIKIWFQNRRMKWKK),[266] and MAP (model amphiphatic peptide) (KLALKLAKALKAALKLA),[272, 273] and they exhibit the ability to be arranged in amphipatic α-helical structures.

The use of peptides with cell-penetrating properties as delivery carriers allows modifications of the peptide sequence to yield carriers addressing different cellular subdomains and/or able to transport various types of cargoes. A cargo can be bound to the cell-penetrating peptide covalently or through either electrostatic or hydrophobic interactions, and its molecular weight can be several times greater than the cell-penetrating peptide.[274]

Details on the nature of cell-penetrating peptides, their proposed mechanisms of translocation, and their involvement in the delivery of therapeutic agents have been reviewed recently.[258, 265, 275] In addition, a range of peptidomimetics, such as peptoids[276-279] and β-peptides[280], structurally inspired by the cell-penetrating peptides have been reported with improved delivery properties.

3.1.2.1. ***Peptoids as Delivery Agents***

Peptoids are N-alkylated Glycine derivatives in which the amino acid side chains are shifted from the α-carbon to the amino functionality (**Figure 3.2**).

a) 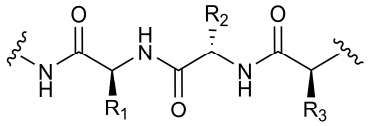

b) 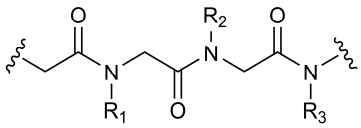

Figure 3.2: schematic comparison between a peptide (a) and an oligomer of N-substituted Glycines or "peptoid" (b) sequence, showing the similarity of spacing of the side chains, and the lack of stereochemistry of the peptoid monomers.

Like peptides, peptoids are prepared by standard solid phase techniques as a succession of building blocks linked together by amide bonds and the distance between two consecutive side chains is the same in both structures.[277, 278, 281, 282] However, peptoids are achiral peptidomimetics (except for any chirality found in any side chain). The advantage of peptoids, as for peptides containing D- and β-peptides, is that they are resistant to proteolysis, and are therefore advantageous for therapeutic applications.[283] Since the secondary structure of peptoids does not involve hydrogen bonding, they are not typically denaturated by solvent, temperature, or chemical denaturants such as urea.

Peptoids inspired on cell-penetrating peptides, such as polyArginine or polyLysine, have been shown to have good cell permeability characteristics in a wide range of cell lines, with the ability to transport a variety of drugs and cargo molecules into cells and tissues.[279, 282, 284, 285] Hybrids of polyLysine-like peptoids with peptide localisation sequences have shown the ability of intracellular targeting.[286, 287]

3.1.3. Nuclear Localisation Sequences

The nuclear envelope or nuclear membrane is a double membrane that is continuous with the endoplasmatic reticulum. It encloses the genetic material in eukaryotic cells and serves as a physical barrier, separating the contents of the nucleus from the cytosol.

Transport of proteins to the nucleus, as opposed to some other cellular compartments,[288, 289] is unique because of the presence of pore complexes in the nuclear membrane. Nuclear pore complexes represent discontinuities in the phospholipid bilayers of the double nuclear membrane that are potentially available for protein transport. Small proteins appear to diffuse freely across the

nuclear membrane, but a selective mechanism regulates the entry of larger proteins.[290]

The selectivity of large nuclear protein import resides in nuclear localisation signals (NLS), which are present only in nuclear proteins. Transport signals are specifically bound and recognised by importins in the cytoplasm, and the resulting complexes cross the nuclear envelope (**Figure 3.3**).[291, 292] They can be located almost anywhere in the amino acid sequence and generally consist of a short sequence (typically four to eight amino acids) that varies for different nuclear proteins but is rich in Lysine and Arginine residues, and usually contains Proline. In many nuclear proteins this sequence is split into two blocks of two to four amino acids, with the blocks separated from each other by about ten amino acids. These blocks are thought to form loops on the protein surface.[293]

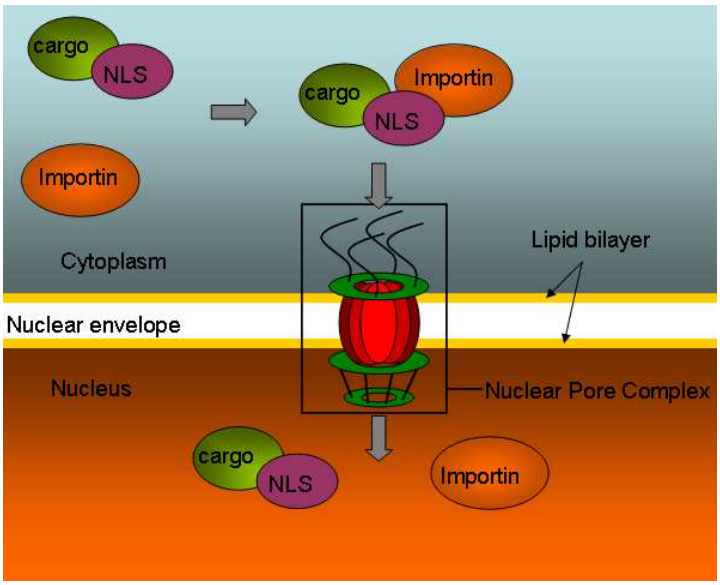

Figure 3.3: Schematic representation of nuclear import. The process starts when proteins or cargos bearing a nuclear localisation singal (NLS) are recognised by importins and form a complex that localises to the nuclear envelope and docks at the nuclear pore. Once translocation through the pore is executed using ATP, the complex is destabilised and dissociated, facilitating cargo release.

Nuclear localisation signals were first indentified in the large viral protein T-antigen, encoded by the SV40 virus and needed for viral DNA replication in the host cell nucleus.[294] This signal comprises a highly basic stretch of amino acids (^{126}PKKKRKV^{132}) containing five consecutive positively charged residues.[295] There is an absolute requirement for a positive charge at the position of the second Lysine, with the next three positive charges having less effect on transport.[294, 296] Since then, several nuclear localisation signals have been identified, together with their import receptors that recognise and bind them.[297-300]

NLS peptides coupled by way of covalent linkers have already been demonstrated to confer nuclear localisation on a variety of proteins, e.g., BSA and ferritin,[296] and even molecules as large as IgM.[301] In addition, the NLS sequence conjugated with a different classes of biomaterials, such as nucleotides,[302] peptidic materials[303] and drugs,[304] have also been reported as an efficient and very specific mechanism for transporting cargos into the nucleus. Thus, NLS may have applications in drug delivery, where the therapeutic agent in question has its specific target site of action within the nucleus, for example some anticancer drugs.

3.1.4. Colchicine & Anticancer Drugs

The water-soluble alkaloid Colchicine (**Figure 3.4**) is extracted from the bulb of meadow saffron or Colchicum. Colchicine blocks or suppresses cell division by inhibiting mitosis, the division of a cell's nucleus. Specifically, it inhibits the development of spindles as the nuclei are dividing by binding to tubulin, one of the main constituents of microtubules.[305] Normally, the cell would use its spindle fibers to line up its chromosomes, make a copy of them, and divide into two new cells with each daughter cell having a single set of chromosomes. With Colchicine present, the spindle fibres do not form, and so the cell cannot move its chromosomes around.[306] The cell may end up copying some or all of the chromosomes anyway, but cannot parcel them out into new cells, and so it never divides.

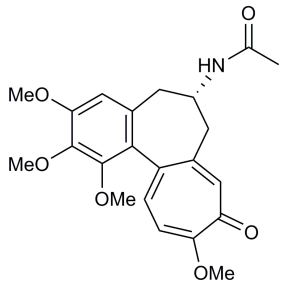

Figure 3.4: Colchicine anticancer drug structure.

Since one of the defining characteristics of cancer cells is a significantly increased rate of mitosis, cancer cells are significantly more vulnerable to Colchicine poisoning than normal cells are. Unfortunatelly, the therapeutic value of Colchicine against cancer is limited by its toxicity against normal cells. However, Colchicine is nowdays used to treat gout and familial Mediterranean fever as it also has anti-inflammatory effects, by inhibiting neutrophil motility

and activity, and the deposition of uric acid crystals which is a vital aspect of the mechanism of gout.[307-310]

The crucial role of the mitotic spindle in cell division has been identified as an important target for anticancer drug development.[311, 312] However, drug delivery in cancer chemotherapy has two main limitations. Firstly, the selectivity of chemotherapeutic agents for cancer cells is often low. As a consequence, the drug does not reach a given concentration close to the tumor cells and higher doses of anticancer drugs must be given resulting in unacceptable toxicity to normal tissues. Secondly, the water solubility of the chemotherapeutic agent must be high in order to gain access to tumor cells surfaces *via* the circulatory system as well as good lipid solubility to allow penetration of the cancer cell plasma membrane upon arrival at the cell surface. These two solution properties are often difficult to design into the same drug molecule. Consequently, there is a need for a new method of administration that could concentrate the drug close to the tumour site.

Several solutions have been proposed for increasing the efficacy of chemotherapy while reducing adverse effects. On one side, carrier systems have been used to enhance cell penetrability and solve solubility problems.[313] And, on the other hand, folic acid has been conjugated to anticancer drugs to generate high specificity of these drugs to cancer cells by receptor-mediated endocytosis as a result of the overexpression of folate receptors on cancer cells, which in turn also reduces permeability barriers due to drug solubility.[314, 315]

3.1.5. Flow Cytometry

Flow cytometry is a powerful technique that allows the measurement of multiple parameters of individual particles in heterogeneous samples. When a sample in solution is injected into a flow cytometer, the particles are randomly distributed in a three-dimensional space and ordered into a stream of single particles that can be interrogated by the machine's detection system. This process is managed by the fluidics system.

Essentially, the fluidics system consists of a central channel/core through which the sample is injected, enclosed by an outer sheath that contains faster flowing fluid. The difference in fluid velocity creates a massive drag effect on the narrowing central chamber, called hydrodynamic focusing, which creates a single line of particles (**Figure 3.5**). Then, each particle passes through one or more laser beams. The light that emerges from each cell passing through a laser beam

is captured. Light scattering or fluorescence emission provides information about the particle's properties.

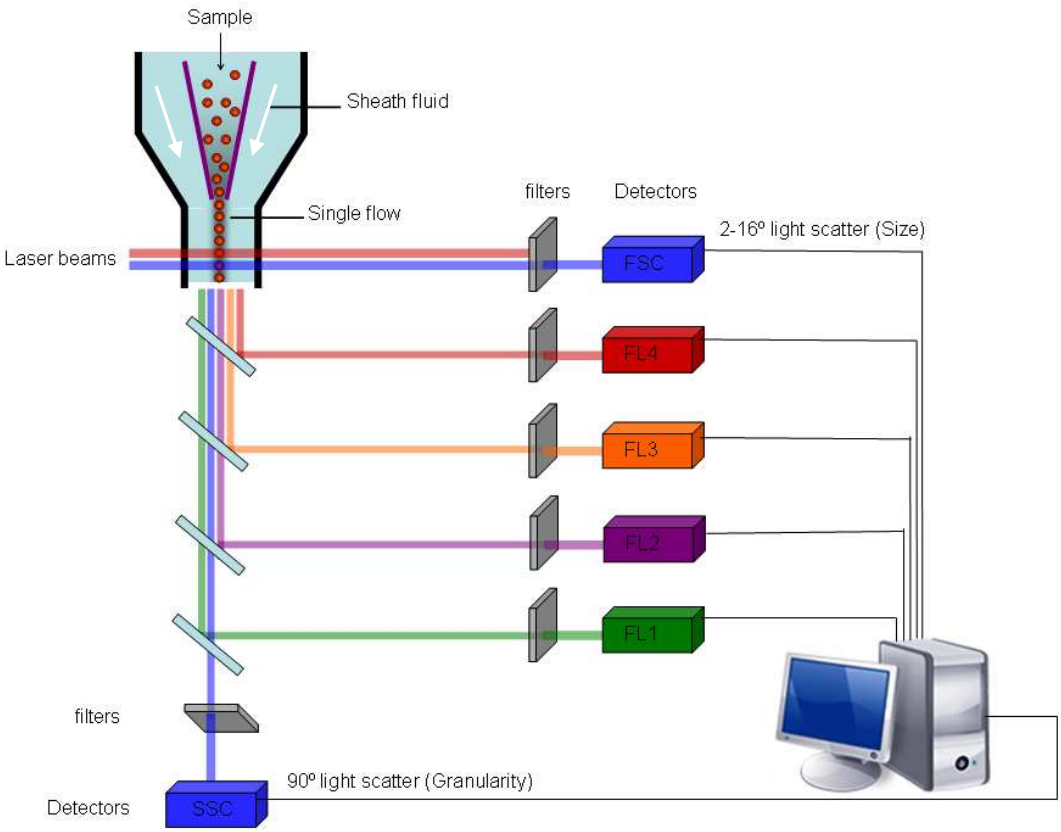

Figure 3.5: Overview of a typical flow cytometry setup.

Light that is scattered in the forward direction is collected by a detector known as the forward scatter channel (FSC) and its intensity equates to the particle's size and can also be used to distinguish between cellular debris and living cells. The side scatter light (SSC) is collected at 90º to the excitation line and provides information about the granular content within a particle. Both FSC and SSC are unique for every particle, and a combination of the two may be used to differentiate different cell types in a heterogeneous sample. On the other hand, fluorescent measurements taken at different wavelengths can provide quantitative and qualitative data about fluorescently-labelled cells. The data gathered can be analysed statistically by flow cytometry software to report cellular characteristics such as size, complexity, phenotype, and health.

3.2. Aim of the Project

The aim of this project was to develop a general method for cellular delivery. Probes were prepared incorporating the TFMAD photophore (**Chapter I**) in order to capture any desired cargo and a fluorescent dye to allow probe detection by microscopy and flow cytometry. One of the probes also contained a nuclear localisation sequence (PKKKRKV) to mediate intracellular delivery (**Scheme 3.1**). Cargos were covalently bound to the probe by irradiation at 365 nm. Optimal conditions for cargo capture were determined by using a peptoid as a model cargo and comparing the cell penetrability abilities of each sample. Probes were characterised by their cellular uptake efficiency, their toxicity and cellular localisation, and finally, they were applied to study their effect on the improvement of delivery efficiency and therapeutic effect of a cancer drug.

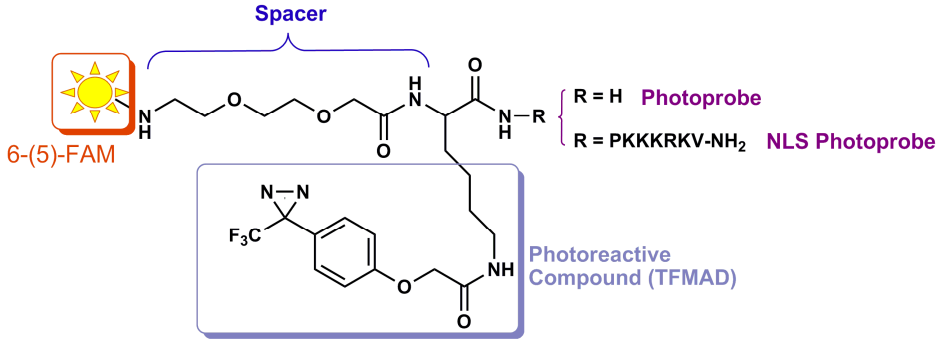

Scheme 3.1: Schematic representation of photoreactive probes prepared in this chapter. Both probes contained 6-(5)-carboxfluorescein dye linked by a PEG spacer to the photoreactive compound TFMAD **4**. The only difference between them was the presence of the NLS sequence (PKKKRKV).

3.3. Probe Synthesis

Probe synthesis was achieved *via* solid phase using Fmoc-Lys(Dde)-OH. The orthogonality of the Dde and Fmoc protecting groups allowed the selective substitution of the two amino functionalities, thus introducing branches for functionalisation.[316]

Dde-OH **34** was prepared from dimedone and acetic acid in the presence of DCC and DMAP in DMF (**Scheme 3.2**). Dde-OH **34** was successfully condensed to the side chain residue of Fmoc-Lys-OH using microwave irradiation and the presence of catalytic amounts of TFA to give Fmoc-Lys(Dde)-OH **35** with an overall yield of 69%.

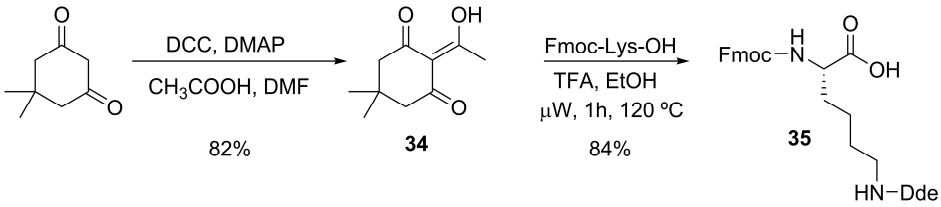

Scheme 3.2: Preparation of Fmoc-Lys(Dde)-OH.

The synthesis of the first photoprobe started with the loading of aminomethyl polystyrene resin with the Rink Amide linker under microwave irradiation for 20 min at 60 ºC followed by Fmoc deprotection with 20% piperidine in DMF. Fmoc-Lys(Dde)-OH was then coupled to the resin under the same conditions and Dde deprotection was carried out with hydroxylamine hydrochloride and imidazole. To the free amino group on the side chain was coupled TFMAD (**Scheme 3.3**).

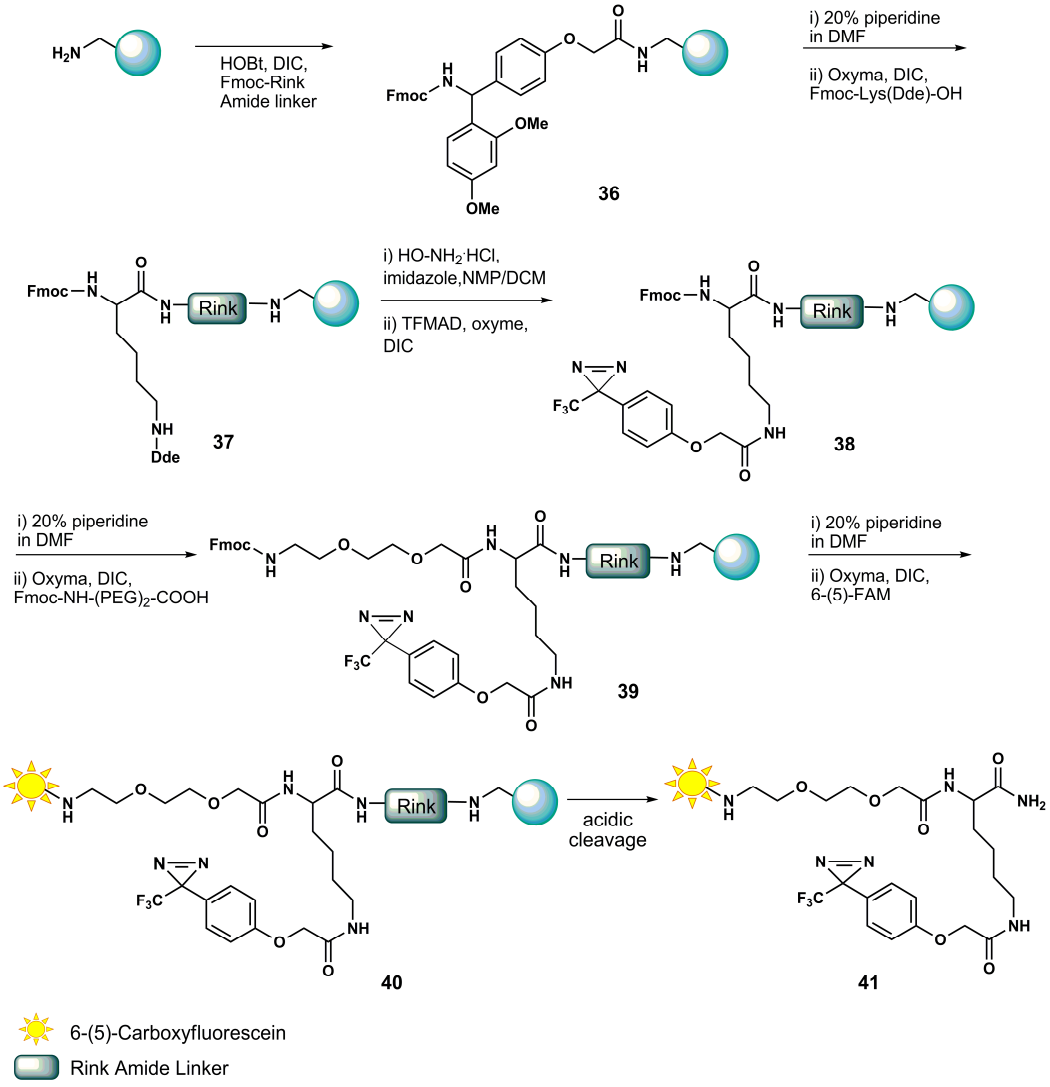

Scheme 3.3: Synthetic route to photoreactive probe **41**.

After TFMAD photophore coupling, deprotection of the Fmoc group and subsequent PEG coupling was performed to separate the photophore and the dye. Fmoc deprotection and 6-(5)-carboxyfluorescein coupling were carried out with a subsequent resin wash with 20% piperidine in DMF before final acidic cleavage from the resin. The probe was obtained in 64% overall yield.

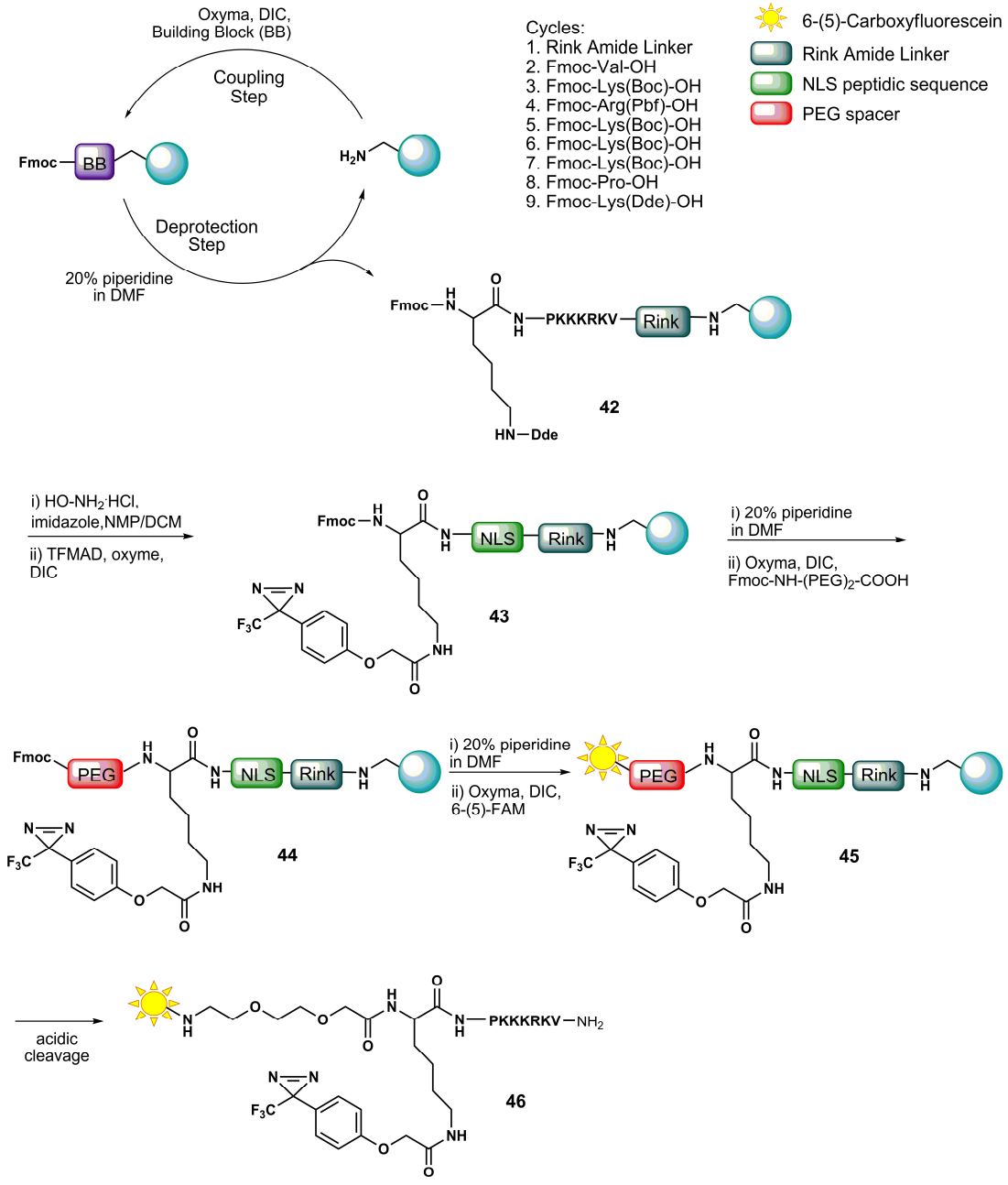

Scheme 3.4: Synthetic route of NLS photoreactive probe **46**.

The NLS photoreactive probe was synthetised following the same strategy (**Sheme 3.4**). Aminomethyl polystyrene resin was loaded with the Rink linker and Fmoc deprotection was carried out. The cycle was repeated seven more

times in order to build the NLS sequence (PKKKRKV). After that, Fmoc-Lys(Dde)-OH was introduced and the same procedure as before was used to give the probe in 24% yield.

MALDI-TOF mass spectra of the NLS photoreactive probe showed the molecular mass of the probe with nitrogen loss $[(\text{Probe-}N_2)+H]^{+\cdot}$ as a result of the laser beam (nitrogen laser) used for sample ionisation that triggers the carbene generation by nitrogen liberation. It also showed the mass of the conjugate product between the NLS photoreactive probe and sinapic acid (SA) used as a matrix for sample ionisation (**Figure 3.6**).

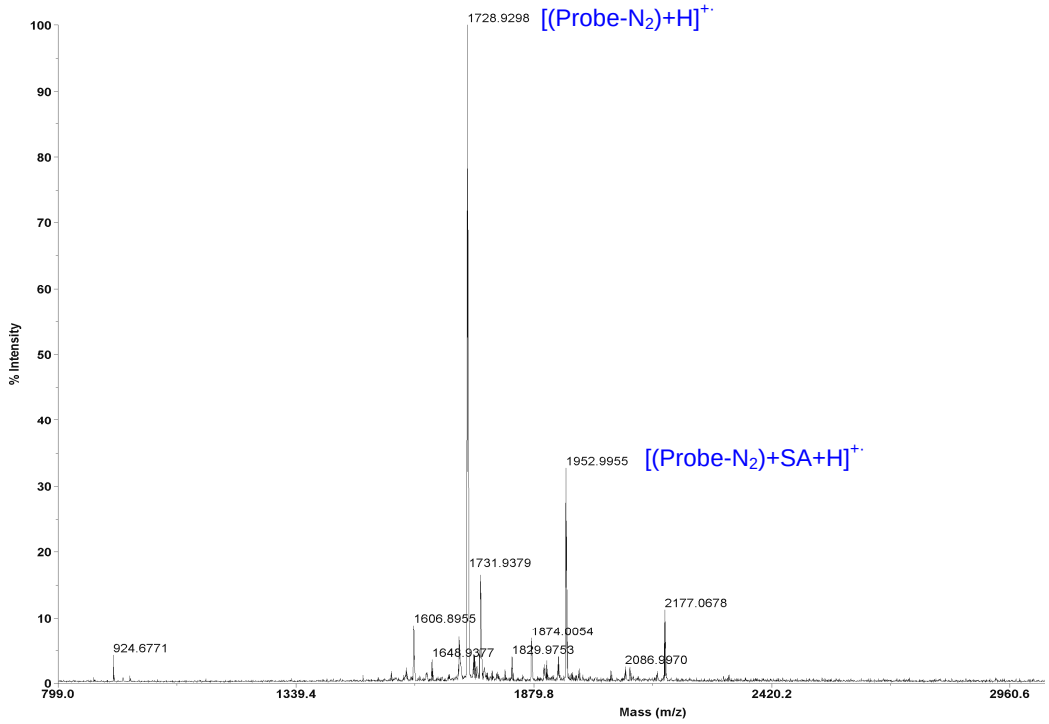

Figure 3.6: Mass spectra of NLS photoreactive probe **46**.

3.4. Time-Dependent Cellular Uptake

The time dependence of the fluorescein-tagged designed probes to enter cells was tested with HeLa cells and analysed by flow cytometry. Probes (10 and 20 μM solutions prepared using the extinction coefficient of 5(6)-carboxyfluorescein were tested in triplicate, using untreated cells and cells incubated with 5(6)-carboxyfluorescein as a negative control. Cells were analysed at different times using 0.4% Trypan Blue to quench any extracellular or membrane-associated fluorescence (**Figure 3.7** and **Graph 3.1**).[317]

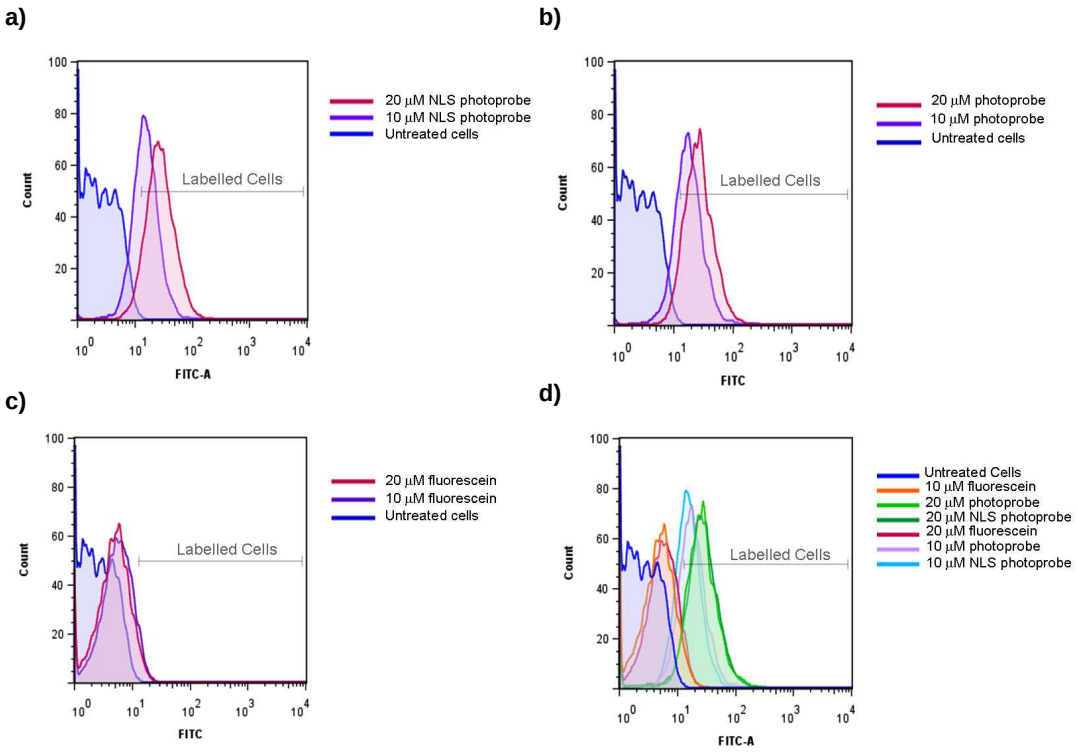

Figure 3.7: Representation of the cell population after 8 h of cellular uptake. a) NLS photoprobe **46**, b) photoprobe **41**, c) carboxyfluorescein, and d) all samples together.

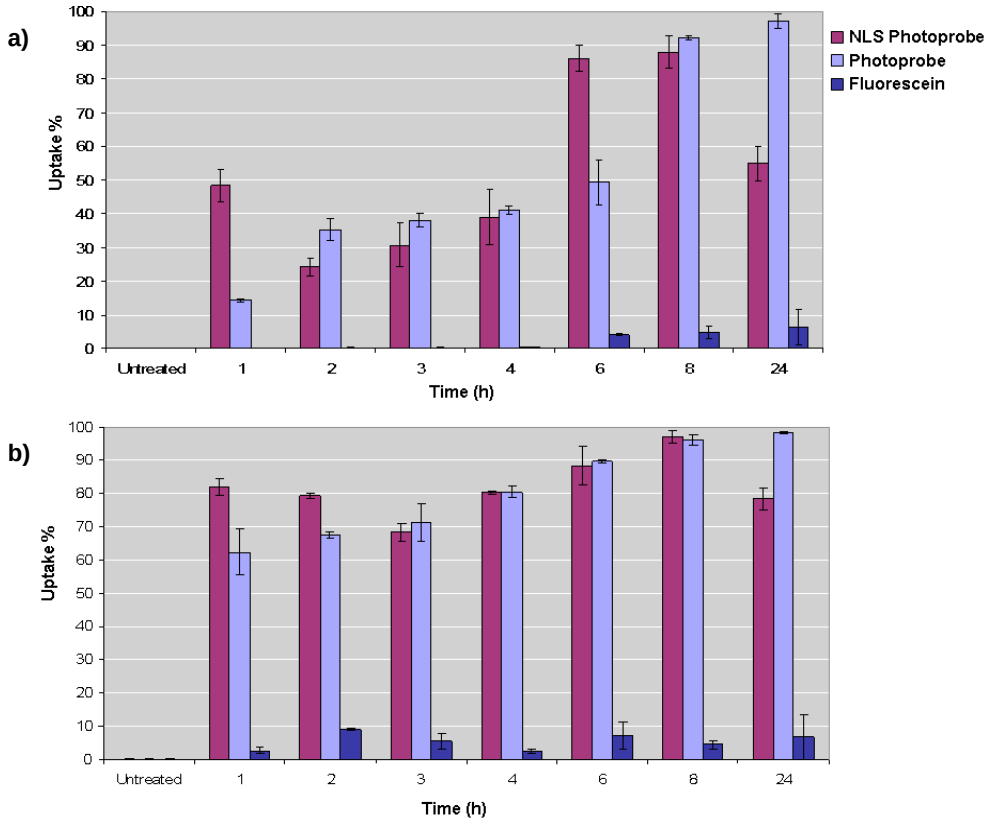

Graph 3.1: Flow cytometry analysis of cellular uptake versus time. Samples were analysed in triplicate with concentrations of a) 10 µM and b) 20 µM of photoprobes **46**, **41** and carboxyfluorescein.

Fluorescence intensity increased in a non-linear manner over time (**Graph 3.1**) pointing to a protein-mediated uptake mechanism, with rapid accumulation within the first 1 h, typically giving half the final uptake after 6h for experiments using the 10 μM probe. As expected probe cellular uptake was dependent on the concentration and was non-toxic to cells.

Both probes showed considerable cell-penetrating properties after 8 h incubation with a 50-fold or a 10-fold increase in mean fluorescence relative to the untreated cellular control or to cells treated with 5(6)-carboxyfluorescein, respectively.

3.5. Probe Cytotoxicity

The cytotoxicity of the two photoprobes was evaluated in HeLa cells exposed to increasing concentrations of each probe for 24 h (**Graph 3.2**). MTT assays use 3-(4,5-dimethylthiazol-2-yl)-2,5-dipheyltetrazolium bromide, a tetrazole which is converted by healthy cells to purple formazan crystals. Once, dissolved, the absorbance of the formazan produced can be measured (λ = 570 nm) and related to the cellular viability (taking untreated control cells as 100% viable).[318]

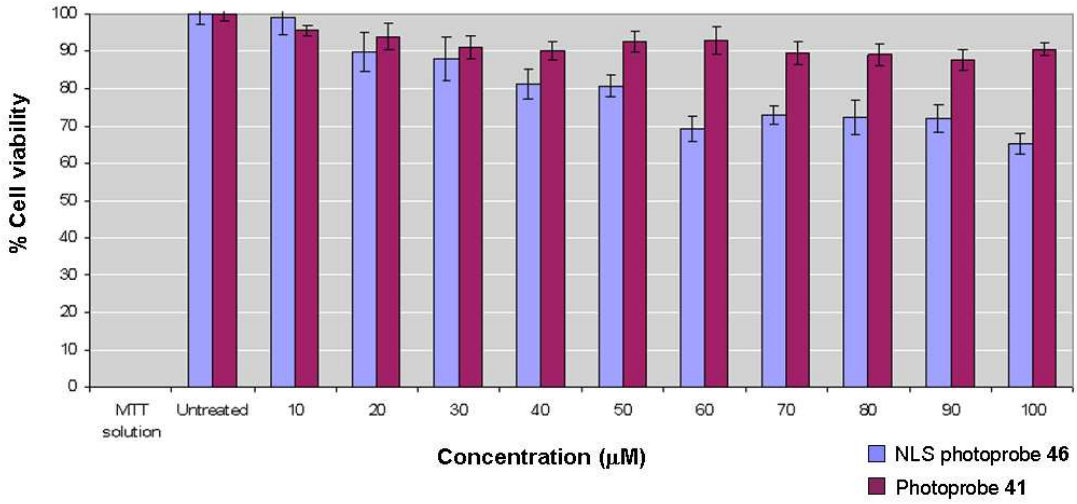

Graph 3.2: Evaluation of toxicity of photoprobe 41 and 46 toward HeLa cells using MTT assays for 24 h (n = 6).

No substantial cytotoxicity was noted in HeLa cells using photoprobe **41** at concentrations up to 100 μM (viability was generally more than 90% in all cases). NLS photoprobe **46** showed a slight toxicity effect for concentrations higher than 50 μM. The experiment demonstrated that concentrations used for the present study (10 and 20 μM) were not cytotoxic.

3.6. Nuclear Localisation

Intracellular localisation of both probes was investigated in HeLa cells using fluorescence microscopy. HeLa cells were incubated with both photoprobes, washed, fixed with a solution of 4 % paraformaldehyde and the nuclei stained with Hoechst-33342 prior to analysis by microscopy. Differences in fluorescent patterns were observed for both probes. Photoprobe **41** was localised in the cytoplasm with some "spot" accumulations (**Figure 3.8).** On the other hand, co-localisation of the photoprobe **46** fluorescence emanating from the nucleus along with Hoechst-33342 could be observed, with perceptible accumulation in the nucleolus (**Figure 3.9**).

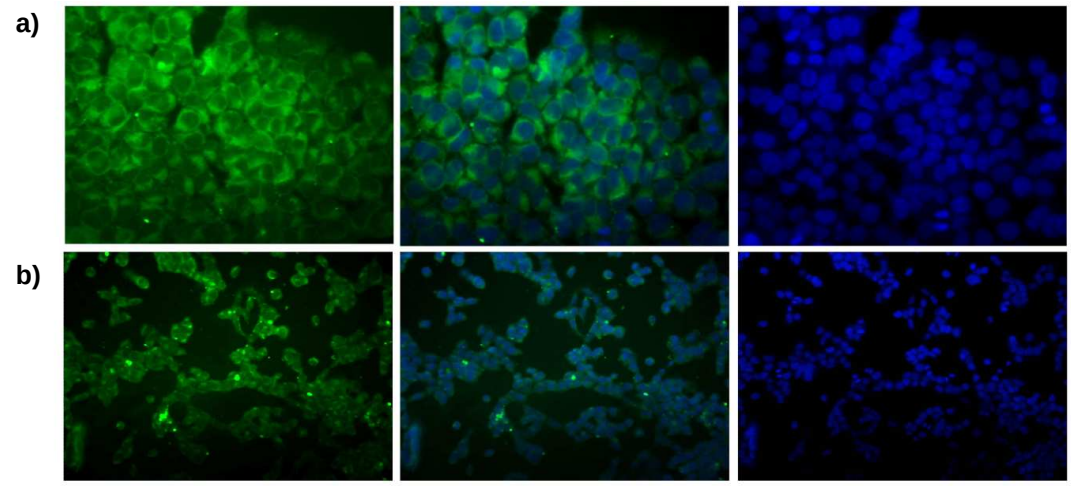

Figure 3.8: Microscopic images of HeLa cells incubated with photoprobe **41** at 50 μM for 2h: (a) 40 x, and (b) 20 x magnified. On the right, FITC fluorescence images form **41**; on the left, fluorescence images of DAPI dye staining the nucleus; and middle image is a merge of both images.

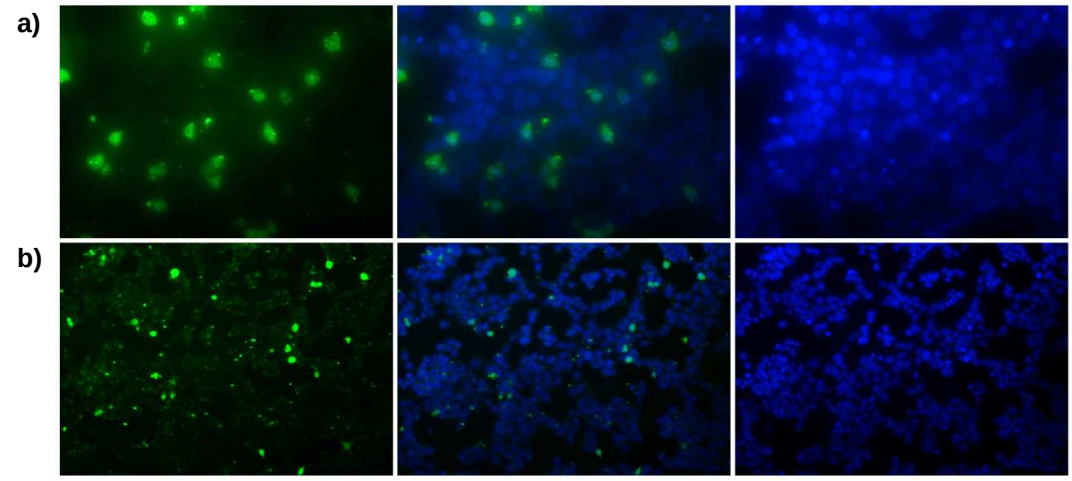

Figure 3.9: Microscopic images of HeLa cells incubated with photoprobe **46** at 50 μM for 2h: (a) 40 x, and (b) 20 x magnified. On the right, FITC fluorescence images form **46**; on the left, fluorescence images of DAPI dye staining the nucleus; and middle image is merge of both images.

Although further microscopy studies would be useful, the results strongly suggested that probe **46** localised into the nucleus as a consequence of the NLS presence unlike probe **41** which localised into the cytoplasm.

3.7. Enhancing Cellular Uptake

In order to establish the capacity of capture, an experiment was carried out where the probe was activated in the presence of a 9-mer lysine peptoid (**Figure 3.10**) with activation of the TFMAD photophore in the solid state (**Scheme 3.5**). This peptoid has the ability to deliver cargos into cells, so if the linkage between the probe and the peptoid was successful, cells would be even more rapidly labelled with carboxyfluorescein.

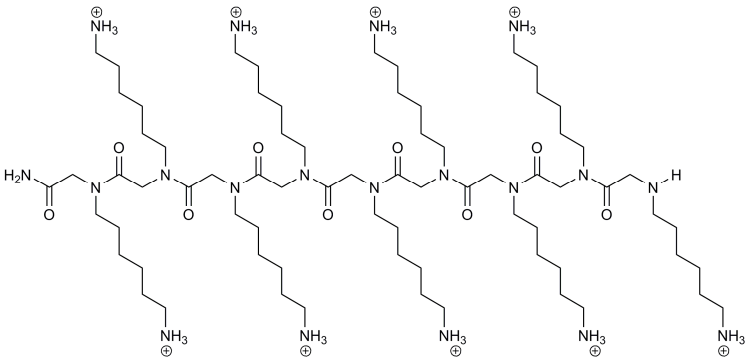

Figure 3.10: Peptoid used in this study.

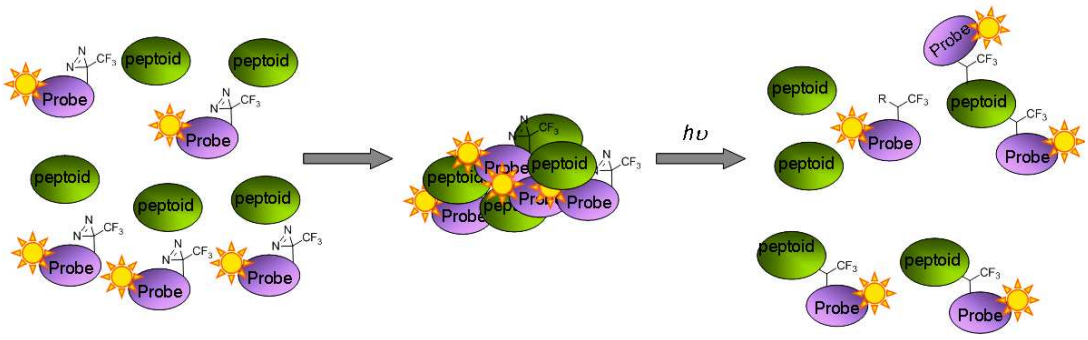

Scheme 3.5: Peptoid and fluorecently labelled probes were mixed together, the solvent was evaporated and the sample irradiated at 365 nm for 40 min, forming different peptoid-probe conjugates which would display a higher degree of penetrability into cells.

The experiment consisted of mixing different ratios of photoreactive probes and peptoid in order to find the best conditions for cross-linking. In a 96 well-plate, solutions of peptoid and photoreactive probe were mixed (mole ratios: 3:1, 2:1, 1:1, 1:2 and 1:3 (peptoid:probe)). Samples were evaporated and after irradiation for 40 minutes at 365 nm, redissolved in PBS. Negative controls were also prepared by activation of the photoprobe without peptoid.

All samples were analysed by MALDI-MS to demonstrate formation of peptoid-probe conjugates. Spectra were quite similar for all samples, all showed a mass 2287 Da which correspond to the adduct formed from probe and the peptoid and thus demonstrate the adduct was formed. A peak 1711 Da was present in all samples (being the most intensive peak) suggesting the formation of probe-probe adducts (**Figure 3.11**).

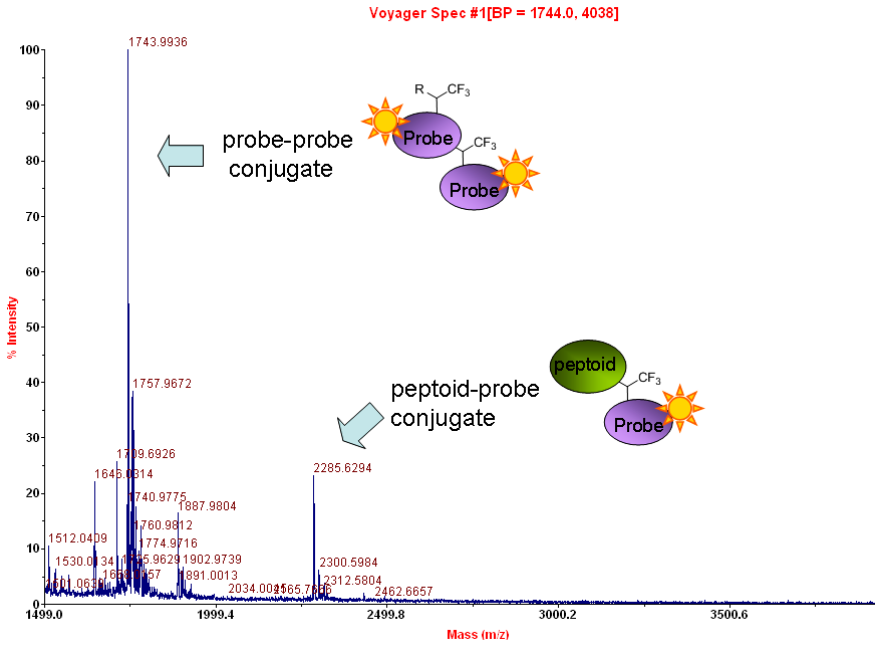

Figure 3.11: MALDI-MS spectrum of a solution 1:1 peptoid-probe after irradiation.

To assess the capture reaction efficiency of the cell-penetrating peptoid derivatives generated, experiments were carried out with HeLa cells. Solutions of 10 μM peptoid-probe conjugate were added to cells and incubated for 8 h. The same volumes of negative control samples were used. After incubation, cells were washed, trypsinised and analysed by flow cytometry (**Graph 3.3**). All cells treated with peptoid-probe conjugate solutions showed a 70 - 90% labelling of the whole population, except for the ratio 1:3, which despite containing the highest amount of probe, showed just 50%. In addition, HeLa cells treated with different concentrations of irradiated probe alone were not labelled at all presumably as a result of their cross-linking with the well plate surface when irradiated.

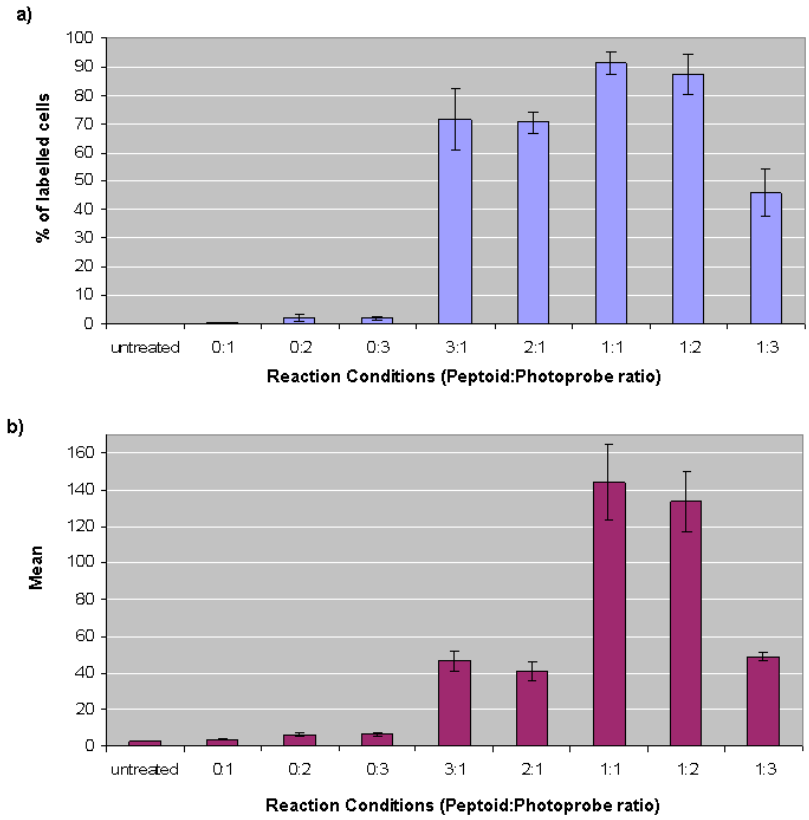

Graph 3.3: Cellular uptake of peptoid-probe adducts in HeLa cells (8 hours, n = 3). Graph a) showing the percentage of labelled cells and b) the fluorescence mean intensity relative to untreated cells.

Fluorescence values suggested that 1:1 and 1:2 were the best ratios for conjugation. Furthermore, the mean fluorescence observed in cellular uptake studies for a 10 μM photoprobe solution incubated for 8 h with HeLa cells was 20-fold and 51-fold higher than for untreated cells with probe **41** (**Graph 3.1**) and peptoid-probe **41** conjugate (**Graph 3.3**), respectively. Therefore, peptoid conjugation increased the cellular uptake properties of probe **41**.

In summary, these experiments confirmed that molecules could be captured by the synthesised photoreactive probe and that the best ratio for conjugate preparation was an equimolar quantity of probe and cargo (peptoid).

3.8. Colchicine Adduct Toxicity

In order to assess the potential use of these molecules as carriers for drug delivery, the delivery of an anticancer drug was evaluated. Conjugates of Colchicine with the NLS photoprobe **46** or photoprobe **41** were prepared (ratio

1:1) as previously described for peptoid capture. Colchicine itself was used as a positive control.

HeLa cells were treated with concentrations of 10, 1, and 0.1 μM of the Colchicine-probe conjugates. After 24 hours, cells were washed and MTT assays were performed and results were represented as cell viability (**Graph 3.4**).

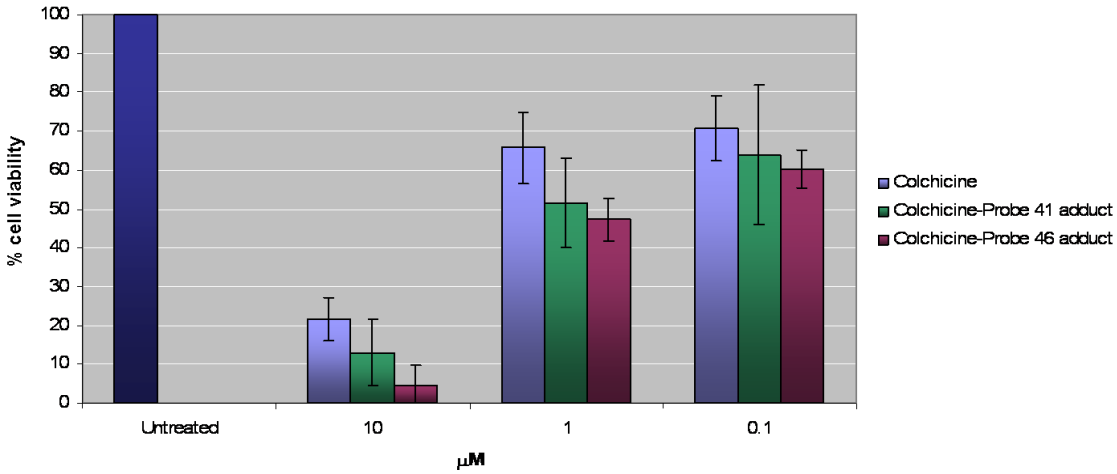

Graph 3.4: MTT assay results from 3 independent assays (n = 5).

Results suggested that the IC_{50} of Colchicine for this assay was between 1 and 10 μM as cell viability decreased from 65% to 20%, respectively. Colchicine-probe adducts also showed the same behaviour but with a small increase in effectiveness (although statistically unchanged). Images of the effect of the drug and its derivatives are shown in **Figure 3.12**.

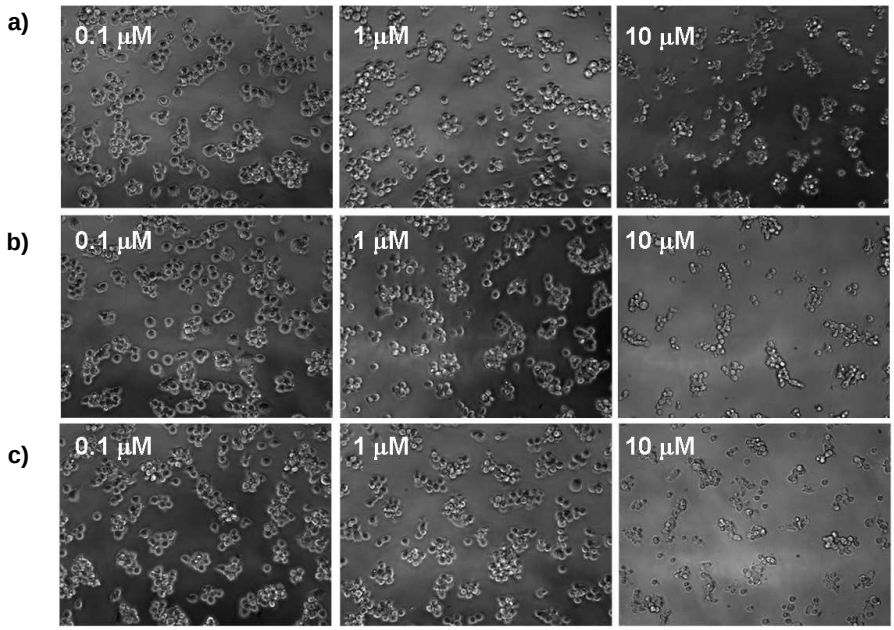

Figure 3.12: Images of cells after 24 h incubation with a) photoreactive probe-Colchicine conjugates; b) NLS photoreactive probe-Colchicine conjucates and c) Colchicine.

Although the Colchicine IC_{50} values did not decrease by orders of magnitude, the study showed that increasing the uptake and localising the drug into the nucleus probably had an effect on Colchicine effectiveness.

3.9. Conclusion

Two photoreactive probes were prepared consisting of a fluorescent dye (fluorescein) and TFMAD **4** linked by a PEG spacer. The difference between the probes was the introduction of an NLS sequence to mediate intra-nuclei targeting. Both probes, somewhat surprisingly, showed good cellular uptake properties, with an increase of 10-fold in fluorescence mean relative to cells treated with carboxyfluorescein which enters to the cell by simple diffusion. Furthermore, both probes showed no cytotoxicity for concentrations used for these studies, and despite the need of further studies, probes **41** and **46** seemed to be localised into the cytoplasm and in the nucleus, respectively.

On one hand, probe **41** was used to determine optimal conditions for cargo capture by irradiation of the diazirine moiety in the presence of a lysine-like peptoid. The best cargo:probe ratios was found to be 1:1 and 2:1. On the other hand, probe **46** was used to capture the anticancer drug Colchicine, which has its effects in the nucleus, and these photo-adducts were compared to the drug itself. Unfortunately, the results showed a minimal increase in Colchicine activity for both probes and no additional effect could be attributed to drug localisation into the nucleus by the NLS sequence.

Nevertheless, this approach opens up a new avenue for the rapid assessment and delivery of any desired compound into cells. The inclusion of the photoreactive moiety to the fluorescent probe construct provides a rapid way to tether compounds and allow analysis of their effects in cells before further studies are carried out or facilitate their cellular localization. Alternatively, these photoreactive probes could also be used for staining or fluorescent tagging specific tissues, cells or indeed cellular compartments by activation of the photoprobes once inside the cell.

***Chapter IV*:**

MICROSPHERES for GENE DELIVERY

4.1. Introduction

The main goal of gene therapy consists of delivering therapeutic genes into the nucleus of target cells to achieve expression of a deficient or incorrectly expressed gene product, thus curing genetic diseases and viral infections, slowing down tumour growth, and stopping neurodegenerative disease.[319] However, difficulties in developing safe and efficient gene delivery vectors able to sustain gene expression for long periods has limited broader clinical application of gene delivery.[320] Viral vectors have been seen as the most efficient transfection method, however they have safety issues. For this reason, efficient non-viral methods for gene delivery are needed. Although a wide range of methods and techniques have been developed, there is the need to increase the efficiency and efficacy of gene transfer and reduce toxicity. Microspheres have proven to be a very successful delivery agent for a range of different biomolecules such as sensors, proteins and oligonucleotides.[321-324] As a result, microspheres could perhaps also be used to deliver DNA into cells. In order to investigate the ability of microspheres to introduce plasmids into cells, TFMAD-functionalised microspheres were prepared and carbene insertion chemistry was used to capture DNA onto microsphere surfaces.

4.1.1. Gene Delivery

The ability to introduce DNA encoding a gene of interest into cells efficiently has been of central importance in gene therapy and biological research. In gene therapy, the expression of a particular gene is desired to correct a genetically predetermined biochemical lack of that activity, to block cell division, or to effect cytotoxicity in tumour cells. In a research context, the aim is transfer DNA in order to increase expression of a gene product under study in transfected cells, or to to oblate completely expression of a particular gene product in order to establish its function.

A plasmid contains trypically 10^3 to 10^4 base pairs with a molecular weight of 10^6 to 10^7 Da and has a supercoiled tertiary structure in aqueous solution with an effective hydrodynamic diameter greater than 100 nm.[325] Uptake of the exogeneous DNA by cells is greatly limited by its size and negative surface charge density.[326] Therefore, it has to be condensed to a size that allows it to be taken up into cells and the negative charges have to be masked.

Most of the DNA delivery systems operate at one of three general levels: DNA condensation and complexation, endocytosis, and nuclear targeting/entry. Negatively charged DNA molecules are usually condensed and/or complexed with cationic transfection reagents before delivery. These complexes are taken up by cells, usually through endocytosis, the route of uptake determines subsequent DNA release, trafficking, and lifetime in the cell. Endocytosis is a multistep process involving binding to specific receptors of the surface, internalisation, formation of endosomes, fusion with lysosomes, and lysis. The low pH and enzymes within endosomes and lysosomes usually bring about degradation of entrapped DNA and associated complexes. Finally, DNA that has survived both endocytotic processing and cytoplasmic nucleases must then dissociate from the condensed complexes and be transported through the nuclear pores and into the nucleus for transcription and expression to occur (**Scheme 4.1**).

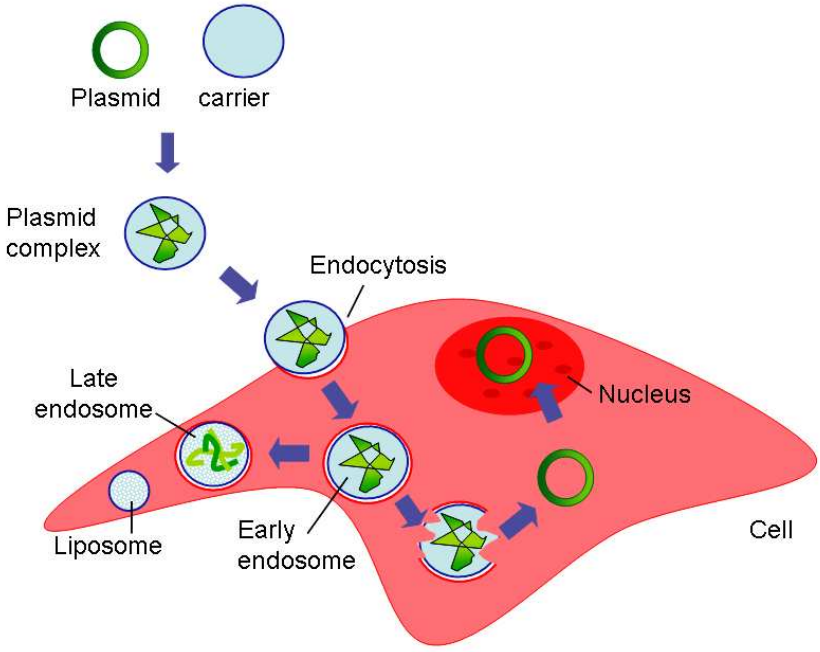

Scheme 4.1: DNA is masked with the delivery system to increase the low uptake across the plasma membrane. The formed complex enter into the cell by endocytosis forming an endosome. The endosome can become a late endosome and the plasmid be degradated or be liberated into the cytoplasm from early endosomes. The plasmid needs to enter into the nucleus for expression.

The low efficiency of DNA delivery from outside the cell to inside the nucleus is a natural consequence of this multistep process. As a result, the number of DNA molecules decreases at each step of the journey to the nucleus.[327] Therefore, the three major barriers to be addressed for an efficient DNA delivery system are the low uptake across the plasma membrane, the inadequate release of DNA molecules in the cytoplasm, and the lack of nuclear targeting. Thus, some improvements in DNA delivery efficiency have been achieved *via* the optimisation of DNA condensation, the size of DNA complexes and cell and tissue targeting while controlling cytotoxicity. All these aspects have been discussed and reviewed elsewhere.[328-331]

4.1.2. Delivery methods

Delivery methods reported in the literature can be divided into viral and non-viral. Viral-mediated gene delivery uses the ability of viruses such as adenoviruses and retroviruses to enter and express their genomes in the host cell. As a result these systems have been found to be highly efficient for delivering DNA into cells.[332] However, this type of vector also present several problems such as toxicity, immunogenicity, size limit of the exogenous DNA, difficulty of large-scale production, purification and storage, and the risk of

inducing oncogenic mutations or generating active viral particles through recombination mechanisms.[333, 334] These limitations of viral vectors justify the interest on the development of improved non-viral gene delivery vectors, which have resulted in the development of a broad range of delivery systems.[335]

The intent of chemical methods is to neutralise or obviate the issue of introducing negatively charged molecules into cells as well as to compact the DNA to facilitate its uptake. The main types of chemicals used for DNA delivery are cationic polymers, liposomes, nanoparticles and cell-penetrating peptides (CPPs) (**Figure 4.1**). The advantages of these gene transfer formulations are their ease of preparation (and scale-up) and their flexibility regarding the size of DNA to be transferred.

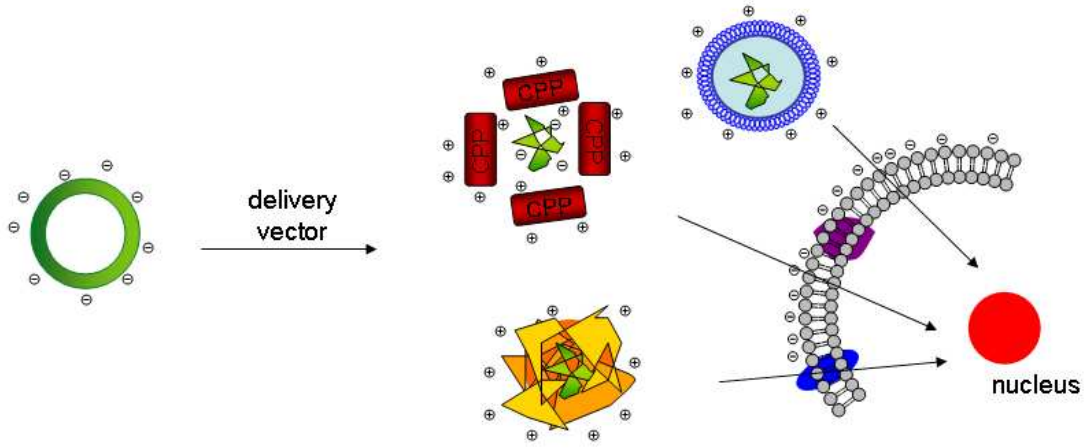

Figure 4.1: Reagents such as cationic polymers, cationic lipids or cell-penetreting peptides (CPPs) coat the DNA, neutralising or even creating an overall positive charge on the molecule.

Cationic polymers tightly associate with negatively charged nucleic acids, providing an excess of positive charge which allows the uptake of the complex by endocytosis.[336, 337] This method successfully delivers nucleic acids into cells for transient expression; that is, for short-term expression studies of a few days in duration. However, this technique is not generally useful for stable or long-term transfection studies that rely upon integration of transferred DNA into the chromosome.[338] Synthetic cationic polymers that have been used to transfer DNA into cells include DEAE-dextran, polybrene[339], and polyethyleneimine (PEIs)[340]. The biodegradable poly-L-lysine (PLL) has also been used as a delivery vehicle for DNA and small drugs for a long time. The advantages are the ease of its degradation by cells and the use of the epsilon amino group of lysine for covalently attaching ligands to the molecule to improve transfection efficiency.[341] However, PLL has a low level of transfection efficiency, primarily owing to lack of

rapid release of PLL-DNA complexes form endosomes, and suffers from immunogenicicty and toxicity.[342, 343]

Polyamidoamine (PAMAM) dendrimers are non-linear polycationic hyperbranched polymers that can bind to DNA. The interaction of dendrimers and plasmid DNA induces condensation of the nucleic acid which facilitates their uptake by endocytosis.[344-346] Commercially available PAMAM dendrimers include the SuperFect, and PolyFect transfection reagents (Qiagen).

Cationic lipids have the ability to form lipid bilayers in aqueous medium called liposomes. The cationic portion of the lipid molecule associates with negatively charged nucleic acids, resulting in compaction of the nucleic acid in a liposome-nucleic acid complex,[347, 348] which enters into the cell by endocytosis or fusion with the plasma membrane via the lipid moieties of the lipoplex.[349] New formulations make use of various lipid mixtures and cationic peptides to improve transfection efficiency, for example the addition of L-dioleoyl phosphatidylethanolamine (DOPE) aims to help DNA release from endosomes once in the cytoplasm as well as to facilitate fusion with the outer cell membrane.[350] Several cationic peptides have been used as a condensation agent to enhance uptake and facilitate the plasmid transfer to the nucleus.[341, 351]

Liposome-mediated delivery offers advantages such as relatively high efficiency of gene transfer, in vitro and in vivo applications,[352] and successful delivery of DNA of all sizes from oligonucleotides to yeast artificial chromosomes.[261, 344, 353-355] Cells transfected using liposome techniques can be used for transient expression studies and long-term experiments. However, their transfection efficiency is still unsatisfactory, especially when compared with viral vectors, and little is known of the role of charged lipids in human gene therapy and the mechanism involved in the process of intracellular gene delivery.[356] In addition, several *in vivo* studies have reported cytotoxicity of cationic lipids upon administration.[357, 358] Nevertheless, the formulations of cationic lipids for DNA transfection such as Lipofectamine, Effectene and Attractene are commercially available.

The use of **CPPs** for gene delivery is particularly interesting because they are able to efficiently condense DNA due to electrostatic interaction, improve cellular internalization and promote endosomal escape, and can provide nuclear localisation of condensates when short NLS peptides are used.[265, 359-361] There are many examples of CPP-mediated delivery of plasmid DNA into cultured cells

and also *in vivo*.[362, 363] However, their transfection efficiency improves when the peptide backbone is chemically modified by fatty tails such as stearic acid which increases efficiency of endosomal escape.[364] Coupling of CPPs to other classes of non-viral gene delivery methods, such as liposomes,[365, 366] PEI polymer[367, 368] or nanoparticles[369-371] contributes to enhance cellular association and increase nuclear delivery efficiency.[372]

Alternatively, the main physical and mechanical methods include microinjection, electroporation and particle bombardment. In general, these methods involve making a transient hole in the membrane to facilitate the delivery of compounds that would not cross the membrane alone. Following permeation, the cell membrane can repair itself. Although efficient, these methods are slow, laborious and toxic.

4.1.3. Microspheres as a Delivery Agent

Microspheres are spherical mono-disperse polymeric particles, typically created by polymerisation techniques. The Bradley group has developed methods for the synthesis of amino functionalised cross-linked polystyrene microspheres of highly defined sizes that can be employed in solid phase multi-step synthesis and have demonstrated to be an efficient delivery agent of biological cargos, including sensors,[321, 373] proteins,[323, 374] RNA,[324] and dyes.[322] Microspheres have not only high uptake efficiency in a wide range of cells,[373, 375, 376] but they also show non-toxicity and may be easily functionalised. In addition, they are not trapped within endosomes, exhibiting cytoplasmic localisation. This is beneficial as the cargo is directly administered in the cytoplasm instead of being trapped within endosomes which can be trafficked to acidic lysosomes and can result in the degradation of the cargo. For all these traits, microspheres could be a very efficient delivery system for gene transfection.

4.2. Aim of the Project

The aim of this project was to investigate the potential of these microspheres as DNA delivery agents while using the reactivity of the TFMAD photophore synthesised in **Chapter I**. Specifically, functionalised microspheres with the TFMAD photophore would be used to attach plasmids randomly onto microsphere surface. In addition, the development of this general non-selective method could be used to immobilise other biomolecules, which could interact with a plasmid and therefore capture it non-covalently. To investigate the ability

of microspheres to deliver plasmid into the cells, a plasmid that encoded green fluorescent GFP protein (pEGFP-C1) was used as a reporter and the level of transfection was monitored by measuring the expression of GFP in cells (**Scheme 4.2**).

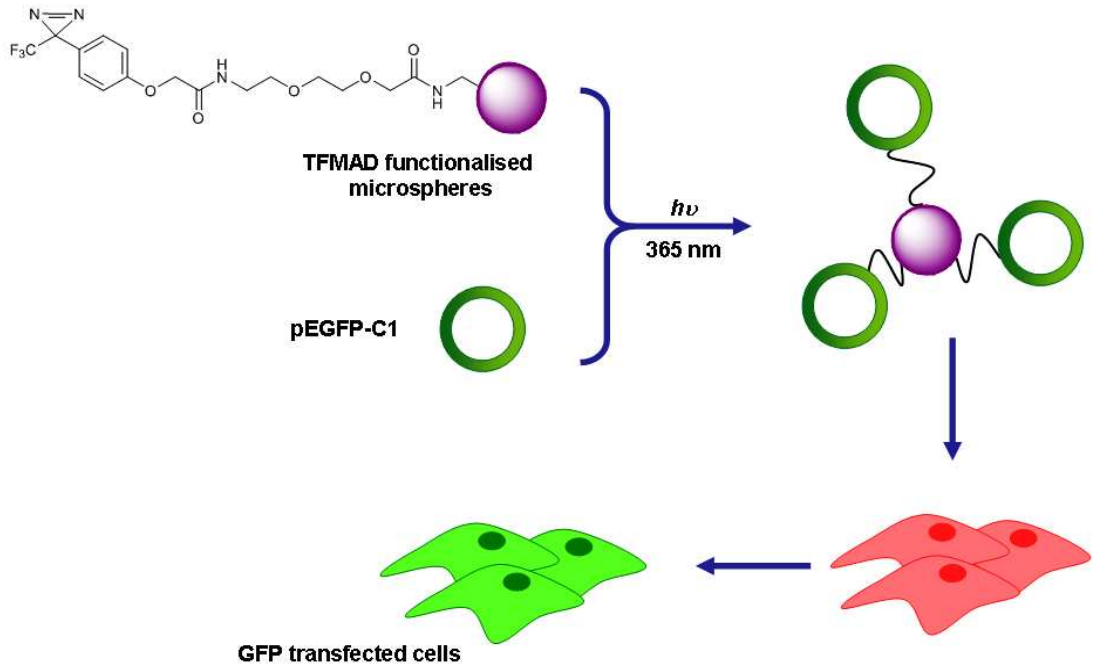

Scheme 4.2: pEGFP is covalently immobilised after activation with UV light of the TFMAD-functionalised microspheres. The plasmid-derivatised microspheres are then beadfected into cells. If the plasmid is successfully transfected into the nucleus, cells will become fluorescent as a result of the expresion of GFP protein encoded by the plasmid.

4.3. Preparation of TFMAD-Functionalised Microspheres

In order to study the ability of TFMAD-functionalised microspheres to capture DNA and efficiently transfer it into the cells, microspheres were synthesised and the influence of different factors such as spacer length, nature of linker and cargo were studied. These variables were chosen for several reasons.

Firstly, the incorporation of spacers helps to reduces steric congestion between attached molecules and the microsphere surface, making them more accessible for further derivatisation. In addition, some spacers enhance biocompatibility and aid the interactions between microspheres and the cell surfaces.[260] Microspheres were synthesised, with either one PEG spacer unit (**51a** and **56a**) or two PEG spacer units (**51b** and **56b**) (**Figure 4.2**).

Secondly, microspheres with a cleavable linker (**51c** and **56c**) were also prepared by functionalising them with a disulfide linker which can be easily cleaved by naturally occurring enzymes or cellular factors.[324] This would allow studies of the release effect of the DNA into the cytoplasm.

And finally, the diazirine group was photolysed under "dry conditions" in order to achieve the maximum conjugation. However, the effect of drying the beads has not been studied before and could damage their morphology. For this reason, a set of microspheres with different length spacers were prepared but with the addition of Arginine (**56a**, **56b**, and **56c** microspheres) in order to add an overall positive charge to the microspheres. This positive charge would make them more attractive to the negatively charged DNA, concentrating the amount of DNA surrounding the microsphere surface and therefore increase the possibility of being captured in solution by the carbenes upon irradiation. The list of synthesised microspheres is shown in **Figure 4.2**.

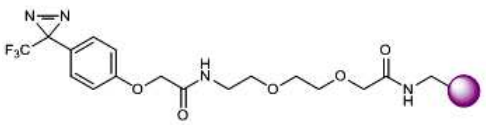

51a

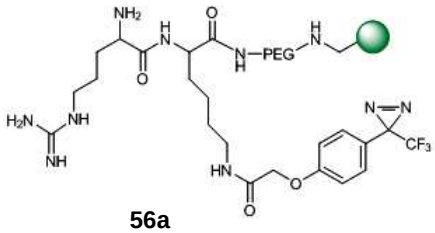

56a

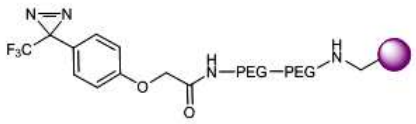

51b

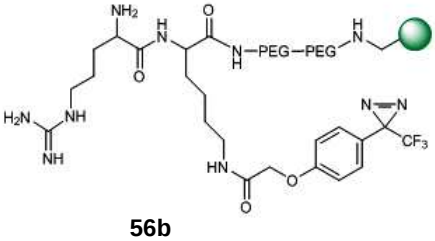

56b

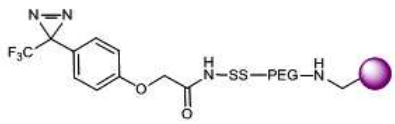

51c

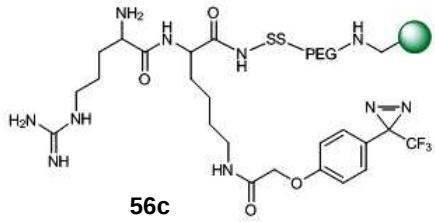

56c

Figure 4.2: Microspheres were functionalised with TFMAD linked through different spacers with and without the presence of an Arginine to induce an overall positive charge.

Amino-functionalised polystyrene microspheres (0.38 μm, 2% sc) were derivatised with an Fmoc-8-amino-3,6-dioxaoctanoic acid spacer unit **27**,

prepared in **chapter II**. The step was repeated under the same conditions to give microspheres **51b** in order to have a longer spacer. Microspheres **51c** were derivatised first with adipic acid and then cystamine to introduce the disulfide bond into the structure (**Scheme 4.3**). Finally, deprotection of the Fmoc group was carried out if necessary and the TFMAD photophore **4** was introduced.

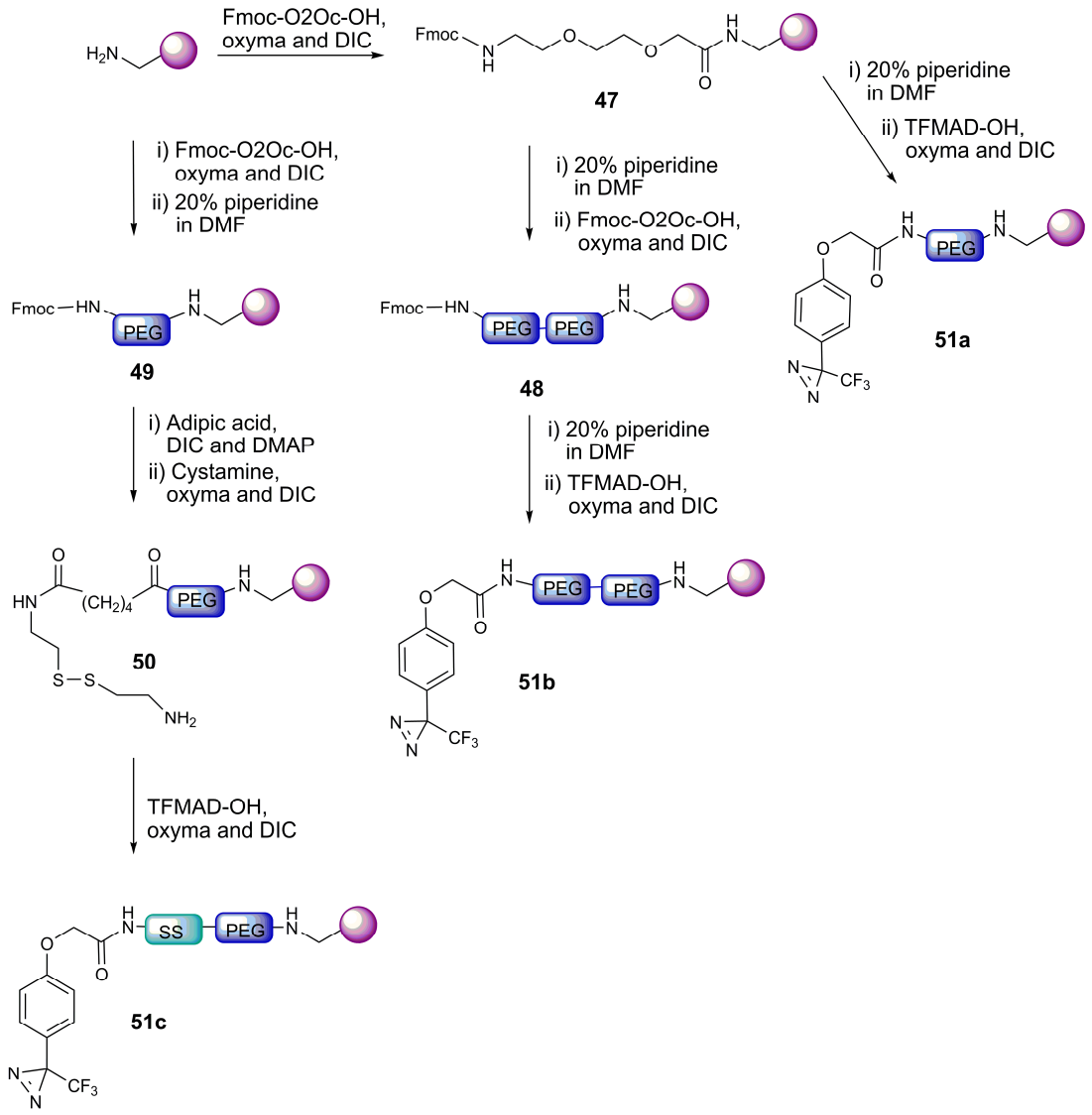

Scheme 4.3: Synthetic route for the preaparation of microspheres without overall positive charge.

For the preparation of positively charged microspheres, Fmoc-Lys(Dde)-OH amino acid **35** (prepared in **Chapter III**) was used in order to introduce branches for derivatisation.[316] Firstly, the free ε-amino group of Lysine was coupled to TFMAD and then, the α-amino group was used to introduce Fmoc-Arg(Boc)$_2$-OH (**Scheme 4.4**).

Coupling and deprotection steps were monitored using the colorimetric ninhydrin test and zeta potential values in order to determine if they were successful. Ninhydrin test provides information about the presence of primary amino groups on the microspheres while the zeta potential value is an important particle characteristic which monitors the diffferent functional groups present on the surface.[377]

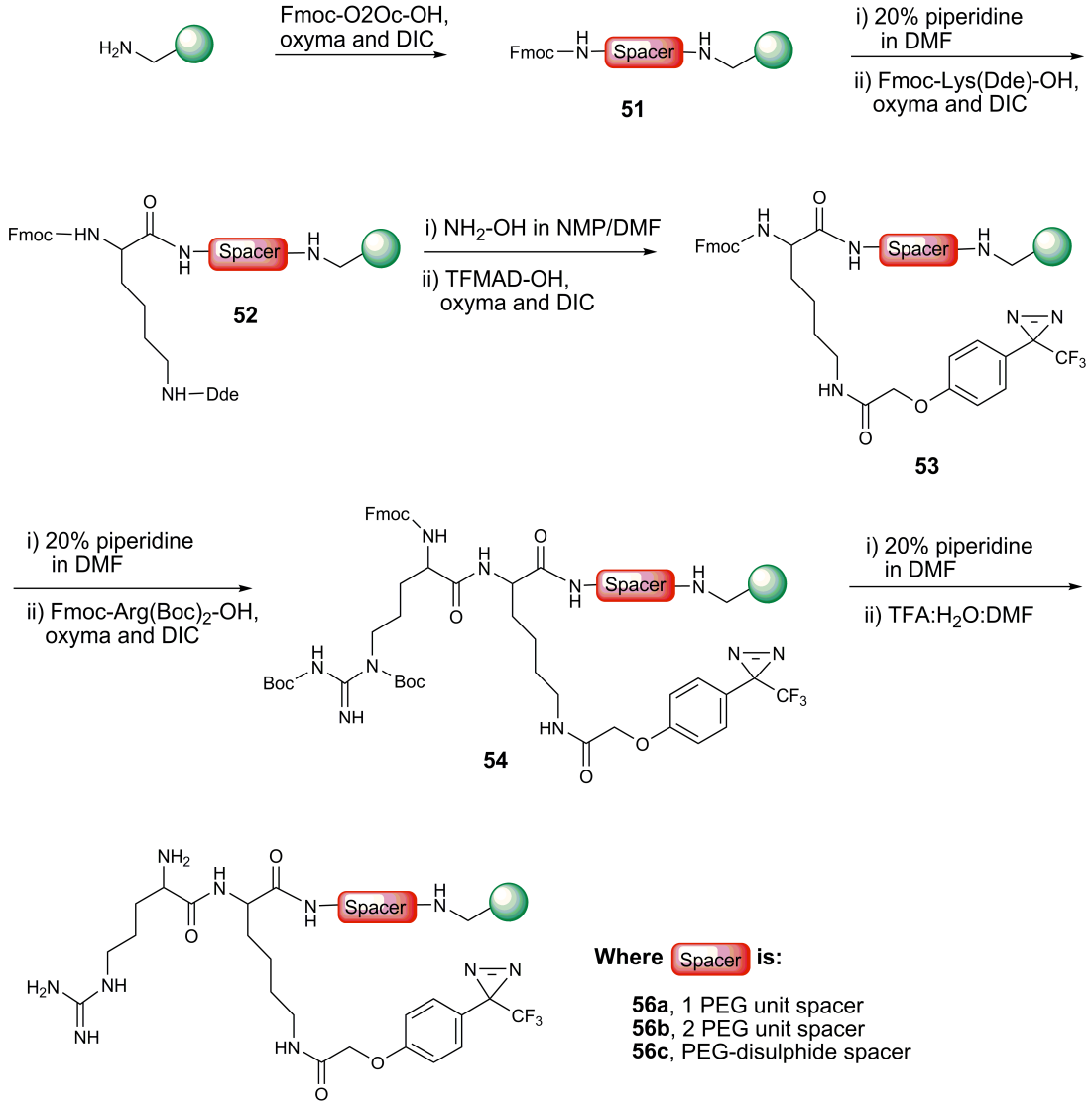

Scheme 4.4: Synthesis of positively charged microspheres **56**.

To be able to remove the protecting Boc group of the guanidinium moiety, strong acidic treatment with TFA was needed. The effect of this treatment on microphere morphology was studied by SEM microscopy. As **Figure 4.3** shows, microspheres did not lose their smooth and rounded form, demonstrating that the last step of the synthesis did not induce damage.

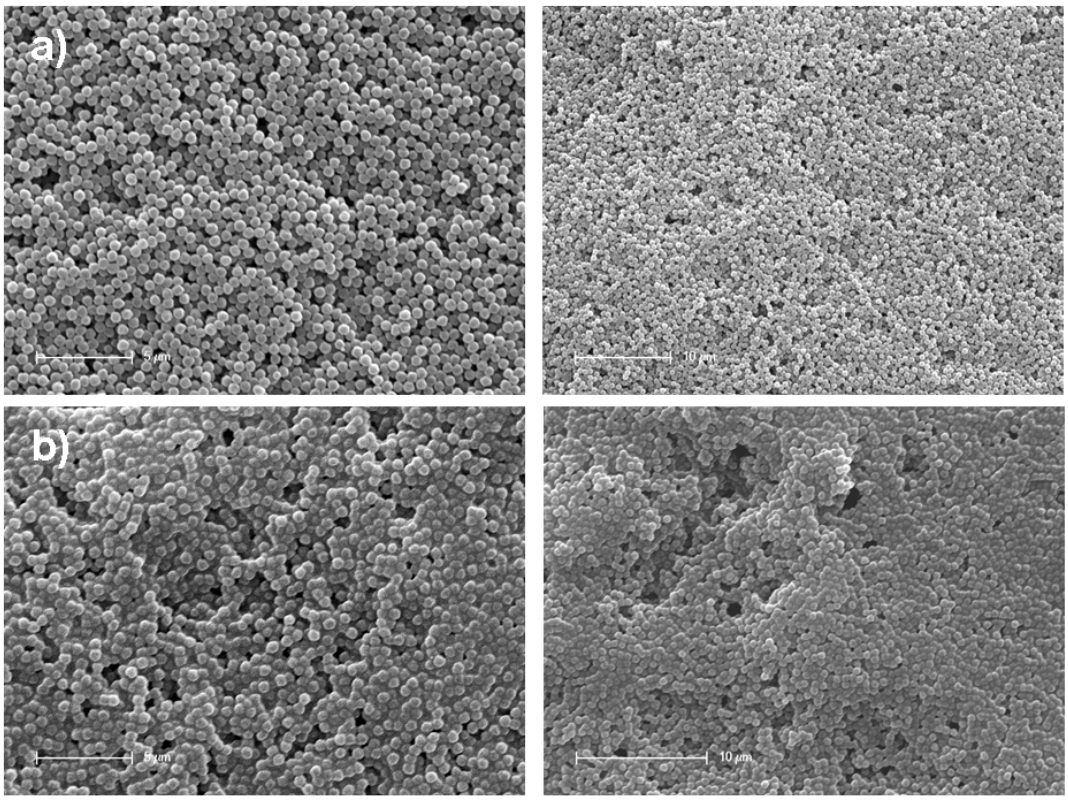

Figure 4.3: Scanning Electron Microscopy images of microspheres. a) microspheres **51a**, which synthesis does not incude acid treatment and b) microspheres **56a** after treatment with acid for Boc deprotection. Scale bar is 5 μm on the left and 10 μm on the right pictures.

4.4. Microsphere Capture Optimisation

In order to find out the best conditions for DNA capture, a 77-mer labelled oligonucleotide with Texas red (TxRd) on the 5' anti-sense strand was chosen as a biological cargo. The capture of this oligonucleotide allowed the easy monitoring of the fluorescently-labelled microspheres by flow cytometry and quantification of the coupling reaction success.

As a first approach, the best conditions for sample irradiation were determined. Previous work using TFMAD showed that capture of molecules was successful when irradiation was carried out in dry conditions; however the effect of dryness as well as irradiation on microspheres needed to be determined. For this purpose, microspheres **51a** and **56a** were irradiated dry and in solution. Microspheres were mixed with the TxRd-oligonucleotide (1:10 equivalents), irradiated in an ice bath, washed and analysed by flow cytometry (**Scheme 4.5**).

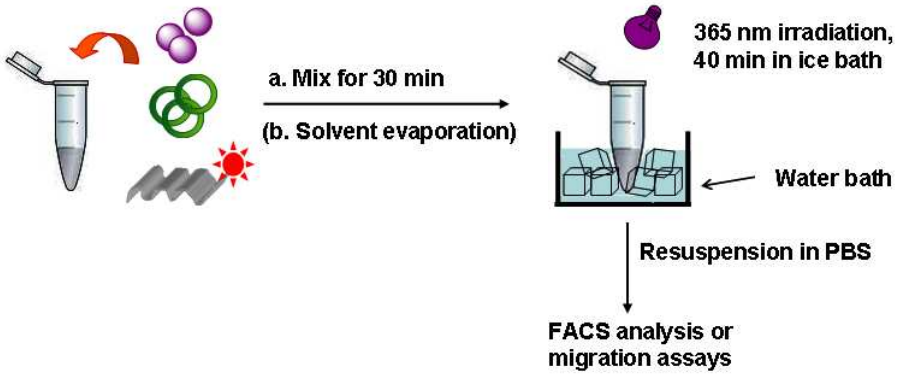

Scheme 4.5: General process for capture of DNA or oligonucleotides onto TFMAD-derivatised microspheres. Microspheres and DNA were mix together gently for 30 minutes. For irradiation in dry conditions solvent was evaporated from samples. Samples were irradiated in an ice bath for 40 minutes at 365 nm, resuspended in PBS and washed. Microspheres were analysed by flow cytometry or gel electrophoresis or added to cells to evaluate transfection abilities.

Flow cytometry showed a remarkable difference depending on the irradiation conditions for the two types of microspheres analysed (**Graph 4.1**). Samples irradiated under dry conditions showed a higher percentage of TxRd-DNA loading, between 55 and 65 %, than microspheres irradiated in solution which showed a maximum of 12 % of labelled beads. The results also suggested that microspheres containing the Arginine residue captured TxRd-oligonucleotides slightly better than microspheres without it; however the percentage of labelling in solution was still too low to be effective.

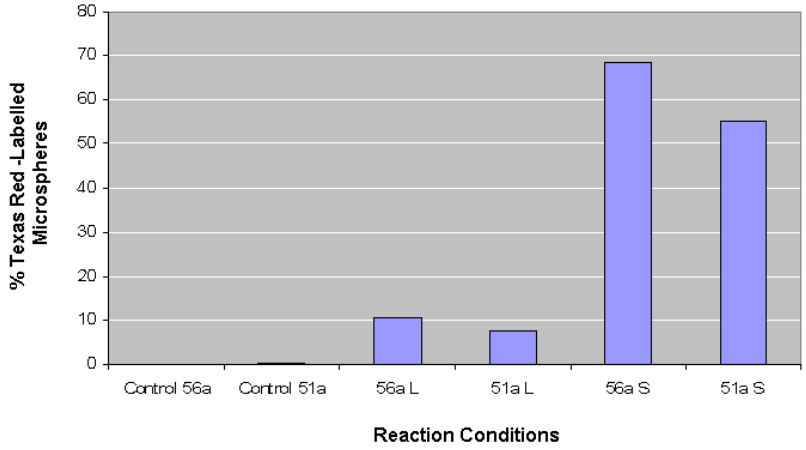

Graph 4.1: Assessment of the capture of Texas Red-oligos by TFMAD-derivatised microspheres. Irradiation of microspheres with DNA (S) in solid phase and (L) in solution conditions with microspheres **51a** and **56a**.

In order to determine the effect of irradiation in dry conditions, the surface morphology of irradiated samples was examined by SEM microscopy (**Figure 4.4**). The results show that the morphology of microspheres was conserved after irradiation under dry conditions and in solution, demonstrating that irradiation at 365 nm for 40 minutes does not damage its structure.

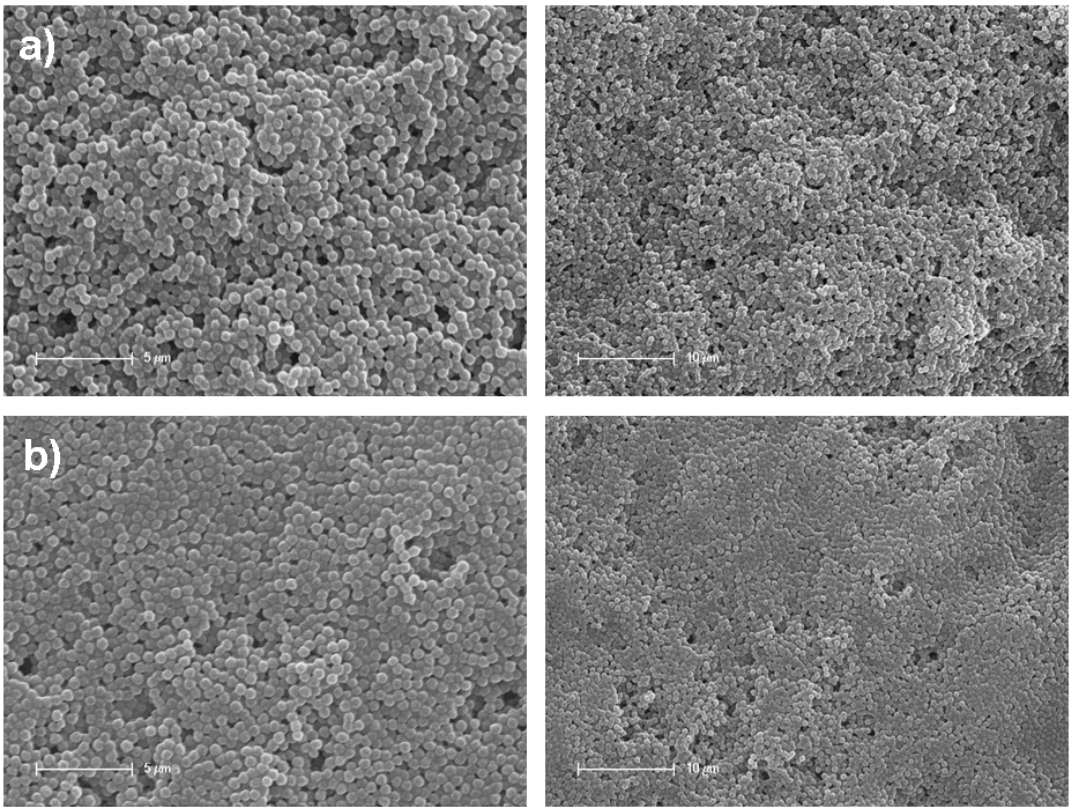

Figure 4.4: SEM images of microspheres. Irradiation of **56a** microsphers a) in solution or b) under dry conditions. Scale bar is 5 µm on the left and 10 µm on the right pictures.

Subsequently, the optimisation of DNA capture yields was studied where microspheres were irradiated with different amounts of pEGFP and the percentage of labelled microspheres was quantively assessed by cytometry using propidium iodide (PI), an intercalating agent that is used to stain nucleic acids.[378] Samples treated in the same way but without irradiation where used as a negative control. Surprisingly, **Graph 4.2** showed that microspheres mixed with the lowest amount of pEGFP had the highest yield. As in previous results, microspheres containing Arginine showed higher capture capacities than microspheres without it.

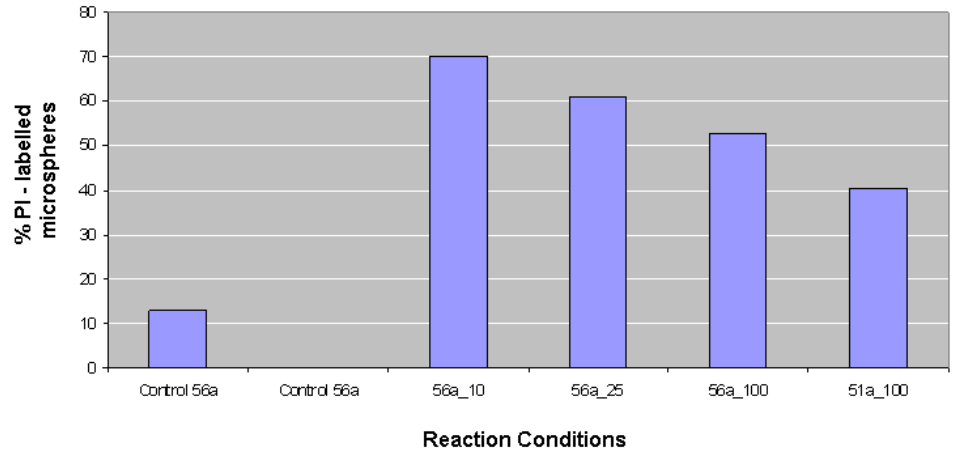

Graph 4.2: Microspheres **51a** and **56a** were used for the optimisation of the amount of DNA for efficient microsphere loading which was quantified by flow cytometry using propidium iodide (PI), a DNA stainer.

In conclusion, these experiments allowed determination of the best conditions for DNA capture onto microspheres. Results showed that the best photoreaction yields were obtained when samples were prepared under dry conditions. Results also showed that up to 70% of microspheres were labelled with DNA and the percentage did not increase with an increase in the DNA concentration. Finally, microsphere morphology examination by SEM microscopy demonstrated that irradiation of samples did not have any significant effect on their structure.

4.5. Covalent Capture and Transfection of pEGFP-C1

Once the optimal conditions for DNA capture were determined, the influence of other factors was studied by analysing the whole microsphere set under the same conditions. Not surprisingly, microspheres prepared in solution (L) showed a lower photoreactive yield compared to microspheres prepared under dry conditions (S) as previously observed (**Graph 4.3**). Nevertheless, the set of microspheres **56** containing Arginine in their structure showed higher percentages of DNA capture than the microspheres **51** that do not contained it. Arginine-containing microsphere with a cleavable linker (**51c**) showed the best capabilities for DNA capture.

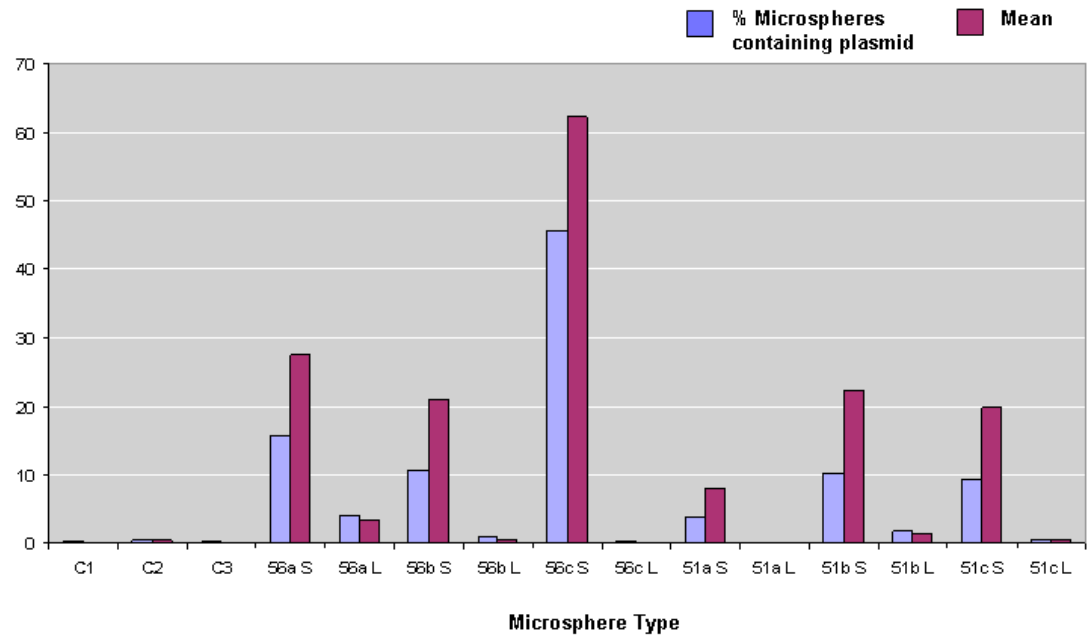

Graph 4.3: Capture of DNA plasmid with different micropheres. Negative controls C1, C2 and C3, represented microspheres treated with plasmid but without irradiation (C1), microspheres without plasmid and PI (C2), and microspheres with plasmid and PI (C3). Samples prepared in dryness are indicated with an S next to the microsphere type and those prepared in solution are indicated with an L.

Complexation of DNA by cationic lipids is usually assessed by gel retardation assays due to a reduction of the DNA mobility on agarose as a result of the hidden negative DNA charge inside the liposomes that leads to the retention of DNA in the wells. Capture of DNA onto the prepared microsphere set was also assessed by gel retardation electrophoresis and compared with plasmid as a negative control and plasmid complexed with lipofectamine (Invitrogen) as a positive control. As expected, plasmid complexed by lipofectamine was partly retained in the well where sample was introduced although the signal was very faint. The reason for that might be the sensitivity of the liposome formation as they were not carried out under optimal conditions (**Figure 4.5**). In the case of microspheres, the same phenomenon occurred, thus a new band which does not migrate to the positive pole appeared very close to the starting gates where samples were introduced, but this time as a result of the impenetrability of microspheres through the agarose gel and not by complexation with liposomes (**Figure 4.5**). The results of the retardation assay basically showed similar results as to flow cytometry analysis, with higher intensity bands corresponding to microsphere-DNA complexes prepared dry.

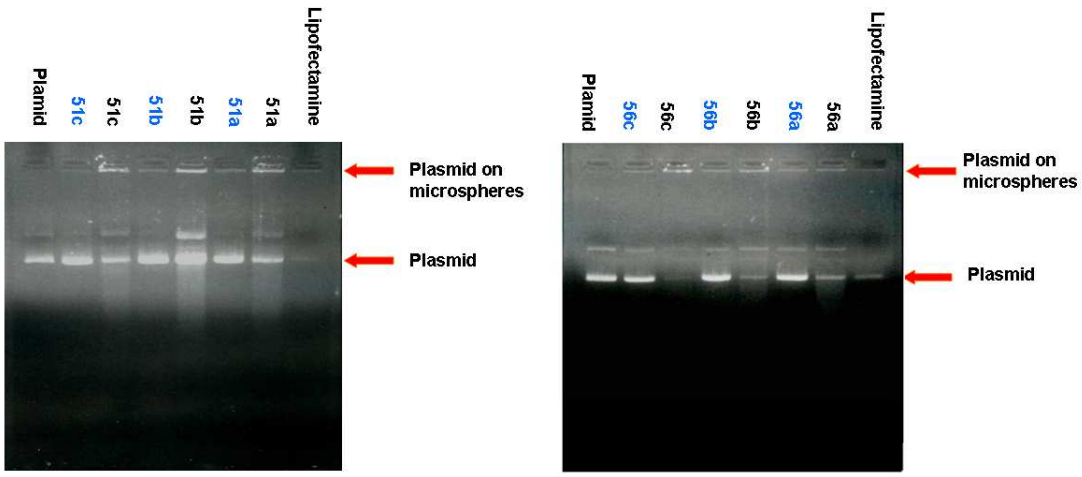

Figure 4.5: Gel retardation assays. pEGFP-C1 attached onto microspheres was loaded in an agarose gel (0.7% agarose, 1 µg/ml ethidium bromide in TBE buffer) and run at 90 V for 45 min. Lipofectamine line corresponded to the positive control and plasmid line corresponded to the negative control, naked plasmid. Microspheres samples in black were prepared in solid conditions and in blue in solution phase.

The transfection abilities of the microsphere set were evaluated on HEK293T cells after 48 and 72 h. Different microspheres bearing pEGFP-C1 were "beadfected" at three different concentrations (43, 86 and 172 µg/mL) and tested in triplicate. The expression of GFP was determined by microscopy and flow cytometry and compared to the values obtained by transfection with lipofectamine 2000 (Invitrogen). Unfortunately, none of the microspheres showed GFP expression (**Graph 4.4**).

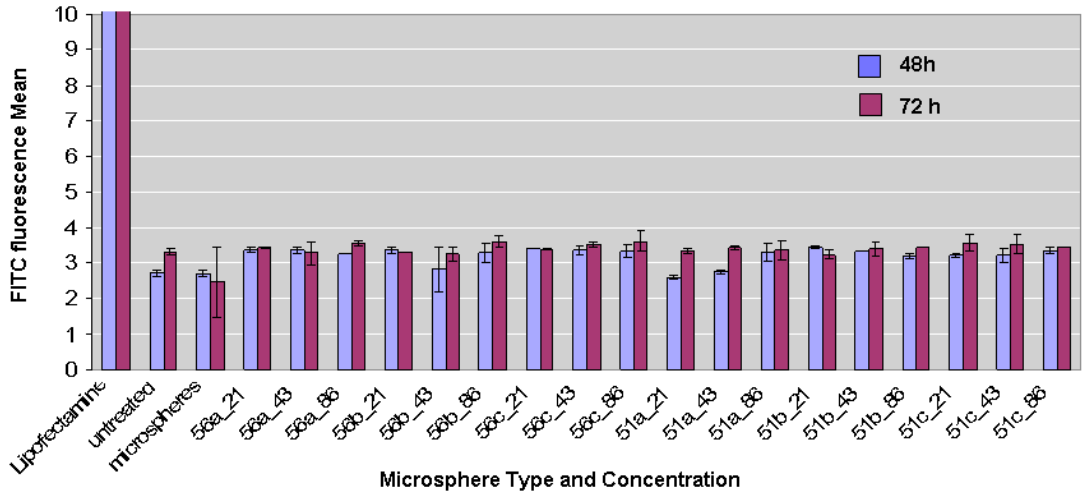

Graph 4.4: Results of transfection effciency of plasmid-microspheres complexes in different concentraions by flow cytometry. Cells transfected by lipofectamine reagent were used as a positive control (fluorescent mean values were 1620 and 1755 at 48 and 72 h, respectively). Negative controls corresponded to untreated cells and cells treated with microspheres without bearing a plasmid. X axes shows they type of microsphere used at three different concentrations: 21, 43, and 86 mg/mL. Each sample was assessed by triplicate.

The condensation of the plasmid has an important role on the efficiency of cellular uptake.[351, 379] As a consequence of the conformation and large size of DNA plasmid which could limit its uptake,[325, 326] microspheres were prepared with the same procedure but loaded with linear plasmid. For this purpose, DNA was treated with a restriction enzyme (StuI, which cut the plasmid in just one place and away from any important encoding area) to obtain the linear plasmid on the microspheres. As previously, capture of DNA onto microspheres was detected by two means, flow cytometry analysis using propidium iodide (**Graph 4.5**) and gel retardation assay (**Figure 4.6**). Flow cytometry analysis showed that microspheres having a net positive charge in their structure had the best capture abilities. Gel retardation assay allowed not only detection of DNA captured onto microspheres as a band in the starting gate, but also showed the shift in migration of the band corresponding to the plasmid after treatment with StuI restriction enzyme.

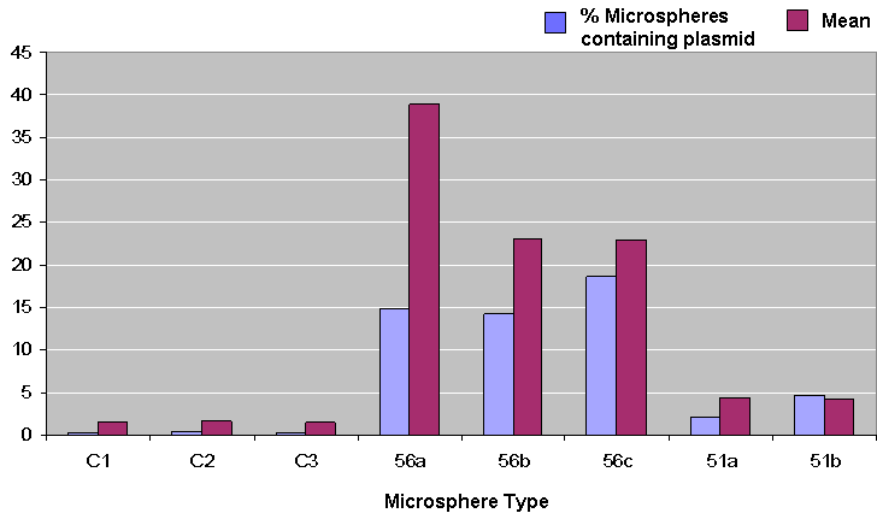

Graph 4.5: Capture of linearised plasmid onto micropheres. Negative controls C1, C2 and C3, represented microspheres treated with plasmid but without irradiation (C1), microspheres without plasmid and PI (C2), and microspheres without plasmid and PI (C3).

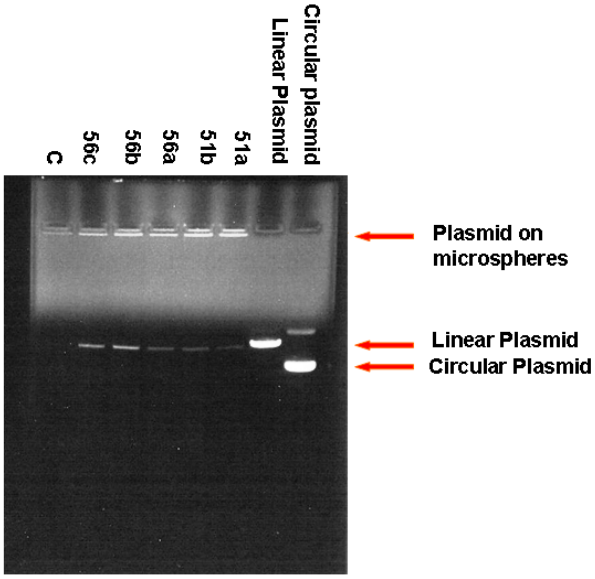

Figure 4.6: Gel electrophoresis after treatment with Stu I. Circular plasmid corresponds to the plasmid without incubation with the restriction enzyme and the linear plasmid corresponds to the plasmid treated with Stu I. The rest are different microspheres irradiated with the circular plasmid and then treated with Stu I.

However, the transfection abilities of microspheres bearing the linearised plasmid on HEK293T cells for 48 and 72 hr at three different concentrations showed no expression of GFP (**Graph 4.6**).

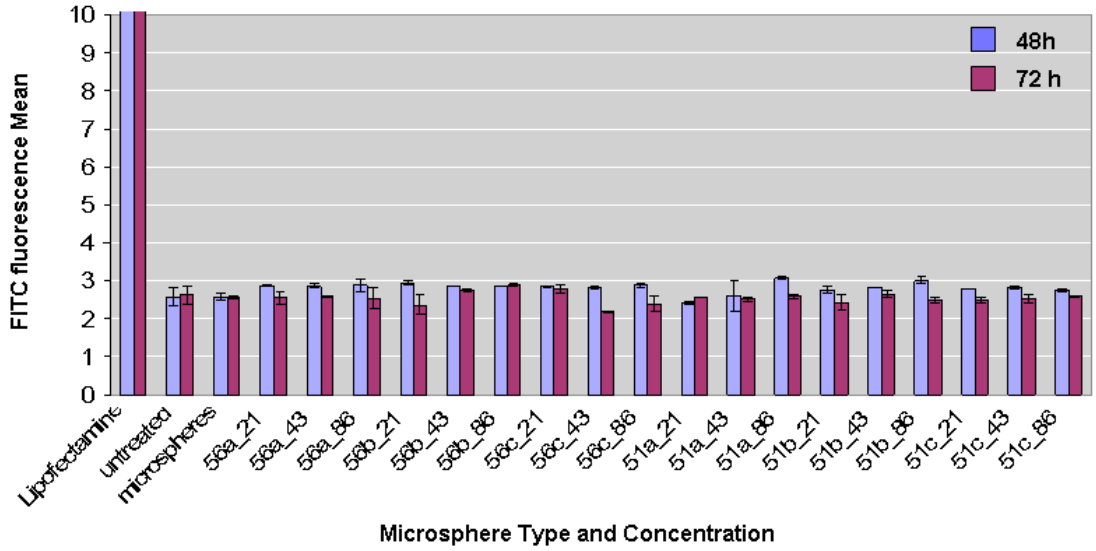

Graph 4.6: Analysis of transfection effciency of plasmid-microspheres complexes. Positive control were cells transfected by lipofectamine and negative controls corresponded to untreated cells and cells treated with microspheres without bearing a plasmid. X axes shows they type of microsphere used at three different concentrations: 43, 86, and 129 mg/mL. Each sample was assessed by triplicate.

The absence of GFP expression led to a second verification of the presence of plasmid on the microspheres. Microspheres carrying a circular plasmid were treated with StuI and ApaI, which cut the plasmid in two different places generating two sequences of different lengths. If microspheres bearing a circular plasmid are treated with these two restriction enzymes, one of the sequences would be still attached onto the surface of the microsphere but the other would be free to move through the gel. With this aim, microspheres irradiated with plasmid were washed thoughtfully. Each sample was divided into two fractions, one was incubated with enzymes and the other without to be able to compare. **Figure 4.7** showed that although microspheres were washed extensively, it was not enough to eliminate DNA that was not covalently attached to the microspheres as the band corresponding to the circular plasmid was still detected. Nevertheless, signal bands corresponding to microspheres treated with the two restriction enzymes did show a decrease in intensity in comparison with the band corresponding to the microspheres without treatment. Indeed, it was demonstrated that the band that stayed at the starting gate without migrating corresponded to the microspheres with plasmid attached onto their surface.

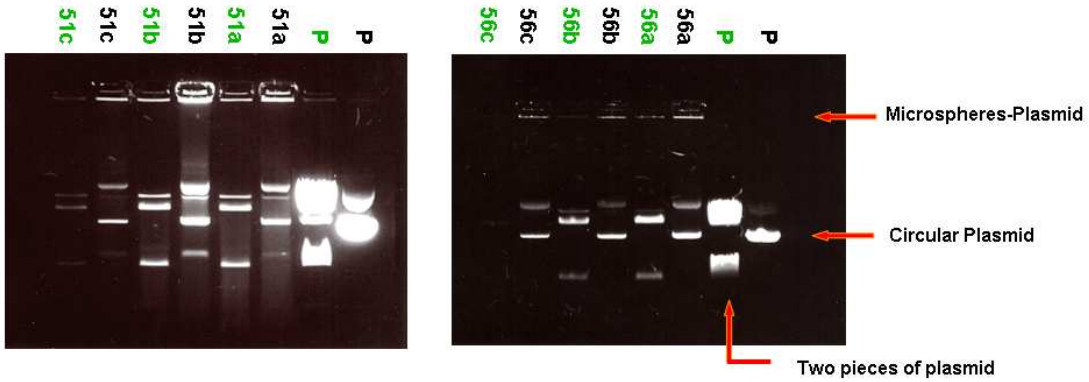

Figure 4.7: Images of the electrophoresis gels carried out with the 6 different samples under the same conditions with (samples in green) and without restriction enzymes treatment (samples in black). P corresponds to the naked plasmid. The reduction of band intensity at the starting gate between samples treated with and without enzyme strongly demonstrate that the band corresponded to the plasmid attached onto micropheres.

Although it was demonstrated that the plasmid could be cross-linked to microspheres making use of the TFMAD, expression of GFP after beadfection of HEK293T cells was not detected. Modification of the length and nature of the spacer did not improve the percentage of labelled beads and no transfection could be determined. These results suggest that the expression of the plasmid could be blocked due to covalent attachment to microspheres or as a result of the plasmid chemical modification by carbene insertion.

4.6. Non-covalent Gene Capture Approach

The impact of random covalent attachment of the plasmid onto the microspheres by the carbene generated after irradiation is not known. It was hypothesised that if the plasmid was attached in an area where no important information was encoded, then the protein would be expressed. However, even so, we do not know if the plasmid stays for too long in the cytoplasm where there are DNA nucleases that can degradate it before being cleaved from the microspheres and moved into the nucleus.

To rule out the effect in gene expression of chemical modification of the plasmid by covalent attachment, a new approach was developed where the DNA plasmid could be attached and disengaged from the microspheres by using peptide nucleic acid (PNA).[380] Specific PNA sequences would be captured by TFMAD on the microspheres so they would be present onto the microsphere surface. These PNA sequence would have the ability to trap the double-stranded DNA onto their surface by hybridising on a specific area of the plasmid.[292]

4.6.1. PNA-DNA Triplex Helix

Binding of PNA to DNA is also very tight and occurs with a specificity similar to that observed in the formation of DNA duplexes.[381] In fact, PNA·DNA duplexes are much more stable that DNA·DNA duplexes, and the introduction of a suitable strand of PNA can displace the corresponding DNA strand from a pre-existing DNA duplex.[382]

Peptide nucleic acid (PNA) recognition of nucleic acids occurs by a variety of mechanisms depending on the PNA sequence and nucleic acid target recognition.[383] In general, triplex strand invasion by homopyrimidine PNAs is the preferred strategy for targeting double strand DNA by PNA.[384] This mechanism involves the local dissociation of the low complementary DNA strands and binding of the sequence complementary PNA oligomers to one of the exposed strands forming extremely stable triplexes (**Figure 4.8**).

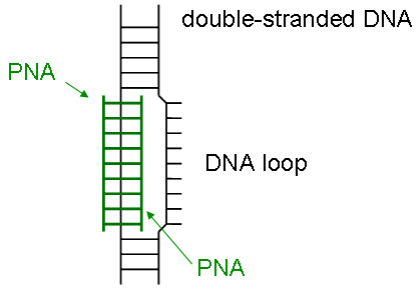

Figure 4.8: Triple strand invasion where PNA·DNA·PNA triple helix is formed with an antiparallel Watson-Crick duplex and a parallel bound Hoongsteen strand.

For the capture of pEGFP-C1, two PNA-peptide conjugates able to form a triple helix PNA·DNA·PNA were prepared by members of the Bradley group.[385] A poly-purine nucleotide sequence of 10 bases, 5'-GGAAGGGAAG-3', was identified in the GFP non-codifying portion of the pEGFP-C1 (bases from 1993 to 2001). A complementary anti-parallel sequence (C-CCTTCCCTTC-NH_2) and the parallel one (N-CCTTCCCTTC-C) of the corresponding PNA target sequence were designed containing rhodamine or fluorescein dyes at the N-terminus separated by a hydrophilic spacer, respectively (**Figure 4.9**).

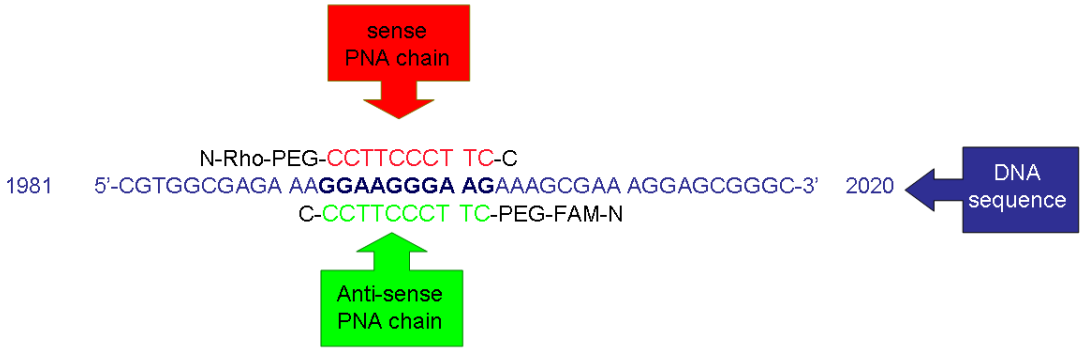

Figure 4.9: Sequence of the PNA used for targetting the DNA tagged sequence of the EGFP plasmid.

4.6.2. Capture of PNA by TFMAD Photophore

As with covalent attachment of the plasmid onto TFMAD-derivatised microspheres, dye-labelled PNA were captured by microspheres upon irradiation. Three different batches were prepared (**Scheme 4.6**), one with each dye-labelled PNA and another with the same quantities of both PNA sequences.

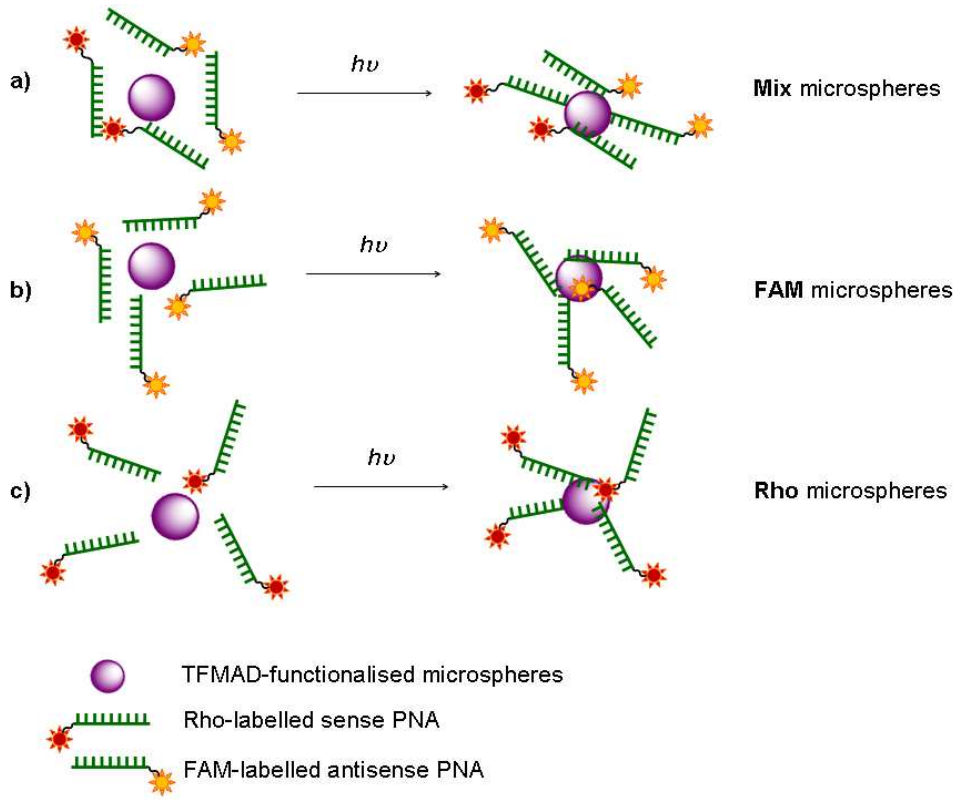

Scheme 4.6: Synthesis of the different PNA conjugated microspheres. Microspheres were irradiated in the presence of a) both PNA sequences, b) FAM-labelled PNA, and c) Rho-labelled PNA.

The capture of fluorescently-labelled PNA onto microspheres was confirmed by flow cytometry where microsphere population clearly showed a shift in fluorescence for all three samples compared to microspheres irradiated without PNA (**Figure 4.10**).

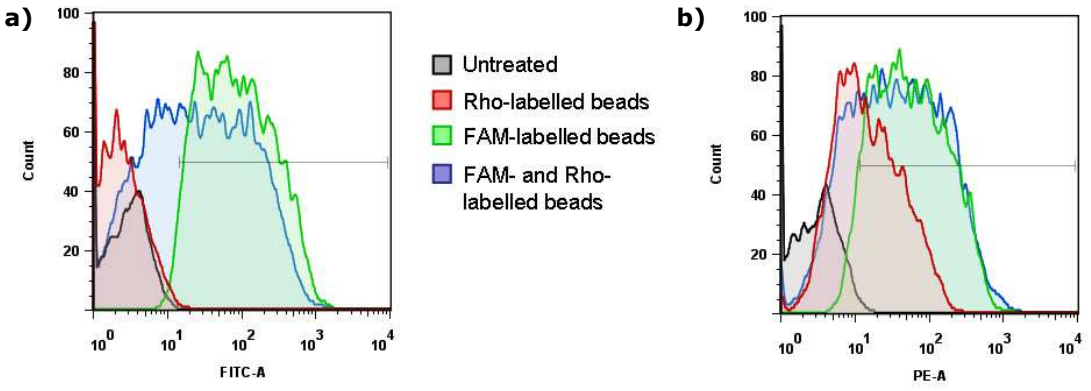

Figure 4.10: Flow cytometry analysis of the beads after irradiation under dry conditions with: no PNA (black), Rho-PNA (red), FAM-PNA (green), and both, Rho-PNA and FAM-PNAs at the same time. Histograms of fluorescent beads using a) a FITC filter, and b) a PE filter.

4.6.3. DNA Hybridisation and Transfection

In order to find out the best conditions for non-covalent capture of DNA onto the PNA-functionalised microspheres, three different strategies were assessed. The first strategy consisted of using **Mix** microspheres directly for DNA hybridisation as these microspheres already contained both PNA sequences. For the second stratey, equal volumes of **FAM**- and **Rho**-microspheres were mixed and used to hybridised the plasmid. And finally, **FAM**-microspheres were hybridised with the plasmid and the addition of the same loading equivalents of Rho-PNA sense sequence (**Scheme 4.7**).

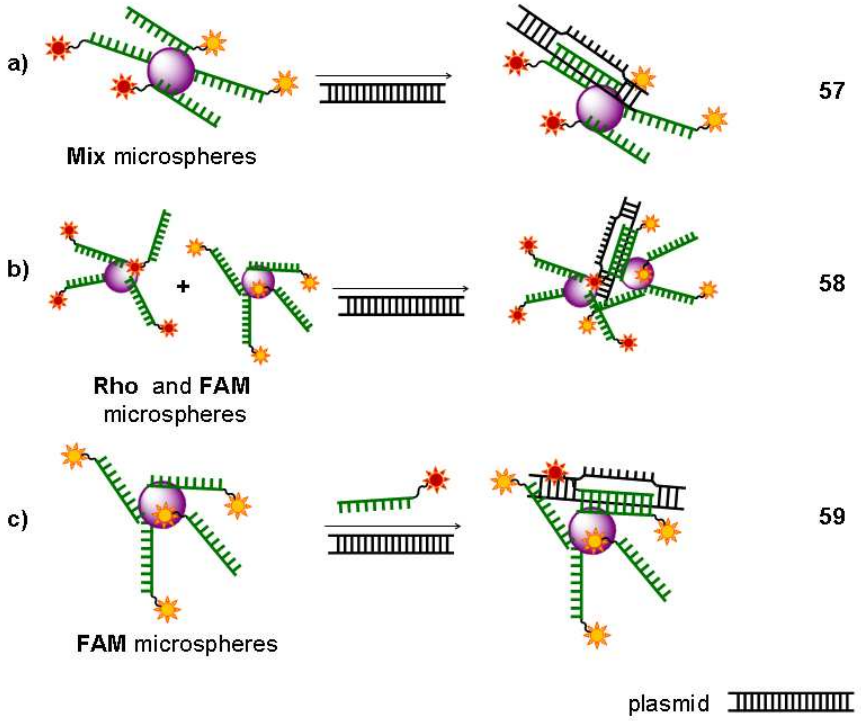

Scheme 4.7: Hybridisation of double-stranded DNA onto PNA-functionalised microspheres by three different strategies: a) using Mix microspheres which contained both PNA sequences, b) using a mixture of Rho- and FAM-PNA functionalised microspheres, and c) using FAM-microspheres but with the addition of the complementary Rho-labelled PNA strand to the mixture. Hybridisation was carried out by heating all samples to 90 ºC and allow to cool down to RT slowly.

DNA hybridiation on microspheres was carried out using different DNA amounts (10, 20, and 40 μL of plasmid solution) for each sample and DNA capture efficiency was evaluated by gel migration assay (**Figure 4.11**).

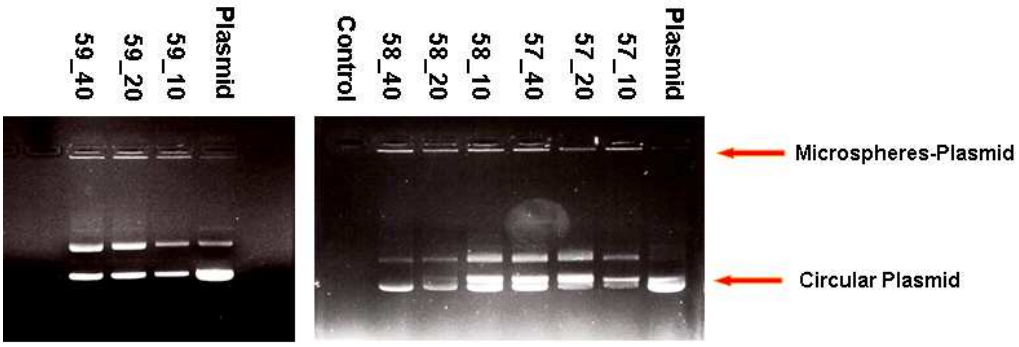

Figure 4.11: Gel retardation assays of PNA-functionalised microspheres hybridised with different plasmid volumes: 10, 20, and 40 μL of plasmid solution (0.4 μg/mL in TE buffer).

Gel retardation assay showed a band at the starting gate corresponding to the double-stranded DNA complexed to microspheres for all samples and at all concentrations of plasmid. Microspheres were then beadfected for 48 and 72 h with HEK293T cells with 2 different concentrations (43 and 86 μg/mL). However no expression of GFP could be detected under any conditions (**Graph 4.7**).

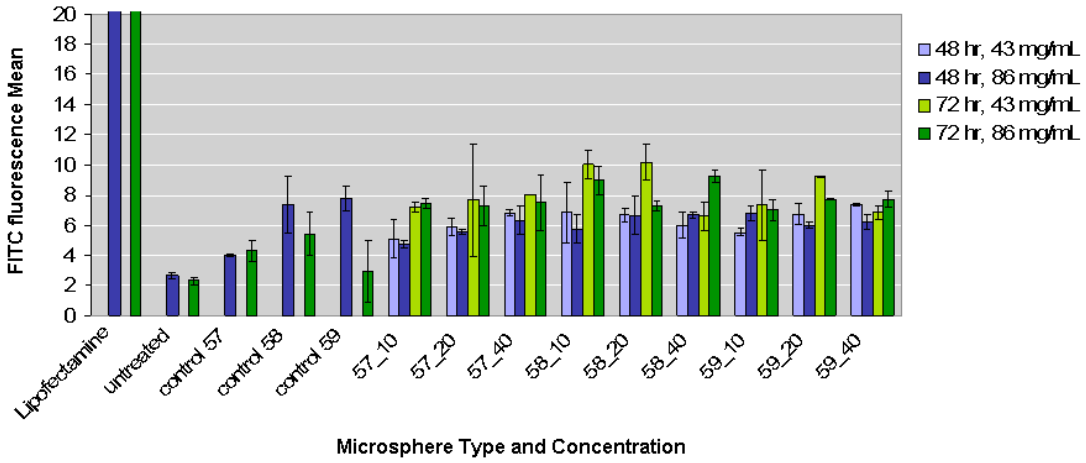

Graph 4.7: Results of transfection effciency of plasmid-microspheres complexes in different concentraions by flow cytometry. Positive control were cells treated with lipofectamine and negative controls corresponded to untreated cells and cells treated with each type of microsphere without bearing a plasmid. X axes shows each type of sample with the DNA amount used for the hybridisation, blue bars correspond to mean fluorescence after 48 hr and green bars after 72 hr. Each sample was assessed by triplicate.

4.7. Conclusions

No transfection was seen with the work shown above. Further experiments are needed to elucidate why the above strategies were not successful. Nevertheless, this work has developed a general loading method using a photo cross-linking reaction for cargos onto microspheres, for example a plasmid or PNA. Two strategies for DNA capture have been studied, by direct covalent immobilisation of the plasmid and by indirect non-covalent immobilisation using PNA-functionalised microspheres. Microspheres with different spacers showed slightly different effects on their ability to capture plasmid. As expected, positively charged microspheres showed better immobilisation abilities, having the highest yields when irradiation was performed under dry conditions. However, the effect of the different spacers on plasmid delivery could not be determined as no GFP expression could be detected.

There are many reasons why plasmid attachment would not be expressed, thus further studies would help to elucidate why this methodology have not been successful. On one side, it would be prudent to find a way to determine the exact amount of plasmid per microsphere in order to know the amount of plasmid used for cell transfection. It could happen that no transfection is detected as a result of an insufficient plasmid quantity. On the other side, other applications that have been successfully developed using microspheres as a delivery vectors could be applied with this methodology in order to compare the applicability of TFMAD-functionalised microspheres.

Chapter V:

EXPERIMENTAL SECTION

5.1. General Information

Solvents were dried by eluting through alumina columns. Unless otherwise noted, materials were obtained from a commercial supplier and were used without further purification. All reactions were performed in pre-dried glassware under nitrogen. All reactions involving diazirines were performed in dim red light. **Microwave** reactions were performed in sealed heavy-walled Pyrex tubes under controlled conditions in a safe and reproducible procedure using an Initiatior 2.0 Microwave (Biotage) fitted with a rotational mixing system. Single mode microwave irradiation was used at a fixed temperature, pressure and irradiation power during the reaction time by an automatic power control. Thin-layer **chromatography** (TLC) was carried out using precoated silica gel 60 F_{250} plates with thickness of 0.25 μm. TLC plates were visualised by short wavelength ultra-violet light (254 nm) and/or stained with DNP acetic anhydride. Flash column chromatography was performed using silica gel 60 (230-400 mesh ASTM, Merck). ^{1}H, ^{13}C and ^{19}F **nuclear magnetic resonance** (NMR) spectra were recorded on Bruker instruments: DMX500, DPX360 and ARX250, respectively. Chemical shifts (δ) are reported in parts per million (ppm) relative to internal solvent signal ($(CH_3)_4Si$, δ = 0.00 for ^{1}H and ^{13}C NMR and CCl_3F for ^{19}F NMR) with coupling constants (J) in Hertz (Hz). Trifluoroacetic acid was used as a reference standard in some studies for ^{19}F NMR (δ = -78.50 for ^{19}F NMR). **Analytical HPLC** was performed on an analytical HPLCs HP Agilent 1100 instrument using a 5 μm C18 reversed-phase Supelco Discovery® column (5 cm

x 4.60 mm) at 1 mL/min eluent solvent and detecting by UV at 220, 254, 260, 282 and 495 nm and evaporative light-scattering detection (ELSD) lamp. Different methods have been created for sample analysis:

Method A: A 5 min method starting from water/MeCN/FA 95:5:0.1 and raising gradually to 5:95:0.1 after 3min, then 1 min isocratic and 1 min to go back to initial values.

Method B: A 10 min method starting from water/MeCN/FA 95:5:0.1 and raising gradually to 5:95:0.1 after 8min, then 1 min isocratic and 1 min to go back to initial values.

Method C**:** A 5 min method starting from water/MeOH/FA 95:5:0.1 and raising to gradually 5:95:0.1 after 3min, then 1 min isocratic and 1 min to go back to initial values.

Mass spectrometric analysis was recorded on an Agilent 1100 series system. Mass spectra were obtained on a VG platform single Quadrupole mass spectrometer in electrospray positive (ES^+) and negative (ES^-) mode. **High resolution mass spectra** were recorded by the MS Department of the University of Edinburgh on a Finnigan MAT 900 XLP high resolution, double focussing mass spectrometer. **MALDI** mass spectra were acquired on a Voyager-DETM STR MALDI-TOF MS (Applied Biosystems). Sinapic acid was used as a matrix solution (10 mg/mL) in 50% MeCN in water with 0.1% TFA. **IR spectra** were recorded on a Bruker Tensor 27 FT-IR with a golden SPECAC gate accessory with neat compounds. Sample **Irradiation** was carried out with a UVP Blak-Ray® lamp, model B100AP, 100 W, which emits a monochromatic light with a wavelength of 365 nm and 2.44 $\mu W/cm^2$ of intensity. **UV-Vis spectroscopy** was performed on an Agilent 8453 UV-Vis spectrophotometer provided with UV-Vis Chemstation software (Agilent).

An **Inkjet printer** (Microdrop, GmbH, Norderstedt, Germany) equipped with a micro-pipette (AD-K-501, 70 μm diameter nozzle) was used for development of microarray preparation methods. The piezodispensing system Scienion S5 sciFLEXARRAYER (Scienion AG, Germany), operating at 230V AC, a temperature 15-30 ºC, 230V AC +/-10%, 50-60 Hz, relative humidity up to 85% was used to prepare the small molecule microarray. **GeneMachines® Hyb4** (Zinsser Analytic GmbH, Frankfurt, Germany) small scale hybridisation station was used for microarray hybridisations. Fluorescence readout of hybridised microarrays was conducted with either a BioAnalyser 4F/4S **fluorescence**

scanner (LaVision Biotec, Bielefeld, Germany) or an AutoLoader microarray scanner (Genetix 4200AL, Axon). Images were analysed using FiPS fluorescence imaging and processing software (LaVision Biotec, Bielefeld, Germany), the output of which was a background-corrected value of an integrated fluorescence intensity of each spot ("spot fluorescence").

Cell experiments were carried out in a HERAsafe KS 18 class II negative-flow cabinet from Heraeus. **Cell cultures** were performed in a HERAcell 150 incubator form Heraeus. **Flow cytometry** was performed on a BD Biosciences FACSAria® system using the BD FACSDiva software for analysis or a DakoCytomation CyAn™ ADP system with Summit software for analysis. **Scanning electron microscopy** (**SEM**) analysis was performed on a Philips XL30CP with PGT Spirit X-ray analysis and HKL channel5 Electron Backscatter Diffraction (EBSD) system. **ZetaSizer Nano** (Malvern Instruments, United Kindom) was used for Z potential measurements. **Cell viability** was assessed using a Benchmark® Bio-Rad microplate reader measuring absorbance at 570 nm. **Microscopy** was performed on a Leica DM IRB inverted fluorescent microscope and processed using Leica FW4000 v 1.2 imaging software (Leica Microsystems Imaging Solutions Ltd., UK).

5.2. General Methods

5.2.1. Kaiser test:

The test is based on the reaction of ninhydrin with primary amines which give a dark blue colour or a yellow colour when no free amino groups are present. Thus, the test is used to monitor the coupling reactions on solid support after each coupling or deprotection step.[386]

On Solid Phase: A few resin beads were transferred to a small glass tube after extensive washing and drying. Then, 3 drops of ninhydrin reagent A and 1 drop of ninhydrin reagent B were added to the resin. The tube was introduced into a heater at 110 ºC for 3 minutes.

On Microspheres: Microspheres were suspended in MeOH (25 μL, 2% sc) and solid particles obtained by centrifugation. Methanol was removed and ninhydrin reagent A (6 μL) and ninhydrin reagent B (2 μL) were added to the solid particles and sonicated before heating to 110 ºC for 3 min.

5.2.2. Malachite Green Test:

A few resin beads were transfer to a small glass vial after an extensive washing and drying. To this, 1 mL of a 0.25% solution of Malachita Green oxalate in ethanol was added followed by a single drop of pure triethylamine. After 2 min at room temperature the solution was discarded and the beads rinsed several times with EtOH (or MeOH) until the solution remained clear. In the presence of acid groups, the beads were coloured dark green; alternatively, they appeared as clear gel pearls.[387]

5.2.3. Cell culture

All cells were cultured in the appropriate culture medium at 37°C/5% CO2 Dulbecco's Modified Eagle Medium (DMEM, Sigma-Aldrich) for HEK293T and Roswell Park's Memorial Institute (RPMI-1640, Sigma-Aldrich) medium for HeLa, supplemented with 10% foetal bovine serum (FBS, Biosera), 100 U/mL penicillin and streptomycin and 4 mM L-glutamine (Gibco). Cells were cultured in T-75 flasks (Nunc) until 70-80% confluency. At this time, the old growth media was removed and the cells were washed with PBS (10 mL) and harvested via trypsination (trypsin/EDTA, Gibco) (1 mL) at 37°C. The detached cells were collected in fresh growth media and diluted to the appropriate cell density for

experiments in fresh growth media. An aliquot was re-seeded to a T-75 flask for re-growth.

5.2.4. Haemocytometry

Cell densities were determined by haemocytometry. An aliquot (10 μL) of cells detached from a T-75 flask and collected in growth media (5 mL) was mixed with 0.2% trypan blue (40 μL, Sigma-Aldrich) and pipetted into a Bright Line TM haemocytometer (an etched glass device with an H-shaped moat forming two cell-counting areas (with 4 quadrants in each area), with surface features enhanced by Neubauer rulings, Sigma-Aldrich). Cell concentrations and the densities required for experiments were determined by **Equations 5.1** and **5.2**, respectively.

$$\text{Concentration (cells/mL)} = (N/Q) \times 5 \times 10^4$$

Equation 5.1: Concentration of cells/mL by haemocytometry, where "N" is the total number of cells counted and "Q" is the number of quadrants counted.

$$V_{Exp}\ (mL) = (V_{Tot} \times C_{Well}) \times (1000/V_{Well})/C_{Tot}$$

Equation 5.2: Volume of cells detached from T-25 flask (V_{Exp}) required in an experiment a total medium volume of V_{Tot} and a concentration per well of C_{Well}. V_{Well} is the volume required per well and C_{Tot} is the concentration of cells/mL as calculated in **Equation 5.1**.

5.2.5. Flow cytometry analysis of cells

In preparation for flow cytometric analysis, the old media was removed from cell cultures and the cells were washed with PBS and harvested by trypsination at 37°C (trypsin/EDTA). Detached cells were collected in growth media. Samples were analysed by flow cytometry using a 488 nm Coherent® Sapphire™ solid state laser with the band pass filters according to the fluorophores under investigation:

Filter name	Band pass Filter	Fluorophores
FITC-A	530/30	Fluorescein or GFP
PE-A	585/42	TAMRA and PI
PE-TxRed	610/20	Texas Red

The BD Biosciences FACSDiva software was used to treat the data. Untreated cells were defined as having 0% uptake or transfection efficiency.

5.2.6. Cytotoxicity assay

Cells were cultured and seeded onto a 96-well plate at a density of 1 x 10^4 cells/well (volume per well: 100 μL). The first row of the well-plate was used as a blank without seeded cells. Cells were incubated (37 ºC/5% CO_2) for 24 hours prior to the addition of samples at different concentrations (10-100 μM). After 24 h, the old media was removed and replaced with 100 μL solution of fresh phenol red-free media (IMDM Iscovers Modified Medium supplemented with L-Glutamine and HEPES, FBS and Den/Stren Glu, GIBCO Invitrogen) containing 3-(4,5-dimethylthiazol-2-yl)-2,5-diphenyltetrazolium bromide (MTT, Sigma-Aldrich) at a concentration of 5 mg/mL. Cells were incubated for 3 h (37 ºC/5% CO_2) before the addition of MTT solubilising solution (10% Triton-X, 0.1 N HCl in isopropanol) (100 μL). Once formazan crystals were dissolved, absorbance of each well was measured at 570 nm with a Bio-Rad microplate reader (version 1.15). Untreated cells were considered to be 100% viable and cell viability was calculated from **Equation 5.3**.[318]

$$\% \text{ Viable Cells} = (Abs_{Exp}/Abs_{Cont}) \times 100$$

Equation 5.3: Viability of cells by MTT assays, where "Abs_{Exp}" refers to the absorbance at 570 nm of cells treated with microspheres and "Abs_{Cont}" refers to the absorbance at 570 nm of untreated control cells.

5.3. Experimental for Chapter 1

5.3.1. Synthesis of aryl(trifluoromethyl)diazirine group

tert-butyl (4-formyl-phenoxy)acetate (9):

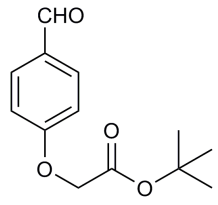

To a dried heavy-walled Pyrex tube containing a small stir bar was added 4-hydroxibenzaldehyde (732 mg, 3 mmol), dry potassium carbonate (622 mg, 4.5 mmol) and potassium iodide (74 mg, 0.45 mmol), and dry acetonitrile (1.2 mL). *Tert*-butyl bromoacetate (415 μL, 3.75 mmol) was added dropwise. The tube containing the reaction mixture was sealed with an aluminium crimp cap fitted with a silicon septum and then it was exposed to microwave irradiation for 40 min at a temperature of 120 ºC. After the irradiation, the reaction tube was cooled to room temperature with high-pressure air. The reaction progress was followed by TLC and DNP was used as a stain. Once the reaction was completed, water (10 mL) and DCM (10 mL) was added and the phases were separated. The aqueous layer was extracted with DCM (3 x 10 mL). The combined organic layers were dried over $MgSO_4$, concentrated *in vacuo* and purified by column chromatography hexane/EtOAc (6:3) to give an orange solid (673 mg, 2.85 mmol 95%).

MS (ES^+) m/z: 237 $[M+H]^+$, 259 $[M+Na]^+$; **HRMS (ES^+)** for $C_{13}H_{17}O_4$: 237.11214 (calc.); 237.11241 (found); **Mp**: 52-53°C (lit.[388] 56-57°C); **^{1}H NMR** ($CDCl_3$, 500 MHz): δ 9.89 (s, 1H), 7.84 (s, 2H), 6.99 (s, 2H), 4.60 (s, 2H), 1.48 (s, 9H); **^{13}C NMR** ($CDCl_3$, 90.6 MHz): δ 191.1, 167.5, 163.1, 132.3, 130.9 (2C), 115.2 (2C), 83.3, 65.9, 28.4 (3C); **IR** (neat) υ_{max} /cm^{-1}: 2977, 1746, 1686, 1598, 1215, 1148; **HPLC** (ELSD) t_R/min: 3.532 (method A);

***Tert*-butyl [4-(2,2,2-trifluoro-1-hydroxy-ethyl)phenoxy]acetate (10):**

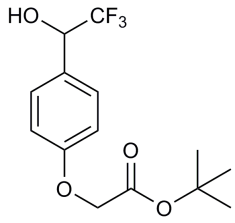

To a mixture of **9** (673 mg, 2.85 mmol) and trifluoromethyl trimethylsilane (425 μm, 3.6 mmol) in THF (9.0 mL), TBAF (1.0 M solution in THF, 29 μL) was added at 0 ºC with stirring. After 15 min, methanol (21 mL) and aqueous 2M HCl solution (10.2 mL) were added to the mixture successively, and the whole mixture was stirred for an additional 10 min. Methanol and tetrahydrofuran were removed under reduced pressure, and the aqueous mixture was extracted with ether (20 mL x 3). The combined organic solutions were washed with brine, dried over $MgSO_4$, and concentrated *in vacuo*. The residue was purified by column chromatography eluting with hexane/ EtOAc (4:1) to give a pale yellow solid (646 mg, 2.12 mmol, 74%).

MS (ES^+) m/z: 324.19 $[M+NH_4]^+$; **HRMS (ES^+)** for $C_{14}H_{21}O_4N_1F_3$: 324.14172 (calc.); 324.14229 (found); **Mp**:61-62°C; **^{1}H NMR** ($CDCl_3$, 500 MHz): δ 7.41 (d, 2H, J = 8.58 Hz), 6.92 (d, 2H, J = 8.3 Hz), 4.94 (q, J = 6.7 Hz, 1H), 4.53 (s, 2H), 4.11 (q, J = 7.1 Hz, 1H, OH),1.52 (s, 9H); **^{13}C NMR** ($CDCl_3$, 90.6 MHz): δ 168.3, 159.0, 129.1, 127.6 (2C), 124.7 (q, ^{1}J = 282.1), 115.0 (2C), 83.0, 72.6 (q, ^{2}J = 31.9 Hz), 65.8, 28.1 (3C); **^{19}F NMR** ($CDCl_3$, 235.9 MHz): δ -79.77; **IR** (neat) υ_{max} /cm^{-1}: 3448, 1735, 1218, 1151 and 1122; **HPLC (ELSD)** t_R/min**:** 3.732 (method A), 7.161 (method B).

***tert*-Butyl [4-(2,2,2-Trifluoro-acetyl)-phenoxy]acetate (11):**

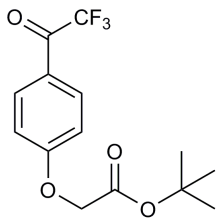

A mixture of **10** (590 mg, 1.93 mmol), Dess-Martin periodinane (2.5 g, 8.55 mmol), and TFA (446 μL, 8.55 mmol) in DCM (20 mL) was stirred at RT for 12 h. After the mixture was diluted with ether (20 mL), and the resulting mixture was poured into saturated aqueous $NaHCO_3$. The organic layer was separated, washed with water, dried over $MgSO_4$ and concentrated *in vacuo*. The residue

was purified by column chromatography eluting with hexane/EtOAc (6:4) to give the product **3** (469 mg, 1.54 mmol, 80%) as a mixture of ketone and hydrate forms (3:1).

MS (ES^+) m/z: 305 $[M+H]^+$; **HRMS (EI)** for $C_{14}H_{15}O_4F_3$: 304.09170 (calc.); 304.09110 (found); **Mp**: 57-58°C; **^{1}H NMR** ($CDCl_3$, 500 MHz): δ 8.04 (d, J = 8.8 Hz, 2H), 6.95 (d, J = 8.8 Hz, 2H), 4.61 (s, 2H), 1.49 (s, 9H); **^{13}C NMR** ($CDCl_3$, 90.6 MHz): δ 179.2 (q, ^2J = 34.7), 167.7, 163.9, 133.0 (2C), 123.9, 123.8, 117.2 (q, ^1J = 291.0), 115.27 (2C), 83.5, 65.8, 28.3 (3C); **^{19}F NMR** ($CDCl_3$, 235.9 MHz): δ -72.37, -77.19. **IR** (neat) υ_{max}/cm^{-1}: 1753, 1693, 1135; **HPLC (ELSD)** t_R/min**:** 3.538 (method A), 6.724 (method B).

***tert*-butyl [4-(2,2,2-trifluoro-1-hydroxyimino-ethyl)phenoxy]acetate (12):**

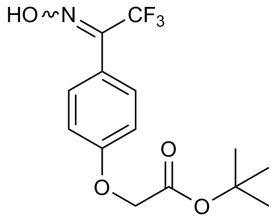

Ketone **11** (469 mg, 1.50 mmol) was dissolved in pyridine (3.5 mL) and placed in a microwave glass flask and sealed. Hydroxylamine hydrochloride (312.7 mg, 4.5 mmol) was added and the reaction was performed under microwave irradiation for 40 min at a temperature of 70 ºC. After cooling the reaction tube at room temperature, pyridine was removed *in vacuo*, and the remaining residue was dissolved in Et_2O (20 mL) and washed with 0.01M HCl (20 mL). The organic layer was washed with H_2O (3 x 20 mL) and dried with $MgSO_4$, and the solvent was removed *in vacuo* to give a colorless liquid (311 mg, 0.97 mmol, 65%), which was purified by flash column chromatography eluting with Et_2O/Hexanes (6:4).

MS (ES^+) m/z: 342 $[M+Na]^+$, 320 $[M+H]^+$; **HRMS (ES^+)** for $C_{14}H_{17}O_4N_1F_3$: 320.11042 (calc.); 320.11072 (found); **Mp**: 62-63°C; **^{1}H NMR** ($CDCl_3$, 500 MHz); δ 9.80 (bs, 1H), 7.42 (d, J = 8.7, 2H), 6.90 (d, J = 8.7, 2H), 4.53 (s, 2H), 1.48 (s, 9H); **^{13}C NMR** ($CDCl_3$, 90.6 MHz): δ 168.1, 159.7, 130.2 (2C), 129.1, 119.8, 118.9 (q, ^1J = 291.0), 114.8 (2C), 83.1, 66.3, 28.3 (3C); **^{19}F NMR** ($CDCl_3$, 235.9 MHz): δ -67.22, -63.64; Multiple splitting patterns arise in ^{1}H and ^{19}F NMRs due to anti/syn configurations of the oxime with a ratio of 3:2. **IR** (neat) υ/cm^{-1}: 3309, 1735, 1247, 1139; **HPLC (ELSD)** Rt/min**:** 7.421 (method B), 4.228 (method C).

***tert*-butyl {4-[2,2,2-trifluoro-1-(O-toluensulfonyl)hydroxyimino-ethyl]-phenoxy}acetate Oxime (13): [93]**

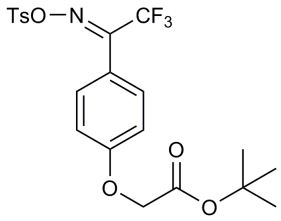

Oxime **12** (162 mg, 0.51 mmol) was dissolved in pyridine (2 mL) and placed in a microwave glass flask and sealed. Tosyl chloride (145 mg, 0.76 mmol) was added, and the reaction was performed under microwave irradiation for 40 min at 130 ºC. Subsequently, pyridine was removed in vacuo, and the remaining residue was dissolved in Et_2O (20 mL) and washed with 0.01 M HCl (10 mL). The organic layer was washed with H_2O (3 x 20 mL) and dried with $MgSO_4$ and the solvent removed giving an orange oil product (173 mg, 0.37 mmol, 72%) which was purified by column chromatography from 20 to 70% DCM in hexane.

MS (ES^+) m/z: 512 $[M+K]^+$, 496 $[M+Na]^+$, 491 $[M+H_2O]^+$, 374 $[M+H]^+$; **HRMS (ES^+)** for $C_{21}H_{26}O_6N_2F_3S_1$: 491.14582 (calc.); 491.14527 (found); **Mp**: 58-60°C; **^{1}H NMR** ($CDCl_3$, 500 MHz): δ 9.85 (bs, OH), 7.88 (d, J = 8.1, 2H), 7.44 (d, J = 8.9, 2H), 7.37 (d, J = 8.1, 2H), 6.94 (d, J = 8.9, 2H), 4.55 (s, 2H),1.48 (s, 9H); **^{13}C NMR** ($CDCl_3$, 90.6 MHz): δ 167.6, 160.7, 153.3 (q, ^{2}J = 33.7), 146.4, 131.5, 131.0 (2C), 130.2 (2C), 129.6 (2C), 120.1 (q, ^{1}J = 277.7), 117.6, 115.1 (2C), 83.2, 65.8, 28.3 (3C),22.1; **^{19}F NMR** ($CDCl_3$, 235.9 MHz): δ -67.27; **IR** (neat) υ_{max}/cm^{-1}: 1741, 1143; **HPLC (ELSD)** t_R/min**:** 4.437 (method A), 7.355 (method B).

***tert*-butyl {4-[3-(trifluoromethyl)diaziridin-3-yl]phenoxy}acetate (14):**

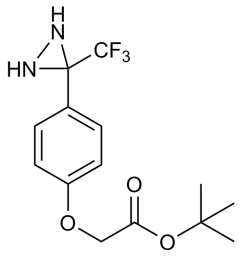

In a thick-walled screw-cap tube, compound **13** (173 mg, 0.37 mmol) was dissolved in Et_2O (0.9 mL). The solution was cooled to -78 ºC, and liquid ammonia (0.2 mL) was added. The tube was screwed tightly closed, and the

solution mixture allowed rising to room temperature. The reaction was stirred for 12h, and the solution was cooled to -78 ºC before removing the cap. Ammonia was removed by allowing the system to rise to RT. The solution was partitioned between Et_2O (5 mL) and H_2O (5 mL), the organic layer was dried with $MgSO_4$, and the solvent was removed in vacuo to give an oil (106 mg, 0.33 mmol, 90%). The product was purified by column chromatography eluting from 10 to 50% EtOAc in hexane.[93]

MS (ES^+) m/z: 319 $[M+H]^+$; **HRMS (ES^+)** for $C_{14}H_{18}O_3N_2F_3$: 319.12640 (calc.); 319.12661 (found); **^{1}H NMR** ($CDCl_3$, 500 MHz): δ 7.52 (d, J = 8.7, 2H), 6.90 (d, J = 8.7, 2H), 4.52 (s, 2H), 2.78 (d, J = 8.7, 1H), 2.21 (d, J = 8.7, 1H), 1.48 (s, 9H); **^{13}C NMR** ($CDCl_3$, 90.6 MHz): δ 168.0, 159.5, 130.2 (2C), 124.9, 123.9 (q, ^{1}J = 278.4), 115.1 (2C), 83.0, 65.9, 57.9 (q, ^{2}J = 36.0), 28.3 (3C); **^{19}F NMR** ($CDCl_3$, 235.9 MHz): δ -76.97; **IR** (neat) υ/cm^{-1}: 3257, 1748, 1514, 1143; **HPLC (ELSD)** Rt/min**:** 3.753 (method A), 7.283 (method B).

***tert*-butyl {4-[3-(trifluoromethyl)-3*H*-diaziren-3-yl]phenoxy}acetate (15):**

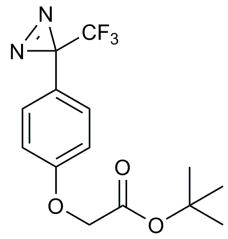

A mixture of diaziridine **21** (266 mg, 0.84 mmol) and Et_3N (201 μL, 1.44 mmol) was stirred with iodine (235 mg, 0.924 mmol) in the dark for 10 min. After the solution was poured into aqueous 1 M NaOH solution and stirred for 5 min. The organic layer was further extracted with NaOH solution and the combined aqueous solution was neutralised with HCl and extracted with EtO_2. The organic layer was dried over magnesium sulfate and evaporated under vacuum to give a redish oil. The residue was purified by column chromatography from 0 to 20% EtOAc in hexane to give a colorless liquid (124 mg, 0.392 mmol, 90%).

MS (ES^+) m/z: 317 $[M+H]^+$, 339 $[M+Na]^+$; **HRMS (EI)** for $C_{14}H_{15}O_3N_2F_3$: 316.10293 (calc.); 316.10389 (found); **^{1}H NMR** ($CDCl_3$, 250 MHz): δ 7.12 (d, J = 8.8 2H), 6.89 (d, J = 9.0, 2H), 4.51 (s, 2H), 1.47 (s, 9H); **^{13}C NMR** ($CDCl_3$, 90.6 MHz): δ 167.8, 159.3, 128.5 (q, ^{3}J = 1.3, 2C), 122.5 (q, ^{1}J = 274.6), 122.2,

115.3 (2C), 83.0, 28.3 (3C), 65.9, 28.5 (q, ^2J = 40.4), 28.3 (3C); **^{19}F NMR** ($CDCl_3$, 235.9 MHz): δ -66.82; **IR** (neat) υ/cm^{-1}: 1751, 1613, 1369 and 825; **HPLC (ELSD)** Rt/min**:** 4.442 (method A), 9.775 (method B), 4.458 (method C).

{4-[3-(trifluoromethyl)-3*H*-diaziren-3-yl]phenoxy}acetic acid (4):

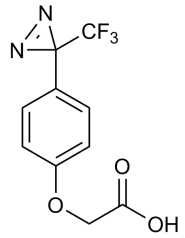

Diazirine **15** (101 mg, 0.390 mmol) was dissolved in a solution of 50% TFA/CH_2Cl_2 (2 mL) and stirred for 20 min. The reaction progress was followed by TLC until it was completed. The solution was concentrated *in vacuo* and redissolved in Et_2O, dried over magnesium sulfate and the solvent evaporated *in vacuo* to give a white solid (100 mg, 0.386 mmol, 99%). The product was pure enough to be used in the next step without further purification.

MS (ES$^-$) m/z: 259 [M-H]$^-$, 519 [2M-H]$^-$; **HRMS (ES$^-$)** for $C_{10}H_6O_3N_2F_3$: 259.03360 (calc.); 259.03424 (found); **Mp:** 53-55°C; **^{1}H NMR** ($CDCl_3$, 500 MHz): δ 10.49 (bs, OH), 7.18 (d, J = 8.8, 2H), 6.85 (d, J =8.7, 2H), 4.71 (s, 2H); **^{13}C NMR** ($CDCl_3$, 90.6 MHz): δ 175.0, 159.4, 129.4 (q, ^3J = 1.3, 2C), 124.7, 123.2 (q, ^1J = 274.6), 116.0 (2C), 65.7 (2C), 28.2 (q, ^2J = 40.6); **^{19}F NMR** ($CDCl_3$, 235.9 MHz): δ -66.19; **IR** (neat) υ/cm^{-1}: 2909 (bs), 1748, 1610 and 1519; **HPLC (ELSD)** Rt/min**:** 3.556 (method A), 4.383 (method C), 6.221 (method D).

4-Bromophenoxytrimethylsilane (17):

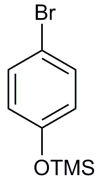

p-Bromophenol **16** (17.30 g, 100 mmol) was dissolved in anhydrous THF (30mL) followed by addition of Et_3N. The reaction mixture was cooled in an ice/water bath and trimethylsilyl chloride (12.7 mL, 100 mmol) was added dropwise with stirring. The thick reaction mixture was stirred at RT for 1 h, and the white precipitate was filtered. The filtrate was diluted with hexane (20mL),

refiltered and evaporated to yield a colourless oil (24.50 g, 99.92 mmol, 99.9%) and used without further purification.

MS (ES^+) m/z: 244 and 246 $[M+H]^+$; **HRMS (EI)** for $C_9H_{13}OBrSi$: 243.99136 (calc.); 243.99176 (found); **^{1}H NMR** ($CDCl_3$, 360 MHz): δ 7.20 (d, J = 8.9, 2H), 6.60 (d, J =8.9, 2H), 0.13 (s, 9H); **^{13}C NMR** ($CDCl_3$, 90.6 MHz): δ 154.6, 132.6 (2C), 122.2 (2C), 114.1, 0.4 (3C); **IR** (neat) υ/cm^{-1}: 1249, 824; **HPLC (ELSD)** Rt/min**:** 4.738 (method C).

4-trifluoroacetyl phenol (18):

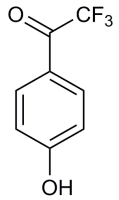

*n*BuLi (80 mL of 2.5 M in hexanes, 150 mmol) was added to a stirred solution of 4-bromophenoxytrimethylsilane **17** (24.50 g, 99.9 mmol) and ethyl trifluoroacetate (17.85 mL, 150 mmol) in THF (500 mL) at -110 °C (cyclohexane/nitrogen cool bath) under argon. The mixture was stirred at -110 °C → -78 °C for 30min, and then the reaction was quenched with 1 M aqueous HCl (500 mL). The reaction mixture was extracted with Et_2O (2 x 100 mL) and the combined organic layer was washed with water (50 mL), brine (50 mL), dried over anhydrous $MgSO_4$, filtered and concentrated. The product (12.77 g, 67.93 mmol, 68%) was used for the following steps without further purification.

MS (ES^-) m/z: 189 $[M-H]^-$; **^{1}H NMR** ($CDCl_3$, 500 MHz): δ 7.91 (d, J = 8.8, 2H), 6.86 (d, J =8.9, 2H); **^{13}C NMR** ($CDCl_3$, 90.6 MHz): δ 180.0 (q, ^2J = 34.8), 163.1, 133.7 (2C), 122.8, 117.2 (q, ^1J = 291.1), 116.5 (2C); **^{19}F NMR** ($CDCl_3$, 235.9 MHz): δ -71.09; **HPLC (ELSD)** Rt/min**:** 3.524 (method C).

5.3.2. Irradiation Studies

Photolysis in solution followed by NMR spectroscopy:

A 20 mM solution of TFMAD (52.034 mg) in deuterated methanol (10 mL) was prepared in a 10-mL microwave vial and sealded with a septum cap. Trifluoroacetic acid was added as a reference standard for ^{19}F NMR. The sample was continuously irradiated with a 100-W black UV light lamp (UVP, model

B-100AP, 230 V) for 112 min at 20°C. Every 2 min, 0.5-mL samples were extracted until 18 min and then in increasing time scales. All samples were analysed by ^{1}H- and ^{19}F- NMR to follow the progress of the reaction.

Photolysis in solution Recorded by UV-Vis Spectroscopy:

A 3.5 mM solution of TFMAD in MeOH (1.5 mL) was added into a quatz cuvette (*l* = 1 cm) and irradiated at 365 nm above 10 cm at RT. At specific periods of time, the absorbance of the sample was recorded until no starting material was observed.

Irradiation in Dry Conditions of TFMAD and Biotin:

TFMAD (5.2 mg, 20 μmol) and biotin (7.33 mg, 30 μmol) were dissolved in deuterated DMSO in a 10-mL glass vial. A sample was collected and analysed by HPLC and NMR. Water was added (5 mL) and the sample was freezed dried to evaporate the solvent. Before irradiation at 365 nm for 10 min, the sample was cooled down to -196°C. The solid was redissolved with deuterated DMSO and analysed by ^{1}H- and ^{19}F-NMR. This operation was repeated two more times and the final solution was analysed further by HPLC and LCMS.

5.4. Experimental for Chapter 2

Fluorescence polarisation solution assays of the 10 putative binding compounds to β-TrCP1 were performed by Douglas Houston from the center for cell Biology in the University of Edinburgh.

5.4.1. Slide Preparation

Slide cleaning:

Glass slides were rinsed in acetone to remove manufacturing grease and residues before being etched by treating them for 2 h in a solution of 10% potassium hydroxide in methanol. Slides were then rinsed with water until no strips were visible on the surface. Slides were then washed with acetone and dried under a nitrogen stream and they were used immediately for functionalisation.[117]

Masking process:

Slides were printed with a solution of 20% (w/v) sucrose in water (12 drops/spot) by an inkjet printing system (Microdrop Technology). The optimal printing voltage was 90 V, as a voltage greater than this resulted in drops breaking up to produce satellite drops, while a lower voltage was insufficient for drops to be generated. Subsequently, slides were dried for 5 min at 40 ºC in an oven before tridecafluoro-1,1,2,2-tetrahydrooctyl-dimethylchlorosilane (TFCS) (10 μL) was added and spread over the slide surface. Slides were incubated at 110 ºC for 2hr in a sealed hybridisation chamber. Slides were then washed liberally, firstly with acetone followed by water, before curing them at 110 ºC for 30 min.

Amino functionalisation of slide:

Aminosilanisation of the groups on the glass surface were carried out by incubating the slides in a solution of 2% 3-aminopropyltriethoxysilane (APTES) in acetonitrile (10 mL) for 30 min. Slides were washed with acetonitrile (2 x 10 min) and ethanol (2 x 10 min) before being cured at 110 ºC for 30 min.

Slide Fluorination:

To a pre-cleaned slide, tridecafluoro-1,1,2,2-tetrahydrooctyl-1-trimethoxysilane (10 μL) was added onto the slide and spread across the

surface. The slide was left for 2h at 110 ºC in a sealed hybridisation chamber. Slides were then washed with acetone and cured for 30 min at 110 ºC.

5.4.2. PhotoSpacer synthesis

5.2.2.1. Linker Synthesis

Ethyl-4-(4'-formyl-phenol)-butyrate (22):

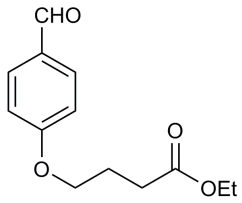

A microwave vessel was prepared with hydroxybenzaldehyde (4.9 g, 40 mmol), dried potassium carbonate (8.3 g, 60 mmol) and potassium iodide (996 mg, 6 mmol). The vessel was closed with a microwave septum cap and then acetonitrile (32 mL) and ethyl bromobutyrate (7.2 mL, 50 mmol) were added. The mixture was heated for 40 min at 120 ºC under microwave irradiation. After the reaction had been completed, the solution was filtered. Water (50 mL) and DCM (100 mL) were added and the phases were separated. The aqueous layer was extracted with DCM (3 x 100 mL) and the combined organic layer was washed with a saturated solution of sodium carbonate (200 mL), dried over magnesium sulphate and evaporated under vacuum. The product was pure enough for the next step (9.19 g, 38.9 mmol, 97% yield).

MS (ES^+) m/z: 237 $[M+H]^+$, 259 $[M+Na]^+$; **HRMS (ES^+)** for $C_{13}H_{17}O_4$: 237.11214 (calc.); 237.11211 (found); **^{1}H NMR** ($CDCl_3$, 360 MHz): δ 9.74 (s, 1H),7.67 (d, J =8.7, 2H), 6.82 (d, J = 8.7, 2H), 4.99 (q, J = 7.1, 2H), 3.94 (t, J = 6.2, 2H), 2.37 (t, J = 7.2, 2H), 1.96 (q_5, J = 6.5, 2H), 1.10 (t, J = 7.2, 3H); **^{13}C NMR** ($CDCl_3$, 90.6 MHz): δ 190.1, 177.3, 165.8, 131.3 (2C), 129.5, 114.4 (2C), 66.5, 59.6, 29.9, 27.1, 13.5; **IR** (neat) υ/cm^{-1}: 2979 and 2941, 1728, 1686, 1251 and 1156; **HPLC (ELSD)** Rt/min**:** 4.020 (method C).

4-[4-(hydroxymethyl)phenoxy]butanoic acid (23):

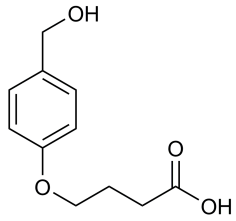

Ethyl-4-(4'-formyl-phenol)-butyrate **22** (9.19 g, 38.9 mmol) was dissolved in ethanol (32 mL) and water (32 mL) was added. NaOH (2.5 g, 62.24 mmol) was added portionwise over 20min. The reaction was stirred at room temperature for 30min. The solution was cooled to 0 ºC and sodium borohydride (1.104 g, 29.18 mmol) was added dropwise. After 1 h, the reaction was concentrated to approximately 30mL and the aqueous portion remaining was cooled to 0 ºC and the reaction quenched by the addition of 2 M HCl. The aqueous mixture was extracted with EtOAc (2 x 300 mL). The combined organic layers were washed with water and brine, dried over magnesium sulphate and concentrated under vacuum to give a greenish white solid (7.03 g, 33.46 mmol, 86%).

MS (ES^-) m/z: 209 $[M-H]^-$; **HRMS (ES^-)** for $C_{11}H_{13}O_4$: 209.08193 (calc.); 209.08164 (found); **^{1}H NMR** (MeOD, 360 MHz): δ 7.13 (d, J =8.6, 2H), 6.76 (d, J =8.6, 2H), 4.91 (bs, OH), 4.40 (s, 2H), 3.86 (t, J = 6.2, 2H), 2.35 (t, J = 7.3, 2H), 1.92 (q_5, J = 7.0, 2H); **^{13}C NMR** (MeOD, 90.6 MHz): δ 157.8, 132.8, 127.7 (2C), 113.5 (2C), 66.0, 63.0, 29.5, 23.9; **IR** (neat) υ/cm^{-1}: 3427, 2603, 1704 and 1246; **HPLC (ELSD)** Rt/min**:** 3.294 (method C).

5.2.2.2. PEG Spacer Unit Synthesis

2-[(Dibenzylamino)ethoxy]ethanol (24):

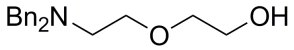

A mixture of 2-(aminoethoxy)ethanol (4.8 mL, 47.5 mmol), potassium carbonate (16.0 g, 118.75 mmol) and benzyl bromide (13.6 mL, 95 mmol) in acetonitrile (250 mL) was stirred at 50 ºC for 20 h. The solid was filtered and the solvent was removed from the filtrate. The residue was dissolved in hydrochloric acid (0.1 M, 50 mL) and washed with ethyl acetate (2 x 50 mL). The aqueous layer was then made basic (pH 9) with sodium hydroxide (4 M) and extracted with dichloromethane (4 x 50 mL). The solvent was dried over $MgSO_4$ and

removed under vacuum to give a yellowish oil (13.0 g, 45.5 mmol, 96%). The product was used in the next step reaction without further purification.

MS (ES^+) m/z: 286.1 $[M+H]^+$; **HRMS (EI)** for $C_{16}H_{19}O_6N_3F_3$: 285.17233 (calc.); 285.17246 (found); **^{1}H NMR** ($CDCl_3$, 360 MHz): δ 7.75-7.25 (m, 10H), 3.75-3.60 (m, 6H), 3.63 (t, J = 5.9, 2H), 3.55 (t, J = 4.9, 2H), 2.77 (t, J = 5.9, 2H); **^{13}C NMR** ($CDCl_3$, 90.6 MHz): δ139.0 (2C), 128.6 (4C), 128.0 (2C), 126.7 (2C), 71.8, 69.3, 61.5, 58.6 (2C), 52.6; **IR** (neat) υ_{max}/cm^{-1}: 3360, 1475, 1366, 1244; **HPLC (ELSD)** t_R/min**:** 3.521 (method C), 3.746 (method D).

[2-(Dibenzylaminoethoxy)ethoxy]acetic acid (25):

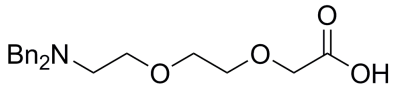

2-[(Dibenzylamino)ethoxy]ethanol (13.0 g, 45.5 mmol) was dissolved in dry THF (100 mL) and cooled to 0 ºC. Sodium hydride (7.30 g, 182.4 mmol; 60% dispersion in oil) was added in portions followed by α-bromoacetic acid (9.44 g, 68.4 mmol). The suspension was refluxed under nitrogen overnight. Water (7 mL) was added carefully followed by stirring for 5 min. More water (200 mL) was added and the aqueous layer washed with a mixture of hexane/diethyl ether (3 x 100 mL) and then neutralised to pH 6-7 with sodium hydroxide (4 M). Solid sodium chloride was added and the mixture was extracted with dichloromethane (5 x 150 mL). The solvent was dried over $MgSO_4$ and removed under vacuum. The crude colorless oil product was used in the next reaction without further purification (8.67 g, 25.2 mmol, 56%).

MS (ES^-) m/z: 342.1 $[M-H]^-$; **HRMS (EI)** for $C_{16}H_{19}O_6N_3F_3$: 343.17781 (calc.); 343.17824 (found); **^{1}H NMR** ($CDCl_3$, 250 MHz): δ 12.21 (bs, OH), 7.72-7.66 (m, 4H), 3.60-7.50 (m, 6H), 4.45 (s, 2H), 4.35-4.28 (m, 2H), 3.98-3.87 (m, 4H), 3.83-3.81 (m, 2H), 3.19 (t, J = 4.96, 2H); **^{13}C NMR** ($CDCl_3$, 90.6 MHz): δ 173.7, 133.2, 130.4 (2C), 128.6 (2C), 128.3, 70.5 (2C), 70.1 (2C), 68.0 (2C), 67.2 (2C), 57.5 (2C), 53.4 (2C); **IR** (neat) υ_{max}/cm^{-1}: 2869, 1728, 1582, 1111,730, 697; **HPLC (ELSD)** t_R/min**:** 3.010 (method C).

[2-(2-aminoethoxy)ethoxy]acetic acid (26):

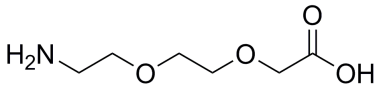

Compound **25** (8.67 g, 25.2 mmol) was dissolved in MeOH (100 mL), palladium (3.0 g, 10% on carbon) was added and the mixture was stirred under hydrogen atmosphere (1 atm) at 45 ºC for 20 h. The catalyst was eliminated by filtration through a celite pad and the solvent removed under vacuum. The residue was triturated with diethyl ether (200 mL) to give a colorless oil (3.86 g, 23.68 mmol, 94%)

MS (ES^+) m/z: 164 $[M+H]^+$; **MS (ES^-)** m/z: 162 $[M-H]^-$; **HRMS (EI)** for $C_{16}H_{19}O_6N_3F_3$: 163.08391 (calc.); 163.08402 (found); **^{1}H NMR** ($CDCl_3$, 600 MHz): δ 4.68 (bs, OH), 4.25 (bs, NH), 4.13 (s, 2H), 3.96-3.70 (m, 6H), 3.36-3.35 (m, 2H); **^{13}C NMR** ($CDCl_3$, 90.6 MHz): δ 170.9, 70.4, 69.67, 67.9, 66.9, 39.1; **IR** (neat) υ_{max}/cm^{-1}: ~2880, 1579, 1097; **HPLC (ELSD)** t_R/min**:** 0.701 (method C).

{2-[(9H-Fluoren-9-ylmethoxycarbonylamino)-methoxy]-ethoxy}-acetic acid (27):

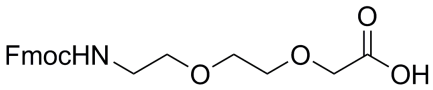

The crude [(2-aminoethoxy)ethoxy]acetic acid (3.86 g, 23.68 mmol) was dissolved in water (120 mL) and sodium bicarbonate (3.98 g, 47.35 mmol) was added with stirring. The resulting solution was cooled in an ice bath and a solution of Fmoc-Cl (6.74 g, 26.04 mmol) in dioxane (240mL) was added dropwise. After stirring at 0°C for 1 h, the reaction mixture was allowed to warm to RT and stirred for a further 2 h. Water was added (50mL), and the aqueous solution was washed with diethyl ether (2 x 30 mL). The aqueous solution was acidified to pH 1-2 with concentrated hydrochloric acid and extracted with dichloromethane (5 x 30 mL). The solvent was dried and removed under vacuum to give an oily product (8.87 g, 23.02 mmol, 97%).

MS (ES^-) m/z: 384.0 $[M-H]^-$; **HRMS (EI)** for $C_{21}H_{23}NO_6$: 385.15199 (calc.); 385.15294 (found); **^{1}H NMR** ($CDCl_3$, 400 MHz): δ 7.73 (d, J = 7.5, 2H), 7.59 (d, J = 7.3, 2H), 7.37 (t, J = 7.3, 2H), 7.28 (t, J = 7.5, 2H), 5.63 (t, J = 5.4, 1H), 4.37 (d, J = 6.9, 2H), 4.19 (t, J = 6.8, 2H), 4.13 (s, 2H), 3.75-3.70 (m, 2H), 3.68-3.63 (m, 2H), 3.61-3.55 (m, 2H), 3.45-3.38 (m, 2H); **^{13}C NMR** ($CDCl_3$,

90.6 MHz): δ 172.7, 156.8, 144.0, 141.3, 127.7, 127.0, 125.1, 120.0, 70.9 (2C), 70.3, 68.3, 66.8, 47.2, 40.8; **IR** (neat) υ_{max}/cm^{-1}: 3324, 1716, 1531, 1253, 1116, 887, 759; **HPLC (ELSD)** t_R/min**:** 4.250 (method C), 7.630 (method D);

5.2.2.3. Photospacer solid phase synthesis

Linker coupling to amino PS resin (28):

Amino polystyrene resin (1.0 g, 1.6 mmol) was swollen in DCM (10 mL). Hydroxymethyl phenyl butanoic acid **23** (1.018 g, 7.8 mmol) and HOBt (650 mg, 4.8 mmol) were dissolved in DMF/DCM (1:1, 20 mL) and then DIC (743 μL, 4.8 mmol) was added to the solution and stirred for 5 min. This solution was added to the resin and left shaking on the rotary wheel for 2.5 h. The resin was then washed with DMF (3 x 1 mL) and DCM (3 x 1 mL) and treated with 1.0 M NaOH(aq)/dioxane (1:1, 20 mL) for 1.5 h. This treatment was necessary to eliminate oligomers of the linker formed during the reaction. The resin was then washed with water (3 x 1 mL), DMF (3 x 1 mL), MeOH (3 x 1 mL), DMF (3 x 1 mL), DCM (3 x 1 mL) and Et_2O (2 x 1 mL) and allowed to dry for 30 min under vacuum. Complete coupling was assessed using the Green Malachita test which gave a positive result for free hydroxyl groups.

Coupling of PEG spacer unit to the linker-Resin (29):

Linker-resin (100 mg, 0.16 mmol) was swollen in DCM (1 mL) for 30 min. PEG spacer unit **27** (123.328 mg, 0.32 mmol) and HOBt (43.24 mg, 0.32 mmol) were dissolved in DCM with a few drops of DMF and stirred at RT. DIC (55 μL, 0.352 mmol) and DMAP (6 mg, 0.048 mmol) were added the mixture and stirred for a further 5 min before addition to the resin. The resin was shaken at RT for 2 h to allow complete esterification. The resin was washed with DMF (3 x 1 mL), DCM (3 x 1 mL), MeOH (3 x 1 mL) and Et_2O (2 x 1 mL) and dried. Malachite Green test was done to check complete coupling of the spacer onto the resin and the absence of free hydroxyl groups.

Fmoc deprotection (30):

Fmoc removal was performed using 20% piperidine in DMF solution for 20 min at RT. The resin was then filtered and washed with DMF (3 x 1 mL), DCM (3 x 1 mL), MeOH (3 x 1 mL) and Et_2O (2 x 1 mL) and dried under vacuum. A positive ninhydrin test result confirmed completion of the reaction.

TFMAD coupling to Spacer-Linker-Resin (31):

The resin was swollen in DCM for 30 min and then washed with DMF (3 x 1 mL). Meanwhile, TFMAD (48 mg, 0.183 mmol) and HOBt (25 mg, 0.183 mmol) were dissolved in DMF (1 mL) and stirred at RT for 10 min. DIC (29mL, 0.183mmol) was added and the mixture stirred for a further 10 min before addition to the resin. The resin was shaken at RT overnight to affect coupling. The resin was washed with DMF (3 x 1 mL), DCM (3 x 1 mL), MeOH (3 x 1 mL) and Et_2O (2 x 1 mL). The resin was dried under vacuum for 30 min.

Acidic Cleavage from the Resin:

The resin (100 mg) was swollen in DCM for 30 min. Then, an acidic cocktail containing DCM:TFA:TIS:water (4.8:4.8:2:2) was added and the resin was agitated on a rotary wheel at RT for 30 min. The resin was removed by filtration and the filtrate diluted with DCM (15 mL). The organic layer was extracted with NaOH 1 M aqueous solution, then acidified with concentrated HCl and extracted again with DCM. The organic solvent was dried over $MgSO_4$ and evaporated under vacuum to give the different photospacer products.

TFMAD-PEG-OH Photospacer (PS1):

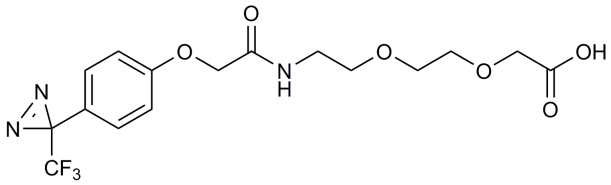

28 mg of yellow oil product (0.0691 mmol) was obtained with a yield of 36%.

MS (ES^-) m/z: 404 $[M-H]^-$; **MS (ES^+)** m/z: 406 $[M+H]^+$; **HRMS (ES^+)** for $C_{16}H_{19}O_6N_3F_3$: 406.12205 (calc.); 406.12182 (found); **^{1}H NMR** ($CDCl_3$, 600 MHz): δ 7.17 (d, J = 8.6, 2H), 7.11 (bs, NH), 6.95 (d, J = 8.8, 2H), 4.53 (s, 2H), 4.13 (s, 2H), 3.71 (m, 2H), 3.63 (m, 4H), 3.57 (m, 2H); **^{13}C NMR** ($CDCl_3$, 150.9 MHz): δ 175.5, 171.2, 160.7, 128.7 (2C), 122.9, 122.5 (q, ^1J = 274.4), 115.5 (2C), 71.5, 70.4, 70.0, 68.9, 67.4, 39.3, 28.0 (q, ^2J = 40.7); **^{19}F NMR** ($CDCl_3$, 235.9 MHz): δ -66.24; **HPLC (ELSD)** Rt/min**:** 4.119 (method C), 5.837 (method D).

TFMAD-(PEG)$_2$-OH photospacer (PS2):

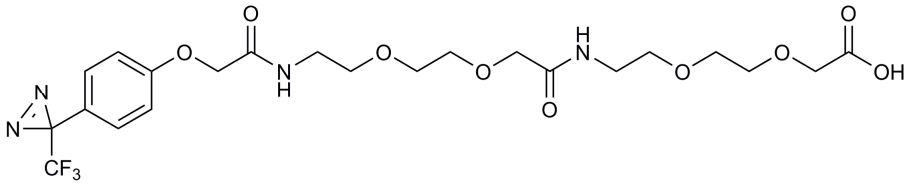

33 mg of yellow oil product (0.06 mmol) was obtained with a yield of 30%.

MS (ES$^-$) m/z: 549 [M-H]$^-$; **MS (ES$^+$)** m/z: 551 [M+H]$^+$, 573 [M+Na]$^+$; **^{1}H NMR** ($CDCl_3$, 360 MHz): δ 7.11 (d, J = 8.6, 2H), 7.02 (d, NH, J = 8.4, 1H), 6.89 (m, 2H), 6.73 (d, NH, J = 8.5, 1H), 4.48 (s, 2H), 4.09 (s, 2H), 3.98 (s, 2H), 3.70-3.35 (m, 16H); **^{13}C NMR** ($CDCl_3$, 90.6 MHz): δ 173.1, 170.9, 170.0, 158.4, 128.7 (2C), 122.8, 122.0 (q, ^{1}J = 274.5), 115.4 (2C), 71.3, 70.8, 70.7, 70.5, 70.3, 70.1, 70.0, 68.9, 67.4, 39.2, 39.1, 28.0 (q, ^{2}J = 40.4); **^{19}F NMR** ($CDCl_3$, 235.9 MHz): δ -66.12; **HPLC (ELSD)** Rt/min**:** 4.112 (method C).

TFMAD-(PEG)$_3$-OH photospacer (PS3):

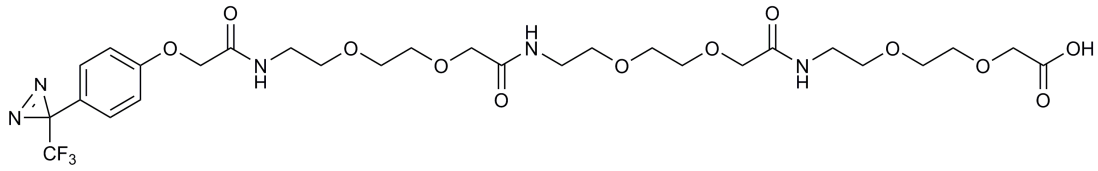

38 mg of yellow oil product (0.055 mmol) was obtained with a yield of 27%.

MS (ES$^-$) m/z: 694 [M-H]$^-$; **MS (ES$^+$)** m/z: 696 [M+H]$^+$; **^{1}H NMR** ($CDCl_3$, 360 MHz): δ 7.11 (d, J = 8.7, 2H), 7.00 (d, NH, J = 8.4, 1H), 6.88 (2H, d J = 8.8), 6.71 (d, NH, J = 8.5, 1H), 4.47 (s, 2H), 4.07 (s, 2H), 3.96 (s, 2H), 3.95 (s, 2H), 3.65-3.40 (m, 24H); **^{13}C NMR** ($CDCl_3$, 90.6 MHz): δ 172.6, 171.1, 170.7, 168.6, 158.4, 128.7 (2C), 122.7, 122.4 (q, ^{1}J = 274.7), 115.4 (2C), 71.1, 71.0, 70.9, 70.6 (2C), 70.5, 70.3, 70.2, 70.0, 69.9, 68.7, 67.4, 39.1, 39.0, 38.9, 28.4 (q, ^{2}J = 40.5); **^{19}F NMR** ($CDCl_3$, 235.9 MHz): δ -66.11; **HPLC (ELSD)** Rt/min**:** 4.158 (method C), 7.338 (method D).

5.4.3. Preparation of Fluorous tagged Photospacers

General solution phase coupling procedure:

To a solution of photospacer, carboxyfluorescein or biotin (1.1 equivalent) in DMF was added (benzotriazol-1-yloxy)trispyrrolidinophosphonium hexafluorophosphate (pyBOP) coupling agent (1.2 equivalent) and stirred at RT

for 45 min. 1-amino-1H,1H,2H,2H-perfluorodecane (1.0 equivalent) and DIEA (1.5 equivalent) in DMF were added and the reaction was irradiated in the microwave for 5 min at 50 ºC and then stirred at RT for 1 h. Evaporation of the product gave the crude which was purified through FSPE using FluoroFlash® silica gel starting with 20% MeOH in water as the wash fraction and 100% MeOH as the elution solution.

Fluorous-tagged Biotin (32):

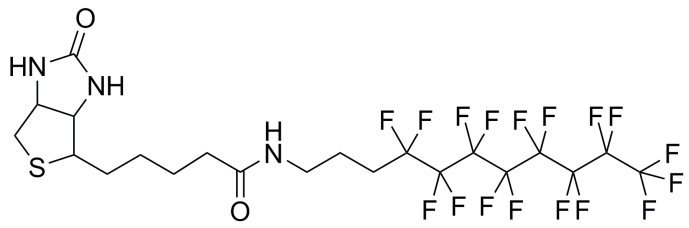

50 mg of product was obtained with a yield of 71%.

MS (ES$^+$) m/z: 704 $[M+H]^+$, 726 $[M+Na]^+$; **^{1}H NMR** (d^6-DMSO with CF_3COOH traces, 500 MHz): δ 7.93 (t, J = 5.3, 1H), 6.96 (d, J = 7.4, 1H), 6.71 (d, J = 8.6, 1H), 4.35-4.32 (m, 1H), 4.17-4.14 (m, 1H), 3.17-3.00 (m, 3H), 2.27-2.15 (m, 2H), 2.07 (t, J = 7.4, 2H), 1.69-1.58 (m, 2H), 1.57-1.42 (m, 2H), 1.36-1.25 (m, 2H), 0.88-0.77 (m, 2H); **^{13}C NMR** (d^6-DMSO with CF_3COOH traces, 125.9 MHz): δ 172.4, 163.1, 132-108 (m), 61.3, 59.5, 55.5, 37.5, 35.3, 28.3, 28.1, 25.4, 24.8, 20.3, 15.7; **^{19}F NMR** (d^6-DMSO, 235.9 MHz): δ -126.23 (2F), -123.54 (2F), -122.93 (2F), -122.90 (6F), -113.76 (2F), -80.66 (3F); **HPLC (ELSD)** Rt/min**:** 4.716 (method C).

Fluorous-tagged 5-(6)-carboxyfluorescein (33):

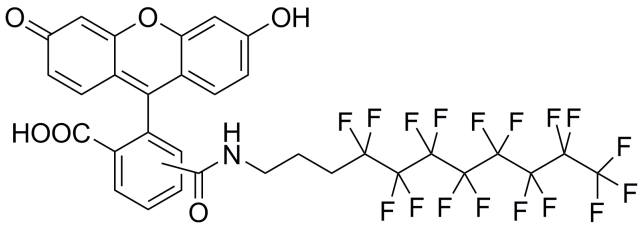

5-(6)-FAM-Ftag

121 mg of product was obtained with a yield of 60% and a mixture of both, 5- and 6- substituted products.

MS (ES$^+$) m/z: 836 $[M+H]^+$; **^{1}H NMR** (MeOD, 360 MHz): δ 8.10 (d, J = 8.0, 1H), 8.03 (d, J = 7.0, 1H), 7.96 (d, J = 8.1, 1H), 7.19 (d, J = 8.1, 1H), 6.58 (s, 2H), 6.50 – 6.40 (m, 3H), 3.27 (t, J = 6.8, 2H), 3.21 (s, 1H), 2.28–2.01 (m,

4H), 1.81 (q_5, J^1 = 7.6, 2H); **^{13}C NMR** (MeOD, 90 MHz): δ 168.6 (168.6), 166.5 (166.3), 158.0 (159.5), 152.1 (154.8), 135.7 (140.1), 133.6 (126.7), 128.3 (2C), 126.4 (126.7), 125.3, 124.3, 123.8, 122.9, 122.0 (117.0), 116.7, 111.8, 109.6 (108.9), 101.7, 40.8, 38.3, 35.1, 27.4 (t, J = 8.6, 1C), 19.5 (m, 1C); ^{1}H and ^{12}C NMRs describe those signals corresponding to 5-substituted product. **^{19}F NMR** (MeOD, 235.9 MHz): δ -127.72 (2F), -124.82 (2F), -124.19 (2F), -123.33 (6F), -115.65 (2F),-82.77 (3F); **HPLC (ELSD)** Rt/min**:** 4.757 (method C).

TFMAD-PEG-Ftag (FPS1):

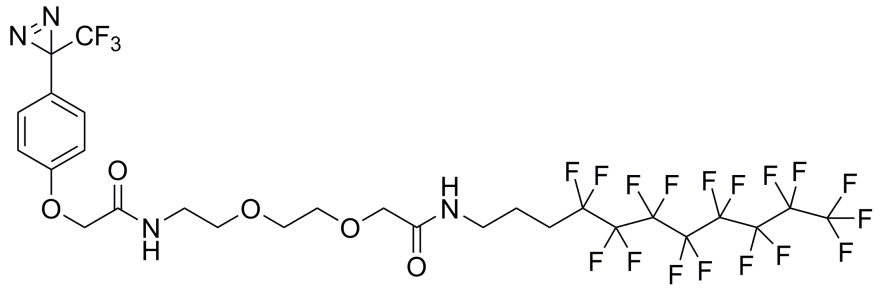

21 mg of product was obtained with a yield of 70%.

MS (ES$^+$) m/z: 865 $[M+H]^+$, 887 $[M+Na]^+$; **^{1}H NMR** (MeOD, 400 MHz): δ 7.24 (d, J = 8.6, 2H), 7.10 (d, J = 9.0, 2H), 4.58 (s, 2H), 4.02 (s, 2H), 3.79-3.71 (m, 2H), 3.68 (s, 4H), 3.65-3.60 (m, 2H), 3.54-3.48 (m, 2H), 2.30-2.20 (m, 2H), 1.90-1.80 (m, 2H); **^{13}C NMR** (MeOD, 125.9 MHz): δ 171.6, 171.6, 169.2, 159.0, 128.0 (2C), 122.3 (q, ^{1}J = 273.0), 121.5, 115.2 (2C), 70.5, 69.9, 69.8, 69.1, 66.7, 42.4, 38.5, 37.6, 28.0 (q, ^{2}J = 28.0); **^{19}F NMR** (MeOD, 235.9 MHz): δ -127.26 (2F), -124.38 (2F), 123.72 (2F), -122.89 (6F), -115.21 (2F), -82.35 (3F), -67.44 (3F); **HPLC (ELSD)** Rt/min**:** 4.966 (method C).

TFMAD-(PEG)$_2$-Ftag (FPS2):

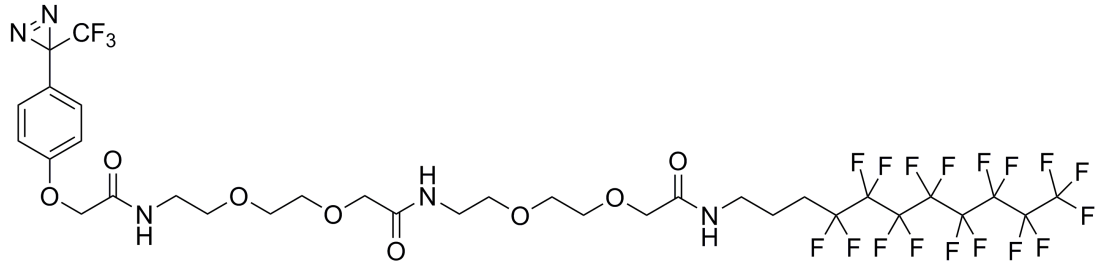

51 mg of product was obtained with a yield of 72%.

MS (ES$^-$) m/z: 1008 $[M-H]^-$, 1054 $[M+FA]^-$; **MS (ES$^+$)** m/z: 1010 $[M+H]^+$, 1032 $[M+Na]^+$; **^{1}H NMR** ($CDCl_3$, 500 MHz): δ 7.20 (d, J = 8.7, 2H), 7.07-7.02

(m, 3H, NHs), 6.96 (d, J = 8.9, 2H), 4.52 (s, 2H), 4.01 (s, 4H), 3.07-3.64 (m, 4H), 3.64-3.56 (m, 8H), 3.54-3.49 (m, 2H), 3.42-3.38 (m, 2H), 2.21-2.11 (m, 2H), 1.33-1.27 (m, 2H); **^{13}C NMR** ($CDCl_3$, 125.9 MHz): δ 170.3, 170.2, 168.1, 158.5, 128.8 (2C), 123.0, 122.1 (q, ^1J = 274.5), 115.4 (2C), 70.8, 70.5, 70.1, 70.0, 69.8, 67.3, 38.8, 38.4, 37.9, 20.9, 28.4 (q, ^2J = 23.0); **^{19}F NMR** ($CDCl_3$, 235.9 MHz): δ -126.06 (2F), -123.50 (2F), 122.67 (2F), -121.28 (6F), -114.07 (2F), -81.18 (3F), -66.46 (3F); **HPLC (ELSD)** Rt/min**:** 4.945 (method C);

TFMAD-(PEG)$_3$-Ftag (FPS3):

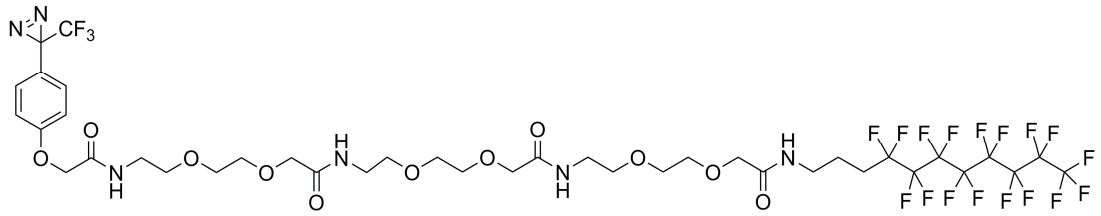

30 mg of product was obtained with a yield of 69%.

MS (ES$^-$) m/z: 1153.8 $[M-H]^-$; 1199.1 $[M+FA]^-$; **^{1}H NMR** ($CDCl_3$, 500 MHz): δ 7.20 (d, J = 8.7, 2H), 6.97 (d, J = 9.0, 2H), 7.16-7.01 (m, NH, 4H), 4.533 (s, 2H), 4.16 (s, 2H), 4.02 (s, 4H), 3.69-3.50 (m, 24H), 3.44-3.39 (m, 2H), 1.29-1.25 (m, 2H), 1.16 (t, J = 4.3, 2H); **^{13}C NMR** ($CDCl_3$, 125.8 MHz): δ 170.8, 170.0, 170.0-169.8 (m), 167.7, 158.2, 128.45 (2C), 122.5, 115.2 (2C), 122.1 (q, ^1J = 274.9), 129.8, 70.8 (3C), 70.7, 70.6, 70.2, 70.1 (2C), 70.0, 69.9, 69.8, 68.5, 67.4, 38.8, 38.6, 38.6, 38.5, 37.9, 29.7, 23.8 (q, ^2J = 24.0); **^{19}F NMR** ($CDCl_3$, 235.9 MHz): δ -126.04 (2F), -123.33 (2F), 121.67 (2F), -119.00 (6F), -114.23 (2F), -80.73 (3F), -65.58 (3F); **HPLC (ELSD)** Rt/min**:** 4.938 (method C);

5.4.4. Biotin-Streptavidin validation experiment

Attachment of Photospacers by Strategy I

A 15 μL solution of 0.3 M of **PS1**, **PS2** or **PS3** photospacer in DMF were transferred to a well plate and mixed with 15 μL of a solution of 0.3 M of HOBt in DMF. This was followed by addition of 15 μL solution of 0.3 M of DIC in DMF and mixing. 10 drops/spot were printed using this solution using a Microdrop printer (90 V and 60 μs). Printed slides were kept in a hybridisation chamber with DMF (1 mL) overnight at 30 ºC. The slides were washed with DMF (2 x 3 min), EtOH

(2 x 3 min), water and acetone and dry with nitrogen. If the slides were not used immediately, they were kept in the dark at 4 ºC.

Attachment of Photospacers by Strategy II

Solutions of 10 mM concentration of **FPS1**, **FPS2** or **FPS3** were prepared in DMF and used for printing 8-10 drops/spot onto fluorinated slides by inkjet printing at 90 V and 60 μs of pulse. The slides were left to dry overnight before small molecule solutions were printed on top.

Biotin/Carboxyfluorescein Immobilisation:

Four different concentration solutions of Biotin/carboxyfluorescein in DMSO (0.1 mM, 1 mM, 10 mM and 100 mM) were prepared and printed on the microarray slides by an inkjet printer (Microdrop). The slides were dried overnight under vacuum. They were then cool down to -196 ºC with liquid nitrogen and irradiated for 40 min at 365 nm with a 100W lamp. The slides were washed with DMSO, EtOH, water and acetone and dried with nitrogen for strategy I or with PBS buffer and distilled water for strategy II. In the case of carboxyfluorescein immobilisation, slides were ready to be scanned using a FITC filter.

Hybridisation with Amersham Cy^{TM}5-Streptavidin (GE Healthcare):

Slides were incubated with 150 μL of a 10 μg/mL streptavidin in PBS (pH 7.4) buffer for 1 h at RT with a hybridisation station (Zinsser Analytic GmbH). Slides were then washed with PBS buffer (3 x 10 min), rinsed with distilled water and dried under a nitrogen stream. Slide scanning was performed using a Cy5 filter by the bioanalyser microarrayer (La Vision BioTech).

5.4.5. Small Molecule Microarray

Small-Molecule Microarray Preparation:

A small molecule microarray was prepared by printing 8 drops per spot of 10 mM **FPS1** solution in DMF (53 rows x 114 columns = 6,042 spots) at a 78 V and 64 μs of pulse using a Scienion S5 sciFLEXARRAYER (Scienion AG, Germany). The slides were left to dry overnight. Using the same settings for voltage and pulse, the 2,000 compounds from the SPECTRUM library (10 mM solutions in DMSO) were printed in triplicate at different locations, distributed along the slide, with 8 drops per spot for each compound. The final diameter per

spot was 200 μm. Slides were left to dry overnight and then irradiated for 40 min at 365 nm from a distance of about 10 cm before washing in distilled water (3 x 10 min) and dried under a nitrogen stream. Slides were scanned with a microarray scanner (Genetix 4200AL, Axon) and analysed with FIPS software (LaVision Biotec, Bielefeld, Germany). If slides were not used immediately, they were kept in the dark at 4 ºC.

Hybridisation with Human β-TrCP I Protein (University of Toronto):

Slides were incubated with 150μL of a 2μM solution of β-TrCP I in TBS containing 0.5% of phosphoBLOCKER™ Blocking Reagent (Cell Biolabs, inc.). Hybridisation was carried out overnight at 4 ºC. Slides were then removed, washed with TBS buffer (3 x 10 min), rinsed with water and dried under a nitrogen stream.

Hybridisation with mouse anti-β-TrCP I (Invitrogen, 37-3400):

1 μL of monoclonal mouse anti-β-TrCP I solution (0.5 mg/mL in PBS, pH 7.4, containing 0.1% sodium azide) was dissolved in 500 μL of TBS buffer containing 1% of phosphoBLOCKER™ Blocking Reagent (Cell Biolabs, inc.). 150 mL of this solution was introduced to the hybridisation station and hybridisation was carried out for 4 h at RT. After that time, slides were removed, washed (3 x 10 min) in TBS buffer, rinsed with water and dried under a nitrogen stream.

Hybridisation with Cy3 conjugated Donkey anti-Mouse IgG Secondary Antibody (Thermo Scientific, PA1-29773):

1 μL of an affinity purified antibody solution (1.4 mg/mL, 500 μg in PBS, pH 7.6, containing 0.05% sodium azide) was dissolved in 500 μL of TBS buffer containing 1% of phosphoBLOCKER™ Blocking Reagent (Cell Biolabs, inc.). 150 mL of this solution was introduced to the hybridisation station and hybridisation was carried out for 1 h at RT. After that time, slides were removed, washed (3 x 10 min) in TBS buffer, rinsed with water and dried under a nitrogen stream.

Denaturising Wash for Slide reusal:

Slides were washed for 1 h at 70 ºC with destilled water and gentle agitation. Slides were then washed with PBS (3 x 3 min) and rinsed with distilled water before drying under nitrogen stream.

5.5. Experimental for Chapter 3

The 9-mer peptoid carrier system used in this chapter was provided by Geraldine Esher, a member of Bradley group.

5.5.1. Photoprobe synthesis

Synthesis of Dde-OH (34):

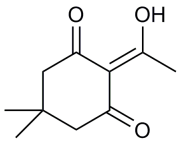

Dimedone (2.06 g, 10 mmol), DMAP (122 mg, 1 mmol) and DCC (1.40 g, 10 mmol) were dissolved in DMF (17 mL) and stirred at RT. Acetic acid (584 μL, 142 mmol, 2 eq) was added to the solution and heated at 80 ºC under microwave irradiation for 1 h. The reaction mixture was filtered and the organic layer was poured into water (20 mL), which was then extracted with Et_2O (3 x 100 mL), dried with MgSO4 and then evaporated *in vacuo*. The crude was passed through a plug of silica to give 1.63 g of a yellowish solid (9 mmol, 90%).

MS (ES^-) m/z: 181 $[M-H]^-$; **HRMS (ES^+)** for $C_{10}H_{15}O_3$: 183.10157 (calc.); 183.10154 (found); **^{1}H NMR** ($CDCl_3$, 500 MHz): δ 2.59 (s, 3H), 2.52 (s, 2H), 2.34 (s, 2H), 1.06 (s, 6H); **^{13}C NMR** ($CDCl_3$, 150.9 MHz): δ 202.4, 197.9, 195.2, 112.4, 52.5, 46.9, 30.7, 28.5, 28.2; **IR** (neat) υ/cm^{-1}: 3324, 2957, 2930, 1665, 1556, 1438; **HPLC (220 nm)** Rt/min**:** 3.776 (method C).

Synthesis of Lys(Dde)-OH (35):

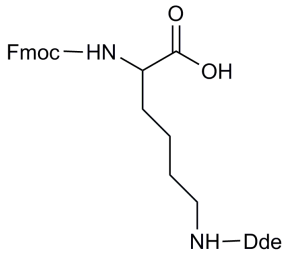

Fmoc-Lys-OH·HCl (10 g, 24.70 mmol) was dissolved in distilled water and DIPEA (5 mL) was added dropwise until a white precipitate was formed. The solution was left to stir for 10 min at room temperature. The precipitate was obtained by filtration and dried under vacuum overnight (8.181 g, 21.17 mmol, 86%).

Fmoc-Lys-OH (900 mg, 2.44 mmol) and Dde-OH (1.302 g, 7.32 mmol) were suspended in ethanol (12 mL) and TFA (18.8 μL, 0.25 mmol) was added dropwise. The mixture was heated under microwave irradiation for 60 min at 120 ºC. Solvent was then removed and the resulting orange residue was dissolved in EtOAC and washed with 1 M aqueous KHSO4 (3 x 100 mL). The organic layer was dried over MgSO4 and evaporated by vacuum. Purification of the crude product was done by column chromatography in 8:1 DCM:MeOH to give 1.093 g of a yellowish powder (2.052 mmol, 84%).

MS (ES^-) m/z: 531 $[M-H]^-$; **MS (ES^+)** m/z: 533 $[M+H]^+$, 555 $[M+H]^+$; **HRMS (ES^+)** for $C_{31}H_{36}O_6N_2$: 533.26571 (calc.); 533.26553 (found); **^{1}H NMR** ($CDCl_3$, 500 MHz): δ 13.32 (br, 1H), 7.77 (d, J = 7.5, 2H), 7.61 (t, J = 8.4, 2H), 7.40 (t, J = 7.4, 2H), 7.30 (t, J = 7.3, 2H), 5.83 (s, 1H, NH), 4.47 (br, 1H), 4.38 (d, J = 6.85, 2H), 4.21 (t, J = 6.9, 2H), 3.42 (s, 2H), 2.59 (s, 4H), 2.38 (m, 3H), 2.01-1.70 (m, 4H), 1.60-1.47 (m, 2H), 1.03 (s, 6H); **^{13}C NMR** ($CDCl_3$, 150.9 MHz): δ 202.5, 198.0, 195.4, 174.1, 156.2, 143.8 (2C), 141.3 (2C), 127.7 (2C), 127.1 (2C), 125.2 (2C), 120.0 (2C), 112.4, 67.1, 53.5, 52.5 (2C), 47.2, 43.3, 32.0, 30.7, 30.2, 28.2 (2C), 22.4, 18.2; **IR** (neat) υ/cm^{-1}: 3294, 2951, 2866, 1715, 1567; **HPLC (ELSD)** Rt/min**:** 4.503 (method C).

Microwave Coupling Reaction Procedure:

The corresponding polystyrene resin (1.23 mmol/g, 1.0 eq) was swollen in DCM (15 mL) for 30 min. A 0.1M solution was prepared with an acidic building block (3.0 eq) and oxyma (3.0 eq) in DCM, and a few drops of DMF were added if necessary for complete dissolution. DIC (3.0 eq) was added to the solution and stirred for 10 min. The solution was then poured into the resin and the suspension was transferred to a microwave vial. The reaction was done at 60 ºC for 20 min. Resin was filtered and washed with DMF (3 x 15mL), DCM (3 x 15mL), MeOH (3 x 15mL) and Et_2O (3 x 15mL) and dried. The completion of the reaction was confirmed with a negative qualitative ninhydrin test.

Room Temperature Coupling Reaction Procedure:

The corresponding polystyrene resin (1.23 mmol/g, 1.0 eq) was swollen in DCM for 30 min. A 0.1 M solution was prepared with the acidic building block (3.0 eq) and oxyma (3.0 eq) in DCM, and a few drops of DMF were added if necessary for complete dissolution. DIC (3.0 eq) was added to the solution and stirred for 10 min. The solution was then added to the resin and the mixture was

agitated in a rotary-wheel for 1 h. Resin was filtered and washed with DMF (3 x 15 mL), DCM (3 x 15 mL), MeOH (3 x 15 mL) and Et_2O (3 x 15mL) and dried. The completion of the reaction was confirmed with a negative qualitative ninhydrin test.

6(5)-Carboxyfluorescein Coupling Reaction:

The corresponding resin was swollen in DCM and a solution of 5(6)-carboxyfluorescein (3.0 eq) and oxyma (3.0 eq) in DMF was prepared. DIC (3.0 eq) was to this solution added and the mixture stirred for 10 min and then poured onto the resin which stirred overnight at room temperature. The resin was washed with DMF (3 x 15 mL), DCM (3 x 15 mL), MeOH (3 x 15 mL) and Et_2O (3 x 15 mL) and dried. The completion of the reaction was confirmed with a negative qualitative ninhydrin test.

Fmoc Deprotection Procedure:

The corresponding resin was swollen in DCM and filtered. A freshly prepared solution of 20% piperidine in DMF was added to the resin and agitated in a rotary-wheel for 20 minutes. Resin was then filtered and washed with DMF (3 x 15 mL), DCM (3 x 15 mL), MeOH (3 x 15 mL) and Et_2O (3 x 15 mL) and dried. The completion of the reaction was confirmed with a positive qualitative ninhydrin test.

Dde Deprotection in Presence of Fmoc Group:

Hydroxylamine hydrochloride (1.25 mg, 1.80 mmol) and imidazole (0.918 g, 1.35 mmol) were suspended in NMP (5 mL) and the mixture was sonicated until complete dissolution. To this solution, DCM (1 mL) was added and the mixture added to the swollen resin with DCM (500 mg, 0.5 mmol) and stirred for 3 h at room temperature. The resin was washed in DCM (3 x 1 mL), DMF (3 x 1 mL), MeOH (3 x 1 mL) and Et_2O (3 x 1 mL) and dried. Deprotection was confirmed with a positive qualitative ninhydrin test.

Resin Cleavage:

Resins **40** and **45** were swollen in DCM for 30 min, washed with DMF (2 x 15 mL), 20% piperidine in DMF solution (3 x 15 mL), DMF (2 x 15 mL), and DCM (2 x 15 mL). A cocktail solution of TFA:TIS:water (90:5:5, 20 μL/mg) was added to the resin and the mixture stirred for 2 h at room temperature. The cleavage mixture was filtered and the resin rinsed with neat TFA (1 mL). The collected

acidic solution was added dropwise to a flask containing cooled diethyl ether (10mL ether/mL of cleavage cocktail) where product was precipitated. The precipitate was centrifuged for 10 min and the supernatant was changed for a new cooled diethyl ether solvent fraction. This action was repeated three times to eliminate TFA and scavengers presence from the flask. Finally, the solid was dried under vacuum.

Photoreactive probe (41):

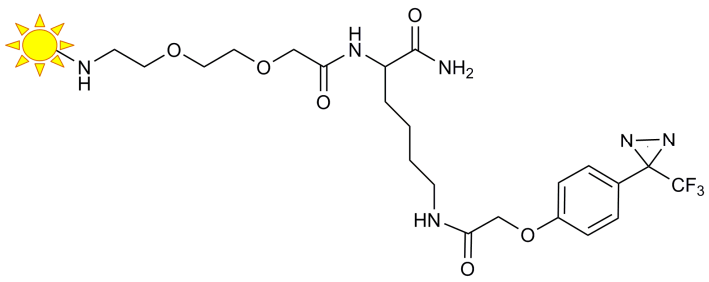

Photoreactive probe **41** was obtained from the cleavage of 50 mg of resin to give 35 mg of an orange powder in 64% yield and 90% purity.

MS (ES^+) m/z: 891 $[M+H]^+$; 913 $[M+Na]^+$; **HRMS (ES^+)** for $C_{43}H_{41}O_{12}N_6F_3$: 891.27884 (calc.); 891.27891 (found); **^{1}H NMR** ($CDCl_3$, 500 MHz): δ 8.30-8.20 (m, 2H), 7.97 (d, J = 7.4, 2H), 7.21 (d, J = 8.4, 2H), 7.09-7.00 (m, 5H), 6.91-6.81 (m, 2H), 6.50 (dd, J = 6.5 and 2.4, 2H), 4.50 (d, J = 9.3, 2H), 4.44 (q, J = 7.2, 2H), 4.03 (s, 2H), 3.74-3.57 (m, 8H), 3.27-3.19 (m, 2H), 1.88-1.62 (m, 2H), 1.60-1.50 (m, 2H), 1.42-1.35 (m, 2H); **^{13}C NMR** ($CDCl_3$, 150.9 MHz): δ 175.8, 174.9, 171.1, 169.0, 166.9, 160.9, 158.9, 152.1, 139.3, 136.7, 132.2, 132.6, 130.9, 129.5, 128.0, 122.3 (q, ^{1}J = 273.8),121.4, 115.2, 114.4 (2C), 105.7, 102.1, 99.9, 70.8, 69.6, 69.2, 69.0, 66.7, 54.2, 39.7, 38.4, 32.0, 28.6, 27.9 (q, ^{2}J = 40.3), 22.5; **^{19}F NMR** ($CDCl_3$, 235.9 MHz): δ -66.05; **HPLC (ELSD)** Rt/min**:** 4.226 and puritiy: 90%.

NLS photoreactive probe (46):

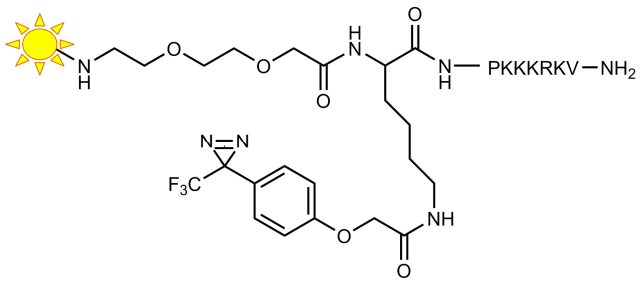

NLS photoreactive probe was obtained form the cleavage of 50 mg of resin to give 26 mg of pure product in 24% yield and 96% purity.

MALDI-TOF MS m/z: 1728.9298 $[(M+H)-N_2]^+$; 1952.9955 [(M+sinapic acid (SA))-$N_2]^+$; **HPLC (ELSD)** Rt/min: 3.117 and puritiy: 96%.

Measure of the sample concentration by UV-Vis spectroscopy:

With the aim of facilitating the probe fluorescence measurement as a consequence of its pH dependency, all samples were dissolved with a solution of 0.1 M NaOH aqueous solution in order to only detect the dianion form which absorbs at 499 nm with a coefficient extinction of 76,900 $M^{-1}cm^{-1}$ and have the best quantum yield (Φ= 0.93).[389] The absorption spectrum was acquired with an 8453 UV-Vis spectrophotometer (Agilent) and concentration calculated using the Beer-Lambert law.

MALDI-TOF MS sample preparation:

1 μL of Sinapinic acid (SA) matrix (10 mg/mL of SA in 50% MeCN in water with 0.1% TFA) was mixed with 1 μL of each sample (1mg/mL in water) on a gold target. Measurements were made using a laser-desorption time-of-flight system (Applied Biosystems). For signal generation, 20-50 laser shots were added up in the single shot mode.

5.5.2. Photoprobe Cellular Uptake

Cellular Uptake experiment:

Cells were suspended to the appropriate cell density in fresh growth media before seeding onto polystyrene well-plates. Cells were incubated (37 ºC/5% CO_2) for 24 hours to allow adhesion. Two concentrations of photoreactive probes and carboxyfluorescein (10 and 20 μM) were added at different times and cells incubated (37 ºC/5% CO_2) in their presence for 1-24 h prior analysis by FACS.

Probes Cytotoxicity:

Toxicity of probes **41** and **46** at different concentrations (10-100 μM) was assessed by the MTT assay described in **Section 5.2.6**. Samples of both probes at different concentrations were added to a 96 well-plate at a density of 10^4 cells/well and assessed in quintuplicate. After 24 h incubation with the probes,

cell viability was measured by the formation of formazan crystals and compared to the positive and negative controls.

Microscopy and Nuclei Staining with Hoechst 33342:

Cells were seeded to the appropriate cell density in a 24-well plate in fresh growth media and incubated (37 ºC/5% CO_2) for 24 h to allow adhesion. The two different probes and carboxyfluorescein were added in a concentration of 10 μM and incubated for 8h. Cells were washed with PBS before staining.

Cells were fixed with a solution of 4% *para*-formaldheyde in PBS (300 μL) for 20 minutes at RT. Cells were washed carefully two more times with PBS (300 mL) before adding a solution of HOECHST dye (300 μL, 0.1 mg/mL) and incubated for 20 minutes at RT. Finally, cells were washed two times with PBS prior to microscopy. Microscopy was performed in PBS with a Leica DM IRB inverted fluorescent microscope or bright field as appropriate. Merged images were performed under identical exposure conditions using Leica FW4000 v 1.2 software.

5.5.3. Peptoid experiment

Peptoid capture by photoreactive probes:

On a 96 well-plate, the same volume of a peptoid solution (2.64 mM, 150 μL/well) was placed into several wells. Different volumes of the photoreactive probe (14.67 mM) were added to achieve the different ratios between peptoid and probe. Also, the 3 highest volumes of probe used were added into empty wells as negative controls and treated as the others. Solvent was evaporated in the speed vac for 1 h, and then the well plate was irradiated from a distance of about 10 cm away for 40 min. Irradiated samples were redissolved in PBS, placed in eppendorfs and kept at 4 ºC until usage. Samples were analysed by MALDI-MS to see if conjugates had been formed.

Peptoid Adduct Cellular Uptake:

Cells were suspended to the appropriate cell density in fresh growth media before seeding onto polystyrene well-plates. Cells were incubated (37 ºC/5% CO_2) for 24 hours to allow adhesion. Then, addition of peptoid conjugates solutions prepared previously were added to each well to have a concentration of 10 μM of peptoid or conjugated peptoid. Cells were incubated in the presence of peptoid-probe adducts (37 ºC/5% CO_2) for 8 h prior to analysis.

5.5.4. Colchicine Adducts Toxicity

Drug capture by photoreactive probes:

1.5 mL of a 100 μM colchicine solution (60 mg) in distilled water were prepared and splitted into 3 wells of a 48-well plate. Then, 50 nmol of each photoreactive probe was added to two of the well plates in order to have the ratio 1:1 of drug-probe and same amounts of photoreactive probe were added to two empty wells as controls. The well plate solution was evaporated using the speed vac and then irradiated for 40 min. Solids were redissolved in distilled water and from these 100 μM solutions, solutions of 10 and 1 μM were prepared by diluting 10 and 100 times with distilled water. These solutions were used to carry out cytotoxicity MTT assays.

Cell viability:

Cells were incubated with colchicine, and conjugates of colchicine with probes **41** and **46** prepared in previous section for 24 h at three different concentrations (10, 1, and 0.1 μM). Each sample and concentration was assessed in quintuplet. Probes **41** and **46** were also added as negative controls for better comparison of samples at these three concentrations. After 24 h incubation, the cytotoxicity assay described in **Section 5.2.6** was carried out and cell viability was determined.

5.6. Experimental for Chapter 4

Amino-functionalised microspheres used in this chapter were provided by Juan Manuel Cardenas-Maestre, a member of the Sánchez-Martín group, with a diameter size of 380 nm and a solid content (sc) of 2%.

5.6.1. TFMAD-Functionalised Microspheres Synthesis

Preparation of PEG Microspheres (47 and 48):

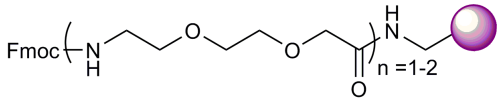

Amino functionalised microspheres (1 mL, solid content 2%, loading 27.6 μmol/g, 1 eq, Z potential = -20.4 mV) were washed in DMF (3 x 1 mL) and suspended in DMF (0.5 mL). Separately, the Fmoc-O_2Oc-OH spacer (2.13mg, 10 eq) was dissolved in DMF (0.5 mL) with HOBt (746 μg, 10 eq) and mixed until complete dissolution had been achieved. Then, diisopropylcarbodiimide (DIC) (0.9 μL, 10 eq) was added to the solution and stirred for 5 min at 25 ºC. The solution was added to amino microspheres and the suspension mixed on a rotary-wheel at 25 ºC for 18h. Microspheres were washed with DMF (3 x 1 mL) and reaction completion was confirmed by a negative qualitative ninhydrin test and a change in Z potential value (-40.0 mV).

Microspheres with a double PEG spacer unit were treated with 20% piperidine in DMF as described below and this step was repeated one more time.

Fmoc Deprotection:

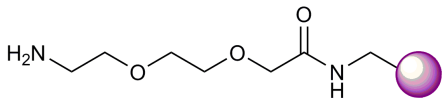

Fmoc-protected microspheres (1 mL, solid content 2%, 1 eq) were centrifuged and DMF was exchange for 1 mL of 20% piperidine in DMF solution. The solution was sonicated and then mixed in a rotary-wheel for 20 min. The process was repeated one more time. Finally, microspheres were washed with DMF (3 x 1 mL) and reaction was confirmed by a positive qualitative ninhydrin test and a change in Z potential value (-0.8 mV).

Preparation of PEG-disulphide Microspheres (50):

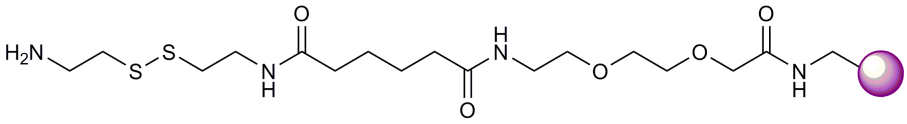

Fmoc-deprotected microspheres **49** (1 mL, solid content 2%, 1 eq) were centrifuged and resuspended into a solution of adipic acid (1.46 mg, 10 eq) and DIC (0.9 μL, 10 eq) that had been mixed for 10 min in DMF. DMAP was then added (0.61 mg, 5 eq) and the suspension was mixed on a rotary-wheel at 25 ºC overnight for 1 h. Microspheres were washed with DMF (3 x 1 mL) and reaction completion was confirmed by a negative result on the ninhydrin test. Subsequently, microspheres were centrifuged and DMF was exchanged for a solution of cytamine (1.52 mg, 10 eq), HOBt (746 μg, 10 eq) and DMAP (0.61 mg, 5 eq) that had been stirred for 10 min after the addition of DIC (0.9 μL, 10 eq). The solution was mixed on a rotary-wheel for 1 h. Finally, microspheres were washed with DMF (3 x 1 mL) and reaction completion was confirmed by a negative qualitative ninhydrin test and a change in Z potential value (-22.0 mV).

TFMAD Coupling onto Microspheres (51a):

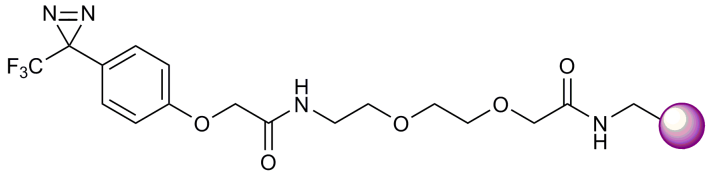

Fmoc-deprotected microspheres **47** (1 mL, solid content 2%, 1 eq) were centrifuged and resuspended into a solution of TFMAD-OH (1.44mg, 10eq) and HOBt (746 μg, 10 eq) that had been mixed for 10 min after addition of DIC (0.9 μL, 10 eq). The suspension was mixed on a rotary-wheel at 25 ºC overnight. The resulting microspheres are washed with DMF (3 x 1 mL) and reaction completion was confirmed by a negative result on the ninhydrin test and a change in Z potential value (-35.5mV). The microspheres were washed with MeOH (3 x 1 mL) and water (3 x 1 mL) and stored at 4 ºC.

Fmoc-Lys(Dde)-OH Coupling to PEG-Microspheres (53):

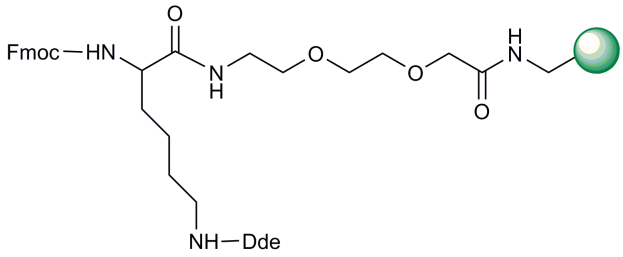

Fmoc-deprotected microspheres **52** (0.5 mL, solid content 2%, 1 eq) were centrifuged and resuspended into a solution of Fmoc-Lys(Dde)-OH (823.4 μg, 10eq) and oxyma (197 μg, 10 eq) that had been mixed for 10 min after addition of DIC (0.214 μL, 10 eq). The suspension was mixed on a rotary-wheel at 25 ºC overnight. The resulting microspheres are washed with DMF (3 x 1 mL) and reaction completion was confirmed by a negative result on the ninhydrin test and a change in Z potential value (-36.6 mV).

Deprotection of Dde and TFMAD coupling (54):

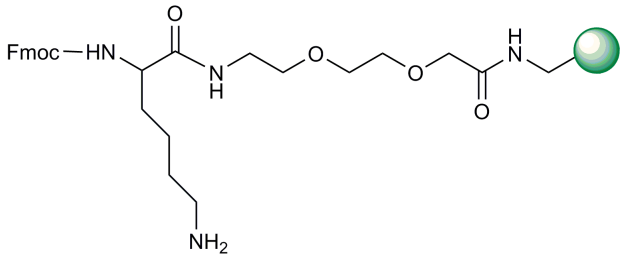

A freshly prepared solution of 1.25g hydroxylamine hydrochloride (1.80 mmol, 1.33 eq) and 918 mg immidazole (1.35 mmol, 1 eq) in 5 mL of NMP was prepared and sonicated until complete dissolution had been achieved. Then, 5 volumes of this solution (1000 μL) were mixed with 1 volume of DMF (200 μL) and the final solution was added to previously centrifuged microspheres **53** (0.5 mL, solid content 2%, 1 eq). The resuspended microspheres were stirred at room temperature for 1.5 h and the procedure was repeated one more time. The resulting microspheres were washed with DMF (3 x 1 mL) and reaction completion was confirmed by a negative result on the ninhydrin test and a change in Z potential value (-8.9 mV).

Dde-deprotected microspheres (0.5 mL, solid content 2%, 1 eq) were centrifuged and resuspended into a solution of TFMAD (388 μg, 10eq) and oxyma (197 μg, 10 eq) that had been mixed for 10 min after addition of DIC (0.214 μL, 10 eq). The suspension was mixed on a rotary-wheel at 25 ºC

overnight. The resulting microspheres are washed with DMF (3 x 1 mL) and reaction completion was confirmed by a negative result on the ninhydrin test and a change in Z potential value (-24.6 mV).

Fmoc deprotection and Fmoc-Arg(Boc)$_2$-OH coupling (55):

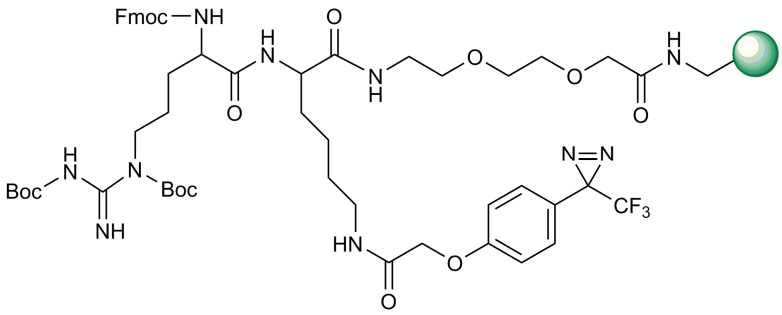

Microspheres **54** (0.5 mL, solid content 2%, 1 eq) were centrifuge and DMF was exchanged for 20% piperidine in DMF solution (1 mL). The solution was sonicated and then mixed in a rotary-wheel for 20 min. The process was repeated one more time. Finally, microspheres were washed with DMF (3 x 1 mL) and reaction was confirmed by a positive qualitative ninhydrin test and a change in Z potential value (-17.4 mV).

Subsequently, microspheres were centrifuged and resuspended into a solution of Fmoc-Arg(Boc)$_2$-OH (824 μg, 10eq) and oxyma (197 μg, 10 eq) that had been mixed for 10 min after addition of DIC (0.214 μL, 10 eq). The suspension was mixed on a rotary-wheel at 25 ºC overnight. The resulting microspheres were washed with DMF (3 x 1 mL) and reaction completion was confirmed by a negative result on the ninhydrin test and a change in Z potential value (-23.4 mV).

Deprotection of Boc and Fmoc protecting groups of Arginine (56a):

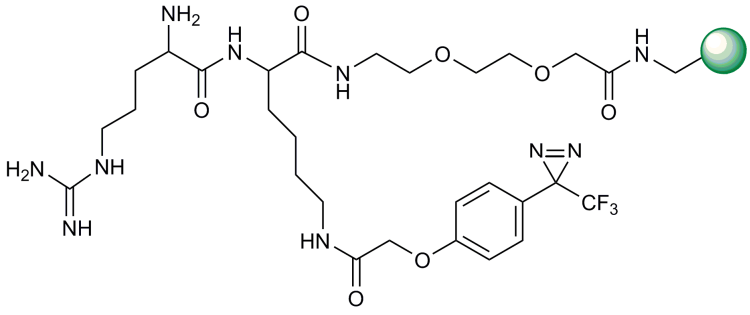

Microspheres **54** (0.5 mL, solid content 2%, 1 eq) were centrifuged and DMF was exchanged for DMF: TFA: TIS: water (64:32:2:2) solution (1 mL)

previously prepared and cooled on ice. Microspheres were resuspended and stirred for 1 h at room temperature. The process was repeated one more time. Microspheres were washed with DMF (3 x 1 mL) and deprotection was confirmed by a positive on ninhydrin test. Subsequently, microspheres were centrifuged and resuspended in of 20% piperidine in DMF (1 mL) and stirred for 20min at room temperature. The process was repeated one more time. Finally, microspheres were washed with DMF (3 x 1 mL) and reaction was confirmed by a change in Z potential value (-5.24 mV).

Preparation of Samples for Scanning Electron Microscopy:

Microspheres (25 μL, 2% sc) were dried on carbon-coated stubs under vacuum (50 ºC, 5 hours) and gold coated by sputtering (approximately 20 nm layer) prior to analysis.

5.6.2. Oligos and pEGFP Covalent Capture on microspheres

TxRd-Oligonucleotide Capture:

Eppendorfs containing 40 μL of microspheres **56a** or **51a** (11.92 nmol of diazirine group, 1 eq) each were prepared and mixed with 10 μL of a 77-mer random sequence oligonucleotide with texas red at 5' position solution (Sigma Aldrich)(100 nmol, 100 μM stock solution, 8.5 eq) and allowed to gently mix for 30 min in the thermomixer. Solvent from one of each microsphere type was evaporated in a speedvac for 30 min at 25 ºC. All samples were placed in an ice bath and irradiated above 10 cm with a UV lamp for 40 min. Dry microspheres were resuspended with 40 μL of nuclease-free deionised water and all were centrifuged and washed three times with nuclease-free deionised water (40 μL) before analysis by flow cytometry.

1 μL of each microsphere sample was suspended into 500 mL of PBS buffer and analysed by flow cytometry using the filter for texas red fluorescence. Untreated microspheres of each type were used as negative controls.

pEGFP Capture:

To an eppendorf containing 15 μL of either **56a** or **51a** microsphere type (0.38 nm in size, 2% sc, 4.5 μmol of reactive group) were added different volumes of pEGFP-C1 stock solution (0.4 μg/mL of plasmid in TE buffer): 10, 25, 50, and 100 μL of plasmid solution per reaction vessel. **51a** microspheres were mixed with the higher volume (100 μL). All samples were left to mix gently in

the thermomixer for 30 min and solvent was then evaporated by speed vacuum for 30 min at 25 ºC. Samples were placed in an ice-water bath and irradiated above 10 cm with a UV lamp for 40 min. Beads were resuspended in nuclease-free deionised water and centrifugated and washed three times before analysis.

5.6.3. Flow Cytometry Analysis of beads Containing Plasmid DNA with Propidium Iodide

For sample analysis, 1 μL of sample was placed in 300 μL of PBS and 6 μL of propidium iodide solution (50 μg/ml in PBS) was added and mixed. Samples were analysed by flow cytometry using Texas Red filter. Untreated microspheres, microspheres with the addition of DNA plasmid and PI or PI only were used as negative controls.

5.6.4. Incubation of beads with Restriction Enzymes

Digestion with FastDigest® StuI (Eco147I, Fermentas):

10 μL of plasmid or 10 μL microspheres bearing plasmid (4 μg of plasmid) was diluted with 22 μL of nuclease-free deionised water and digested with 4 μL of StuI restriction enzyme for 10 min in 4 μL of 1 x Tango buffer at 37 ºC in a water buffer. Samples were washed with nuclease-free deionised water (10 μL).

Double digestion with FastDifest® Stu I and ApaI (Fermentas):

10 μL of plasmid (0.4 μg/mL) or 10 μL of microspheres containing plasmid were diluted with 14 μL of nuclease-free water. To this solution, 4 μL of StuI and 4 μL of ApaI restriction enzymes were added with the subsequent addition of 8 μL of 1 x Tango buffer. The final solution was incubated for 15 min at 37 ºC in a water bath. Samples containing microspheres were centrifuged and washed two times with nuclease-free water before further usage.

5.6.5. Non-covalent Capture of pEGFP

NLS-PNS Conjugate Capture:

Three eppendorfs were prepared with a 100 μL of **51a** microspheres (0.38 μm in size, 2% sc) and mixed with solutions of Rho- or FITC-labelled PNA solutions (550 μM) as follows:

MIX microspheres: 25 μL of Rho- + 25μL FAM-PNA solutions

FAM microspheres: 50 μL of Rho-PNA solution

Rho microspheres: 50 μL of FITC-PNA solution

Solvent from samples was evaporated in a speedvac for 1 h at 25 ºC and samples were then irradiated at 365 nm above 10 cm with a UV lamp for 40 min. Samples were resuspended with nuclease-free deionised water (100 μL). The loading of each sample was determined by measuring the concentration of labelled-PNA left in the supernatant solution by UV-Vis spectrometry (**Table 5.1** and **Appendix III**). Finally, beads were washed three times with nuclease-free deionised water.

Microspheres	Loading in 100 μL microspheres	Reaction Yield (%)
Mix	15.7 nmol Rho-PNA / 20.4 nmol FAM-PNA	65
FAM	41.5 nmol FAM-PNA	74
Rho	42.6 nmol Rho-PNA	76

Table 5.1: Determination of the fluorescently-labelled PNA loading onto microspheres by UV-Vis spectrometry of the supernatant solutions.

pEGFP Capture by NLS-PNA functionalised microspheres:

Three different conditions were used for the hybridisation of plasmid onto the PNA-containing microspheres. First, microspheres containing the Rho- and FAM-labelled PNA sequences **(Mix** microspheres) were used directly for the hybridisation (**57**). Second, identical amounts of microspheres containing antisense (**FAM** microspheres) and sense sequences (**Rho** microspheres) were mixed and used for hybridisation with plasmid with no additions (**58**). And third, microspheres containing FAM-labelled PNA sequences (**FAM** microspheres) were incubated with the plasmid and the addition of the Rho-labelled PNA solution (8 μL, 21 mM solution) containing the same equivalents of the antisense sequence

on the microsphere (**59**). Samples of 15 μL of each microsphere type were mixed with 10, 20, or 40 μL of pEGFP-C1 solution. Hybridisation was carried out in a TC-312 thermocycler (Techne, Wolf Lavoratoried Ltd.) with a program starting from 5 min at 95 ºC and then 1 min decreasing the temperature 3 ºC until reaching RT. Samples were washed three times with DNAase-free deionised water before analysis or beadfection.

5.6.6. Gel Retardation Assays

A 0.7% agarose gel in thickness was prepared with 243 mg of agarose I-B in 35 mL 1 x TBE buffer and diluted by warming the solution into a water bath at 60 ºC for 20 min. Once 3.5 μL of GelRed Nucleic Acid Stain (10,000x in water, Biotium) were added to the solution and mixed, the mixture was poured into the mould and allowed to cool down to RT for 1 h. Meanwhile, microsphere solutions were prepared by diluting 5 μL of microsphere solutions obtained after irradiation in enzyme digestion with TBE buffer (20 μL) and addition of 4 μL of loading dye. Samples were mixed well before injecting them into the gel. Negative control samples were prepared by dilution of 1 μL of plasmid solution in TBE buffer and 4 μL of loading dye. Positive samples were prepared by dissolving 1 μL of plasmid (0.4 μg/μl in TE buffer) with 1 μL of Lipofectamine in 25 μL of TBE buffer. Positive controls were left for 20 minute of gentle mixing before adding 4 μL of loading dye. The migration gel was run for 45 min at 90 V.

5.6.7. Cell assays

Lipofection with Lipofectamine™ 2000:

HeLa and HEK293T cells were seeded in the appropriate growth media to 24-well plates at a density of 3 x 10^4 cell/well (well volume = 350 μL). After 24 hours and with a confluence of 90%, the old media was removed from the cells, washed with PBS and replaced with fresh serum- and antibiotic-free Opti-MEM® I Reduced Serum Medium (500 μL). The well plate was incubated before addition of the complexes.

For each transfection sample, Lipofectamine™ 2000 (2 μL) was incubated in Opti-MEM® media (50 μL) at 25°C for 5 min. EGFP-plasmid (0.8 μg, 2 μL of a stock solution of 0.4 μg/μL of plasmid in TE buffer) was diluted in Opti-MEM® media (50 μL) and mixed gently. Then, the two diluted solutions were combined (100 μL) and incubated at 25°C for 20min. This solution was added to the well plate and mixed gently by rocking the plate back and forth.

After 24-72 hours cells were washed, harvested by trypsination and prepared for flow cytometric analysis as described in general procedures.

Beadfection of HEK293T Cells:

HEK cells were suspended to the appropriate cell density in fresh growth media before seeding onto polystyrene well-plates (Nunc). Cells were incubated (37°C/5% CO_2) for 24 hours to allow adhesion.

Separately, DNA plasmid-containing microspheres were dispersed in fresh growth media to a concentration of 43, 86, and 172 μg/mL. The old media was removed from cells and replaced with fresh media containing microspheres. Cells were incubated in the presence of microspheres (37°C/5% CO_2) for 48 and 72 hours prior to analysis by flow cytometry and microscopy.

Appendix I

NMR Spectres of TFMAD **4** Photolysis:

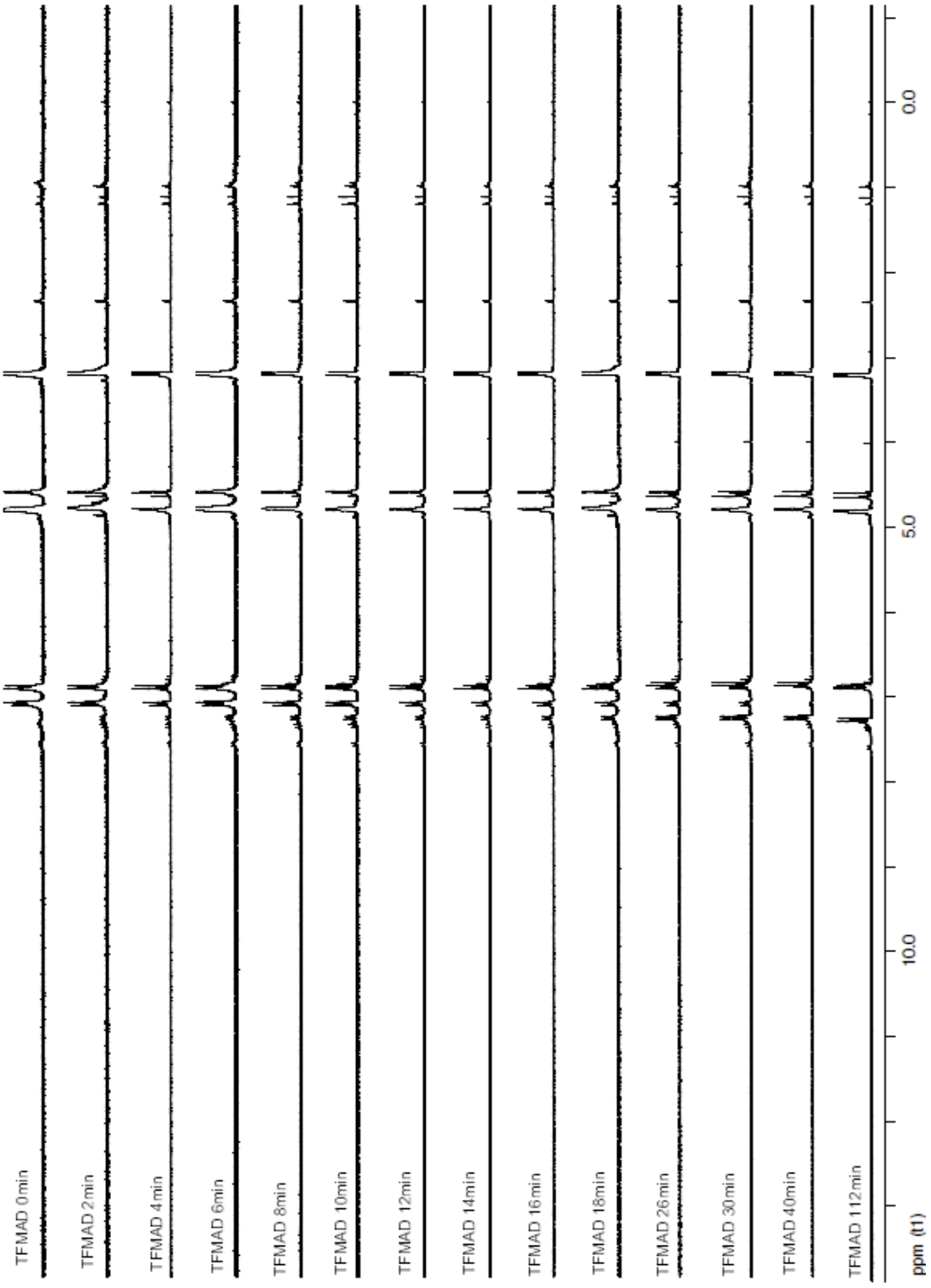

Figure A.1: Photoreaction of **4** in CD_3OD at room temperature monitored by ^{1}H-NMR (Arx250, CD_3OD, 250MHz, 20 °C).

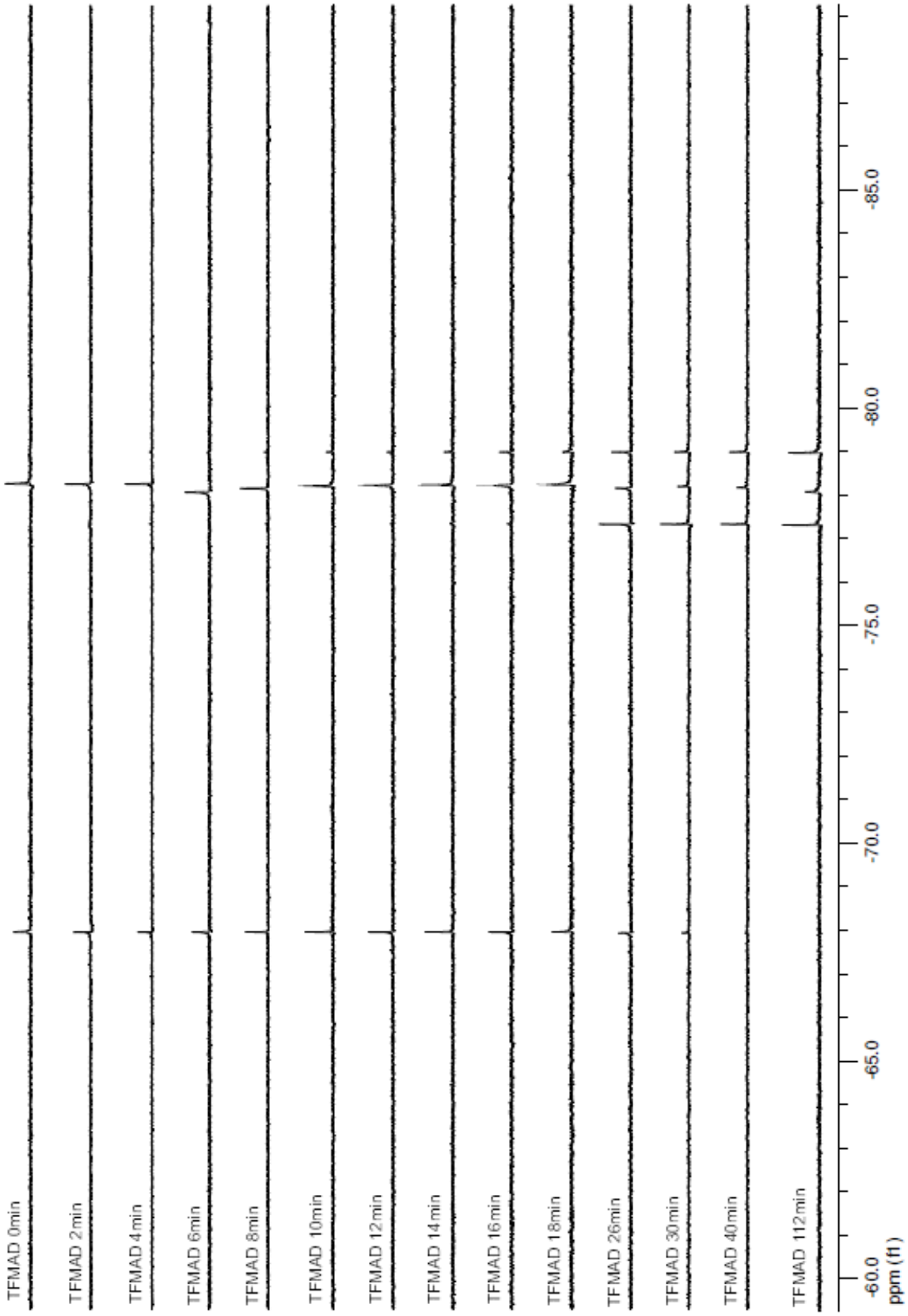

Figure A.2: Photoreaction of **4** in CD_3OD at room temperature monitored by ^{19}F-NMR (Arx250, CD_3OD, 235.9MHz, 20 °C) using TFA as an external standard (δ = 69.987 ppm).

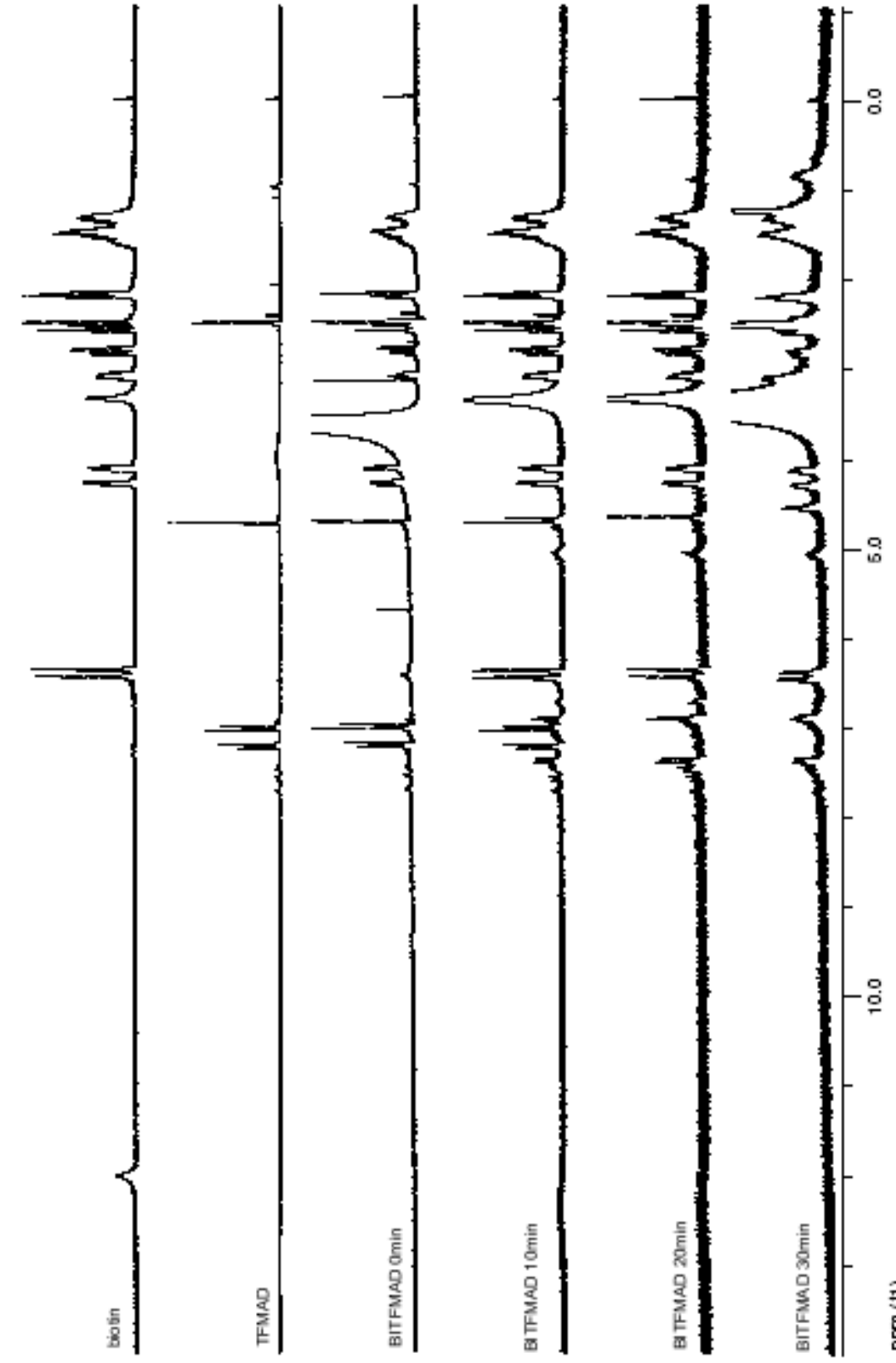

Figure A.3: Photoreaction of **4** and biotin in dry conditions and at -196 ºC monitored by ^{1}H-NMR (Arx250, d^{6}-DMSO, 250MHz).

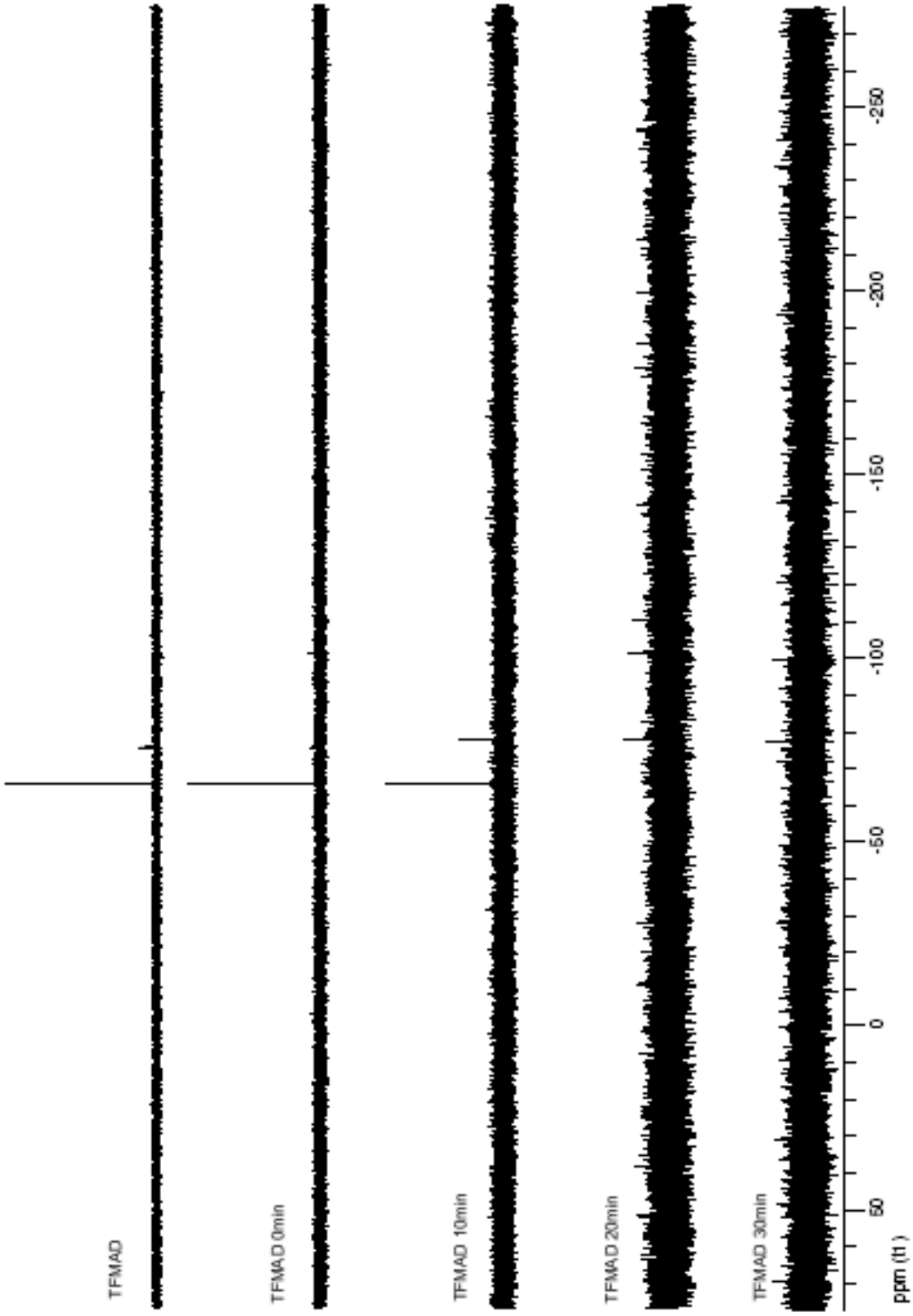

Figure A.4: Photoreaction of **4** and biotin in dry conditions and at -196 ºC monitored by ^{19}F-NMR (Arx250, d^{6}-DMSO, 235.9MHz).

Appendix II

List of the compounds generated from the top 25 potential binders from SPECTRUM library found on the three binding assays carried out towards β-TrCP1. The list also includes compounds that were not found active as negative controls. Highlighted compounds corresponded to those compounds found active towards β-TrCP1 by solution binding assays.

1	Pyrromycin	**41**	Juglone
2	Pyrvinium Pamoate	**42**	Pomiferin
3	Doxorubicin	**43**	Tyrothricin
4	Dehydrovariabilin	**44**	Thiridazine Hydrochloride
5	Bisanhydrotutilantinone	**45**	Dalbergione
6	Fenofibrate	**46**	Ethisterone
7	Rutilantinone	**47**	Apigenin
8	Dichlorophene	**48**	Haematoporphyrin
9	Naphazoline Hydrochloride	**49**	2001-039
10	Hexachlorophene	**50**	Quinacrine Hydrochloride
11	Bithionate Sodium	**51**	Derrubone
12	Auraptene	**52**	Chlorhexidine
13	Pararosaniline Pamoate	**53**	Purpurin
14	Tannic Acid	**54**	Perillyl Alcohol
15	Benzbromarone	**55**	Thiostrepton
16	Daunorubicin	**56**	Indapamide
17	Gentian Violet	**57**	Epirubicin Hydrochloride
18	Gambogic Acid Amide	**58**	Carbetapentane Citrate
19	3,4'-Dimethoxyflavone	**59**	Ornidazole
20	Probucol	**60**	2001-039
21	Trazodone Hydrochloride	**61**	Methyl Robustone
22	Dibutyl Phthalate	**62**	Triamterene
23	Pyrimethamine	**63**	Adenosine Phsophate
24	Gossypol	**64**	Danthron
25	Grayanotoxin I	**65**	Physcion
26	Pimozide	**66**	Acriflavinium Hydrochloride
27	Curcumin	**67**	1770-173
28	Methyl 7-Deshydroxypyrogallin-4-ccarcarboxylate	**68**	Colistin sulphate
29	Nisldipine	**69**	Polymyxin B sulfate
30	Phloretin	**70**	Sulfacetamide
31	Theaflavin Digallate	**71**	Scopolamine Hydrobromide
32	Temefos	**72**	Mecamylamine Hydrochloride
33	Propranolol Hydrochloride (+/-)	**73**	Sisomicin sulphate
34	Resveratrol	**74**	Mephenesin
35	Aristolochich acid	**75**	Pirenzepine Hydrochloride
36	Eugenyl Benzoate	**76**	Dropropizine
37	4'-methoxychalcone	**77**	Methylbenzethonium Chloride
38	Gossypetin	**78**	Bambuterol Hydrochloride
39	Oxidopamine Hydrochloride	**79**	Quinine Sulfate
40	Theaflavin Monogallates	**80**	Chlormezanone

Table A.1: List of 80 selected compounds form SPECTRUM library. Highlighted compound were found active for inhibition of β-TrCP1 by fluorescence polaritsation assays.

Appendix III

Calibration and determination of the extinction coefficient of FAM-PNA conjugate at 501 and 560 nm:

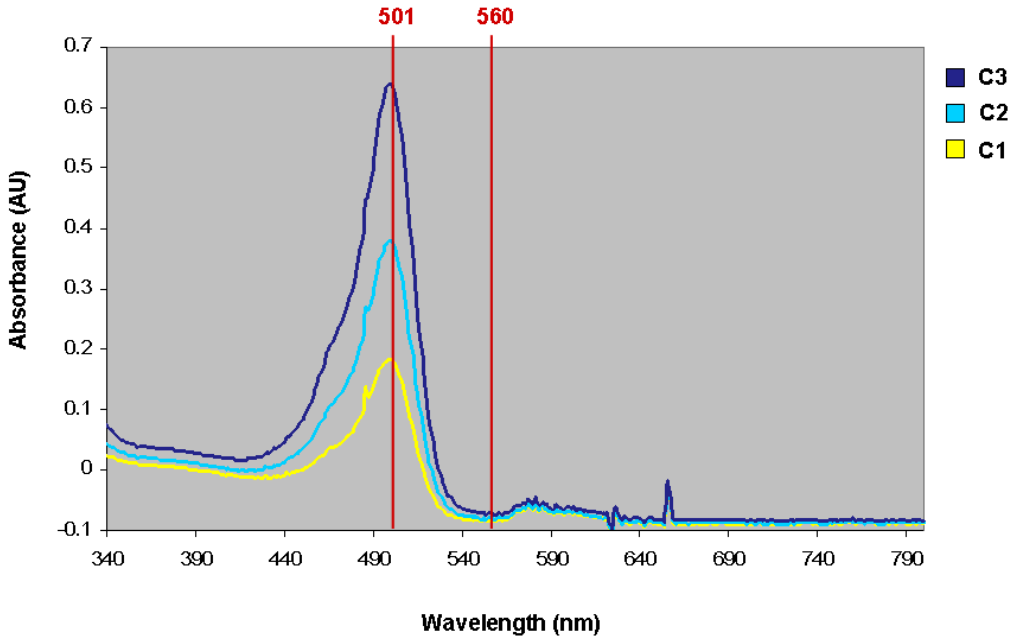

Figure A.5: Absorbance spectra of three different concentrations of FAM-labelled PNA sequence.

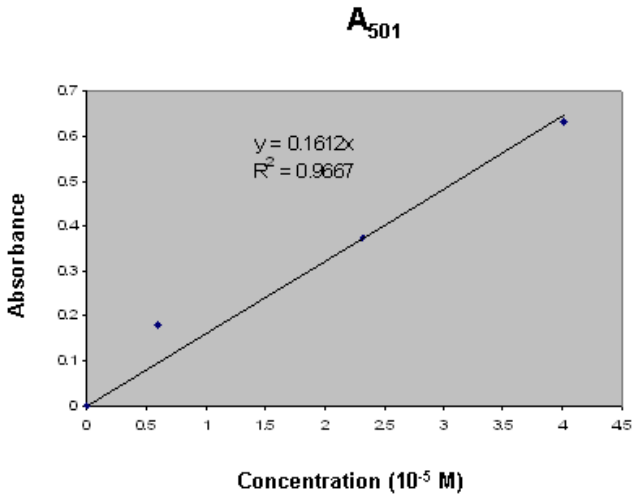

C (10^{-5}M)	A_{560}
0	0
0.59	0.1800
2.32	0.3741
4.01	0.6337

Graph A.1: Determination of the extinction coefficient of fluorescein at 501 nm with the absorbance values obtained for each concentration.

FAM-labelled PNA sequence has an ε of 16,117 $M^{-1}cm^{-1}$ at 501 nm and a null value at 560 nm.

Calibration and determination of the extinction coefficient of Rho-labelled PNA sequence at 501 and 560 nm

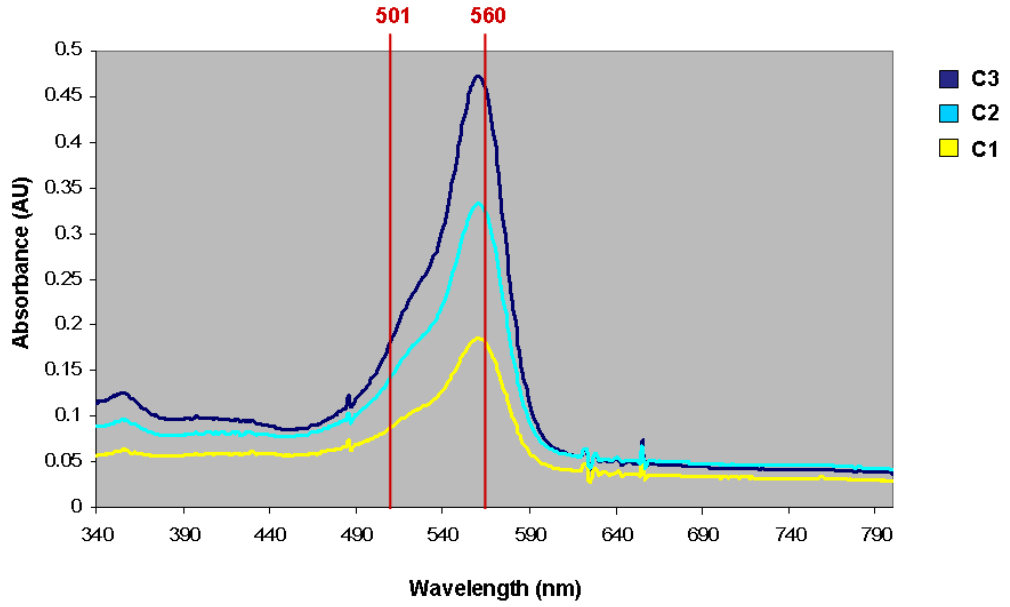

Figure A.6: Absorbance spectra of three different concentrations of Rho-labelled PNA sequence.

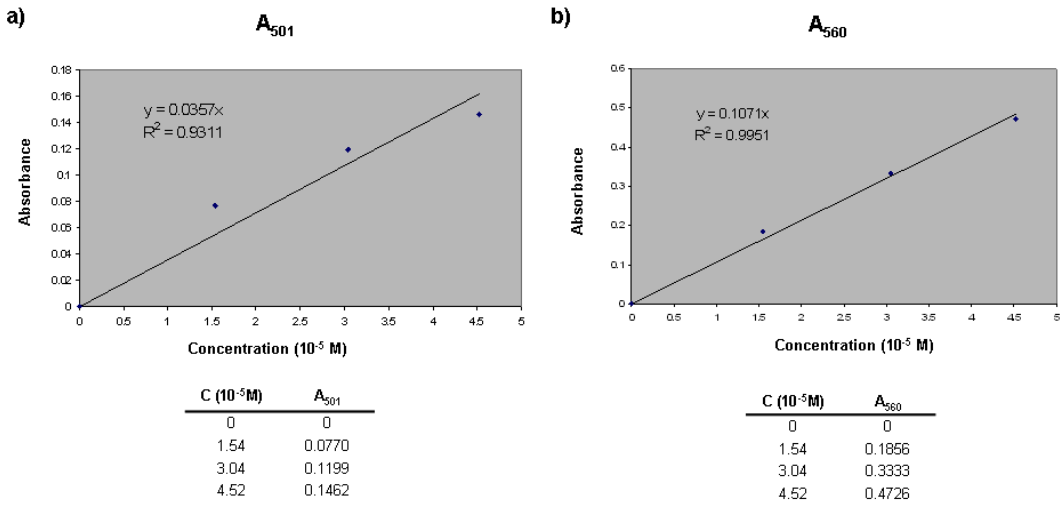

C (10^{-5}M)	A_{501}
0	0
1.54	0.0770
3.04	0.1199
4.52	0.1462

C (10^{-5}M)	A_{560}
0	0
1.54	0.1856
3.04	0.3333
4.52	0.4726

Graph A.2: Determination of the extinction coefficient of Rhodamine at 501 and 560 nm with the absorbance values obtained for each concentration.

Rho-labelled PNA sequence has an ε of 3,570 $M^{-1}cm^{-1}$ at 501 nm and 10,720 $M^{-1}cm^{-1}$ at 560 nm.

Measurements with supernatant samples:

λ (nm)	Absorbance		
	Rho	Mix	FAM
501	0.02282	0.224532	0.157685
560	0.156965	0.172842	0

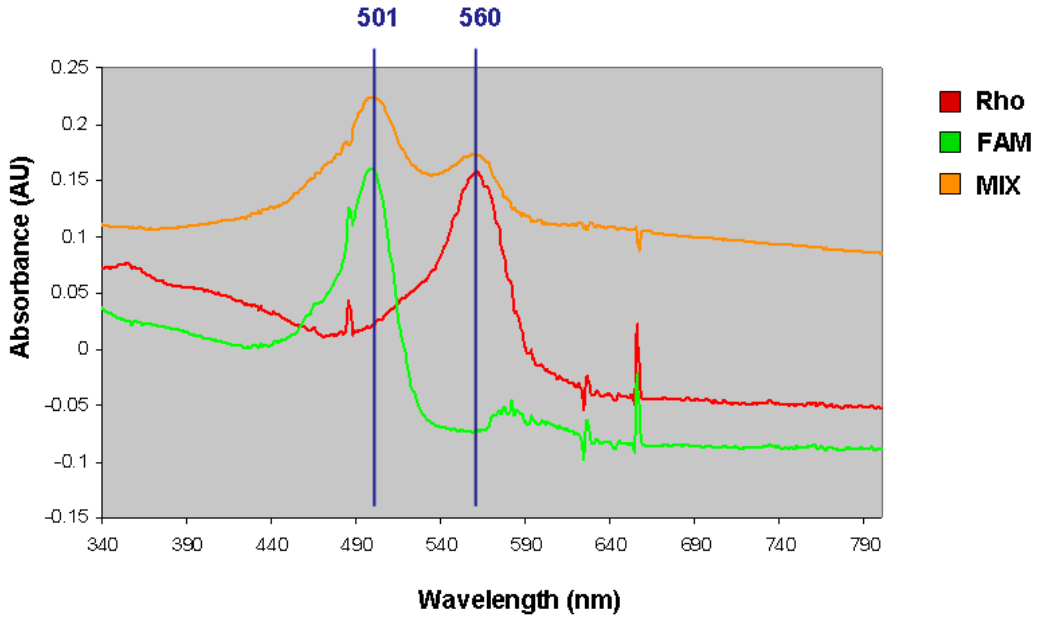

Figure A.7: Absorbance spectra of the three supernatant samples collected after irradiation at 365 nm with TFMAD-functionalised microspheres. The number of nmols present in the supernatant was calculated and extracted form the initial number of nmols to determine the microsphere loading.

References

1. F. Kotzybahibert, I. Kapfer and M. Goeldner, *Angewandte Chemie-International Edition in English*, 1995, **34**, 1296-1312.
2. Y. Hatanaka, H. Nakayama and Y. Kanaoka, *Reviews on Heteroatom Chemistry*, 1996, **14**, 213-243.
3. J. Brunner, *Annual Review of Biochemistry*, 1993, **62**, 483-514.
4. G. Dorman and G. D. Prestwich, *Trends in Biotechnology*, 2000, **18**, 64-77.
5. H. Bayley, *Photogenerated Reagents in Biochemistry and Molecular Biology*, Elsevier DScience Publishers B. V., Amsterdam, The Netherlands, 1983.
6. T. Bender, M. Huss, H. Wieezorek, S. Grond and P. von Zezschwitz, *European Journal of Organic Chemistry*, 2007, 3870-3878.
7. M. Hashimoto, Y. Kato and Y. Hatanaka, *Tetrahedron Letters*, 2006, **47**, 3391-3394.
8. T. Hiramatsu, Y. Guo and T. Hosoya, *Organic & Biomolecular Chemistry*, 2007, **5**, 2916-2919.
9. N. S. Kumar and R. N. Young, *Bioorg Med Chem*, 2009, **17**, 5388-5395.
10. T. Kuroda, K. Suenaga, A. Sakakura, T. Handa, K. Okamoto and H. Kigoshi, *Bioconjugate Chemistry*, 2006, **17**, 524-529.
11. C. Walling and M. J. Gibian, *Journal of the American Chemical Society*, 1965, **87**, 3361-3364.
12. R. E. Galardy, L. C. Craig and M. P. Printz, *Nature-New Biology*, 1973, **242**, 127-128.
13. J. F. Brennan and J. Beutel, *Journal of Physical Chemistry*, 1969, **73**, 3245-3249.
14. G. Dorman and G. D. Prestwich, *Biochemistry*, 1994, **33**, 5661-5673.
15. R. E. Galardy, L. C. Craig, J. D. Jamieson and M. P. Printz, *Journal of Biological Chemistry*, 1974, **249**, 3510-3518.
16. N. Williams and P. S. Coleman, *Journal of Biological Chemistry*, 1982, **257**, 2834-2841.
17. H. Bayley and J. R. Knowles, *Methods Enzymol*, 1977, **46**, 69-114.
18. H. Bayley and J. V. Staros, in *Azides and Nitrenes*, ed. E. F. V. Screiven, Academic Press, San Diego, CA, Editon edn., 1984, p. Chapter 9.
19. E. Leyva, M. S. Platz, G. Persy and J. Wirz, *Journal of the American Chemical Society*, 1986, **108**, 3783-3790.
20. M. S. Platz, *Accounts of Chemical Research*, 1995, **28**, 487-492.
21. C. J. Shields, D. R. Chrisope, G. B. Schuster, A. J. Dixon, M. Poliakoff and J. J. Turner, *Journal of the American Chemical Society*, 1987, **109**, 4723-4726.
22. Y. Z. Li, J. P. Kirby, M. W. George, M. Poliakoff and G. B. Schuster, *Journal of the American Chemical Society*, 1988, **110**, 8092-8098.
23. W. L. Karney and W. T. Borden, *Journal of the American Chemical Society*, 1997, **119**, 3347-3350.

24. E. W. Meijer, S. Nijhuis and F. Vanvroonhoven, *Journal of the American Chemical Society*, 1988, **110**, 7209-7210.

25. J. F. W. Keana and S. X. Cai, *Journal of Organic Chemistry*, 1990, **55**, 3640-3647.

26. M. G. Rosenberg and U. H. Brinker, *European Journal of Organic Chemistry*, 2006, 5423-5440.

27. J. H. Atherton and R. Fields, *Journal of the Chemical Society C-Organic*, 1968, 1507.

28. J. H. Atherton and R. Fields, *Journal of the Chemical Society C-Organic*, 1968, 2276.

29. D. M. Dankbar and G. Gauglitz, *Analytical and Bioanalytical Chemistry*, 2006, **386**, 1967-1974.

30. Brunswic.Dj and Cooperma.Bs, *Biochemistry*, 1973, **12**, 4074-4078.

31. E. Schmitz, *Angewandte Chemie-International Edition*, 1964, **3**, 333.

32. J. R. Knowles, *Accounts of Chemical Research*, 1972, **5**, 155.

33. J. Shafer, Baronows.P, R. Laursen, F. Finn and Westheim.Fh, *Journal of Biological Chemistry*, 1966, **241**, 421.

34. P. S. Linsley, C. Blifeld, M. Wrann and C. F. Fox, *Nature*, 1979, **278**, 745-748.

35. Y. Takagaki, C. M. Gupta and H. G. Khorana, *Biochemical and Biophysical Research Communications*, 1980, **95**, 589-595.

36. J. Stackhouse and F. H. Westheimer, *Journal of Organic Chemistry*, 1981, **46**, 1891-1898.

37. V. Chowdhry and F. H. Westheimer, *Journal of the American Chemical Society*, 1978, **100**, 309-310.

38. D. H. R. Barton, J. C. Jaszberenyi, E. A. Theodorakis and J. H. Reibenspies, *Journal of the American Chemical Society*, 1993, **115**, 8050-8059.

39. R. Moya-Barrios, F. L. Cozens and N. P. Schepp, *Journal of Organic Chemistry*, 2009, **74**, 1148-1155.

40. J. M. Delfino, S. L. Schreiber and F. M. Richards, *Journal of the American Chemical Society*, 1993, **115**, 3458-3474.

41. T. Weber and J. Brunner, *Journal of the American Chemical Society*, 1995, **117**, 3084-3095.

42. J. Brunner, H. Senn and F. M. Richards, *Journal of Biological Chemistry*, 1980, **255**, 3313-3318.

43. M. Platz, A. S. Admasu, S. Kwiatkowski, P. J. Crocker, N. Imai and D. S. Watt, *Bioconjugate Chemistry*, 1991, **2**, 337-341.

44. M. Hashimoto and Y. Hatanaka, *European Journal of Organic Chemistry*, 2008, 2513-2523.

45. H. J. Abendroth and G. Henrich, *Angewandte Chemie-International Edition*, 1959, **71**, 283-283.

46. S. R. Paulsen, *Angewandte Chemie-International Edition*, 1960, **72**, 781-782.

47. E. Schmitz and R. Ohme, *Chemische Berichte-Recueil*, 1961, **94**, 2166-2173.

48. A. Blencowe and W. Hayes, *Soft Matter*, 2005, **1**, 178-205.

49. R. A. Moss, *Accounts of Chemical Research*, 1989, **22**, 15-21.

50. A. H. Ross, R. Radhakrishnan, R. J. Robson and H. G. Khorana, *Journal of Biological Chemistry*, 1982, **257**, 4152-4161.

51. D. A. Modarelli, S. Morgan and M. S. Platz, *Journal of the American Chemical Society*, 1992, **114**, 7034-7041.

52. H. Bayley and J. R. Knowles, *Biochemistry*, 1978, **17**, 2420-2423.

53. R. Bonneau, B. Hellrung, M. T. H. Liu and J. Wirz, *Journal of Photochemistry and Photobiology a-Chemistry*, 1998, **116**, 9-19.

54. R. A. G. Smith and J. R. Knowles, *Journal of the American Chemical Society*, 1973, **95**, 5072-5073.

55. R. A. G. Smith and J. R. Knowles, *Journal of the Chemical Society-Perkin Transactions 2*, 1975, 686-694.

56. M. Nassal, *Liebigs Annalen Der Chemie*, 1983, 1510-1523.

57. C. von Ballmoos, J. Brunner and P. Dimroth, *Proceedings of the National Academy of Sciences of the United States of America*, 2004, **101**, 11239-11244.

58. M. Hashimoto, Y. Hatanaka and K. Nabeta, *Bioorganic & Medicinal Chemistry Letters*, 2000, **10**, 2481-2483.

59. R. F. R. Church and M. J. Weiss, *Journal of Organic Chemistry*, 1970, **35**, 2465.

60. G. A. Korshunova, N. V. Sumbatyan, A. N. Topin and M. T. Mtchedlidze, *Molecular biology*, 2000, **34**, 823-839.

61. G. L. Closs and B. E. Rabinow, *Journal of the American Chemical Society*, 1976, **98**, 8190-8198.

62. J. A. Kerr, B. V. Ogrady and Trotmand.Af, *Journal of the Chemical Society a -Inorganic Physical Theoretical*, 1967, 897.

63. N. Kanoh, T. Nakamura, K. Honda, H. Yamakoshi, Y. Iwabuchi and H. Osada, *Tetrahedron*, 2008, **64**, 5692-5698.

64. H. Tomioka, *Research on Chemical Intermediates*, 1994, **20**, 605-634.

65. K. Peters and F. M. Richards, *Annual Review of Biochemistry*, 1977, **46**, 523-551.

66. V. Chowdhry and F. H. Westheimer, *Annual Review of Biochemistry*, 1979, **48**, 293-325.

67. Y. Sadakane and Y. Hatanaka, *Analytical Sciences*, 2006, **22**, 209-218.

68. D. B. Ureta, P. O. Craig, G. E. Gomez and J. M. Delfino, *Biochemistry*, 2007, **46**, 14567-14577.

69. P. O. Craig, D. B. Ureta and J. M. Delfino, *Protein Science*, 2002, **11**, 1353-1366.

70. F. M. Richards, R. Lamed, R. Wynn, D. Patel and G. Olack, *Protein Science*, 2000, **9**, 2506-2517.

71. G. E. Gomez, A. Cauerhff, P. O. Craig, F. A. Goldbaum and J. M. Delfino, *Protein Science*, 2006, **15**, 744-752.

72. M. Nassal, *Journal of the American Chemical Society*, 1984, **106**, 7540-7545.

73. L. B. Shih and H. Bayley, *Analytical Biochemistry*, 1985, **144**, 132-141.

74. J. C. Kauer, S. Ericksonviitanen, H. R. Wolfe and W. F. Degrado, *Journal of Biological Chemistry*, 1986, **261**, 695-700.

75. M. Suchanek, A. Radzikowska and C. Thiele, *Nature Methods*, 2005, **2**, 261-267.

76. G. A. Korshunova, N. V. Sumbatyan, A. N. Topin and M. T. Mtchedlidze, *Molecular biology*, 2000, **34**, 823-839.

77. M. Zofall and B. Bartholomew, *Nucleic Acids Research*, 2000, **28**, 4382-4390.

78. J. J. Tate, J. Persinger and B. Bartholomew, *Nucleic Acids Research*, 1998, **26**, 1421-1426.

79. D. Forget, M. F. Langelier, C. Therien, V. Trinh and B. Coulombe, *Molecular and Cellular Biology*, 2004, **24**, 1122-1131.

80. K. Musierforsyth and P. Schimmel, *Biochemistry*, 1994, **33**, 773-779.

81. A. N. Mayer and F. Barany, *Gene*, 1995, **153**, 1-8.

82. S. D. Westerheide and J. M. Boss, *Nucleic Acids Research*, 1999, **27**, 1635-1641.

83. D. Pruss, B. Bartholomew, J. Persinger, J. Hayes, G. Arents, E. N. Moudrianakis and A. P. Wolffe, *Science*, 1996, **274**, 614-617.

84. S. M. Sengupta, M. VanKanegan, J. Persinger, C. Logie, B. R. Cairns, C. L. Peterson and B. Bartholomew, *Journal of Biological Chemistry*, 2001, **276**, 12636-12644.

85. H. Sigrist, A. Collioud, J. F. Clemence, H. Gao, R. Luginbuhl, M. Sanger and G. Sundarababu, *Optical Engineering*, 1995, **34**, 2339-2348.

86. N. Kanoh, S. Kumashiro, S. Simizu, Y. Kondoh, S. Hatakeyama, H. Tashiro and H. Osada, *Angewandte Chemie-International Edition*, 2003, **42**, 5584-5587.

87. N. Kanoh, M. Kyo, K. Inamori, A. Ando, A. Asami, A. Nakao and H. Osada, *Analytical Chemistry*, 2006, **78**, 2226-2230.

88. N. Kanoh, A. Asami, M. Kawatani, K. Honda, S. Kumashiro, H. Takayama, S. Simizu, T. Amemiya, Y. Kondoh, S. Hatakeyama, K. Tsuganezawa, R. Utata, A. Tanaka, S. Yokoyama, H. Tashiro and H. Osada, *Chemistry-an Asian Journal*, 2006, **1**, 789-797.

89. S. J. Dilly, M. J. Bell, A. J. Clark, A. Marsh, R. M. Napier, M. J. Sergeant, A. J. Thompson and P. C. Taylor, *Chemical Communications*, 2007, 2808-2810.

90. A. Collioud, J. F. Clemence, M. Sanger and H. Sigrist, *Bioconjugate Chemistry*, 1993, **4**, 528-536.

91. N. Kanoh, K. Honda, S. Simizu, M. Muroi and H. Osada, *Angewandte Chemie-International Edition*, 2005, **44**, 3559-3562.

92. K. Kuramochi, T. Haruyama, R. Takeuchi, T. Sunoki, M. Watanabe, M. Oshige, S. Kobayashi, K. Sakaguchi and F. Sugawara, *Bioconjugate Chemistry*, 2005, **16**, 97-104.

93. K. Stromgaard, D. R. Saito, H. Shindou, S. Ishii, T. Shimizu and K. Nakanishi, *Journal of Medicinal Chemistry*, 2002, **45**, 4038-4046.

94. C. Sridar, Y. Kobayashi, H. Brevig, U. M. Kent, S. G. Puppali, J. M. Rimoldi and P. F. Hollenberg, *Drug Metabolism and Disposition*, 2006, **34**, 1849-1855.

95. G. K. S. Prakash, R. Krishnamurti and G. A. Olah, *Journal of the American Chemical Society*, 1989, **111**, 393-395.

96. A. Ruhmann and C. Wentrup, *Tetrahedron*, 1994, **50**, 3785-3796.

97. T. Hosoya, T. Hiramatsu, T. Ikemoto, M. Nakanishi, H. Aoyama, A. Hosoya, T. Iwata, K. Maruyama, M. Endo and M. Suzuki, *Organic & Biomolecular Chemistry*, 2004, **2**, 637-641.

98. M. T. McHedlidze, N. V. Sumbatyan, D. A. Bondar, M. V. Taranenko and G. A. Korshunova, *Russian Journal of Bioorganic Chemistry*, 2003, **29**, 177-184.

99. M. Hashimoto and Y. Hatanaka, *Analytical Biochemistry*, 2005, **348**, 154-156.

100. T. Hiramatsu, Y. Guo and T. Hosoya, *Organic & Biomolecular Chemistry*, 2007, **5**, 2916-2919.

101. M. T. H. Liu, O. Banjoko, Y. Yamamoto and I. Moritani, *Tetrahedron*, 1975, **31**, 1645-1648.

102. H. Ismail, S. Lee and M. S. Workentin, *Langmuir*, 2010, **26**, 14958-14964.

103. S. L. Schreiber, *Nature Chemical Biology*, 2005, **1**, 64-66.

104. B. R. Stockwell, *Nature*, 2004, **432**, 846-854.

105. N. Tolliday, P. A. Clemons, P. Ferraiolo, A. N. Koehler, T. A. Lewis, X. H. Li, S. L. Schreiber, D. S. Gerhard and S. Eliasof, *Cancer Research*, 2006, **66**, 8935-8942.

106. D. P. Walsh and Y. T. Chang, *Chemical Reviews*, 2006, **106**, 2476-2530.

107. N. Winegarden and J. Woodgett, *Future Drug Discovery*, 2006, 1-5.

108. D. E. Leyden, *Silanes, Surfaces, and Interfaces*, Gordon and Breach, New York, 1986.

109. E. P. Plueddemann, *Silane Coupling Agents*, Pleneum, New York, 1991.

110. K. L. Mittal, *Silane and Other Coupling Agents*, VSP, Utrecht, 1992.

111. J. J. Pesek, *Chemically Modifies Surfaces*, Cambridge, 1994.

112. G. T. Hermanson and G. T. Hermanson, in *Bioconjugate Techniques*, Editon edn., 1996, pp. 562-581.

113. A. Y. Fadeev and T. J. McCarthy, *Langmuir*, 1999, **15**, 3759-3766.

114. J. B. Brzoska, N. Shahidzadeh and F. Rondelez, *Nature*, 1992, **360**, 719-721.

115. A. N. Parikh, D. L. Allara, I. B. Azouz and F. Rondelez, *Journal of Physical Chemistry*, 1994, **98**, 7577-7590.

116. J. B. Brzoska, I. Benazouz and F. Rondelez, *Langmuir*, 1994, **10**, 4367-4373.

117. S. H. North, E. H. Lock, T. R. King, J. B. Franek, S. G. Walton and C. R. Taitt, *Analytical Chemistry*, 2010, **82**, 406-412.

118. E. T. Vandenberg, L. Bertilsson, B. Liedberg, K. Uvdal, R. Erlandsson, H. Elwing and I. Lundstrom, *Journal of Colloid and Interface Science*, 1991, **147**, 103-118.

119. D. M. Marsden, R. L. Nicholson, M. Ladlow and D. R. Spring, *Chemical Communications*, 2009, 7107-7109.

120. B. T. Houseman and M. Mrksich, *Trends in Biotechnology*, 2002, **20**, 279-281.

121. J. J. Diaz-Mochon, G. Tourniaire and M. Bradley, *Chemical Society Reviews*, 2007, **36**, 449-457.

122. B. T. Houseman and M. Mrksich, *Chemistry & Biology*, 2002, **9**, 443-454.

123. Z. Guo, R. A. Guilfoyle, A. J. Thiel, R. F. Wang and L. M. Smith, *Nucleic Acids Research*, 1994, **22**, 5456-5465.

124. M. S. Shchepinov, S. C. CaseGreen and E. M. Southern, *Nucleic Acids Research*, 1997, **25**, 1155-1161.

125. P. J. Hergenrother, K. M. Depew and S. L. Schreiber, *Journal of the American Chemical Society*, 2000, **122**, 7849-7850.

126. J. R. Falsey, M. Renil, S. Park, S. J. Li and K. S. Lam, *Bioconjugate Chemistry*, 2001, **12**, 346-353.

127. I. Shin, S. Park and M. R. Lee, *Chemistry-a European Journal*, 2005, **11**, 2894-2901.

128. M. R. Lee and I. Shin, *Angewandte Chemie-International Edition*, 2005, **44**, 2881-2884.

129. M. Kurosu and W. A. Mowers, *Bioorganic & Medicinal Chemistry Letters*, 2006, **16**, 3392-3395.

130. D. S. Thorpe and S. Walle, *Biochemical and Biophysical Research Communications*, 2000, **269**, 591-595.

131. M. Kohn, R. Wacker, C. Peters, H. Schroder, L. Soulere, R. Breinbauer, C. M. Niemeyer and H. Waldmann, *Angewandte Chemie-International Edition*, 2003, **42**, 5830-5834.

132. R. Benters, C. M. Niemeyer and D. Wohrle, *Chembiochem*, 2001, **2**, 686-694.

133. J. Wang, M. Uttamehandani, H. Y. Sun and S. Q. Yao, *Qsar & Combinatorial Science*, 2006, **25**, 1009-1019.

134. M. Uttamchandani, J. Wang and S. Q. Yao, *Molecular Biosystems*, 2006, **2**, 58-68.

135. M. Uttamchandani, D. P. Walsh, S. Q. Yao and Y. T. Chang, *Current Opinion in Chemical Biology*, 2005, **9**, 4-13.

136. Q. C. Xu and K. S. Lam, *Journal of Biomedicine and Biotechnology*, 2003, 257-266.

137. M. Kohn, *Journal of Peptide Science*, 2009, **15**, 393-397.

138. A. J. Vegas, J. H. Fuller and A. N. Koehler, *Chemical Society Reviews*, 2008, **37**, 1385-1394.

139. S. P. A. Fodor, J. L. Read, M. C. Pirrung, L. Stryer, A. T. Lu and D. Solas, *Science*, 1991, **251**, 767-773.

140. S. Singh-Gasson, R. D. Green, Y. J. Yue, C. Nelson, F. Blattner, M. R. Sussman and F. Cerrina, *Nature Biotechnology*, 1999, **17**, 974-978.

141. S. W. Li, D. Bowerman, N. Marthandan, S. Klyza, K. J. Luebke, H. R. Garner and T. Kodadek, *Journal of the American Chemical Society*, 2004, **126**, 4088-4089.

142. D. S. Shin, K. N. Lee, B. W. Yoo, J. Kim, M. Kim, Y. K. Kim and Y. S. Lee, *Journal of Combinatorial Chemistry*, 2010, **12**, 463-471.

143. S. W. Li, N. Marthandan, D. Bowerman, H. R. Garner and T. Kodadek, *Chemical Communications*, 2005, 581-583.

144. R. Frank, *Tetrahedron*, 1992, **48**, 9217-9232.

145. R. Frank, *Journal of Immunological Methods*, 2002, **267**, 13-26.

146. R. Frank, *Combinatorial Chemistry & High Throughput Screening*, 2002, **5**, 429-440.

147. U. Reineke, A. Kramer and J. Schneider-Mergener, *Combinatorial Chemistry in Biology*, 1999, **243**, 23-36.

148. A. Darji, K. Niebuhr, M. Hense, J. Wehland, T. Chakraborty and S. Weiss, *Infection and Immunity*, 1996, **64**, 2356-2358.

149. S. Pfefferhennig, H. Wessner, M. Hennig, Z. Dauter, G. Hausdorf and W. E. Hohne, *Proteins-Structure Function and Genetics*, 1993, **16**, 437-439.

150. W. Martens, I. Greiserwilke, T. C. Harder, K. Dittmar, R. Frank, C. Orvell, V. Moennig and B. Liess, *Veterinary Microbiology*, 1995, **44**, 289-298.

151. R. Frank and J. Schneider-Mergener, *Peptide arrays on membrane supports: a laboratory manual*, Springer Verlag, Heidelberg, 2002.

152. U. Reineke, R. Volkmer-Engert and J. Schneider-Mergener, *Current Opinion in Biotechnology*, 2001, **12**, 59-64.

153. A. Kramer, U. Reineke, L. Dong, B. Hoffmann, U. Hoffmuller, D. Winkler, R. Volkmer-Engert and J. Schneider-Mergener, *Journal of Peptide Research*, 1999, **54**, 319-327.

154. H. E. Blackwell, *Current Opinion in Chemical Biology*, 2006, **10**, 203-212.

155. D. Scharn, H. Wenschuh, U. Reineke, J. Schneider-Mergener and L. Germeroth, *Journal of Combinatorial Chemistry*, 2000, **2**, 361-369.

156. D. Scharn, L. Germeroth, J. Schneider-Mergener and H. Wenschuh, *Journal of Organic Chemistry*, 2001, **66**, 507-513.

157. N. Heine, L. Germeroth, J. Schneider-Mergener and H. Wenschuh, *Tetrahedron Letters*, 2001, **42**, 227-230.

158. J. Niggemann, K. Michaelis, R. Frank, N. Zander and G. Hofle, *Journal of the Chemical Society-Perkin Transactions 1*, 2002, 2490-2503.

159. M. D. Bowman, R. C. Jeske and H. E. Blackwell, *Organic Letters*, 2004, **6**, 2019-2022.

160. Q. Lin, J. C. O'Neill and H. E. Blackwell, *Organic Letters*, 2005, **7**, 4455-4458.

161. G. MacBeath, A. N. Koehler and S. L. Schreiber, *Journal of the American Chemical Society*, 1999, **121**, 7967-7968.

162. B. T. Houseman, E. S. Gawalt and M. Mrksich, *Langmuir*, 2003, **19**, 1522-1531.

163. T. Horlacher, M. A. Oberli, D. B. Werz, L. Krock, S. Bufali, R. Mishra, J. Sobek, K. Simons, M. Hirashima, T. Niki and P. H. Seeberger, *Chembiochem*, 2010, **11**, 1563-1573.

164. M. A. Oberli, M. Tamborrini, Y. H. Tsai, D. B. Werz, T. Horlacher, A. Adibekian, D. Gauss, H. M. Moller, G. Pluschke and P. H. Seeberger, *Journal of the American Chemical Society*, 2010, **132**, 10239-10241.

165. A. N. Koehler, A. F. Shamji and S. L. Schreiber, *Journal of the American Chemical Society*, 2003, **125**, 8420-8421.

166. D. Barnes-Seeman, S. B. Park, A. N. Koehler and S. L. Schreiber, *Angewandte Chemie-International Edition*, 2003, **42**, 2376-2379.

167. Q. C. Xu and K. S. Lam, *Tetrahedron Letters*, 2002, **43**, 4435-4437.

168. O. Melnyk, X. Duburcq, C. Olivier, F. Urbes, C. Auriault and H. Gras-Masse, *Bioconjugate Chemistry*, 2002, **13**, 713-720.

169. X. Duburcq, C. Olivier, F. Malingue, R. Desmet, A. Bouzidi, F. L. Zhou, C. Auriault, H. Gras-Masse and O. Melnyk, *Bioconjugate Chemistry*, 2004, **15**, 307-316.

170. X. Duburcq, C. Olivier, R. Desmet, M. Halasa, O. Carion, B. Grandidier, T. Heim, D. Stievenard, C. Auriault and O. Melnyk, *Bioconjugate Chemistry*, 2004, **15**, 317-325.

171. G. Y. J. Chen, M. Uttamchandani, Q. Zhu, G. Wang and S. Q. Yao, *Chembiochem*, 2003, **4**, 336-339.

172. M. Uttamchandani, E. W. S. Chan, G. Y. J. Chen and S. Q. Yao, *Bioorganic & Medicinal Chemistry Letters*, 2003, **13**, 2997-3000.

173. M. L. Lesaicherre, M. Uttamchandani, G. Y. J. Chen and S. Q. Yao, *Bioorganic & Medicinal Chemistry Letters*, 2002, **12**, 2079-2083.

174. M. L. Lesaicherre, M. Uttamchandani, G. Y. J. Chen and S. Q. Yao, *Bioorganic & Medicinal Chemistry Letters*, 2002, **12**, 2085-2088.

175. M. C. Bryan, L. V. Lee and C.-H. Wong, *Bioorganic & Medicinal Chemistry Letters*, 2004, **14**, 3185-3188.

176. F. Fazio, M. C. Bryan, H. K. Lee, A. Chang and C. H. Wong, *Tetrahedron Letters*, 2004, **45**, 2689-2692.

177. D. A. Calarese, H. K. Lee, C. Y. Huang, M. D. Best, R. D. Astronomo, R. L. Stanfield, H. Katinger, D. R. Burton, C. H. Wong and I. A. Wilson, *Proceedings of the National Academy of Sciences of the United States of America*, 2005, **102**, 13372-13377.

178. T. Feizi, F. Fazio, W. C. Chai and C. H. Wong, *Current Opinion in Structural Biology*, 2003, **13**, 637-645.

179. C. Y. Huang, D. A. Thayer, A. Y. Chang, M. D. Best, J. Hoffmann, S. Head and C. H. Wong, *Proceedings of the National Academy of Sciences of the United States of America*, 2006, **103**, 15-20.

180. J. L. Childs-Disney, M. Wu, A. Pushechnikov, O. Aminova and M. D. Disney, *ACS Chemical Biology*, 2007, **2**, 745-754.

181. M. Kohn, M. Gutierrez-Rodriguez, P. Jonkheijm, S. Wetzel, R. Wacker, H. Schroeder, H. Prinz, C. M. Niemeyer, R. Breinbauer, S. E. Szedlacsek and H. Waldmann, *Angewandte Chemie-International Edition*, 2007, **46**, 7700-7703.

182. M. B. Soellner, K. A. Dickson, B. L. Nilsson and R. T. Raines, *Journal of the American Chemical Society*, 2003, **125**, 11790-11791.

183. M. Lee and I. Shin, *Organic Letters*, 2005, **7**, 4269-4272.

184. *Hungary Pat.*, WO 2008/023208, 2007.

185. A. S. Blawas and W. M. Reichert, *Biomaterials*, 1998, **19**, 595-609.

186. J. Pascal, W. Dirk, K. Maja, E. Hans, C. M. C. Peter , K. Jürgen, C. M. Jan , N. Dirk, S. Hendrik, W. Ron, B. Rolf, M. N. Christof and W. Herbert, *Angewandte Chemie International Edition*, 2008, **47**, 4421-4424.

187. B. T. Houseman, J. H. Huh, S. J. Kron and M. Mrksich, *Nature Biotechnology*, 2002, **20**, 270-274.

188. W. S. Dillmore, M. N. Yousaf and M. Mrksich, *Langmuir*, 2004, **20**, 7223-7231.

189. J. M. Astle, L. S. Simpson, Y. Huang, M. M. Reddy, R. Wilson, S. Connell, J. Wilson and T. Kodadek, *Chemistry & Biology*, 2010, **17**, 38-45.

190. Z. C. Pei, H. Yu, M. Theurer, A. Walden, P. Nilsson, M. D. Yan and O. Ramstrom, *Chembiochem*, 2007, **8**, 166-168.

191. R. Y. P. Lue, G. Y. J. Chen, Y. Hu, Q. Zhu and S. Q. Yao, *Journal of the American Chemical Society*, 2004, **126**, 1055-1062.

192. M. L. Lesaicherre, R. Y. P. Lue, G. Y. J. Chen, Q. Zhu and S. Q. Yao, *Journal of the American Chemical Society*, 2002, **124**, 8768-8769.

193. H. B. Shi, K. Liu, A. Xua and S. Q. Yao, *Chemical Communications*, 2009, 5030-5032.

194. K. Godula and C. R. Bertozzi, *Journal of the American Chemical Society*, 2010, **132**, 9963-9965.

195. M. C. Bryan, O. Plettenburg, P. Sears, D. Rabuka, S. Wacowich-Sgarbi and C. H. Wong, *Chemistry & Biology*, 2002, **9**, 713-720.

196. A. Studer, S. Hadida, R. Ferritto, S.-Y. Kim, P. Jeger, P. Wipf and D. P. Curran, *Science*, 1997, **275**, 823-826.

197. K. S. Ko, F. A. Jaipuri and N. L. Pohl, *Journal of the American Chemical Society*, 2005, **127**, 13162-13163.

198. J. H. Butler, M. Cronin, K. M. Anderson, G. M. Biddison, F. Chatelain, M. Cummer, D. J. Davi, L. Fisher, A. W. Frauendorf, F. W. Frueh, C. Gjerstad, T. F. Harper, S. D. Kernahan, D. Q. Long, M. Pho, J. A. Walker and T. M. Brennan, *Journal of the American Chemical Society*, 2001, **123**, 8887-8894.

199. A. J. Vegas, J. E. Bradner, W. P. Tang, O. M. McPherson, E. F. Greenberg, A. N. Koehler and S. L. Schreiber, *Angewandte Chemie-International Edition*, 2007, **46**, 7960-7964.

200. S. K. Mamidyala, K. S. Ko, F. A. Jaipuri, G. Park and N. L. Pohl, *Journal of Fluorine Chemistry*, 2006, **127**, 571-579.

201. G. S. Chen and N. L. Pohl, *Organic Letters*, 2008, **10**, 785-788.

202. C. M. Santos, A. Kumar, W. Zhang and C. Z. Cai, *Chemical Communications*, 2009, 2854-2856.

203. R. L. Nicholson, M. L. Ladlow and D. R. Spring, *Chemical Communications*, 2007, 3906-3908.

204. B. Y. M. Collet, T. Nagashima, M. S. Yu and N. L. B. Pohl, *Journal of Fluorine Chemistry*, 2009, **130**, 1042-1048.

205. N. Winssinger, J. L. Harris, B. J. Backes and P. G. Schultz, *Angewandte Chemie-International Edition*, 2001, **40**, 3152-+.

206. N. Winssinger, S. Ficarro, P. G. Schultz and J. L. Harris, *Proceedings of the National Academy of Sciences of the United States of America*, 2002, **99**, 11139-11144.

207. H. D. Urbina, F. Debaene, B. Jost, C. Bole-Feysot, D. E. Mason, P. Kuzmic, J. L. Harris and N. Winssinger, *Chembiochem*, 2006, **7**, 1790-1797.

208. D. Pouchain, J. J. Diaz-Mochon, L. Bialy and M. Bradley, *ACS Chemical Biology*, 2007, **2**, 810-818.

209. J. J. Diaz-Mochon, L. Bialy, L. Keinicke and M. Bradley, *Chemical Communications*, 2005, 1384-1386.

210. J. J. Diaz-Mochon, L. Bialy and M. Bradley, *Chemical Communications*, 2006, 3984-3986.

211. N. Winssinger, R. Damoiseaux, D. C. Tully, B. H. Geierstanger, K. Burdick and J. L. Harris, *Chemistry & Biology*, 2004, **11**, 1351-1360.

212. S. A. Ruiz and C. S. Chen, *Soft Matter*, 2007, **3**, 168-177.

213. U. R. Müller, D. V. Nicolau, U. Müller and R. Papen, in *Microarray Technology and Its Applications*, eds. E. Greenbaum, M. Aizawa, O. S. Andersen, R. H. Austin, J. Barber, H. C. Berg, V. Bloomfield, R. Callender, B. Chance, S. Chu, L. J. DeFelice, J. Deisenhofer, G. Feher, H. Frauenfelder, I. Giaever, S. M. Gruner, J. Herzfeld, M. S. Humayun, P. Joliot, L. Keszthelyi, R. S. Knox, A. Lewis, S. M. Lindsay, D. Mauzerall, E. V. Mielczarek, M. Niemz, V. A. Parsegian, L. S. Powers, E. W. Prohofsky, A. Rubin, M. Seibert, D. Thomas and S. J. Williamson, Springer Berlin Heidelberg, Editon edn., 2005, pp. 73-88.

214. U. R. Müller, D. V. Nicolau and M. Doktycz, in *Microarray Technology and Its Applications*, eds. E. Greenbaum, M. Aizawa, O. S. Andersen, R. H. Austin, J. Barber, H. C. Berg, V. Bloomfield, R. Callender, B. Chance, S. Chu, L. J. DeFelice, J. Deisenhofer, G. Feher, H. Frauenfelder, I. Giaever, S. M. Gruner, J. Herzfeld, M. S. Humayun, P. Joliot, L. Keszthelyi, R. S. Knox, A. Lewis, S. M. Lindsay, D. Mauzerall, E. V. Mielczarek, M. Niemz, V. A. Parsegian, L. S. Powers, E. W. Prohofsky, A. Rubin, M. Seibert, D. Thomas and S. J. Williamson, Springer Berlin Heidelberg, Editon edn., 2005, pp. 63-72.

215. P. R. Kumaresan and K. S. Lam, in *Exploiting Chemical Diversity for Drug Discovery*, eds. M. Entzeroth and P. A. Bartlett, Molecular Biosystems, Editon edn., 2006, vol. 2, pp. 259-270.

216. Y. S. Sun, J. P. Landry, Y. Y. Fei and X. D. Zhu, *Langmuir*, 2008, **24**, 13399-13405.

217. J. E. Bradner, O. M. McPherson, R. Mazitschek, D. Barnes-Seeman, J. P. Shen, J. Dhaliwal, K. E. Stevenson, J. L. Duffner, S. B. Park, D. S. Neuberg, P. Nghiem, S. L. Schreiber and A. N. Koehler, *Chemistry & Biology*, 2006, **13**, 493-504.

218. C. M. Salisbury, D. J. Maly and J. A. Ellman, *Journal of the American Chemical Society*, 2002, **124**, 14868-14870.

219. A. K. Shiau, M. E. Massari and C. C. Ozbal, *Combinatorial Chemistry & High Throughput Screening*, 2008, **11**, 231-237.

220. L. T. Mazzola and S. P. A. Fodor, *Biophysical Journal*, 1995, **68**, 1653-1660.

221. G. J. Wegner, A. W. Wark, H. J. Lee, E. Codner, T. Saeki, S. P. Fang and R. M. Corn, *Analytical Chemistry*, 2004, **76**, 5677-5684.

222. J. P. Landry, X. D. Zhu and J. P. Gregg, *Optics Letters*, 2004, **29**, 581-583.

223. Y. Y. Fei, J. P. Landry, Y. S. Sun, X. D. Zhu, J. T. Luo, X. B. Wang and K. S. Lam, *Rev Sci Instrum*, 2008, **79**, 013708.

224. Y. S. Sun, J. P. Landry, Y. Y. Fei, X. D. Zhu, J. T. Luo, X. B. Wang and K. S. Lam, *Analytical Chemistry*, 2009, **81**, 5373-5380.

225. Y. Y. Fei, J. P. Landry, Y. S. Sun, X. D. Zhu, X. B. Wang, J. T. Luo, C. Y. Wu and K. S. Lam, *Journal of Biomedical Optics*, 2010, **15**.

226. J. L. Duffner, P. A. Clemons and A. N. Koehler, *Current Opinion in Chemical Biology*, 2007, **11**, 74-82.

227. R. L. Nicholson, M. Welch, M. Ladlow and D. R. Spring, *ACS Chemical Biology*, 2007, **2**, 24-30.

228. F. G. Kuruvilla, A. F. Shamji, S. M. Sternson, P. J. Hergenrother and S. L. Schreiber, *Nature*, 2002, **416**, 653-657.

229. M. Uttamchandani, D. P. Walsh, S. M. Khersonsky, X. Huang, S. Q. Yao and Y. T. Chang, *Journal of Combinatorial Chemistry*, 2004, **6**, 862-868.

230. S. E. Tully, M. Rawat and L. C. Hsieh-Wilson, *Journal of the American Chemical Society*, 2006, **128**, 7740-7741.

231. M. Uttamchandani, W. L. Lee, J. Wang and S. Q. Yao, *Journal of the American Chemical Society*, 2007, **129**, 13110-13117.

232. S. M. Gopalakrishnan, J. Karvinen, J. L. Kofron, D. J. Burns and U. Warrior, *Journal of Biomolecular Screening*, 2002, **7**, 317-323.

233. H. Miao, J. A. Tallarico, H. Hayakawa, K. Munger, J. L. Duffner, A. N. Koehler, S. L. Schreiber and T. A. Lewis, *Journal of Combinatorial Chemistry*, 2007, **9**, 245-253.

234. S. J. Kwon, M. Y. Lee, B. Ku, D. H. Sherman and J. S. Dordick, *ACS Chemical Biology*, 2007, **2**, 419-425.

235. C. A. David, T. Middleton, D. Montgomery, H. Ben Lim, W. Kati, A. Molla, X. L. Xuei, U. Warrior, J. L. Kofron and D. J. Burns, *Journal of Biomolecular Screening*, 2002, **7**, 259-266.

236. S. Dickopf, M. Frank, H. D. Junker, S. Maier, G. Metz, H. Ottleben, H. Rau, N. Schellhaas, K. Schmidt, R. Sekul, C. Vanier, D. Vetter, J. Czech, M. Lorenz, H. Matter, M. Schudok, H. Schreuder, D. W. Will and H. P. Nestler, *Analytical Biochemistry*, 2004, **335**, 50-57.

237. S. Melkko, J. Scheuermann, C. E. Dumelin and D. Neri, *Nature Biotechnology*, 2004, **22**, 568-574.

238. R. L. W. Roska, T. G. S. Lama, J. P. Hennes and R. E. Carlson, *Journal of the American Chemical Society*, 2009.

239. I. Miyazaki, S. Simizu, K. Ishida and H. Osada, *Chembiochem*, 2009, **10**, 838-843.

240. I. Miyazaki, H. Okumura, S. Simizu, Y. Takahashi, N. Kanoh, Y. Muraoka, Y. Nonomura and H. Osada, *Chembiochem*, 2009, **10**, 845-852.

241. H. Y. Sun, S. Chattopadhaya, J. Wang and S. Q. Yao, *Analytical and Bioanalytical Chemistry*, 2006, **386**, 416-426.

242. Q. Zhu, M. Uttamchandani, D. B. Li, M. L. Lesaicherre and S. Q. Yao, *Organic Letters*, 2003, **5**, 1257-1260.

243. D. N. Gosalia and S. L. Diamond, *Proceedings of the National Academy of Sciences of the United States of America*, 2003, **100**, 8721-8726.

244. J. Wang, M. Uttamchandani, J. Q. Li, M. Y. Hu and S. Q. Yao, *Chemical Communications*, 2006, 3783-3785.

245. S. Fournel and S. Muller, *Current Protein & Peptide Science*, 2003, **4**, 261-276.

246. A. H. Smith, J. M. Vrtis and T. Kodadek, *Advances in Clinical Chemistry, Vol. 38*, 2004, **38**, 217-+.

247. O. J. Barrett, J. L. Childs and M. D. Disney, *Chembiochem*, 2006, **7**, 1882-1885.

248. K. L. Hsu and L. K. Mahal, *Current Opinion in Chemical Biology*, 2009, **13**, 427-432.

249. M. Uttamchandani, J. L. Neo, B. N. Z. Ong and S. Moochhala, *Trends in Biotechnology*, 2009, **27**, 53-61.

250. Z. Peng and Y. Bang-Ce, *J Agric Food Chem*, 2006, **54**, 6978-6983.

251. C. Visintin, A. E. Aliev, D. Riddall, D. Baker, M. Okuyama, P. M. Hoi, R. Hiley and D. L. Selwood, *Organic Letters*, 2005, **7**, 1699-1702.

252. C. M. Pickart, *Annual Review of Biochemistry*, 2001, **70**, 503-533.

253. M. Hart, J. P. Concordet, I. Lassot, I. Albert, R. del los Santos, H. Durand, C. Perret, B. Rubinfeld, F. Margottin, R. Benarous and P. Polakis, *Current Biology*, 1999, **9**, 207-210.

254. Q. T. Li and I. M. Verma, *Nature Reviews Immunology*, 2002, **2**, 725-734.

255. J. T. Winston, P. Strack, P. Beer-Romero, C. Y. Chu, S. J. Elledge and J. W. Harper, *Genes & Development*, 1999, **13**, 270-283.

256. D. A. LaVan, D. M. Lynn and R. Langer, *Nature Reviews Drug Discovery*, 2002, **1**, 77-84.

257. I. Roy and M. N. Gupta, *Chemistry & Biology*, 2003, **10**, 1161-1171.

258. S. Deshayes, M. C. Morris, G. Divita and F. Heitz, *Cellular and Molecular Life Sciences*, 2005, **62**, 1839-1849.

259. C. Adrian and M. Hogbern, *Pysiologist*, 1960, 56-62.

260. R. M. Sanchez-Martin, M. Muzerelle, N. Chitkul, S. E. How, S. Mittoo and M. Bradley, *Chembiochem*, 2005, **6**, 1341-1345.

261. P. L. Felgner, T. R. Gadek, M. Holm, R. Roman, H. W. Chan, M. Wenz, J. P. Northrop, G. M. Ringold and M. Danielsen, *Proceedings of the National Academy of Sciences of the United States of America*, 1987, **84**, 7413-7417.

262. O. Pillai and R. Panchagnula, *Current Opinion in Chemical Biology*, 2001, **5**, 447-451.

263. B. K. Nanjwade, H. M. Bechra, G. K. Derkar, F. V. Manvi and V. K. Nanjwade, *European Journal of Pharmaceutical Sciences*, 2009, **38**, 185-196.

264. N. W. S. Kam, T. C. Jessop, P. A. Wender and H. J. Dai, *Journal of the American Chemical Society*, 2004, **126**, 6850-6851.

265. S. Trabulo, A. L. Cardoso, M. Mano and M. C. P. de Lima, *Pharmaceuticals*, 2010, **3**, 961-993.

266. D. Derossi, G. Chassaing and A. Prochiantz, *Trends in Cell Biology*, 1998, **8**, 84-87.

267. J. B. Rothbard, S. Garlington, Q. Lin, T. Kirschberg, E. Kreider, P. L. McGrane, P. A. Wender and P. A. Khavari, *Nature Medicine*, 2000, **6**, 1253-1257.

268. A. Prochiantz, *Current Opinion in Neurobiology*, 1996, **6**, 629-634.

269. L. R. Jones, E. A. Goun, R. Shinde, J. B. Rothbard, C. H. Contag and P. A. Wender, *Journal of the American Chemical Society*, 2006, **128**, 6526-6527.

270. H. J. P. Ryser and W. C. Shen, *Proceedings of the National Academy of Sciences of the United States of America*, 1978, **75**, 3867-3870.

271. M. Pooga, M. Hallbrink, M. Zorko and U. Langel, *Faseb Journal*, 1998, **12**, 67-77.

272. Y. K. Reshetnyak, O. A. Andreev, U. Lehnert and D. M. Engelman, *Proceedings of the National Academy of Sciences of the United States of America*, 2006, **103**, 6460-6465.

273. T. Vagt, O. Zschornig, D. Huster and B. Koksch, *Chemphyschem*, 2006, **7**, 1361-1371.

274. R. E. Lanford, P. Kanda and R. C. Kennedy, *Cell*, 1986, **46**, 575-582.

275. B. Gupta, T. S. Levchenko and V. P. Torchilin, *Advanced Drug Delivery Reviews*, 2005, **57**, 637-651.

276. P. A. Wender, J. B. Rothbard, T. C. Jessop, E. L. Kreider and B. L. Wylie, *Journal of the American Chemical Society*, 2002, **124**, 13382-13383.

277. R. J. Simon, R. S. Kania, R. N. Zuckermann, V. D. Huebner, D. A. Jewell, S. Banville, S. Ng, L. Wang, S. Rosenberg, C. K. Marlowe, D. C. Spellmeyer, R. Y. Tan, A. D. Frankel, D. V. Santi, F. E. Cohen and P. A. Bartlett, *Proceedings of the National Academy of Sciences of the United States of America*, 1992, **89**, 9367-9371.

278. I. Peretto, R. M. Sanchez-Martin, X. H. Wang, J. Ellard, S. Mittoo and M. Bradley, *Chemical Communications*, 2003, 2312-2313.

279. P. A. Wender, D. J. Mitchell, K. Pattabiraman, E. T. Pelkey, L. Steinman and J. B. Rothbard, *Proceedings of the National Academy of Sciences of the United States of America*, 2000, **97**, 13003-13008.

280. N. Umezawa, M. A. Gelman, M. C. Haigis, R. T. Raines and S. H. Gellman, *Journal of the American Chemical Society*, 2002, **124**, 368-369.

281. M. G. Paulick, K. M. Hart, K. M. Brinner, M. Tjandra, D. H. Charych and R. N. Zuckermann, *Journal of Combinatorial Chemistry*, 2006, **8**, 417-426.

282. J. E. Murphy, T. Uno, J. D. Hamer, F. E. Cohen, V. Dwarki and R. N. Zuckermann, *Proceedings of the National Academy of Sciences of the United States of America*, 1998, **95**, 1517-1522.

283. S. M. Miller, R. J. Simon, S. Ng, R. N. Zuckermann, J. M. Kerr and W. H. Moos, *Bioorganic & Medicinal Chemistry Letters*, 1994, **4**, 2657-2662.

284. T. Schroder, K. Schmitz, N. Niemeier, T. S. Balaban, H. F. Krug, U. Schepers and S. Brase, *Bioconjugate Chemistry*, 2007, **18**, 342-354.

285. Y. Utku, E. Dehan, O. Ouerfelli, F. Piano, R. N. Zuckermann, M. Pagano and K. Kirshenbaum, *Molecular Biosystems*, 2006, **2**, 312-317.

286. A. Unciti-Broceta, F. Diezmann, C. Y. Ou-Yang, M. A. Fara and M. Bradley, *Bioorganic & Medicinal Chemistry*, 2009, **17**, 959-966.

287. T. Schroder, N. Niemeier, S. Afonin, A. S. Ulrich, H. F. Krug and S. Brase, *Journal of Medicinal Chemistry*, 2008, **51**, 376-379.

288. G. Blobel and B. Dobberstein, *Journal of Cell Biology*, 1975, **67**, 835-851.

289. G. Blobel and B. Dobberstein, *Journal of Cell Biology*, 1975, **67**, 852-862.

290. E. M. Derobertis, *Cell*, 1983, **32**, 1021-1025.

291. R. W. Wozniak, M. P. Rout and J. D. Aitchison, *Trends in Cell Biology*, 1998, **8**, 184-188.

292. D. A. Jans, C. K. Chan and S. Huebner, *Med. Res. Rev.*, 1998, **18**, 189-223.

293. J. Robbins, S. M. Dilworth, R. A. Laskey and C. Dingwall, *Cell*, 1991, **64**, 615-623.

294. D. Kalderon, B. L. Roberts, W. D. Richardson and A. E. Smith, *Cell*, 1984, **39**, 499-509.

295. E. Vives, P. Brodin and B. Lebleu, *Journal of Biological Chemistry*, 1997, **272**, 16010-16017.

296. R. E. Lanford and J. S. Butel, *Cell*, 1984, **37**, 801-813.

297. T. Boulikas, *Journal of Cellular Biochemistry*, 1994, **55**, 32-58.

298. L. M. McLane and A. H. Corbett, *Iubmb Life*, 2009, **61**, 697-706.

299. A. Lange, R. E. Mills, C. J. Lange, M. Stewart, S. E. Devine and A. H. Corbett, *Journal of Biological Chemistry*, 2007, **282**, 5101-5105.

300. R. S. Faustino, T. J. Nelson, A. Terzic and C. Perez-Terzic, *Clinical Pharmacology & Therapeutics*, 2007, **81**, 880-886.

301. Y. Yoneda, T. Semba, Y. Kaneda, R. L. Noble, Y. Matsuoka, T. Kurihara, Y. Okada and N. Imamoto, *Experimental Cell Research*, 1992, **201**, 313-320.

302. M. A. Zanta, P. Belguise-Valladier and J. P. Behr, *Proceedings of the National Academy of Sciences of the United States of America*, 1999, **96**, 91-96.

303. P. Chen, J. Wang, K. Hope, L. Q. Jin, J. Dick, R. Camron, J. Brandwein, M. Minden and R. M. Reilly, *Journal of Nuclear Medicine*, 2006, **47**, 827-836.

304. M. Sibrian-Vazquez, T. J. Jensen, R. P. Hammer and M. G. H. Vicente, *Journal of Medicinal Chemistry*, 2006, **49**, 1364-1372.

305. G. G. Borisy and E. W. Taylor, *Journal of Cell Biology*, 1967, **34**, 525.

306. R. L. Margolis and L. Wilson, *Proceedings of the National Academy of Sciences of the United States of America*, 1977, **74**, 3466-3470.

307. L. W. Moreland and G. V. Ball, *Arthritis and Rheumatism*, 1991, **34**, 782-786.

308. F. D. Malkinson, *Archives of Dermatology*, 1982, **118**, 453-457.

309. A. Garciagonzalez and M. H. Weisman, *Seminars in Arthritis and Rheumatism*, 1992, **22**, 139-150.

310. A. Livneh, D. Zemer, P. Langevitz, J. Shemer, E. Sohar and M. Pras, *Seminars in Arthritis and Rheumatism*, 1993, **23**, 206-214.

311. E. von Angerer, *Curr Opin Drug Discov Devel*, 2000, **3**, 575-584.

312. M. A. Jordan, D. Thrower and L. Wilson, *Cancer Research*, 1991, **51**, 2212-2222.

313. E. M. Gipps, P. Groscurth, J. Kreuter and P. P. Speiser, *Journal of Pharmaceutical Sciences*, 1988, **77**, 208-209.

314. S. Wang and P. S. Low, *Journal of Controlled Release*, 1998, **53**, 39-48.

315. C. P. Leamon and P. S. Low, *Journal of Biological Chemistry*, 1992, **267**, 24966-24971.

316. J. J. Diaz-Mochon, L. Bialy and M. Bradley, *Organic Letters*, 2004, **6**, 1127-1129.

317. J. Hed, G. Hallden, S. G. O. Johansson and P. Larsson, *Journal of Immunological Methods*, 1987, **101**, 119-125.

318. T. Mosmann, *Journal of Immunological Methods*, 1983, **65**, 55-63.

319. I. M. Verma and N. Somia, *Nature*, 1997, **389**, 239-242.

320. D. J. Glover, H. J. Lipps and D. A. Jans, *Nature Reviews Genetics*, 2005, **6**, 299-U229.

321. R. M. Sanchez-Martin, M. Cuttle, S. Mittoo and M. Bradley, *Angewandte Chemie-International Edition*, 2006, **45**, 5472-5474.

322. M. Bradley, L. Alexander, K. Duncan, M. Chennaoui, A. C. Jones and R. M. Sanchez-Martin, *Bioorganic & Medicinal Chemistry Letters*, 2008, **18**, 313-317.

323. M. Bradley, L. Alexander and R. M. Sanchez-Martin, *Journal of Fluorescence*, 2008, **18**, 733-739.

324. L. M. Alexander, R. M. Sanchez-Martin and M. Bradley, *Bioconjugate Chemistry*, 2009, **20**, 422-426.

325. F. D. Ledley, *Pharmaceutical Research*, 1996, **13**, 1595-1614.

326. J. Rejman, V. Oberle, I. S. Zuhorn and D. Hoekstra, *Biochemical Journal*, 2004, **377**, 159-169.

327. A. S. Boutorine and E. V. Kostina, *Biochimie*, 1993, **75**, 35-41.

328. A. P. Rolland, *Critical Reviews in Therapeutic Drug Carrier Systems*, 1998, **15**, 143-198.

329. J. Zabner, A. J. Fasbender, T. Moninger, K. A. Poellinger and M. J. Welsh, *Journal of Biological Chemistry*, 1995, **270**, 18997-19007.

330. C. W. Pouton and L. W. Seymour, *Advanced Drug Delivery Reviews*, 1998, **34**, 3-19.

331. R. I. Mahato, Y. Takakura and M. Hashida, *Critical Reviews in Therapeutic Drug Carrier Systems*, 1997, **14**, 133-172.

332. M. L. Edelstein, M. R. Abedi and J. Wixon, *Journal of Gene Medicine*, 2007, **9**, 833-842.

333. A. Rolland and P. L. Felgner, *Advanced Drug Delivery Reviews*, 1998, **30**, 1-3.

334. R. G. Amado and I. S. Y. Chen, *Science*, 1999, **285**, 674-676.

335. M. D. Brown, A. G. Schatzlein and I. F. Uchegbu, *International Journal of Pharmaceutics*, 2001, **229**, 1-21.

336. J. S. Pagano and A. Vaheri, *Archiv Fur Die Gesamte Virusforschung*, 1965, **17**, 456-464.

337. McCutcha.Jh and J. S. Pagano, *Journal of the National Cancer Institute*, 1968, **41**, 351.

338. P. Mellon, V. Parker, Y. Gluzman and T. Maniatis, *Cell*, 1981, **27**, 279-288.

339. S. Kawai and M. Nishizawa, *Molecular and Cellular Biology*, 1984, **4**, 1172-1174.

340. O. Boussif, F. Lezoualch, M. A. Zanta, M. D. Mergny, D. Scherman, B. Demeneix and J. P. Behr, *Proceedings of the National Academy of Sciences of the United States of America*, 1995, **92**, 7297-7301.

341. W. Zauner, M. Ogris and E. Wagner, *Advanced Drug Delivery Reviews*, 1998, **30**, 97-113.

342. A. Akinc and R. Langer, *Biotechnology and Bioengineering*, 2002, **78**, 503-508.

343. S. D. Patil, D. G. Rhodes and D. J. Burgess, *Aaps Journal*, 2005, **7**, E61-E77.

344. J. Haensler and F. C. Szoka, *Bioconjugate Chemistry*, 1993, **4**, 372-379.

345. J. F. KukowskaLatallo, A. U. Bielinska, J. Johnson, R. Spindler, D. A. Tomalia and J. R. Baker, *Proceedings of the National Academy of Sciences of the United States of America*, 1996, **93**, 4897-4902.

346. S. E. How, A. Unciti-Broceta, R. M. Sanchez-Martin and M. Bradley, *Organic & Biomolecular Chemistry*, 2008, **6**, 2266-2269.

347. A. V. Kabanov and V. A. Kabanov, *Bioconjugate Chemistry*, 1995, **6**, 7-20.

348. F. LabatMoleur, A. M. Steffan, C. Brisson, H. Perron, O. Feugeas, P. Furstenberger, F. Oberling, E. Brambilla and J. P. Behr, *Gene Therapy*, 1996, **3**, 1010-1017.

349. X. Gao and L. Huang, *Gene Therapy*, 1995, **2**, 710-722.

350. W. J. Guo and R. J. Lee, *Bioscience Reports*, 2000, **20**, 419-432.

351. B. Schwartz, M. A. Ivanov, B. Pitard, V. Escriou, R. Rangara, G. Byk, P. Wils, J. Crouzet and D. Scherman, *Gene Therapy*, 1999, **6**, 282-292.

352. P. L. Felgner, Y. J. Tsai, L. Sukhu, C. J. Wheeler, M. Manthorpe, J. Marshall and S. H. Cheng, *DNA Vaccines*, 1995, **772**, 126-139.

353. S. Capaccioli, G. Dipasquale, E. Mini, T. Mazzei and A. Quattrone, *Biochemical and Biophysical Research Communications*, 1993, **197**, 818-825.

354. J. T. Lee and R. Jaenisch, *Nucleic Acids Research*, 1996, **24**, 5054-5055.

355. B. T. Lamb and J. D. Gearhart, *Current Opinion in Genetics & Development*, 1995, **5**, 342-348.

356. M. C. P. de Lima, S. Simoes, P. Pires, H. Faneca and N. Duzgunes, *Advanced Drug Delivery Reviews*, 2001, **47**, 277-294.

357. S. Dokka, D. Toledo, X. G. Shi, V. Castranova and Y. Rojanasakul, *Pharmaceutical Research*, 2000, **17**, 521-525.

358. M. C. Filion and N. C. Phillips, *Biochimica Et Biophysica Acta-Biomembranes*, 1997, **1329**, 345-356.

359. M. E. Martin and K. G. Rice, *Aaps Journal*, 2007, **9**, E18-E29.

360. F. Heitz, M. C. Morris and G. Divita, *British Journal of Pharmacology*, 2009, **157**, 195-206.

361. V. P. Torchilin, *Biopolymers*, 2008, **90**, 604-610.

362. M. C. Morris, L. Chaloin, J. Mery, F. Heitz and G. Divita, *Nucleic Acids Research*, 1999, **27**, 3510-3517.

363. S. Veldhoen, S. D. Laufer and T. Restle, *International Journal of Molecular Sciences*, 2008, **9**, 1276-1320.

364. T. Lehto, R. Abes, N. Oskolkov, J. Suhorutsenko, D. M. Copolovici, I. Mager, J. R. Viola, O. E. Simonson, K. Ezzat, P. Guterstam, E. Eriste, C. I. E. Smith, B. Lebleu, S. El Andaloussi and U. Langel, *Journal of Controlled Release*, 2010, **141**, 42-51.

365. R. E. Vandenbroucke, S. C. De Smedt, J. Demeester and N. N. Sanders, *Biochimica Et Biophysica Acta-Biomembranes*, 2007, **1768**, 571-579.

366. L. Hyndman, J. L. Lemoine, L. Huang, D. J. Porteous, A. C. Boyd and X. S. Nan, *Journal of Controlled Release*, 2004, **99**, 435-444.

367. C. Rudolph, C. Plank, J. Lausier, U. Schillinger, R. H. Muller and J. Rosenecker, *Journal of Biological Chemistry*, 2003, **278**, 11411-11418.

368. E. Kleemann, M. Neu, N. Jekel, L. Fink, T. Schmehl, T. Gessler, W. Seeger and T. Kissel, *Journal of Controlled Release*, 2005, **109**, 299-316.

369. J. A. MacKay, W. Li, Z. Huang, E. E. Dy, G. Huynh, T. Tihan, R. Collins, D. F. Deen and F. C. Szoka, *Molecular Therapy*, 2008, **16**, 893-900.

370. I. A. Khalil, K. Kogure, S. Futaki, S. Hama, H. Akita, M. Ueno, H. Kishida, M. Kudoh, Y. Mishina, K. Kataoka, M. Yamada and H. Harashima, *Gene Therapy*, 2007, **14**, 682-689.

371. A. El-Sayed, I. A. Khalil, K. Kogure, S. Futaki and H. Harashima, *Journal of Biological Chemistry*, 2008, **283**, 23450-23461.

372. I. A. Khalil, S. Futaki, M. Niwa, Y. Baba, N. Kaji, H. Kamiya and H. Harashima, *Gene Therapy*, 2004, **11**, 636-644.

373. R. M. Sanchez-Martin, L. Alexander and M. Bradley, *Fluorescence Methods and Applications: Spectroscopy, Imaging, and Probes*, 2008, **1130**, 207-217.

374. R. M. Sanchez-Martin, L. Alexander, M. Muzerelle, J. M. Cardenas-Maestre, A. Tsakiridis, J. M. Brickman and M. Bradley, *Chembiochem*, 2009, **10**, 1453-1456.

375. A. Tsakiridis, L. M. Alexander, N. Gennet, R. M. Sanchez-Martin, A. Livigni, M. Li, M. Bradley and J. M. Brickman, *Biomaterials*, 2009, **30**, 5853-5861.

376. N. Gennet, L. M. Alexander, R. M. Sanchez-Martin, J. M. Behrendt, A. J. Sutherland, J. M. Brickman, M. Bradley and M. Li, *New Biotechnology*, 2009, **25**, 442-449.

377. H. Butt, K. Graf and M. Kappl, *Physics and chemistry of interfaces*, Wiley-VCH Berlag GmbH & Co., Germany, 2003.

378. T. Suzuki, K. Fujikura, T. Higashiyama and K. Takata, *Journal of Histochemistry & Cytochemistry*, 1997, **45**, 49-53.

379. F. L. Sorgi, S. Bhattacharya and L. Huang, *Gene Therapy*, 1997, **4**, 961-968.

380. L. J. Branden, A. J. Mohamed and C. I. E. Smith, *Nature Biotechnology*, 1999, **17**, 784-787.

381. M. Egholm, O. Buchardt, L. Christensen, C. Behrens, S. M. Freier, D. A. Driver, R. H. Berg, S. K. Kim, B. Norden and P. E. Nielsen, *Nature*, 1993, **365**, 566-568.

382. P. E. Nielsen, M. Egholm, R. H. Berg and O. Buchardt, *Science*, 1991, **254**, 1497-1500.

383. M. E. Hansen, T. Bentin and P. E. Nielsen, *Nucleic Acids Research*, 2009, **37**, 4498-4507.

384. T. Bentin, G. I. Hansen and P. E. Nielsen, *Nucleic Acids Research*, 2006, **34**, 5790-5799.

385. E. Hebert, *Biology of the Cell*, 2003, **95**, 59-68.

386. E. Kaiser, Colescot.Rl, Bossinge.Cd and P. I. Cook, *Analytical Biochemistry*, 1970, **34**, 595-&.

387. M. E. Attardi, G. Porcu and M. Taddei, *Tetrahedron Letters*, 2000, **41**, 7391-7394.

388. K. E. Borbas, P. Mroz, M. R. Hamblin and J. S. Lindsey, *Bioconjugate Chemistry*, 2006, **17**, 638-653.

389. R. Sjoback, J. Nygren and M. Kubista, *Spectrochimica Acta Part a-Molecular and Biomolecular Spectroscopy*, 1995, **51**, L7-L21.